

## Cruise report for Lophelia and Nereus 2014

Operating authority:

Sven Lovén Centre for Marine Sciences, Tjärnö, University of Gothenburg, Sweden

Owner: University of Gothenburg, Sweden

Name of master: Carl-Henrik Gustavsson

Scientist in charge: Lisbeth Jonsson

Principal investigators:

Tomas Lundälv

Ann Larsson

Susanna Strömberg

### Table of activities

Date	Ship name	Activities			
		ROV	Recording of bottom transects	Collection of corals*	Deployment/retrieval of current meters
21 Jan	Nereus	X		X	
26 Feb	Nereus	X			X
27 Mar	Nereus	X			X
10 Apr	Nereus	X			X
20 May	Lophelia	X	X		
21 May	Lophelia	X	X		
22 May	Lophelia	X	X		
23 May	Lophelia	X	X		
27 May	Lophelia	X	X	X	
20 Nov	Lophelia	X		X	
9 Dec	Lophelia	X			X

\* All necessary permits were in place: the Ytre Hvaler National Park Board and the Norwegian Directorate for Nature Management permit for coral collections, 2010/107-432.3; 2013-46; the Norwegian Fisheries Directorate CITES export permit EX-23-2014, and the Swedish Board of Agriculture CITES import permit Dnr: 4.10.18-10009/14 Nr: 51200-14.

### Scientific publications stemming from the activities

Strömberg SM, Östman C (2017). The cnidome and internal morphology of *Lophelia pertusa* (Linnaeus, 1758) (Cnidaria, Anthozoa). *Acta Zoologica* **98**: 191–213

Strömberg SM (2016) Early life history of the cold-water coral *Lophelia pertusa* –with implications for dispersal. Ph.D. thesis at the University of Gothenburg

Georgian SE, Dupont S, Kurman M, Butler A, Strömberg SM, Larsson AI, Cordes EE (2016). Biogeographic variability in the physiological response of the cold-water coral *Lophelia pertusa* to ocean acidification. *Marine Ecology* **37**:1345-1359

van Oevelen D, Mueller CE, Lundälv T, Middelburg JJ (2016). Food selectivity and processing by the cold-water coral *Lophelia pertusa*. *Biogeosciences* **13**:5789-5798

Middelburg J, Mueller C, Veuger B, Larsson AI, Form A, van Oevelen D (2015). Discovery of symbiotic nitrogen fixation and chemoautotrophy in cold-water corals. *Scientific reports*, 5:17962, DOI: 10.1038/srep17962

The publications are attached

# SCIENTIFIC REPORTS



OPEN

## Discovery of symbiotic nitrogen fixation and chemoautotrophy in cold-water corals

Jack J. Middelburg<sup>1</sup>, Christina E. Mueller<sup>2</sup>, Bart Veuger<sup>2</sup>, Ann I. Larsson<sup>3</sup>, Armin Form<sup>4</sup> & Dick van Oevelen<sup>2</sup>

Received: 19 June 2015

Accepted: 09 November 2015

Published: 08 December 2015

Cold-water corals (CWC) are widely distributed around the world forming extensive reefs at par with tropical coral reefs. They are hotspots of biodiversity and organic matter processing in the world's deep oceans. Living in the dark they lack photosynthetic symbionts and are therefore considered to depend entirely on the limited flux of organic resources from the surface ocean. While symbiotic relations in tropical corals are known to be key to their survival in oligotrophic conditions, the full metabolic capacity of CWC has yet to be revealed. Here we report isotope tracer evidence for efficient nitrogen recycling, including nitrogen assimilation, regeneration, nitrification and denitrification. Moreover, we also discovered chemoautotrophy and nitrogen fixation in CWC and transfer of fixed nitrogen and inorganic carbon into bulk coral tissue and tissue compounds (fatty acids and amino acids). This unrecognized yet versatile metabolic machinery of CWC conserves precious limiting resources and provides access to new nitrogen and organic carbon resources that may be essential for CWC to survive in the resource-depleted dark ocean.

Microbes involved in nitrogen transformations occur in symbiosis with a wide range of marine eukaryotes, including shipworms, diatoms, sponges and tropical corals<sup>1,2</sup>. Symbiotic relationships in tropical corals include not only interactions between the coral and photoautotrophic dinoflagellates (zooxanthellae), but also involves cyanobacteria that reduce dinitrogen gas (N<sub>2</sub>) to ammonia that subsequently can be used by the dinoflagellate-coral association<sup>2-4</sup> or oxidized to nitrate by nitrifying symbiotic microbes<sup>5</sup>. This intense nitrogen cycling in tropical corals is key to understanding their functioning<sup>2</sup> and enables them to survive in the oligotrophic tropical seas<sup>6,7</sup>.

Cold-water corals are ecosystem engineers distributed at water depths more than 50 m across the globe<sup>8,9</sup> and provide a habitat for >2700 species<sup>10</sup>. They live in the dark ocean and are therefore thought to depend on the arrival of organic matter produced in the distant sunlit surface ocean<sup>11,12</sup>. This organic matter rapidly degrades during the downward transit rendering a low availability of energy and organic nutrients in the deep sea. CWC have therefore adopted opportunistic feeding strategies utilizing various organic resources and preferentially retaining nitrogen<sup>13,14</sup>. CWCs are hotspot of organic matter processing relative to bare sediments and therefore contribute disproportionately to oxygen consumption and dissolved inorganic carbon and nutrient releases<sup>11,12,15</sup>. Khrifounoff *et al.*<sup>15</sup> reported high coral ammonium excretion rates while the ammonium concentration in the surrounding water was low, implying a high ammonium turnover. Maier *et al.*<sup>16,17</sup> studied dissolved inorganic nutrient release by CWC and found consistent release of phosphate and ammonium and sometimes release of nitrite and nitrate as well. Ambient water concentrations were as low at ~1 μmol L<sup>-1</sup>, as found also for other Atlantic cold-water coral reefs<sup>18</sup>, suggesting high nutrient turnover rates, while the release of nitrate and nitrite hints at nitrification activity by the CWC holobiont, i.e. the coral and its associated microbes.

These apparent conflicting observations can be reconciled if CWC retain nitrogen by efficient recycling or have access to new nitrogen sources that compensates for losses. Here we use <sup>15</sup>N-labeled dinitrogen, nitrate and ammonium to elucidate nitrogen transformation pathways by the cold-water coral *Lophelia pertusa*, a holobiont that is dominant in the North Atlantic<sup>9,13</sup>. Moreover, we use <sup>13</sup>C-labelled bicarbonate to investigate whether inorganic carbon was fixed by chemoautotrophs and transferred into coral tissue and different tissue components

<sup>1</sup>Department of Earth Sciences, Utrecht University, P.O. Box 80.021, 3508 TA Utrecht, The Netherlands. <sup>2</sup>Department of Ecosystem Studies, Royal Netherlands Institute for Sea Research (NIOZ-Yerseke), P.O. Box 140, 4400 AC Yerseke, The Netherlands. <sup>3</sup>Dept. of Marine Sciences, Tjärnö, University of Gothenburg, 452 96 Strömstad, Sweden. <sup>4</sup>GEOMAR, Helmholtz Centre for Ocean Research, Düsternbrooker Weg 20, 24105 Kiel, Germany. Correspondence and requests for materials should be addressed to J.J.M. (email: j.b.m.middelburg@uu.nl)

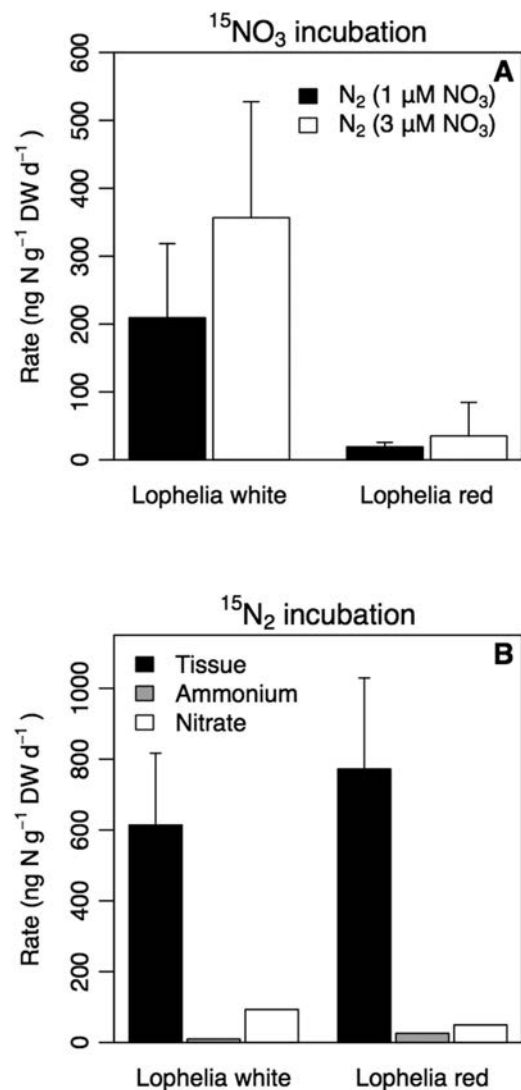


**Figure 1.** (A)  $^{15}\text{NO}_3^-$  addition experiment. Denitrification associated with white and red *L. pertusa* from the Trondheim Fjord. Tracer was added at two concentration levels (see M&M). (B)  $^{15}\text{N}_2$  addition experiment. Fixation of  $\text{N}_2$  based on tracer incorporation in coral tissue of red and white *L. pertusa* (Trondheim Fjord) and transfer to dissolved  $\text{NH}_4^+$  and  $\text{NO}_3^-$  pools. Results are shown as average  $\pm$  SD.

including hydrolysable amino acids (HAAs), total fatty acids (TFAs) and phospholipid-derived fatty acids (PLFAs). Compound specific isotope analysis of bacterial PLFAs allowed us to trace the flow of carbon from the dissolved inorganic carbon pool via chemoautotrophic bacteria to the CWC.

## Results

**Nitrogen cycling.** Both the white and red phenotypes of *L. pertusa* from Trondheim fjord (Norwegian Shelf) were studied for nitrogen transformation activities using  $^{15}\text{N}$  labeled substrates. Addition of  $^{15}\text{NO}_3^-$  resulted in the formation of  $^{15}\text{N}$ -labelled nitrogen gas within 24 hours (Fig. 1A). Denitrification rates in white *L. pertusa* were significantly higher than those in the red phenotype at low nitrate (Kruskal-Wallis,  $p < 0.05$ ).

Within 24 hours,  $^{15}\text{N}$  added in the form of  $\text{N}_2$  was traced into the organic coral tissue of both color morphs (Fig. 1B), indicating that the holobiont *L. pertusa* performs  $\text{N}_2$  fixation, an energy-demanding process, in the dark ocean. Moreover, nitrogen fixation was higher than denitrification for both phenotypes indicating that CWC are a source of fixed nitrogen to the deep ocean. Within 24 hours, net fixation was about 85–90% of gross nitrogen fixation. About 6–13% of the  $^{15}\text{N}_2$  fixed by nitrogen-fixing symbionts was excreted directly as ammonium by the symbionts or regenerated to ammonium and subsequently nitrified (Fig. 1B) indicating a tight coupling between ammonium release and consumption. Gross production and consumption of ammonium based on isotope dilution calculations<sup>19</sup> varied between 2.4 and 6.9  $\mu\text{g N g}^{-1} \text{ DW d}^{-1}$  and 0.7 and 1.2  $\mu\text{g N g}^{-1} \text{ DW d}^{-1}$ , respectively (Table 1) and were much higher than rates of nitrification, denitrification and nitrogen fixation. Nitrification contributed less than 1% to ammonium consumption indicating most ammonium was assimilated into organic compounds.

Treatment	Total Production $\mu\text{g N g}^{-1}\text{ DW d}^{-1}$	Net production $\mu\text{g N g}^{-1}\text{ DW d}^{-1}$	Consumption $\mu\text{g N g}^{-1}\text{ DW d}^{-1}$	Nitrification $\text{ng N g}^{-1}\text{ DW d}^{-1}$
<i>L. pertusa</i> white 1 $\mu\text{M}$	6.9 $\pm$ 1.1	5.7 $\pm$ 1.1	1.2 $\pm$ 0.1	14.6 $\pm$ 15.7
<i>L. pertusa</i> white 3 $\mu\text{M}$	5.0 $\pm$ 0.2	4.1 $\pm$ 0.1	0.9 $\pm$ 0.3	5.9 $\pm$ 1.4
<i>L. pertusa</i> red 1 $\mu\text{M}$	6.0 $\pm$ 2.0	5.2 $\pm$ 1.8	0.8 $\pm$ 0.5	3.0 $\pm$ 4.8
<i>L. pertusa</i> red 3 $\mu\text{M}$	2.4 $\pm$ 0.5	2.3 $\pm$ 0.3	0.7 $\pm$ 0.6	1.4 $\pm$ 2.4

**Table 1. Results from the  $^{15}\text{NH}_4^+$  addition experiment.** Total and net ammonium production, total consumption and nitrification by red and white *L. pertusa* from Trondheim fjord. All data are the average  $\pm$  SD and were obtained after an addition of 1 or 3  $\mu\text{M NH}_4^+$  and incubation during two days. Note that nitrification rates are expressed in ng rather than  $\mu\text{g N}$ .

CWC	Carbon Fixation $\text{ng C g}^{-1}\text{ DW d}^{-1}$	Ammonium incorporation $\text{ng N g}^{-1}\text{ DW d}^{-1}$
<i>L. pertusa</i> white, Tisler	931 $\pm$ 294	261 $\pm$ 155
<i>L. pertusa</i> white, Trondheim	1016 $\pm$ 363	139 $\pm$ 22
<i>L. pertusa</i> red, Trondheim	1394 $\pm$ 464	191 $\pm$ 59

**Table 2. Dissolved inorganic carbon and ammonium incorporation in tissue of red and white *L. pertusa*.** Results are shown as average  $\pm$  SD.

**Carbon fixation and ammonium assimilation.** White and red *L. pertusa* from Trondheim fjord were exposed to  $^{15}\text{N}$ -labelled ammonium and  $^{13}\text{C}$ -labelled dissolved inorganic carbon for 4 to 10 days. Both  $^{15}\text{N}$  and  $^{13}\text{C}$  were incorporated into coral tissue (Table 2), with no significant differences between color morphs for either ammonium or inorganic carbon fixation. Inorganic carbon fixation by CWC represents the first evidence for chemoautotrophy and we therefore executed a similar experiment with white *L. pertusa* from Tisler reef (Norwegian Skagerrak). Tisler reef *L. pertusa* also assimilated ammonium and inorganic carbon in its tissue and with similar rates (Kruskal-Wallis,  $p > 0.05$ ; Table 2). The added  $^{13}\text{C}$  was also incorporated into coral skeleton with rates of  $23 \pm 16 \mu\text{g C g}^{-1}\text{ DW d}^{-1}$  and  $33 \pm 17 \mu\text{g C g}^{-1}\text{ DW d}^{-1}$ , for white and red *L. pertusa* from Trondheim fjord respectively, while corals from the Tisler reef showed an incorporation rate of  $46 \pm 25 \mu\text{g C g}^{-1}\text{ DW d}^{-1}$ .

For the Tisler reef experiment the fate of assimilated inorganic substrates was also traced into specific tissue components (Fig. 2A), including total fatty acids ( $^{13}\text{C}$ ), polar-lipid derived fatty acids ( $^{13}\text{C}$ ) and amino acids ( $^{13}\text{C}$ ,  $^{15}\text{N}$ ). The  $^{15}\text{N}$  and  $^{13}\text{C}$  assimilated were incorporated into all amino acids (Fig. 2B), but D-alanine, a bacterial biomarker. Highest tracer recoveries were in glutamine, asparagine and methionine, but also significant amounts were incorporated in essential amino acids such as isoleucine and leucine.

Within the polar-lipid derived fatty acids about a quarter of  $^{13}\text{C}$  label was incorporated into C16:0, C16:1 $\omega$ 7 and C18:1 $\omega$ 7 (Fig. 2C) which are characteristically dominant in nitrifying and sulfur-oxidizing bacteria<sup>20</sup>. Interestingly, some long-chain PLFAs (C22:1 $\omega$ 9c, C22:4 $\omega$ 6, C22:5 $\omega$ 3 and C20:5 $\omega$ 3) were also readily labeled with  $^{13}\text{C}$  (Fig. 2C) and thus have been produced *de novo* by the coral since bacteria generally only produce short chain PLFA. This trophic transfer of  $^{13}\text{C}$  from the bacterial symbionts to the coral host evidently shows that chemoautotrophic bacteria supplement the coral's carbon and energy demand.

## Discussion

**Nitrogen cycling in CWC.** Living in the resource-depleted dark ocean CWC feed on a variety of organic resources including algae, bacteria, zooplankton, phytodetritus and dissolved organic matter<sup>13,14</sup>. This flexibility in heterotrophic feeding enables CWC to optimally acquire the scarce resources. However, high rates of ammonium excretion<sup>15–17</sup> implicate large nitrogen losses. It is evident that long-term survival also implies conserving limiting resources via efficient recycling. All targeted nitrogen processes were actively mediated by the cold-water coral holobiont *L. pertusa* (Fig. 3). The co-occurrence of ammonium production and assimilation, nitrification, denitrification, and nitrogen fixation indicates a complete nitrogen cycle in cold-water reefs similar to that inferred for tropical reefs<sup>2,21</sup>.

The  $^{15}\text{N}_2$  labeling results presented here (Fig. 1B) are consistent with recent studies<sup>22,23</sup> reporting gene sequences of cyanobacteria and the bacterial genus *Vibrio* in *L. pertusa* samples, each of them able to perform the required metabolic pathways for nitrogen fixation<sup>3,4,24</sup>. These, or related microbes, may be involved in  $\text{N}_2$  fixation by the cold-water coral holobiont. Since photoautotrophy can be excluded in the dark ocean, the microbial symbionts fixing nitrogen in *L. pertusa* are most likely supported by organic compounds released by their coral host to fuel  $\text{N}_2$  fixation<sup>2,6</sup>. Respiration by the corals and pelagic microbes may temporarily lower oxygen concentration in the reef water<sup>25</sup> and thereby favor the activity of the oxygen sensitive  $\text{N}_2$ -fixation enzyme nitrogenase<sup>1,6,24</sup>.

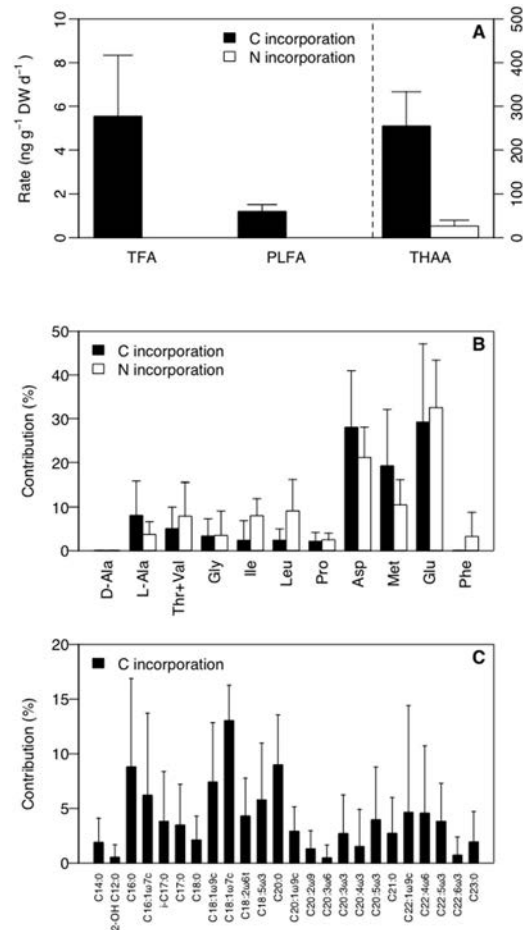


**Figure 2.** Assimilation of ammonium and fixation of dissolved inorganic carbon into coral tissue and tissue components (total fatty acids (TFA), Polar-lipid derived fatty acids (PLFA) and total hydrolysable amino acids (THAA) of white *L. pertusa* from the Tisler reef. (A) Incorporation of dissolved inorganic carbon into TFA, PLFA and THAA pools and assimilation of ammonium into THAA, left axis for TFA and PLFA and right axis for THAA (B) incorporation of dissolved inorganic carbon and ammonium into individual amino acids and (C) incorporation of dissolved inorganic carbon into individual PLFA. Results are shown as average  $\pm$  SD.

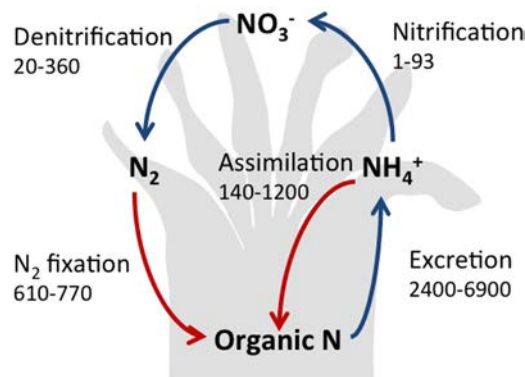


**Figure 3.** A simplified overview of nitrogen cycling ( $\text{ng N g}^{-1} \text{DW d}^{-1}$ ) in cold-water corals. Red arrows indicate processes contributing to nitrogen acquisition/retention. Rates are based on those presented in Fig. 1 and Tables 1 and 2.

Low oxygen concentrations may also stimulate denitrification, the microbial reduction of nitrate to dinitrogen as observed in our experiments (Fig. 1A). It is unclear when or where denitrification occurs in *L. pertusa*, but the required anaerobic conditions suggests that denitrification can occur during polyp retraction, in micro-niches in the coral mucus layer or in the gut cavity<sup>26</sup>. Denitrification rates were higher in white than red *L. pertusa* (Fig. 1A). This difference is consistent with the dominance of mixotrophic Rodobacteraceae in white *L. pertusa*<sup>22</sup>, a family that includes denitrifiers<sup>27</sup>.

Our experiments provided multiple indications for an actively nitrifying community. First, <sup>15</sup>N added in the form of ammonium was readily transferred to nitrate (Table 1). Second, 6–13% of the <sup>15</sup>N<sub>2</sub> fixed by nitrogen-fixing symbionts was regenerated and subsequently nitrified (Fig. 1B). Nitrification activity in CWC is consistent with the recent documentation of marine group 1 Thaumarchaeota in *L. pertusa* at Rockall Bank<sup>28</sup>, a group of organisms involved in nitrification<sup>29</sup>. Moreover, PLFA biomarkers for nitrifying and sulphur-oxidizing bacteria (C16:0, C16:1 $\omega$ 7 and C18:1 $\omega$ 7) incorporated most of the inorganic <sup>13</sup>C among the PLFA (Fig. 2C).

This versatility in CWC nitrogen recycling reduces loss of nitrogen, allows for adjustment to changing availability in quantity and quality of resources and may thus be key to survival in the resource-depleted dark ocean. Moreover, nitrogen fixation by microbial symbionts provides corals with new organic nitrogen, complementing organic nitrogen obtained from their diet (Fig. 3). Ammonium production (2400–6900 ng N per gram dw per day) approximates total nitrogen acquisition via heterotroph feeding and nitrogen fixation (610–770 ng N per gram dw per day), indicating that nitrogen fixation contributes between 9 and 32% to CWC nitrogen requirement. This additional N source may explain the release of mucus with a lower than Redfield C:N ratio<sup>25</sup>.

Although this efficient nitrogen recycling and nitrogen fixation may be beneficial for CWC functioning, simple calculations indicate that is of limited importance for the nitrogen cycle of the deep ocean. On the basis of an average nitrogen fixation rate of 667 ng N per gram dw per day (Fig. 1B) or 204 ng N per polyp per day, and ~12,000 polyps per m<sup>2</sup> (11), one obtains ~0.9 g N m<sup>-2</sup> y<sup>-1</sup>. This is likely an upper estimate because of the high density of polyps in the studied system, but it is similar to nitrogen fixation rates found in coastal sediments<sup>30,31</sup>. Assuming a CWC reef extension similar to that of tropical coral reefs<sup>8</sup>, this relates to a global nitrogen fixation rate of ~0.5 Tg N y<sup>-1</sup>, which is an insignificant contribution to global open ocean nitrogen fixation (~140 to ~177 Tg N y<sup>-1</sup>), and only a small contribution to total shelf nitrogen fixation (~17 Tg N y<sup>-1</sup><sup>32</sup>).

**Chemoautotrophy in CWC.** *L. pertusa* showed significant rates of inorganic carbon fixation in organic tissue (Table 2) and tissue components (HAA, TFA and PLFA; Fig. 2A), indicating a role of chemolithoautotrophs in moderating carbon flow to the coral. The energy for chemoautotrophy comes from the oxidation of substances such as ammonium or reduced sulfur. The observed stoichiometry of 10–100  $\mu$ mol HCO<sub>3</sub><sup>-</sup> fixed for about 1  $\mu$ mol NO<sub>3</sub><sup>-</sup> produced differs considerably from the typical nitrifier stoichiometry of 0.1  $\mu$ mol HCO<sub>3</sub><sup>-</sup> fixed for 1  $\mu$ mol NO<sub>3</sub><sup>-</sup> produced. This stoichiometric mismatch indicates that other chemoautotrophs, such as sulfur oxidizing bacteria of which sequences have been observed in *L. pertusa*<sup>22</sup>, also may have contributed to inorganic carbon fixation. PLFA results indicate that most of the <sup>13</sup>C label was recovered in C16:0, C16:1 $\omega$ 7 and C18:1 $\omega$ 7. These PLFA are abundant not only in nitrifying, but also sulfur-oxidizing bacteria<sup>20</sup>.

While inorganic carbon was initially fixed by chemoautotrophic symbionts, the carbon was subsequently transferred to the coral as evidenced by the appearance of label in PLFA with a chain length > 20, in particular C22:1 $\omega$ 9c, C22:4 $\omega$ 6, C22:5 $\omega$ 3 and C20:5 $\omega$ 3, which must have been produced by the animal. However, whether coral preys on chemoautotrophic bacteria contained within the mucus layer<sup>33</sup> or whether the bacteria release organic compounds, which the coral then takes up remains to be resolved.

Microbial assimilation of inorganic carbon and ammonium and subsequent transfer to the coral is also evident from the labeling pattern of coral amino acids (Fig. 2B). The <sup>13</sup>C and <sup>15</sup>N assimilated was primarily recovered in glutamine and asparagine, consistent with known pathways of ammonium assimilation and amino acid synthesis<sup>34</sup>. Striking are the high enrichment of methionine and formation of isoleucine, leucine, phenylalanine and valine+threonine (lumped because not well resolved in the chromatogram), because these are considered to be essential amino acids, which many animals are considered either incapable of synthesizing or only synthesizing it in insufficient amounts to meet their metabolic needs<sup>34</sup>. These results are in agreement with *de novo* synthesis observed for tropical corals<sup>34</sup>, indicating that tropical and cold-water coral holobionts are able to synthesize putative “essential” amino acids. The *de novo* synthesis of amino acids by CWC poses a challenge to the use of compositional and isotope data in diet studies that are based on putative heterotrophic feeding. These newly formed essential amino acids may be transferred up the reef-associated food web, because of corallivory by echinoids as recently reported on Atlantic reefs<sup>35</sup>.

The intensive recycling of nitrogen, the assimilation of ammonium and inorganic carbon into coral tissue and the *de novo* synthesis of putative essential amino acids and fatty acids (including C20:5 $\omega$ 3 and C22:6 $\omega$ 3) suggest that natural abundance isotope and biomarker approaches should be used with care when based on the concept of putative heterotrophic feeding. Intensive recycling of nitrogen, *in situ* nitrogen fixation and assimilation of ammonium may cause changes in bulk coral tissue  $\delta^{15}$ N values complicating diet and trophic level inferences from natural abundance isotope ratios. Similarly, compound-specific isotope analysis of amino acids is increasingly used to infer diet and trophic transfers, including deep-sea corals<sup>36–38</sup>. The underlying rationale is a division between non-essential and essential amino acids. Our data clearly show that, at least for *L. pertusa*, all amino acids can be generated *de novo*, including the putative essential isoleucine, leucine and threonine+valine. However, comparing inorganic carbon fixation from this study with coral respiration<sup>39,40</sup> it appears that chemoautotrophy provides less than 2% of the energy supply to *L. pertusa*.

Overall, chemoautotrophy, nitrogen fixation and efficient recycling of nitrogen by microbial symbionts may be prerequisites for the longevity of CWC in the dark, resources-limited ocean. However, our findings require follow-up studies to elucidate the importance of chemoautotrophy, nitrogen fixation and efficient nitrogen recycling for CWC

Treatment	Measurement	Process	Incubation Period (d)	Trondheim fjord (P420)	Tisler reef (SLCT)
Nitrogen cycling					
$^{15}\text{N}_2$	$^{15}\text{N}$ Tissue $^{15}\text{NH}_4^+$ & $^{15}\text{NO}_3^-$	$\text{N}_2$ -fixation Ammonium regeneration Nitrification	1	<i>L. pertusa</i> white, red	
$^{15}\text{NO}_3^-$	$^{15}\text{N}_2$	Denitrification	1	<i>L. pertusa</i> white, red	
$^{15}\text{NH}_4^+$	$^{15}\text{NH}_4^+$ & $\text{NH}_4^+$ & $^{15}\text{NO}_3^-$	Ammonium regeneration & consumption Nitrification	2	<i>L. pertusa</i> white, red	
Assimilation					
$^{15}\text{NH}_4^+$	$^{15}\text{N}$ Tissue*	Ammonium assimilation	4–10	<i>L. pertusa</i> white, red	<i>L. pertusa</i> white*
$^{13}\text{C}$ -DIC	$^{13}\text{C}$ Tissue*	DIC-fixation	4–10	<i>L. pertusa</i> white, red	<i>L. pertusa</i> white*

**Table 3. Experimental design and procedures.** All experiments were carried out either during the Poseidon cruise P420 or at the Sven Lovén Centre in Tjärnö (SLC-T). \*detailed tissue analysis including  $^{15}\text{N}/^{13}\text{C}$  HAAs,  $^{13}\text{C}$  TFAs and  $^{13}\text{C}$  PLFAs were only conducted on corals harvested at the Tisler reef.

food web functioning, for carbon and nitrogen budgets and the use of deep-sea corals for paleoenvironmental reconstructions.

## Material and Methods

The experiments were either carried out on board of the RV Poseidon during the cruise P420 to Trondheim fjord (Norway) or in the laboratory at the Sven Lovén Centre for Marine Sciences in Tjärnö, Sweden (Table 3).

**Sampling locations and maintenance.** The corals used in this study were harvested from two different locations. Red and white *L. pertusa* were collected at 30–40 m deep in the Trondheim fjord using the manned submersible JAGO during the Poseidon cruise P420 in September 2011. Coral fragments were cut on-board in small pieces (~2–4 g DW (dry weight) piece<sup>-1</sup> and ~7–11 polyps piece<sup>-1</sup>) to fit the incubation bottles and were acclimated 2 to 3 days in a 500 L tank filled with seawater at a temperature of 7–8 °C. No food was supplied during the acclimation period. Red and white corals from Trondheim fjord were used to measure transfer from the inorganic carbon pool to coral organic tissue and for a detailed nitrogen cycling study involving quantification of  $\text{N}_2$ -fixation, nitrification, denitrification and ammonium assimilation/release. Shipboard incubations with CWC from Trondheim fjord for nitrogen transformation activities were done at 7 °C and in the dark, and replicated three times for each treatment and color morph. Besides the shaking provided by the movement of the ship, every 6 to 8 hours each incubation bottle was gently shaken by hand to mix the incubation water.

At the Tisler reef <sup>13</sup>, white *L. pertusa* branches were collected specifically for a detailed investigation of the assimilation of ammonium and the fixation of dissolved inorganic carbon and incorporation into coral tissue components (fatty acids, amino acids). The Tisler reef is located at a water depth of 75–155 m at the border between Norway and Sweden and samples were taken at 110 m using the remotely operated vehicle Sperre Subfighter 7500 DC. After transporting the corals in cooling boxes filled with cold seawater (7–8 °C) to the Sven Lovén Centre, samples were clipped to a similar size as those from Trondheim fjord (3.9 ± 4.3 g DW piece<sup>-1</sup> and 9.3 ± 1.1 polyps piece<sup>-1</sup>). The Tisler corals were maintained in aquaria (10 L) placed in a dark thermo-constant room (7 °C) for 3 months. The aquaria were continuously flushed with sand-filtered (1–2 mm particle size) water from 45 m depth out of the adjacent Koster fjord (salinity 31–34) (~1 l min<sup>-1</sup>). Corals were fed with larvae (nauplii) of the brine shrimp *Artemia* spp. every 3 to 4 days following common procedures at Sven Lovén Centre at Tjärnö<sup>14,40</sup>.

**Experimental procedures.** Nitrogen transformation processes are often tightly coupled with the product of one process functioning as the substrate for the other process (e.g. ammonium regenerated is partly re-assimilated or nitrified during the incubation period). This complicates the experimental design and the interpretation of data. However, it also means that microbial activities can be identified in more than one treatment and that it provides some information on the importance of such couplings.

**$^{15}\text{N}_2$  addition experiment.**  $^{15}\text{N}_2$  enriched seawater was produced prior to the experiment by injecting  $^{15}\text{N}_2$  gas in degassed artificial seawater following the protocol of Mohr *et al.*<sup>41</sup> to guarantee homogenous labeling of dissolved nitrogen. Red (2.6 ± 0.6 g DW piece<sup>-1</sup>, 8.7 ± 3.1 polyps piece<sup>-1</sup>) and white (2.3 ± 0.1 g DW piece<sup>-1</sup>, 7.3 ± 0.6 polyps piece<sup>-1</sup>) *L. pertusa* pieces were placed separately in gas-tight glass bottles (70 ml) filled without headspace with GF/F filtered seawater. After closing the bottles, 7 ml of the  $^{15}\text{N}_2$  enriched seawater was injected through the rubber septum of the lid (replacing an equal volume of unlabeled water), resulting in an enrichment of 10 atom%  $^{15}\text{N}$  in the incubation vial. Control corals were incubated without  $^{15}\text{N}_2$  enriched seawater while controls for nutrient and background isotopic values were incubated without corals and with and without label addition. Incubations lasted 24-h so that the coral-associated microbes had enough time to process the  $\text{N}_2$ , while at the same time anoxic conditions of the incubation could be avoided. From the experimental setup, oxygen consumption rates (3.6 μmol O<sub>2</sub> g<sup>-1</sup> DW d<sup>-1</sup> at 7 °C)<sup>39</sup> and oxygen solubility (280 μM at 7 °C) we anticipated a 50% depletion during the incubation. At the end of the incubations coral pieces were removed from the bottles and stored frozen

for later analysis of  $^{15}\text{N}$  in the host and symbiont tissue (net  $\text{N}_2$ -assimilation). The water was filtered, pooled per treatment (to obtain enough material for analysis) and stored frozen for analysis of nutrient concentrations and  $^{15}\text{N}$  enrichment of ammonium and nitrate. The appearance of  $^{15}\text{N}$  tracer in ammonium and nitrate pools reflects direct excretion of ammonium or regeneration of fixed nitrogen and subsequent nitrification (Fig. 1B). Nitrification following nitrogen fixation reflects heterogeneous oxygen conditions.

**$^{15}\text{NO}_3^-$  addition experiment.** Red ( $1.7 \pm 0.6$  g DW piece $^{-1}$ ,  $3.5 \pm 1.3$  polyps piece $^{-1}$ ) and white *L. pertusa* pieces ( $1.7 \pm 0.7$  g DW piece $^{-1}$ ,  $3.5 \pm 1.3$  polyps piece $^{-1}$ ) were placed in gas tight glass bottles (70 ml) filled with GF/F filtered seawater enriched with two concentrations of  $^{15}\text{NO}_3^-$  ( $1 \mu\text{M}$ ,  $3 \mu\text{M}$ ), because ambient concentrations and nitrogen transformation rates were not known beforehand. The control treatment (no coral) contained only filtered seawater or filtered seawater enriched with  $^{15}\text{NO}_3^-$  at two concentrations and was incubated in parallel. A 24-h incubation period was chosen to give the coral enough time to process the  $^{15}\text{NO}_3^-$  while avoiding anoxic conditions (see  $\text{N}_2$ -fixation). Incubations were terminated by injection of  $\text{HgCl}_2$  and bottles were stored upside down for analysis of  $^{15}\text{N}_2$ .

**$^{15}\text{NH}_4^+$  addition experiment.** Red *L. pertusa* ( $3.7 \pm 0.6$  g DW piece $^{-1}$ ,  $11.3 \pm 1.5$  polyps piece $^{-1}$ ) and white *L. pertusa* ( $4.4 \pm 1.1$  g DW piece $^{-1}$ ,  $10.4 \pm 2.5$  polyps piece $^{-1}$ ) were incubated in 250 ml glass bottles filled with 200 ml GF/F filtered sea water enriched with  $^{15}\text{NH}_4^+$  at two different concentrations ( $1 \mu\text{M}$  and  $3 \mu\text{M}$  above the  $0.5 \mu\text{M}$  background). The control treatment (without coral) contained either filtered seawater or filtered seawater enriched with  $^{15}\text{NH}_4^+$  at the two different treatment levels. After incubation for 48-h corals were removed (the larger incubation bottles prevented low oxygen conditions), the water was filtered (GF/F) and frozen for further analysis of nutrients and  $^{15}\text{N}$ -enrichment of  $\text{NO}_3^-$  and  $\text{NH}_4^+$ . The appearance of  $^{15}\text{N}$  in the nitrate pool is due to nitrification. The change in ammonium concentration and isotopic enrichment of  $\text{NH}_4^+$  were used to quantify ammonium production and consumption using an isotope dilution technique<sup>19</sup>, originally developed for soils and coastal sediments. As with any isotope labeling technique applied to spatial heterogeneous systems, inferred rates may be biased by non-uniform label distributions.

**$^{13}\text{C}$ -DIC and  $^{15}\text{NH}_4^+$  additions.** Ammonium assimilation and fixation of dissolved inorganic carbon were measured in CWC from Trondheim fjord during the cruise and from Tisler reef in the laboratory at Tjärnö (Table 3). During the cruise red and white *L. pertusa* samples from Trondheim fjord were placed separately in incubation chambers (4 L) filled with GF/F filtered sea water and maintained at  $8^\circ\text{C}$  in a water bath. A stirrer in the middle of the chamber maintained water circulation. After a 12-hr period to acclimate from the transfer from the 500L maintenance to 4L experimental chamber,  $^{13}\text{C}$ -DIC and  $^{15}\text{NH}_4^+$  were added to the water to attain an enrichment of 30 atom% for both  $^{15}\text{N}$  and  $^{13}\text{C}$ . The treatment was replicated three times. Control corals were incubated in parallel without label addition for isotopic background measurements. Every 2.5 days, water was completely exchanged but for about 10% to maintain corals submerged, and new label was added. Incubations lasted for 4 to 10 days to determine the time scale of C and N incorporation into tissue. At the end of the incubation, corals were stored at  $-20^\circ\text{C}$ , freeze-dried and kept frozen for further analysis.

In the laboratory, white *L. pertusa* samples from Tisler reef were placed in incubation chambers (10 L) in a thermo-stated room at  $7^\circ\text{C}$ . A motor-driven paddle on top of the chamber (2 rpm) maintained water circulation. Prior to the experiment, chambers were filled with  $0.2 \mu\text{m}$  filtered seawater from 45 m depth out of the Koster fjord (salinity of 33,  $7^\circ\text{C}$ ). Three coral fragments were randomly selected and placed in a single chamber. After a 12-hr incubation to acclimate from the transfer from the maintenance to experimental chamber,  $^{13}\text{C}$ -DIC and  $^{15}\text{NH}_4^+$  were added to the water to attain an 10 atom% enrichment for both substrates. The experiment was duplicated. Control corals were incubated in parallel without label addition for isotopic background measurements. After an incubation time of 4 days, coral samples were frozen at  $-20^\circ\text{C}$ , freeze-dried and stored frozen for further analysis.

**Chemical analyses.** Concentration and isotopic composition of dissolved  $\text{N}_2$  ( $^{28}\text{N}_2$ ,  $^{29}\text{N}_2$ ,  $^{30}\text{N}_2$ ) were determined in the headspace of the incubation bottle, after injection of He which replaced 5 ml of sample water and vigorous shaking, using a Thermo Electron Flash EA 1112 analyzer (EA) coupled to a Delta V isotope ratio mass spectrometer (EA-IRMS) as described in<sup>42</sup>.

$\text{NH}_4^+$ ,  $\text{NO}_2^-$  and  $\text{NO}_3^-$  concentration in water samples were determined using automated colorimetric techniques (precision  $\text{NH}_4^+ \pm 2\%$  SD,  $\text{NO}_2^-/\text{NO}_3^- \pm 3\%$  SD). The isotopic composition of  $\text{NH}_4^+$  and  $\text{NO}_3^-$  in the sample was determined in two steps<sup>42</sup>. In the first step,  $\text{MgO}$  was added to the water sample to convert the  $\text{NH}_4^+$  to  $\text{NH}_3$ , which was subsequently trapped on an acidified ( $\text{H}_2\text{SO}_4$ ) GF/D filter packed between two Teflon filters floating on the sample surface. In the second step, the remaining  $\text{NO}_3^-$  was converted to  $\text{NH}_4^+$  by the addition of Devarda's Alloy, which was then again trapped on an acidified GF/D filter package as in step one. Finally, both filters were measured for their isotopic composition by EA-IRMS.

For isotope analysis of coral tissues, frozen corals were freeze-dried, weighed and homogenized by grinding with a ball mill for 20 seconds (MM 2000, Retsch, Haan, Germany). A subsample ( $\sim 30$  mg) of ground coral material was decalcified by stepwise acidification with 12M HCl until complete carbonate removal. The remaining organic fraction (tissue + organic skeleton matrix) was measured for C and N concentration and isotopic composition by EA-IRMS. The  $^{13}\text{C}$  incorporation into the skeleton was determined following<sup>43</sup>.

Coral samples from Tisler Reef were also analyzed for tracer incorporation into total fatty acids (TFA), phospholipid-derived fatty acids (PLFA) and hydrolysable amino acids (HAAs). TFAs were extracted from 0.7 g of grounded coral with a modified Bligh and Dyer method. The PLFA fraction of the total fatty acid extract was separated by silica column (Merck Kieselgel 60)<sup>44</sup>. The TFA and PLFA extracts were derivatized by mild alkaline transmethylation to obtain fatty acid methyl esters (FAME). Preparation of methyl esters was carried out

following<sup>44,45</sup>. Concentration and carbon isotopic composition of individual TFAs and PLFAs were measured on a gas-chromatograph combustion-interface isotope-ratio mass spectrometer (GC-c-IRMS)<sup>45</sup>.

Hydrolyzable amino acids were extracted and analyzed using a modified protocol<sup>46</sup>. Ground coral samples were first decalcified by repeated addition of 12M HCl drops. The remaining material was then hydrolyzed in 6M HCl at 110 °C for 20h and purified by cation exchange chromatography (Dowex 50WX8 resin). HAAs were derivatized with isopropanol and pentafluoropropionic anhydride and analyzed by GC-c-IRMS for individual AAs concentrations and <sup>13</sup>C and <sup>15</sup>N enrichment.

**Calculations.** The processing rates/ uptake rates of <sup>15</sup>N or <sup>13</sup>C are presented as total N or C processed per gram of DW ground coral. The excess <sup>15</sup>N or <sup>13</sup>C is calculated from the difference in heavy isotope fraction (F) between sample and background multiplied by the quantity of nitrogen or carbon<sup>45,47</sup>:  $\text{excess} = (F_{\text{sample}} - F_{\text{background}}) \times (\text{ng of N or C in sample})$ , where  $F = R/(R + 1)$  and the isotope ratio R is calculated directly from the measured  $\delta^{15}\text{N}$  or  $\delta^{13}\text{C}$ . In order to convert the <sup>15</sup>N and <sup>13</sup>C processing rates to total rates, they were multiplied by the <sup>15</sup>N [i.e.,  $^{15}\text{N}/(^{15}\text{N} + ^{14}\text{N})$ ] or <sup>13</sup>C [i.e.,  $^{13}\text{C}/(^{13}\text{C} + ^{12}\text{C})$ ] fraction of the respective substrate at the start of the incubation, but for the ammonium regeneration data. These were estimated from the concentration and isotopic enrichment of  $\text{NH}_4^+$  using the isotopic dilution model<sup>19</sup>, which allows estimation of gross and net  $\text{NH}_4^+$  production and consumption rates. For the nitrification rate measurements, the <sup>15</sup>N enrichment of the total  $\text{NH}_4^+$  pool was influenced by strong  $\text{NH}_4^+$  production during the incubations. To compensate for the resulting isotopic dilution, we used the average <sup>15</sup>N enrichment of the  $\text{NH}_4^+$  pool during the incubation period that was calculated from the start value (calculated from natural <sup>14</sup>NH<sub>4</sub><sup>+</sup> concentrations and added <sup>15</sup>NH<sub>4</sub><sup>+</sup> addition) and the end value (directly measured in the extracted  $\text{NH}_4^+$ ). Nitrification and denitrification rates determined for coral incubations were corrected for incubation water activity by subtracting the rates obtained from the control incubations. All results are reported as average  $\pm$  SD. Differences were tested with ANOVA or Kruskal-Wallis if criteria for ANOVA were not met.

## References

- Fiore, C. L., Jarett, J. K., Olson, N. D. & Lesser, M. P. Nitrogen fixation and nitrogen transformations in marine symbioses. *Trends Microb.* **18**, 455–463 (2010).
- Radecker, N., Pogoreutz, C., Voolstra, C. R., Wiedenmann, J. & Wild, C. Nitrogen cycling in corals: the key to understanding holobiont functioning? *Trends Microb.* **23**, 490–497 (2015).
- Lesser, M. P., Mazel, C. H., Gorbunov, M. Y. & Falkowski, P. G. Discovery of symbiotic nitrogen-fixing cyanobacteria in corals. *Science* **305**, 997–1000 (2004).
- Lesser, M. P. *et al.* Nitrogen fixation by symbiotic cyanobacteria provides a source of nitrogen for the scleractinian coral *Montastraea cavernosa*. *Mar. Ecol. Progr. Ser.* **346**, 143–152 (2007).
- Wafar, M., Wafar, S. & David, J. J. Nitrification in reef corals. *Limnol. Oceanogr.* **35**, 725–730 (1990).
- O'Neil, J. M. & Capone, D. G. in *Nitrogen in the Marine Environment*, (eds Capone, D. G. *et al.*) 949–989, Elsevier (2008).
- Cardini, U., Bednarz, V. N., Foster, R. A. & Wild, C. Benthic N<sub>2</sub> fixation in coral reefs and the potential effect of human-induced environmental change. *Ecol. Evol.*, **4**, 1706–1727 (2014).
- Roberts, J. M., Wheeler, A. J. & Freiwald, A. Reefs of the deep, The biology and geology of cold-water coral ecosystems. *Science* **312**, 543–547 (2006).
- Davies, A. J. & Guinotte, J. M. Global Habitat Suitability for Framework-Forming Cold-Water Corals. *PLOS One* **6**, e18483; doi: 10.1371/journal.pone.0018483 (2011).
- Roberts, J. M. & Cairns, S. D. Cold-water corals in a changing ocean. *Cur. Op. Env. Sust.* **7**, 118–126 (2014).
- van Oevelen, D. *et al.* The cold-water coral community as a hot spot for carbon cycling on continental margins: A food-web analysis from Rockall Bank (northeast Atlantic). *Limnol. Oceanogr.* **54**, 1829–1844 (2009).
- Cathalot, C. *et al.* Cold-water coral reefs and adjacent sponge grounds: Hotspots of benthic respiration and organic carbon cycling in the deep sea. *Front. Mar. Sci.* **2**, 37. doi: 10.3389/fmars.2015.00037 (2015).
- Lavaleye, M. *et al.* Cold-water corals on the Tisler reef: Preliminary observations on the dynamic reef environment. *Oceanogr.* **22**, 76–84 (2009).
- Mueller, C. E., Larsson, A. I., Veuger, B., Middelburg, J. J. & van Oevelen, D. Opportunistic feeding on various organic food sources by the cold-water coral *Lophelia pertusa*. *Biogeosciences* **11**, 123–133 (2014).
- Khripounoff, A. *et al.* Deep cold-water coral ecosystems in the Brittany submarine canyons (Northeast Atlantic): Hydrodynamics, particle supply, respiration, and carbon cycling. *Limnol. Oceanogr.* **59**, 87–98 (2014).
- Maier, C. *et al.* Dynamics of nutrients, total organic carbon, prokaryotes and viruses in onboard incubations of cold-water corals. *Biogeosciences* **8**, 2609–2620 (2011).
- Maier, C., Hegeman, J., Weinbauer, M. G. & Gattuso, J. P. Calcification of the cold-water coral *Lophelia pertusa* under ambient and reduced pH. *Biogeosciences* **6**, 1671–1680 (2009).
- Findlay, H. S. *et al.* Fine-scale nutrient and carbonate system dynamics around cold-water coral reefs in the northeast Atlantic. *Sci. Rep.* **4**, 3671 doi: 10.1038/srep03671 (2014).
- Blackburn, T. H. & Henriksen, K. Nitrogen cycling in different types of sediments from Danish waters. *Limnol. Oceanogr.* **28**, 477–493 (1983).
- Van Gaever, S. L. *et al.* Trophic specialisation of metazoan meiofauna at the Hayenkon Mosby Mud Volcano: fatty acid biomarker isotope evidence. *Mar. Biol.* **156**, 1289–1296 (2009).
- Wegley, L., Edwards, R., Rodriguez-Brito, B., Liu H. & Rohwer, F. Metagenomic analysis of the microbial community associated with the coral *Porites astreoides*. *Environ. Microb.* **9**, 2707–2719 (2007).
- Neulinger, S. C., Jarnegren, J., Ludvigsen, M., Lochte, K. & Dullo, W.-C. Phenotype-Specific Bacterial Communities in the Cold-Water Coral *Lophelia pertusa* (Scleractinia) and Their Implications for the Coral's Nutrition, Health, and Distribution. *Appl. Environ. Microb.* **74**, 7272–7285 (2008).
- Kellogg, C. A., Lisle, J. T. & Galkiewicz, J. P. Culture-Independent Characterization of Bacterial Communities Associated with the Cold-Water Coral *Lophelia pertusa* in the Northeastern Gulf of Mexico. *Appl. Environ. Microb.* **75**, 2294–2303 (2009).
- Urdaci, M. C., Stal, L. J. & Marchand, M. Occurrence of nitrogen fixation among *Vibrio* spp. *Arch. Microb.* **150**, 224–229 (1988).
- Wild, C. *et al.* Organic matter release by cold water corals and its implication for fauna-microbe interaction. *Mar. Ecol. Progr. Ser.* **372**, 67–75 (2008).
- Buhl-Mortensen, P. Aquarium observations on the deep-water coral *Lophelia pertusa* (L., 1758) (scleractinia) and selected associated invertebrates. *Ophelia* **54**, 83–104 (2001).
- Swingle, W. D. *et al.* The complete genome sequence of *Roseobacter denitrificans* reveals a mixotrophic rather than photosynthetic metabolism. *J. Bacter.* **189**, 683–690 (2007).

28. Van Bleijswijk, J. *et al.* Microbial assemblage on a cold-water coral mound at the SE Rockall Bank (NE Atlantic): interactions with hydrography and topography. *Biogeosciences* **12**, 4483–4496 (2015).
29. Wuchter, C. *et al.* Archaeal nitrification in the ocean. *Proc. Natl. Acad. Sci.* **103**, 12317–12322 (2006).
30. Capone, D. G. Benthic nitrogen fixation, in: *Nitrogen Cycling in Coastal Marine Environment*, (eds. Carpenter, E. J. & Capone D. G.), 85–123, John Wiley & Sons Ltd., New York (1983).
31. Bertics, V. J. *et al.* Occurrence of benthic microbial nitrogen fixation coupled to sulfate reduction in the seasonally hypoxic Eckernfjorde Bay, Baltic Sea. *Biogeosciences*, **10**, 1243–1258 (2013).
32. Voss, M. *et al.* The marine nitrogen cycle: recent discoveries, uncertainties and the potential relevance of climate change. *Philos. Trans. R. Soc. Lond. Series B*, **368**, 20130121 (2013).
33. Weinbauer, M. G., Ogier, J. & Maier, C. Microbial abundance in the coelenteron and mucus of the cold-water coral *Lophelia pertusa* and in bottom water of the reef environment. *Aq. Biol.* **16**, 209–216 (2012).
34. Fitzgerald, L. M. & Szmant, A. M. Biosynthesis of 'essential' amino acids by scleractinian corals. *Biochem. J.* **322**, 213–221 (1997).
35. Stevenson, A. & Rocha, C. Evidence for the bioerosion of deep-water corals by echinoids in the Northeast Atlantic. *Deep-Sea Res. Part I* **71**, 73–78 (2013).
36. Sherwood, O. A. *et al.* Increasing subtropical North Pacific Ocean nitrogen fixation since the Little Ice Age. *Nature* **505**, 78–81 (2014).
37. Sherwood, O. A. *et al.* Nutrient regime shift in the western North Atlantic indicated by compound-specific  $\delta^{15}\text{N}$  of deep-sea gorgonian corals. *Proc. Natl. Acad. Sci.* **108**, 1011–1015 (2011).
38. Schiff J. T. *et al.* Compound specific amino acids  $\delta^{13}\text{C}$  patterns in a deep-sea proteinaceous coral: Implications for reconstructing detailed  $\delta^{13}\text{C}$  records of exported primary production. *Mar. Chem.* **166**, 82–91 (2014).
39. Dodds, L. A., Roberts, J. M., Taylor, A. C. & Marubini, F. Metabolic tolerance of the cold-water coral *Lophelia pertusa* (Scleractinia) to temperature and dissolved oxygen change. *J. Exp. Mar. Biol. Ecol.* **349**, 205–214 (2007).
40. Larsson, A. I., Lundälv, T. & van Oevelen, D. Skeletal growth, respiration rate and fatty acid composition in the cold water coral *Lophelia pertusa* under varying food conditions. *Mar. Ecol. Progr. Ser.* **483**, 169–184 (2013).
41. Mohr, W., Grosskopf, T., Wallace, D. W. R. & LaRoche, J. Methodological Underestimation of Oceanic Nitrogen Fixation Rates. *PLOS One* **5**(9), e12583 doi: 10.1371/journal.pone.0012583 (2010).
42. Gribsholt, B. *et al.* Nitrogen processing in a tidal freshwater marsh: A whole-ecosystem (15)N labeling study. *Limnol. Oceanogr.* **50**, 945–1959 (2005).
43. Mueller C. *et al.* The symbiosis between *Lophelia pertusa* and *Eunice norvegica* stimulates coral calcification and worm assimilation. *PLoS ONE* **8**(3): e58660 doi: 10.1371/journal.pone.0058660 (2013).
44. Boschker, H. T. S., de Brouwer, J. F. C. & Cappenberg, T. E. The contribution of macrophyte-derived organic matter to microbial biomass in salt-marsh sediments: Stable carbon isotope analysis of microbial biomarkers. *Limnol. Oceanogr.* **44**, 309–319 (1999).
45. Middelburg, J. J. *et al.* The fate of intertidal microphytobenthos carbon: An *in situ* C-13-labeling study. *Limnol. Oceanogr.* **45**, 1224–1234 (2000).
46. Veuger, B., Middelburg, J. J., Boschker, H. T. S. & Houtekamer, M. Analysis of N-15 incorporation into D-alanine: A new method for tracing nitrogen uptake by bacteria. *Limnol. Oceanogr.-Methods* **3**, 230–240 (2005).
47. Middelburg, J. J. Stable isotopes dissect aquatic food webs from the top to the bottom. *Biogeosciences* **11**, 2357–2371 (2014).

## Acknowledgements

L. Jonsson, the JAGO-team (J. Schauer and K. Hissmann) and crew from R.V. Poseidon are thanked for their help in coral sampling. We thank P. van Rijswijk and members of the analytical lab of NIOZ-Yerseke for sample analysis. We acknowledge the feedback received during the review process. This research was supported by the Calmaro project funded by the European Community's Seventh Framework Program (FP7/2007-2013 granted to JM), the Netherlands Earth System Science Center (NESSC to JM) and the Netherlands Organisation of Scientific Research (VIDI 864.13.007 to DvO).

## Author Contributions

J.M. and D.v.O. wrote the manuscript, J.M., D.v.O. and C.M. designed the experiments, C.M., B.V., A.L. and A.F. performed research, and all authors discussed the experimental data.

## Additional Information

**Competing financial interests:** The authors declare no competing financial interests.

**How to cite this article:** Middelburg, J. J. *et al.* Discovery of symbiotic nitrogen fixation and chemoautotrophy in cold-water corals. *Sci. Rep.* **5**, 17962; doi: 10.1038/srep17962 (2015).



This work is licensed under a Creative Commons Attribution 4.0 International License. The images or other third party material in this article are included in the article's Creative Commons license, unless indicated otherwise in the credit line; if the material is not included under the Creative Commons license, users will need to obtain permission from the license holder to reproduce the material. To view a copy of this license, visit <http://creativecommons.org/licenses/by/4.0/>



## ORIGINAL ARTICLE

# Biogeographic variability in the physiological response of the cold-water coral *Lophelia pertusa* to ocean acidification

Samuel E. Georgian<sup>1</sup>, Sam Dupont<sup>2</sup>, Melissa Kurman<sup>1</sup>, Adam Butler<sup>1</sup>, Susanna M. Strömberg<sup>3</sup>, Ann I. Larsson<sup>3</sup> & Erik E. Cordes<sup>1</sup>

<sup>1</sup> Department of Biology, Temple University, Philadelphia, PA, USA

<sup>2</sup> Department of Biological and Environmental Sciences, Sven Lovén Centre for Marine Sciences – Kristineberg, University of Gothenburg, Fiskebäckskil, Sweden

<sup>3</sup> Department of Marine Sciences – Tjärnö, University of Gothenburg, Strömstad, Sweden

## Keywords

Calcification; cold-water coral; deep sea; energetics; ocean acidification; physiology.

## Correspondence

Samuel E. Georgian, Department of Biology, Temple University, 1900 N. 12th Street, Philadelphia, PA 19122, USA.  
E-mail: georgian@temple.edu

Accepted: 14 March 2016

doi: 10.1111/maec.12373

## Abstract

While ocean acidification is a global issue, the severity of ecosystem effects is likely to vary considerably at regional scales. The lack of understanding of how biogeographically separated populations will respond to acidification hampers our ability to predict the future of vital ecosystems. Cold-water corals are important drivers of biodiversity in ocean basins across the world and are considered one of the most vulnerable ecosystems to ocean acidification. We tested the short-term physiological response of the cold-water coral *Lophelia pertusa* to three pH treatments (pH = 7.9, 7.75 and 7.6) for Gulf of Mexico (USA) and Tisler Reef (Norway) populations, and found that reductions in seawater pH elicited contrasting responses. Gulf of Mexico corals exhibited reductions in net calcification, respiration and prey capture rates with decreasing pH. In contrast, Tisler Reef corals showed only slight reductions in net calcification rates under decreased pH conditions while significantly elevating respiration and capture rates. These differences are likely the result of environmental differences (depth, pH, food supply) between the two regions, invoking the potential for local adaptation or acclimatization to alter their response to global change. However, it is also possible that variations in the methodology used in the experiments contributed to the observed differences. Regardless, these results provide insights into the resilience of *L. pertusa* to ocean acidification as well as the potential influence of regional differences on the viability of species in future oceans.

## Introduction

The ability of marine organisms to persist and provide ecosystem services may be severely reduced in the future due to ocean acidification, the gradual decrease in pH and perturbation of the carbonate system of the world's oceans as a consequence of increasing atmospheric CO<sub>2</sub> (IPCC 2013; Wittmann & Pörtner 2013). These changes critically threaten ecosystem function in a wide variety of biomes including coral reefs, coastal systems, the open ocean, polar regions and the deep sea (reviewed in Hofmann *et al.*

2010). While most published studies have focused on the physiological effects elicited by exposure to decreased pH (Riebesell & Gattuso 2015), the potential of local adaptation to modulate the effects of ocean acidification has received less attention (Sunday *et al.* 2011). Studies that have directly compared the responses of multiple populations to acidification have revealed remarkable plasticity, suggesting that regional variability may play an important role in determining the fate of marine organisms in future oceans (*e.g.* Langer *et al.* 2009; Parker *et al.* 2011; Pisteveos *et al.* 2011; Sunday *et al.* 2011; Pancic *et al.* 2015).

The deep sea alone stores 25% of anthropogenic carbon (Canadell *et al.* 2007; Sabine & Feely 2007), providing a crucial buffering capacity that may mitigate the immediate effects of climate change in surface waters but ultimately places all deep-sea ecosystems at risk. The same adaptations that allow organisms to be successful in the cold and generally food-limited deep-sea environment (for example, slower metabolism, slower growth, lower protein content and lower enzyme levels; Drazen & Seibel 2007; Seibel & Drazen 2007) may partially impair their ability to physiologically compensate for rapid changes in pH (Seibel & Walsh 2003; Melzner *et al.* 2009). Among the most vulnerable groups in the deep sea are cold-water corals, organisms that already survive and calcify at low pH and saturation states (Davies & Guinotte 2011; Thresher *et al.* 2011; Lunden *et al.* 2013; Georgian *et al.* 2016). Cold-water corals support high levels of biodiversity by creating complex three-dimensional habitat and providing essential ecosystem services such as carbon sequestration and nutrient cycling (Wild *et al.* 2004; van Oevelen *et al.* 2009). As benthic waters become increasingly acidified, cold-water coral communities could be lost in the coming decades, in many cases before they have been discovered.

There is evidence to suggest that the physiological mechanisms underlying the calcification pathway in cold-water corals may provide some resilience to ocean acidification. Cold-water corals actively elevate the pH of their internal calcifying fluid by as much as 1.0 pH unit higher than external seawater, approximately double the increase observed in shallow-water corals (McCulloch *et al.* 2012). This plausibly represents an evolutionary strategy to counter the chronically low carbonate saturation state in deep-sea environments, and may serve as an indication that cold-water corals could be resilient to future acidification (McCulloch *et al.* 2012). However, there are only a few isolated observations of cold-water corals at or near the saturation horizon *in situ*, and most of these are of solitary corals, suggesting that undersaturated, low pH conditions are not suitable for framework formation. Therefore, it is imperative to experimentally quantify both calcification and the metabolic response of cold-water corals to low pH and saturation states in order to evaluate their future in an increasingly acidified ocean.

Only a small number of ocean acidification experimental studies have been conducted on cold-water corals to date, and the results have been both highly variable and contrasting. Most notably, a 6-month study found that net calcification rates in the cold-water coral *Lophelia pertusa* linearly increased with elevated CO<sub>2</sub> partial pressure (pCO<sub>2</sub>) values as high as 982 microatmospheres (µatm) (corresponding to a pH of 7.75), although calcification occurred at extremely low levels in all treatments (Form & Riebesell 2012). There

was no change in calcification rates between ambient (445 µatm) and projected (867 µatm) pCO<sub>2</sub> treatments in short-term shipboard experiments on *Madrepora oculata* (Maier *et al.* 2012). Similarly, Hennige *et al.* (2014) found no change in calcification in *L. pertusa* growth in acidified conditions as high as 750 ppm (pH of approximately 7.77), but documented a significant decline in respiration over a 21-day period. In contrast, a recent 3-month study on both *L. pertusa* and *M. oculata* found no significant change in either respiration or calcification rates even with CO<sub>2</sub> concentrations as high as 1000 ppm (pH of approximately 7.73; Maier *et al.* 2013a,b). Calcification, skeletal density and energy reserves in *Dendrophyllia cornigera* did not change significantly during a 314-day acidification experiment with pH values as low as 7.81; however, in the same study, *Desmophyllum dianthus* exhibited a significant, 70% reduction in calcification (Movilla *et al.* 2014). Finally, two short-term experiments demonstrated that *L. pertusa* had considerably reduced calcification under reduced pH values of 7.75 (Maier *et al.* 2009) and 7.6 (Lunden *et al.* 2014a). Therefore, while individual studies have provided important insights into the possible response of cold-water corals, the large variability among and within studies renders the potential resilience of cold-water corals to expected levels of acidification uncertain at best.

It is possible that discrepancies in the observed response of cold-water corals to acidification have been caused in part by natural variation among the studied populations. Cold-water corals are found in a variety of habitats in every ocean basin (Guinotte *et al.* 2006; Davies *et al.* 2008), with limited gene flow among regions (Le Goff-Vitry *et al.* 2004; Morrison *et al.* 2011; Lunden *et al.* 2014a). Therefore, biogeographically separated populations may exhibit highly variable responses to acidification due to local adaptation or acclimation to different pH regimes. In the present study, we tested how near-future levels of ocean acidification affected the net calcification, respiration and capture rates of biogeographically and genetically distinct *L. pertusa* populations from the Gulf of Mexico and the Tisler Reef (Norwegian Skagerrak). Ultimately, these data are an important first step in understanding natural variation at the regional scale, and highlight the importance of considering the role of biogeography when assessing the effects of global change on wide-ranging species.

## Material and Methods

### Gulf of Mexico

#### Site description and sample collections

Corals were collected in June 2013 onboard the E/V *Nautilus* using the remotely operated vehicle (ROV) *Hercules* at

the Viosca Knoll 826 (VK826) lease block in the Northern Gulf of Mexico (Fig. 1a, b). The VK826 site contains the largest continuous cold-water coral habitat yet discovered in the Gulf of Mexico (Schroeder 2002; Cordes *et al.* 2008). The site is characterized by a large carbonate mound approximately 500 m in diameter (Davies *et al.* 2010) as well as a series of smaller mounds on the order of tens of meters across (Georgian *et al.* 2014), both containing a high density of living *Lophelia pertusa* thickets. A diverse fauna of octocorals, black corals, fish and associated invertebrate species utilize the *L. pertusa* reef structure as habitat at the site (Cordes *et al.* 2008; Lessard-Pilon *et al.* 2010). Water samples collected by ROV directly over the reef revealed that pH on the total scale (pH<sub>T</sub>) ranged from 7.89–8.03, salinity-normalized total alkalinity ranged from 2288.7–2334.7  $\mu\text{mol}\cdot\text{kg}^{-1}$  and the aragonite saturation state ( $\Omega_A$ ) ranged from 1.33–1.69 (Table 1; Lunden *et al.* 2013). Water temperature varies considerably throughout the year, with values as low as 6.5 °C in winter months, and as high as 11.6 °C in the summer (Mienis *et al.* 2012). Dissolved oxygen concentrations at the site are extremely low compared to other *L. pertusa* habitats, ranging between 2.6–3.2  $\text{ml}\cdot\text{l}^{-1}$ , but are consistent with values for other Gulf of Mexico benthic habitats (Schroeder 2002; Davies *et al.* 2008). The site experiences relatively strong current flows averaging 8  $\text{cm}\cdot\text{s}^{-1}$ , with peak currents as high as 38  $\text{cm}\cdot\text{s}^{-1}$  (Mienis *et al.* 2012).

Corals were sampled within a depth range of 450–500 m from visually distinct colonies separated by at least 20–30 m to avoid sampling identical genotypes (*sensu* Lunden *et al.* 2014a) and returned to the surface in a temperature-insulated ‘biobox’. After collection, corals

were transferred to Temple University (Philadelphia, PA, USA) and housed in a 550-l maintenance aquarium system as described in Lunden *et al.* (2014b) for approximately 7 months prior to experimentation.

#### Experimental design

One experimental tank (60 l) was established for each of the following target treatments: *in situ* (pH<sub>T</sub> 7.9), slightly acidified (pH<sub>T</sub> 7.75) and highly acidified (pH<sub>T</sub> 7.6). Actual pH<sub>T</sub> and  $\Omega_A$  closely matched target conditions (Table 1), and were significantly different among treatments [analysis of variance (ANOVA) with Holm–Sidak *post-hoc* tests,  $P < 0.001$ ]. Treatments were randomly assigned to a tank, and corals were then randomly assigned to treatments. Temperature (average of  $8.1 \pm 0.2$  °C), salinity (average of  $35.1 \pm 0.04$  psu), dissolved oxygen (average of  $6.4 \pm 0.1$   $\text{ml}\cdot\text{l}^{-1}$ ) and total alkalinity (average of  $2328 \pm 23$   $\mu\text{mol}\cdot\text{kg}^{-1}$ ) did not differ significantly across treatments (Table 1; Kruskal–Wallis ANOVA,  $P > 0.05$ ). Temperature was measured once every 5 min using Hobo temperature loggers (Onset UA-001-64), salinity was measured daily using a handheld refractometer and dissolved oxygen was measured twice weekly using a Strathkelvin 782 dual oxygen meter and SI130 microcathode electrode. Corals were fed Marine Snow<sup>®</sup> three times per week (0.25 ml Marine Snow-1 seawater<sup>-1</sup>) but were starved for 24 h prior to the measurement of physiological rates. Total alkalinity was adjusted to approximately 2300  $\mu\text{mol}\cdot\text{kg}^{-1}$  to match *in situ* conditions by addition of 12 N HCl to seawater made using the Instant Ocean<sup>®</sup> salt mix. Total alkalinity was measured three times per week by acid titration on a

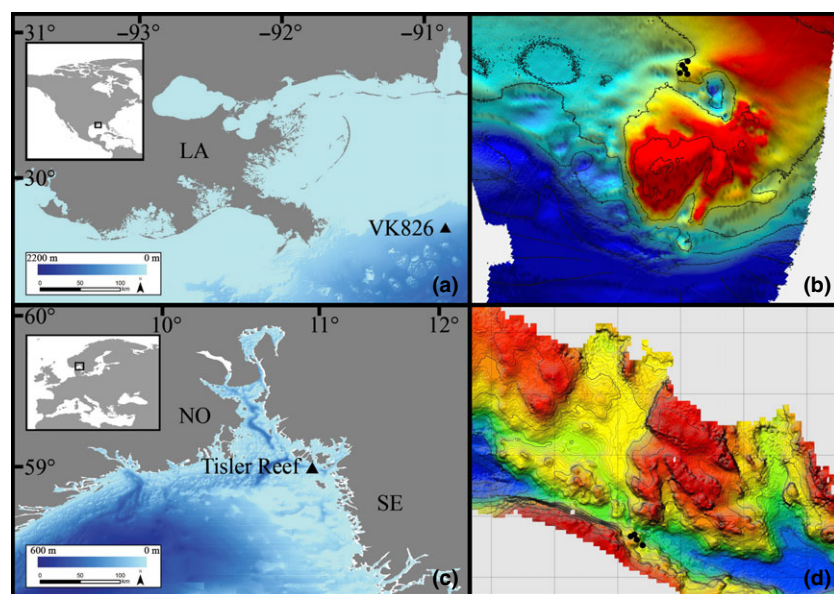


**Fig. 1.** Map of study sites and sample collections. (a): Location of the VK826 site within the Gulf of Mexico. (b): Multibeam bathymetry of the VK826 site with sampling locations indicated by black circles. (c): Location of Tisler Reef in the Skagerrak, Norway. (d): Multibeam bathymetry of Tisler Reef (Lavaleye *et al.* 2009) with sampling locations indicated by black circles. LA, Louisiana; NO, Norway; SE, Sweden.

**Table 1.** Seawater carbonate parameters measured near collection sites and in experimental aquaria. Experimental measurements are given as the 14-day experimental average ( $\pm$  SD), with pH measured daily on the total scale (pH<sub>T</sub>) and total alkalinity (TA,  $\mu\text{mol}\cdot\text{kg}^{-1}$ ) measured twice weekly. Aragonite saturation state ( $\Omega_A$ ) and CO<sub>2</sub> partial pressure (pCO<sub>2</sub>) (microatmospheres,  $\mu\text{atm}$ ) values were calculated in CO2SYS. Gulf of Mexico *in situ* measurements are averages for the VK826 site (Lunden *et al.* 2013). Tisler Reef *in situ* measurements are from a neighboring *Lophelia pertusa* reef in the Skagerrak, Norway (Maier *et al.* 2009).

treatment	target pH	Gulf of Mexico				Tisler Reef			
		pH <sub>T</sub>	TA	$\Omega_A$	pCO <sub>2</sub>	pH <sub>T</sub>	TA	$\Omega_A$	pCO <sub>2</sub>
<i>in situ</i>	–	7.93	2313	1.43	505	8.06	2313	1.89	383
control	7.90	7.92 ( $\pm 0.03$ )	2333 ( $\pm 16$ )	1.51 ( $\pm 0.10$ )	552 ( $\pm 42$ )	7.91 ( $\pm 0.03$ )	2312 ( $\pm 21$ )	1.38 ( $\pm 0.08$ )	579 ( $\pm 41$ )
low pH	7.75	7.76 ( $\pm 0.03$ )	2334 ( $\pm 17$ )	1.07 ( $\pm 0.07$ )	831 ( $\pm 54$ )	7.76 ( $\pm 0.03$ )	2312 ( $\pm 29$ )	1.00 ( $\pm 0.05$ )	845 ( $\pm 61$ )
very low pH	7.60	7.62 ( $\pm 0.03$ )	2331 ( $\pm 15$ )	0.80 ( $\pm 0.05$ )	1165 ( $\pm 76$ )	7.60 ( $\pm 0.04$ )	2309 ( $\pm 26$ )	0.74 ( $\pm 0.07$ )	1208 ( $\pm 132$ )

Mettler-Toledo DL15 autotitrator and checked against certified reference material (Batch 134, Dickson Lab, La Jolla, CA, USA). pH<sub>T</sub> was adjusted using American Marine Pinpoint pH Controllers, which automatically bubble either gaseous CO<sub>2</sub> or ambient air to lower or raise pH, respectively. Each pH system was calibrated weekly on the total scale with standard Tris-HCl and 2-aminopyridine/HCl (AMP-HCl) buffers. The aragonite saturation state was calculated from pH<sub>T</sub>, total alkalinity, temperature and salinity using CO2SYS software (Pierrot *et al.* 2006). Partial water changes (4 l) were performed weekly.

Experiments for the Gulf of Mexico population began in February 2014. Nine colonies consisting of between five and 15 live polyps (average of  $10.8 \pm 3.2$  polyps) were used per treatment. After the colonies were moved to the experimental tanks, pH<sub>T</sub> was slowly decreased to the target level for each treatment over a period of 48 h. Prior to experimental measurements, corals were acclimated to treatment conditions for 1 week. After the acclimation period, respiration, feeding and buoyant weight were measured as described below at the start and end of a 2-week experimental period.

#### Physiological measurements

Net calcification was assessed using the buoyant weighing technique (Jokiel *et al.* 1978; Davies 1989), which has been successfully used in numerous growth studies for both shallow- (Anthony *et al.* 2008; Dove *et al.* 2013) and deep-water (Orejas *et al.* 2011; Form & Riebesell 2012; Larsson *et al.* 2013; Lunden *et al.* 2014a) corals. The buoyant weight of each colony was obtained at the start and end of the 2-week experimental period by weighing fragments submerged in seawater and attached by a hook to an analytical balance (Denver Instrument, precision of 0.1 mg). Buoyant weights were converted to dry weights in air using the density of the skeleton and of the seawater. A correction for the contribution of tissue to buoyant weights (following Davies 1989) was applied to obtain the dry weight of the skeleton alone. Net

calcification was then calculated as the change in skeletal dry weight over the 2-week experimental period, expressed as % starting weight-day<sup>-1</sup>.

The respiration rate of each colony was measured as oxygen consumption in an 800-ml closed acrylic chamber during hour-long incubations. Dissolved oxygen concentrations were measured in  $\mu\text{mol}\cdot\text{l}^{-1}$  using a Strathkelvin 782 dual oxygen meter and SI130 microcathode electrode. The electrode was calibrated at the experimental temperature with a dual point calibration using 100% air-saturated water and a deoxygenated sodium sulfite solution. Temperature was controlled by submerging the chamber in a water bath, and a Hobo temperature logger (Onset UA-001-64) was mounted inside the chamber to monitor for temperature changes during incubations, which never exceeded  $\pm 0.2$  °C. Incubations were conducted with seawater from experimental aquaria so that the starting pH matched treatment conditions. Circulation within the chamber was obtained using a magnetic stir plate set at a stir speed of approximately 80 rpm. This generated sufficient flow to prevent oxygen depletion at the electrode tip, and also appeared to elicit a more natural polyp behavior. Microbial respiration ( $0.6 \pm 0.08 \mu\text{mol O}_2\cdot\text{l}^{-1}\cdot\text{h}^{-1}$ ,  $n = 12$ ) was accounted for by measuring empty chambers and was subtracted from live coral measurements. Corals were allowed to acclimate to conditions in the chamber for half an hour prior to measurements, and oxygen saturation never fell below 90% during incubations. At the end of the experiment, each colony was dried at 60 °C until reaching a constant mass (48–96 h), placed in a muffle furnace at 450 °C for 4 h to combust all organic matter, and reweighed to calculate the ash-free dry mass of each colony.

The feeding rate of each colony was measured as the capture rate of adult *Artemia salina* during a 1-h period in 0.8 l incubation chambers containing a starting prey density of 125 *A. salina* l<sup>-1</sup>. *A. salina* stocks were fed cultured algae after hatching until reaching maturity (3–6 weeks) and had an average length of  $3.54 \pm 0.9$  mm

during both experiments. Circulation was provided using a magnetic stir plate (stir speed of approximately 80 rpm). This provided sufficient flow to provide a constant flow of prey items past each *Lophelia pertusa* polyp (visual observation). Incubations were conducted with seawater from experimental aquaria so that the starting pH matched treatment conditions. Coral colonies were allowed to acclimate to the incubation chamber for 30 min prior to the addition of prey items. Capture rate was standardized to polyp number and reported as  $A. salina$ -polyp<sup>-1</sup>·h<sup>-1</sup>.

### Tisler Reef corals

#### Site description and sample collections

*Lophelia pertusa* colonies were collected in January 2014 from the Tisler Reef in the Norwegian Skagerrak (Fig. 1c, d). The Tisler Reef is a relatively shallow (70–155 m) cold-water coral reef composed of living *L. pertusa* colonies as well as extensive dead skeletal structures (Lavaleye *et al.* 2009). It covers an area of approximately 240 km<sup>2</sup>, making it one of the largest inshore cold-water coral reefs. Following the discovery of the reef in 2002 and the documentation of extensive pre-existing damage from bottom trawling, the reef was protected in 2003 by Norwegian fishery regulations (Lundälv & Jonsson 2003; Fosså & Skjoldal 2010). The reef experiences strong currents up to 50 cm·s<sup>-1</sup>, with tidally influenced downwelling providing the bulk of nutrition to the reef (Wagner *et al.* 2011). Water temperature typically fluctuates between 6 and 9 °C (Lavaleye *et al.* 2009). While the carbonate chemistry directly above the reef has not been measured, a neighboring *L. pertusa* reef at the same depth within the Norwegian Skagerrak had a pH<sub>T</sub> of 8.06, total alkalinity of 2313 μmol·kg<sup>-1</sup> and a Ω<sub>A</sub> of 1.89 (Table 1; Maier *et al.* 2009).

All required permits were obtained from the Norwegian Fisheries Directorate prior to collection. Corals of the white color morph were collected from discrete colonies at a depth of approximately 100 m using the R/V Nereus and ROV Sperre SUB-Fighter 7500, and transported to the Sven Lovén Centre for Marine Sciences (University of Gothenburg) at Tjärnö. Corals were maintained in flow-through aquaria with sand-filtered water (32–35 psu and 8 °C) with water intake from 45 m depth. In June 2014, corals were moved to the Sven Lovén Centre facility at Kristineberg and maintained in a 40 l flow-through aquarium (32–35 psu and 8 °C) with water intake from 32 m. Corals were allowed to acclimate to the conditions at the Kristineberg facility for 1 month prior to the start of the experiment. The experiment for the Tisler Reef population began in August 2014.

#### Experimental design

While we attempted to minimize methodological differences between the Gulf of Mexico and Tisler Reef experiments, some modifications (described below) were necessary due to the available facilities and equipment, as well as differences in the *Lophelia pertusa* colonies themselves. Corals were randomly assigned to 20-l experimental flow-through aquaria at the Kristineberg facility with an average flow rate of 1.5 ± 0.2 l·min<sup>-1</sup>. Two replicate aquaria were established for each treatment, each containing four coral colonies (n = 8 per treatment). pH was controlled to within ± 0.05 in each experimental aquarium using the AquaMedic pH computer (Bissendorf, Germany) via the direct injection of gaseous CO<sub>2</sub>. pH was measured daily on the total scale on filtered water samples (0.45 micron acetate syringe filter) using a Metrohm (827 pH lab) electrode calibrated using standard Tris-HCl and AMP-HCl buffers (Unité d'Océanographie Chimique, Université de Liège, Belgium). Total alkalinity was measured twice weekly on filtered water samples (0.45 micron acetate syringe filter) by acid titration on a Titroline Alpha Plus titrator (SI Analytics). pH<sub>T</sub> and Ω<sub>A</sub> were statistically indistinguishable between replicate tanks (Kruskal–Wallis ANOVA, P > 0.05) but statistically distinct among all treatments (Kruskal–Wallis ANOVA with Student–Newman–Keuls *post-hoc*, P < 0.001). Temperature averaged 7.9 ± 0.07 °C across all treatments, and was not statistically different in any treatment (Kruskal–Wallis ANOVA, P > 0.9). It was not possible to control salinity (average of 33.3 ± 0.4 psu), which was slightly lower than in the Gulf of Mexico experiment, but was statistically identical across treatments (Kruskal–Wallis ANOVA, P > 0.9). Dissolved oxygen was also slightly lower than in the Gulf of Mexico experiment, averaging 5.71 ± 0.3 ml·l<sup>-1</sup>, but was identical across treatments (Kruskal–Wallis ANOVA, P > 0.9). Total alkalinity averaged 2310 ± 24 μmol·kg<sup>-1</sup>, and was not statistically different across treatments (Kruskal–Wallis ANOVA, P = 0.813). Because total alkalinity was within the normal range for *L. pertusa* at this site, it was not altered in the experimental aquaria.

#### Physiological measurements

Net calcification was measured using the total alkalinity anomaly (Smith & Key 1975; Ohde & Hossain 2004) rather than buoyant weighing, because in preliminary trials, small colonies (such as those available from the Tisler Reef) were prone to considerably more error using the buoyant weighing method (data not shown). Corals were individually placed in closed glass chambers (220 ml) in a water bath that maintained temperature to ±0.2 °C during all trials. To avoid hypoxia or the severe reductions of pH during incubations, ambient air was continuously bubbled into the side of the chambers at a slow

rate (1–2 bubbles·s<sup>-1</sup>). This also provided adequate circulation within the chamber. A 60-ml water sample was collected by syringe before and after the 12-h incubation period, and measured for total alkalinity in duplicate as described above. In addition, three seawater-only chambers were measured along with each treatment group to account for microbial activity. Changes in alkalinity within the control chambers were subtracted from the results from the chambers with corals. Net calcification was then calculated as  $\mu\text{mol CaCO}_3\cdot\text{gTW}^{-1}\cdot\text{h}^{-1}$  using the following formula:

$$\text{calcification} = 0.5 \times V \times [(\Delta\text{TA}_F) - (\Delta\text{TA}_C)] / T \times \text{TW}, \quad (1)$$

where *V* is the volume of seawater in liters,  $\Delta\text{TA}_F$  is the average change in total alkalinity during the incubation of each fragment,  $\Delta\text{TA}_C$  is the average change in total alkalinity during the control incubations, *T* is the incubation time in hours and *TW* is the final tissue weight of each fragment in grams. To allow for comparison to other studies, we then calculated net calcification as % starting weight·day<sup>-1</sup>. While the excretion of nutrients can introduce error into this method, we did not account for this here because previous studies have described the influence as negligible (Maier *et al.* 2012; Hennige *et al.* 2014).

Respiration trials were conducted for each coral colony as described above; however, due to the smaller size of the colonies (average size of  $5.5 \pm 1.5$  polyps compared to an average of  $10.8 \pm 3.2$  polyps in the Gulf of Mexico experiment), a smaller chamber (400 ml) was used for incubations. Microbial respiration was accounted for by measuring oxygen consumption in an empty chamber, but was consistently negligible at  $0.98 \pm 0.18$  (SD)  $\mu\text{mol O}_2\cdot\text{l}^{-1}\cdot\text{h}^{-1}$  (*n* = 16). Measurements of the dried tissue weight and capture rate of *A. salina* adults were conducted for each coral colony as described above.

#### Statistical analysis

The water chemistry parameters of experimental aquaria were compared separately for the Tisler Reef and Gulf of Mexico experiments using a one-way ANOVA with Holm–Sidak *post-hoc* tests if the data were normally distributed with equal variances. Otherwise, we used a Kruskal–Wallis ANOVA with Student–Newman–Keuls *post-hoc* tests. Following a model selection process using the Akaike information criterion to select the best model type, linear regressions were used to assess the relationship between each physiological rate and pH. Analyses of covariance (ANCOVAs) were then used to compare the response of Tisler Reef and Gulf of Mexico corals to reduced pH. Statistical analyses were conducted in JMP

version 12.1.0 (ANOVAs and linear regressions, SAS Institute Inc., Cary, NC, USA) and R version 3.1.2 (ANCOVAs, R Development Core Team 2008) using an alpha level of 0.05. All data are presented as averages  $\pm$  SD unless otherwise stated.

## Results

### Tissue and behavior

There was no observed tissue or polyp mortality in any treatment in either the Gulf of Mexico or Tisler Reef experiments. Qualitatively, Gulf of Mexico corals exhibited greater signs of visual stress in acidified treatments, including frequently retracted polyps, extended mesentery filaments (acontia) and increased mucus production. In contrast, Tisler Reef corals exhibited no obvious visual indications of stress; polyps in all treatments were generally extended and active, especially in the presence of food. Corals from both sites maintained a full coverage of coenosarc tissue layer in all treatments, preventing the direct exposure of skeleton to seawater.

### Net calcification

Within the Gulf of Mexico experiment, net calcification under *in situ* conditions ( $\text{pH}_T = 7.9$ ) was variable, ranging from 0.026–0.048%·day<sup>-1</sup> with an average of  $0.036 \pm 0.007\%$ ·day<sup>-1</sup>. Net calcification was linearly dependent on pH, with a decrease of  $-0.1485\%$ ·day<sup>-1</sup>·pH unit<sup>-1</sup> (linear regression,  $r^2 = 0.84$ ,  $P < 0.001$ ) (Table 2, Fig. 2). Corals in the  $\text{pH}_T = 7.75$  treatment had a reduced but positive net calcification rate of  $0.0176 \pm 0.012\%$ ·day<sup>-1</sup>, while corals in the 7.6 treatment exhibited net dissolution of skeletal material at an average rate of  $-0.009 \pm 0.003\%$ ·day<sup>-1</sup>, although it was not possible to determine whether gross calcification occurred but at a lower rate than dissolution.

Tisler Reef corals exhibited higher and more variable net calcification in the control treatment, with rates ranging from 0.047–0.085%·day<sup>-1</sup> and an average rate of  $0.067 \pm 0.016\%$ ·day<sup>-1</sup>. Net calcification in the low pH treatment ( $\text{pH}_T = 7.75$ ) averaged  $0.056 \pm 0.015\%$ ·day<sup>-1</sup>, and all colonies exhibited positive net calcification in the undersaturated treatment ( $\text{pH}_T = 7.6$ ) with an average of  $0.048 \pm 0.011\%$ ·day<sup>-1</sup>. While net calcification in Tisler Reef corals decreased ( $-0.0593\%$ ·day<sup>-1</sup>·pH unit<sup>-1</sup>) significantly under reduced pH conditions (Table 2; linear regression,  $r^2 = 0.25$ ,  $P = 0.013$ ), all colonies exhibited positive net calcification even in undersaturated conditions.

An ANCOVA demonstrated significant differences in the slopes (ANCOVA,  $F_{1,47} = 12.96$ ,  $P < 0.001$ ) and

**Table 2.** Results of the linear regression models assessing the relationship between pH and physiological rates for Gulf of Mexico and Tisler Reef corals.

site	rate	$r^2$	equation	$F$	$P$
Gulf of Mexico	calcification	0.84	$y = 0.1485x - 1.1385$	134.68	<0.0001
	respiration	0.68	$y = 14.25x - 106.07$	54.10	<0.0001
	feeding	0.16	$y = 2.9105x - 20.913$	4.60	0.042
Tisler Reef	calcification	0.25	$y = 0.0593x - 0.4024$	7.39	0.013
	respiration	0.52	$y = -11.054x + 92.955$	23.33	<0.0001
	feeding	0.32	$y = -11.106x + 96.437$	10.21	0.00418

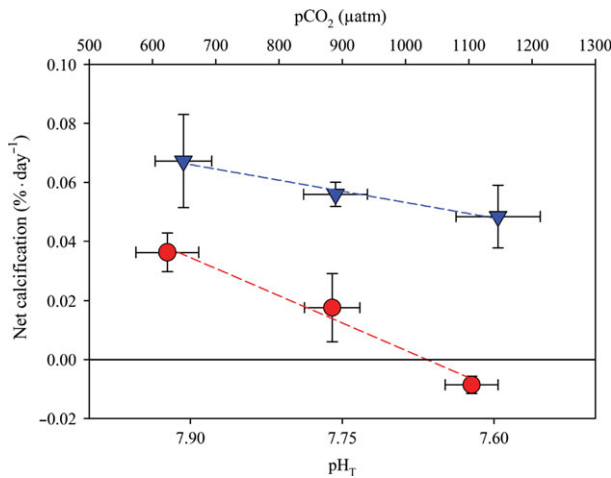


**Fig. 2.** Net calcification (%·day<sup>-1</sup>) of coral colonies after 14 days in each pH treatment [pH on the total scale (pH<sub>T</sub>) = 7.9, 7.75, 7.6]. Tisler Reef experimental data shown as blue triangles. Gulf of Mexico experimental data shown as red circles. Vertical error bars indicate the SD for net calcification measurements; horizontal error bars indicate the SD of pH measured over the experimental period. Dashed lines indicate linear regressions for the Gulf of Mexico (red;  $r^2 = 0.84$ ,  $P < 0.001$ ) and Tisler Reef (blue;  $r^2 = 0.25$ ,  $P = 0.01$ ) data. The slope [analysis of covariance (ANCOVA),  $F_{1,47} = 12.96$ ,  $P < 0.001$ ] and intercept (ANCOVA,  $F_{1,48} = 157.69$ ,  $P < 0.0001$ ) of the site regressions are significantly different. pCO<sub>2</sub>, CO<sub>2</sub> partial pressure; atm, microatmospheres.

intercepts (ANCOVA,  $F_{1,48} = 157.69$ ,  $P < 0.0001$ ) of the Gulf of Mexico and Tisler Reef linear regressions, indicating that reduced seawater pH caused larger reductions in net calcification in the Gulf of Mexico population (Table 3). The combined net calcification rates (%·day<sup>-1</sup>) of both Tisler Reef and Gulf of Mexico corals in the control treatment (pH<sub>T</sub> = 7.9) were negatively correlated with their starting dry weight, indicating that smaller corals from both sites calcified at a proportionally higher rate than large colonies (linear regression,  $r^2 = 0.27$ ,  $P < 0.05$ ).

**Respiration**

Gulf of Mexico and Tisler Reef corals exhibited contrasting metabolic responses to acidification (Fig. 3). In the

**Table 3.** Results of the analyses of covariance testing whether the relationship between pH and physiological rates differed significantly between Gulf of Mexico and Tisler Reef corals. See Table 2 for results of the individual linear regression models.

rate	effect	residual df	SS	$F$	$P$
calcification	slope	47	0.0016	13.0	<0.001
	intercept	48	0.0242	157.7	<0.0001
respiration	slope	47	128.07	72.1	<0.0001
	intercept	48	89.47	20.3	<0.0001
feeding	slope	47	39.3	15.0	<0.001
	intercept	48	932.1	275.5	<0.0001

df = degrees of freedom; SS = sum of squares.

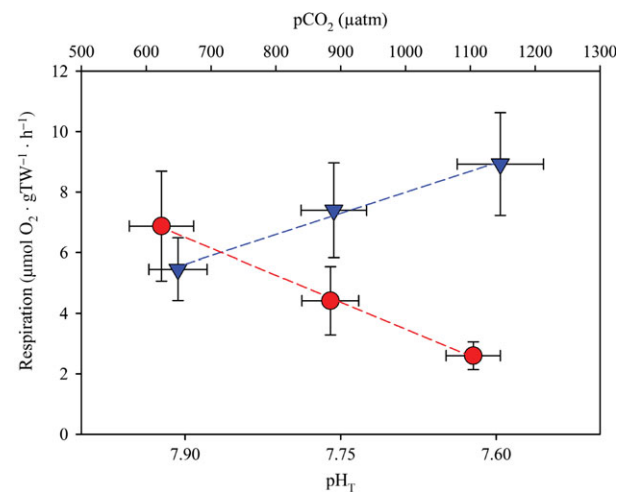


**Fig. 3.** Respiration rate [ $\mu\text{mol O}_2 \cdot \text{g tissue weight (TW)}^{-1} \cdot \text{h}^{-1}$ ] of coral colonies after 14 days in each pH treatment [pH on the total scale (pH<sub>T</sub>) = 7.9, 7.75, 7.6]. Tisler Reef experimental data shown as blue triangles. Gulf of Mexico experimental data shown as red circles. Vertical error bars indicate the SD for respiration rate measurements; horizontal error bars indicate the SD of pH measured over the experimental period. Dashed lines indicate linear regressions for the Gulf of Mexico (red;  $r^2 = 0.68$ ,  $P < 0.0001$ ) and Tisler Reef (blue;  $r^2 = 0.52$ ,  $P < 0.0001$ ) data. The slope [analysis of covariance (ANCOVA), slope,  $F_{1,47} = 72.1$ ,  $P < 0.0001$ ] and intercept (ANCOVA, intercept,  $F_{1,48} = 20.3$ ,  $P < 0.0001$ ) of the site regressions are significantly different. pCO<sub>2</sub>, CO<sub>2</sub> partial pressure; atm, microatmospheres.

control treatments ( $\text{pH}_T = 7.9$ ), Gulf of Mexico corals respired at an average rate of  $6.9 \pm 1.8 \mu\text{mol O}_2 \cdot \text{gTW}^{-1} \cdot \text{h}^{-1}$ , with a range of  $4.8\text{--}9.5 \mu\text{mol O}_2 \cdot \text{gTW}^{-1} \cdot \text{h}^{-1}$ . Across all treatments, respiration in Gulf of Mexico corals was highly variable ( $2.1\text{--}9.5 \mu\text{mol O}_2 \cdot \text{gTW}^{-1} \cdot \text{h}^{-1}$ ), with an average rate of  $4.4 \pm 1.1 \mu\text{mol O}_2 \cdot \text{gTW}^{-1} \cdot \text{h}^{-1}$  in the low pH treatment ( $\text{pH}_T = 7.75$ ) and  $2.6 \pm 0.5 \mu\text{mol O}_2 \cdot \text{gTW}^{-1} \cdot \text{h}^{-1}$  in the very low pH treatment ( $\text{pH}_T = 7.6$ ). Respiration was significantly dependent on pH, with reduced respiration observed under lower pH conditions (Table 2; linear regression,  $r^2 = 0.68$ ,  $P < 0.0001$ ).

Tisler Reef corals respired at an average rate of  $5.5 \pm 1.8 \mu\text{mol O}_2 \cdot \text{gTW}^{-1} \cdot \text{h}^{-1}$  in the control treatment ( $\text{pH}_T = 7.9$ ),  $7.4 \pm 1.6 \mu\text{mol O}_2 \cdot \text{gTW}^{-1} \cdot \text{h}^{-1}$  in the low pH treatment ( $\text{pH}_T = 7.75$ ) and  $8.9 \pm 1.7 \mu\text{mol O}_2 \cdot \text{gTW}^{-1} \cdot \text{h}^{-1}$  in the very low pH treatment ( $\text{pH}_T = 7.6$ ). Respiration was significantly dependent on pH, with considerably elevated rates observed under reduced-pH conditions (Table 2, Fig. 3; linear regression,  $r^2 = 0.52$ ,  $P < 0.0001$ ). The Tisler Reef and Gulf of Mexico populations exhibited significantly different respiration responses to pH (ANCOVA, slope,  $F_{1,47} = 72.1$ ,  $P < 0.0001$ ; ANCOVA, intercept,  $F_{1,48} = 20.3$ ,  $P < 0.0001$ ; Table 3), with Tisler Reef corals respiring at a higher rate under reduced seawater pH and Gulf of Mexico corals respiring at a lower rate.

### Capture rate

The capture rate of Gulf of Mexico corals was relatively low across all pH treatments (Fig. 4), averaging  $2.1 \pm 1.2$  prey-polyp $^{-1} \cdot \text{h}^{-1}$  in the control treatment ( $\text{pH}_T = 7.9$ ),  $1.7 \pm 0.5$  prey-polyp $^{-1} \cdot \text{h}^{-1}$  in the low pH treatment ( $\text{pH}_T = 7.75$ ) and  $1.3 \pm 0.9$  prey-polyp $^{-1} \cdot \text{h}^{-1}$  in the very low pH treatment ( $\text{pH}_T = 7.6$ ). Reductions in seawater pH were correlated with a small but significant reduction in capture rate (linear regression,  $r^2 = 0.16$ ,  $P = 0.04$ ; Table 2), although the removal of a single outlier in the control treatment rendered this relationship insignificant (linear regression,  $r^2 = 0.07$ ,  $P = 0.11$ ).

The Tisler Reef population exhibited a markedly different feeding response to reduced seawater pH (Fig. 4). Corals in the control treatment ( $\text{pH}_T = 7.9$ ) fed at a relatively variable rate ranging from  $6.7\text{--}10.3$  prey-polyp $^{-1} \cdot \text{h}^{-1}$ , with an average capture rate of  $8.6 \pm 1.5$  prey-polyp $^{-1} \cdot \text{h}^{-1}$ . Reduced pH conditions were significantly correlated with elevated capture rates (linear regressions,  $r^2 = 0.32$ ,  $P < 0.01$ ), with the highest capture rates observed in the low pH treatment ( $\text{pH}_T = 7.75$ ; average of  $10.4 \pm 2.1$  prey-polyp $^{-1} \cdot \text{h}^{-1}$ ) and the very low pH treatment ( $\text{pH}_T = 7.6$ ; average of  $12.0 \pm 2.9$  prey-polyp $^{-1} \cdot \text{h}^{-1}$ ). An ANCOVA test revealed that the slopes

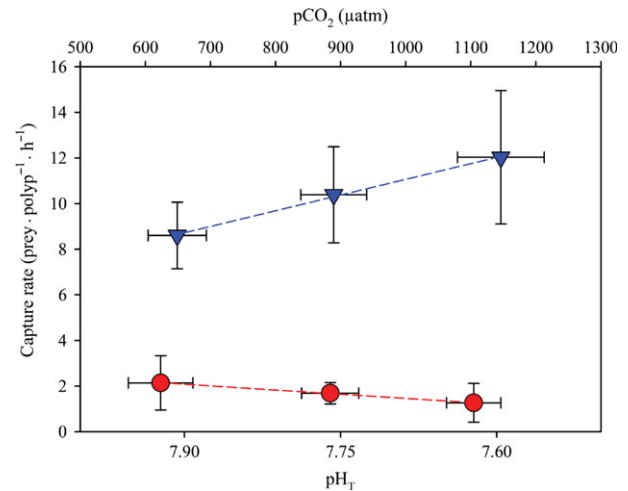


**Fig. 4.** Capture rate (prey-polyp $^{-1} \cdot \text{h}^{-1}$ ) of coral colonies after 14 days in each pH treatment [pH on the total scale ( $\text{pH}_T$ ) = 7.9, 7.75, 7.6]. Tisler Reef experimental data shown as blue triangles. Gulf of Mexico experimental data shown as red circles. Vertical error bars indicate the SD for capture rate measurements; horizontal error bars indicate the SD of pH measured over the experimental period. Dashed lines indicate linear regressions for the Gulf of Mexico (red;  $r^2 = 0.16$ ,  $P = 0.04$ ) and Tisler Reef (blue;  $r^2 = 0.32$ ,  $P < 0.01$ ) data. The slope [analysis of covariance (ANCOVA), slope,  $F_{1,47} = 15.0$ ,  $P < 0.001$ ] and intercept (ANCOVA, intercept,  $F_{1,48} = 275.5$ ,  $P < 0.0001$ ) of the site regressions are significantly different. pCO<sub>2</sub>, CO<sub>2</sub> partial pressure, atm, microatmospheres.

(ANCOVA,  $F_{1,47} = 15.0$ ,  $P < 0.001$ ) and intercepts (Table 3; ANCOVA,  $F_{1,48} = 275.5$ ,  $P < 0.0001$ ) of the Gulf of Mexico and Tisler Reef regression models were significantly different, indicating that the two populations had contrasting feeding responses to reduced pH.

### Discussion

Recent experimental work has revealed considerable variation in the physiological response of cold-water corals to ocean acidification (Maier *et al.* 2009, 2012, 2013a,b; Form & Riebesell 2012; Hennige *et al.* 2014; Lunden *et al.* 2014a), rendering the future of cold-water coral ecosystems unclear. In the present study, we demonstrated that contrasting responses to identical pH changes can be observed between two populations of the cold-water coral *Lophelia pertusa*. Gulf of Mexico corals exhibited reduced physiological performance in all tested parameters, a commonly observed stress-response in marine invertebrates (*e.g.* Kaniewska *et al.* 2012). In contrast, Tisler Reef corals were able to maintain net calcification by elevating respiration and capture rates, a strategy that may confer some resilience to acidification if it can be maintained over extended time periods (*e.g.* Stumpp *et al.* 2011).

Differences in experimental methodology may explain some of the large variability observed among *L. pertusa* populations, both in this and in previous studies. One of the major experimental differences in the present study was the use of a flow-through system in the Tisler Reef experiment and recirculating aquaria in the Gulf of Mexico experiment. Previous cold-water coral physiology studies have utilized both systems, perhaps accounting for some of the variability among studies. Despite evidence that recirculating systems are adequate for housing shallow-water (Barron *et al.* 2010) and deep-sea (Lunden *et al.* 2014a,b) corals, it is plausible that this difference partially accounted for the lower physiological performance observed in the Gulf of Mexico corals, as previous studies have found reduced physiological rates in recirculating systems (e.g. Otsoshi *et al.* 2003; but see Tomoda *et al.* 2005). However, we did not observe any detectable buildup of waste products (nitrate, nitrite or ammonia; data not shown) during the course of the present study. In addition, the Instant Ocean<sup>®</sup> artificial seawater used in the current study matches the chemical composition of seawater better than other artificial mixes (Atkinson & Bingman 1998), and has been successfully used in a large number of physiology experiments (Marchant *et al.* 2010; Castillo *et al.* 2014; Lunden *et al.* 2014a). Regardless, it is possible that the recirculating system was sub-optimal and could partially explain the lower absolute net calcification measurements recorded for the Gulf of Mexico corals.

Another experimental difference that may partially explain our results was the use of the alkalinity anomaly technique for the Tisler Reef experiment and the buoyant weighing technique for the Gulf of Mexico experiment. While both methods have abundant support in the coral literature (Maier *et al.* 2009, 2013b; Ries *et al.* 2010; Cohen & Fine 2012; Form & Riebesell 2012; Larsson *et al.* 2013), it is plausible that this discrepancy partially explains the considerably higher net calcification rates in the Tisler Reef corals. The total alkalinity anomaly technique may overestimate calcification if microbial activity considerably reduces alkalinity during incubations; however, our seawater-only control chambers did not reveal such an effect. In addition, the net calcification rates measured in this study for Tisler Reef corals using the total alkalinity anomaly (control average of  $0.067 \pm 0.02\% \cdot \text{day}^{-1}$ ) were comparable to previous rates measured at Tisler Reef using the buoyant weighing technique (average of  $0.046 \pm 0.02\% \cdot \text{day}^{-1}$ ; Larsson *et al.* 2013), and studies directly comparing the two methods have not revealed significant differences in either tropical (Holcomb *et al.* 2010) or cold-water corals (Maier *et al.* 2013b).

The net calcification rates measured in this study were well within the range previously reported for *L. pertusa*

(Maier *et al.* 2009, 2012; Form & Riebesell 2012; Larsson *et al.* 2013; Hennige *et al.* 2014). However, we observed considerable variability both within and between the Gulf of Mexico and Tisler Reef populations. Under control conditions ( $\text{pH}_T = 7.9$ ), the net calcification rate of the Tisler Reef corals was approximately double the rate observed in the Gulf of Mexico corals. This difference may be partially due to the smaller size of the Tisler Reef fragments, as we found that net calcification in the control treatment was negatively correlated with starting weight. Previous work has also found that smaller, more apical *L. pertusa* fragments have a higher growth rate (Brooke & Young 2009). High variability was also observed among individuals from the same site and within the same treatment. However, published measurements of *L. pertusa* calcification revealed even greater variation; in one study alone, net calcification rates ranged from  $0.0027\% \cdot \text{day}^{-1}$  to  $0.19\% \cdot \text{day}^{-1}$  depending on the age and position of polyps within colonies (Maier *et al.* 2009).

Net calcification in both populations significantly declined under reduced pH, although only the Gulf of Mexico corals exhibited the net dissolution of existing skeletal material under very low pH conditions ( $\text{pH}_T = 7.6$ ). In contrast, the Tisler Reef corals maintained positive net calcification across all pH treatments, in part because calcification did not decrease as steeply with reduced pH as in the Gulf of Mexico corals. The stark contrast in the ability of the Tisler Reef and Gulf of Mexico corals to maintain calcification in conditions expected by the end of the century has considerable implications for their future viability. Previous studies have also found that *L. pertusa* from the North Atlantic maintains positive net calcification even when grown in undersaturated conditions (e.g. Form & Riebesell 2012; Maier *et al.* 2013b; Hennige *et al.* 2015), while the only study from the Gulf of Mexico documented net dissolution in undersaturated conditions (Lunden *et al.* 2014a). Recent experimental work has shown that cold-water corals are able to tightly regulate the pH of their internal calcifying fluid through the active removal of protons (Anagnostou *et al.* 2012; McCulloch *et al.* 2012; Wall *et al.* 2015). As a result, the saturation state of the calcifying fluid is elevated to several times that of the external seawater, allowing for  $\text{CaCO}_3$  precipitation even when the external seawater is undersaturated. However, decreasing seawater pH considerably increases the energy required to maintain this large pH gradient, with an estimated 10% energy increase per 0.1 pH unit decrease (McCulloch *et al.* 2012). Therefore, while this work provides a viable mechanism for calcification under acidified conditions, there are likely to be potential disruptions to the energy budget of the coral and associated changes to

the rate of calcification and other key physiological processes.

Given the increased energy required to calcify under reduced pH, the observed calcification response may have been partially controlled by the metabolic rates of each population. Respiration has been shown to be coupled to calcification under both ambient and reduced pH conditions in tropical (e.g. Kaniewska *et al.* 2012) and cold-water corals (Maier *et al.* 2013a). Aerobic respiration is required to fuel adenosine triphosphate-driven processes in corals, and is critically linked to the active transport of  $H^+$  and  $Ca^{2+}$  ions during calcification (Al-Horani *et al.* 2003). In the present study, Tisler Reef and Gulf of Mexico corals exhibited contrasting metabolic responses to acidification. The Gulf of Mexico corals experienced significantly reduced respiration rates in both low pH treatments, suggesting the onset of metabolic depression, a mechanism that enhances survival under short-lived disturbances at the cost of some biological functioning (Guppy & Withers 1999; Thomsen & Melzner 2010). In contrast, the Tisler Reef corals significantly elevated respiration rates in response to acidified seawater. This metabolic strategy has the potential to supply enough additional energy to maintain positive net calcification even under acidified conditions, but may create an energetic imbalance that can only be sustained by catabolizing energy reserves (Rodrigues & Grottoli 2007) or obtaining additional energy from the environment.

The ability to increase energy intake from the environment via elevated feeding has been shown to reduce or negate the effects of acidification and other stressors in tropical corals (Cohen & Holcomb 2009). However, no previous study has assessed whether cold-water corals are capable of altering their capture rate in response to climate change conditions. In the present study, the Gulf of Mexico corals had lower capture rates under control conditions ( $pH_T = 7.9$ , average rate of  $2.1 \pm 1.2$  *A. salina*-polyp $^{-1}$ ·h $^{-1}$ ) than have previously been measured for *L. pertusa* ( $7.8$  *A. salina*-polyp $^{-1}$ ·h $^{-1}$ ; Tsounis *et al.* 2010). In contrast, the Tisler Reef corals had a higher capture rate of *A. salina* prey under control conditions ( $pH_T = 7.9$ , average rate of  $8.6 \pm 1.5$  *A. salina*-polyp $^{-1}$ ·h $^{-1}$ ), and significantly elevated feeding under reduced pH conditions. It is possible that the considerably lower baseline feeding rate in the Gulf of Mexico corals was due in part to inter-polyp competition for prey, as the Gulf of Mexico corals had a higher number of polyps ( $10.8 \pm 3.2$  polyps-colony $^{-1}$ ) compared to the Tisler Reef corals ( $5.5 \pm 1.5$  polyps-colony $^{-1}$ ) but the same prey concentration was used in both experiments. Previous research on the effects of intra-specific, inter-polyp competition in scleractinian corals has had mixed results, with some studies demonstrating that competition

reduced feeding rates and resource acquisition (Merks *et al.* 2004; Einbinder *et al.* 2009; Wijgerde *et al.* 2011), and others finding that denser polyp spacing within colonies enhanced feeding rates (McFadden 1986; Wijgerde *et al.* 2012). Inter-polyp competition has not yet been observed in cold-water corals, and as *L. pertusa* is capable of self-recognition to avoid intra-specific competition (Hennige *et al.* 2014), it is possible that even closely spaced polyps do not actively compete for food. Nevertheless, it may be fruitful for future research to explore the effects of polyp number and spacing on *L. pertusa*'s feeding rate, as well as the interactive effects of water flow, pH and prey density.

Regardless of the mechanism underlying the higher capture rates observed in the Tisler Reef corals, the increased energy input from feeding likely facilitated their elevated respiration (see Larsson *et al.* 2013) and subsequent maintenance of positive net calcification rates in undersaturated conditions. This type of response would only be favorable in environments where there is a relatively high-quality and reliable food source, such as the shallower cold-water coral systems in Norway [average lateral deposition of particulate organic carbon (POC) at Tisler Reef of  $459$  mg C·m $^{-2}$ ·day $^{-1}$ ; Wagner *et al.* 2011]. In contrast, the lower food availability at the deeper Gulf of Mexico VK826 site (modeled POC flux of  $46$  mg C·m $^{-2}$ ·day $^{-1}$ ; Georgian *et al.* 2014) may not favor this strategy as pH and saturation state decline. Despite the apparent resilience conferred on Tisler Reef corals via elevated feeding, predictions that food will become more limited in future oceans may hamper the ability of *in situ* cold-water corals to utilize this strategy in response to climate change. Ocean acidification has been predicted to reduce surface phytoplankton by 4–10%, leading to a decrease in the POC flux to the deep sea by 6–13% (Mora *et al.* 2013). In some areas, particularly in the Gulf of Mexico, the anthropogenic eutrophication of marine systems will act to increase the size and extent of 'dead zones'; coupled with the effects of global warming and deoxygenation, many regions in the deep sea may become severely food limited in future oceans (Rabouille *et al.* 2008; Stramma *et al.* 2010). However, in addition to zooplankton capture, *L. pertusa* utilizes alternative food sources including dissolved organic matter, bacteria and algal detritus (Mueller *et al.* 2014), and may be able to increase uptake from these sources.

A number of factors may have been responsible for the contrasting responses observed in Tisler Reef and Gulf of Mexico populations, including genetic differences, acclimation to local environmental conditions and experimental differences. Given the limited gene flow between Gulf of Mexico and Northern Atlantic *L. pertusa* populations (Morrison *et al.* 2011; Lunden *et al.* 2014a), it is not

surprising that they exhibited a very different baseline physiology as well as a contrasting response to acidification. Recent evidence has demonstrated that genetic differences may partially explain the considerable intra-specific variation observed in the physiological tolerance of tropical coral species (Meyer *et al.* 2009; Pandolfi *et al.* 2011). Numerous *L. pertusa* studies from the Northern Atlantic and Mediterranean Sea have found higher respiration rates (Hennige *et al.* 2014), capture rates (Purser *et al.* 2010; Tsounis *et al.* 2010) and calcification rates (Maier *et al.* 2009) than measured in the present study or previously reported for the Gulf of Mexico (Lunden *et al.* 2014a). If biogeographically separated populations of *L. pertusa* exhibit a large variability in their response to ocean acidification, as suggested by the literature and the results presented here, some populations may already be relatively resilient to acidification, giving the species as a whole a higher adaptive potential to more effectively respond to acidification and other stressors.

Acclimation to local environmental conditions may also be partially responsible for the contrasting physiological responses of Tisler Reef and Gulf of Mexico populations. In our study, Tisler Reef corals were collected from a much shallower depth (100 m) than Gulf of Mexico corals (450 m). In addition to experiencing a chronically higher saturation state than the Gulf of Mexico, this means that the Tisler Reef has a higher influx of high-quality food (Wagner *et al.* 2011). Deep-sea environments are generally food limited because only a fraction of surface productivity is transported to deep waters before being degraded (Deuser 1986), meaning that both the quantity and quality of food reaching the sea floor are highly depth-dependent. Plausibly, Tisler Reef corals are accustomed to having the necessary resources to increase their capture rate and subsequently elevate their metabolism in order to allocate additional energy to calcification during periods of environmental stress.

## Conclusions

Cold-water coral habitats are protected as Vulnerable Marine Ecosystems by the United Nations and have long been recognized as critical drivers of diversity and ecosystem function in the deep sea (reviewed in Thurber *et al.* 2014). Considering the potential for major declines in cold-water coral ecosystems due to ocean acidification and other stressors, it is imperative to better understand their potential range of responses. In this study, we found evidence that corals from the Tisler Reef may be somewhat resilient to acidification over a short time period, but it is not clear whether this strategy will be sustainable in the long term given the large increase in feeding

required to maintain calcification under low pH conditions. Importantly, these results demonstrate that the existing variability among cold-water coral physiological studies may strongly depend on biogeographic variability, genetic and environmental differences, and inconsistencies in experimental designs. Future research would benefit from comparative studies both within and among large biogeographic regions that link observed physiological responses to ocean acidification and other stressors with differences in local environmental conditions. Such an approach would provide key insights into the mechanisms underlying the resilience or sensitivity of separated populations, and identify the environmental conditions that may drive local adaptation or acclimatization to global ocean change. While our current understanding of the mechanisms and rates of adaptive capacity to environmental change does not suggest that the rate of coral evolution will be able to keep up with the pace of global changes (Hoegh-Guldberg 2014), it is possible that pre-existing local adaptations to different or more variable pH regimes might provide such a capacity at a global scale (Hofmann *et al.* 2010). Ultimately, more work is needed to assess whether natural variability among cold-water coral populations will provide a significant avenue of resilience in future oceans.

## Acknowledgements

Funding was provided by the Gulf of Mexico Research Institute to the Ecosystem Impacts of Oil & Gas Inputs to the Gulf consortium, and through a National Science Foundation (NSF) Ocean Acidification Grant (OCE-1220478 to E.E.C. and to R. Kulathinal). Additional funding was provided by Integrated Marine Biogeochemistry and Ecosystem Research and the U.S. Ocean Carbon and Biochemistry. This work would not have been possible without support from the crews of the *E/V Nautilus* and *ROV Hercules*, and the *R/V Nereus* and *ROV Sperre SUB-Fighter 7500*. We would like to thank A. Ventura, S. Schulz and B. Lundve for their assistance at the Kristineberg Marine Station. S.D. is funded through a Linnaeus grant from the Swedish Research Councils Vetenskapsrådet and The Swedish Research Council Formas. S.M.S. and A.I.L. were funded by The Swedish Research Council Formas (contracts 215-2010-1604 and 215-2012-1134). S.E.G. was funded by the National Science Foundation Graduate Research Fellowship Program (DGE-1144462) and by the NSF Graduate Research Opportunities Worldwide program. Any opinions, findings and conclusions or recommendations expressed in this material are those of the authors and do not necessarily reflect the views of the National Science Foundation.

## References

- Al-Horani F.A., Al-Moghrabi S.M., De Beer D. (2003) The mechanism of calcification and its relation to photosynthesis and respiration in the scleractinian coral *Galaxea fascicularis*. *Marine Biology*, **142**, 419–426.
- Anagnostou E., Huang K.F., You C.F., Sikes E.L., Sherrell R.M. (2012) Evaluation of boron isotope ratio as a pH proxy in the deep sea coral *Desmophyllum dianthus*: evidence of physiological pH adjustment. *Earth Planetary Science Letters*, **349**, 251–260.
- Anthony K.R.N., Kline D.I., Diaz-Pulido G., Dove S., Hoegh-Guldberg O. (2008) Ocean acidification causes bleaching and productivity loss in coral reef builders. *Proceedings of the National Academy of Sciences of the United States of America*, **105**, 17442–17446.
- Atkinson M.J., Bingman C. (1998) Elemental composition of commercial sea salts. *Journal of Aquaculture and Aquatic Sciences*, **8**, 39–43.
- Barron M.G., McGill C.J., Courtney L.A., Marcovich D.T. (2010) Experimental bleaching of a reef-building coral using a simplified recirculating laboratory exposure system. *Journal of Marine Biology*, **2010**, 415167.
- Brooke S., Young C.M. (2009) *In situ* measurement of survival and growth of *Lophelia pertusa* in the northern Gulf of Mexico. *Marine Ecology Progress Series*, **397**, 153–161.
- Canadell J.G., Le Quéré C., Raupach M.R., Field, C. B., Buitenhuis, E. T., Ciais, P., Conway, T. J., Gillett, N. P., Houghton, R. A., & Gregg, M. (2007) Contributions to accelerating atmospheric CO<sub>2</sub> growth from economic activity, carbon intensity, and efficiency of natural sinks. *Proceedings of the National Academy of Sciences of the United States of America*, **104**, 18866–18870.
- Castillo K.D., Ries J.B., Bruno J.F., Westfield I.T. (2014) The reef-building coral *Siderastrea siderea* exhibits parabolic responses to ocean acidification and warming. *Proceedings of the Royal Society B: Biological Sciences*, **281**, 20141856.
- Cohen S., Fine M. (2012) Measuring gross and net calcification of a reef coral under ocean acidification conditions: methodological considerations. *Biogeosciences Discussions*, **9**, 8241–8272.
- Cohen A.L., Holcomb M. (2009) Why corals care about ocean acidification: uncovering the mechanism. *Oceanography*, **22**, 118–127.
- Cordes E.E., McGinley M.P., Podowski E.L., Becker E.L., Lessard-Pilon S., Viada S.T., Fisher C.R. (2008) Coral communities of the deep Gulf of Mexico. *Deep Sea Research I*, **55**, 777–787.
- Davies P.S. (1989) Short-term growth measurements of corals using an accurate buoyant weighing technique. *Marine Biology*, **101**, 389–395.
- Davies A.J., Guinotte J.M. (2011) Global habitat suitability for framework-forming cold-water corals. *PLoS ONE*, **6**, e18483.
- Davies A.J., Wisshak M., Orr J.C., Roberts J.M. (2008) Predicting suitable habitat for the cold-water coral *Lophelia pertusa* (Scleractinia). *Deep Sea Research I*, **55**, 1048–1062.
- Davies A.J., Duineveld G., van Weering T., Mienis, F., Quattrini, A. M., Seim, H. E., Bane, J. M., & Ross, S. W. (2010) Short-term environmental variability in cold-water coral habitat at Viosca Knoll, Gulf of Mexico. *Deep-Sea Research I*, **57**, 199–212.
- Deuser W.G. (1986) Seasonal and interannual variations in deep-water particle fluxes in the Sargasso Sea and their relation to surface hydrography. *Deep-Sea Research I*, **33**, 225–246.
- Dove S.G., Kline D.I., Pantos O., Angly F.E., Tyson G.W., Hoegh-Guldberg O. (2013) Future reef decalcification under a business-as-usual CO<sub>2</sub> emission scenario. *Proceedings of the National Academy of Sciences of the United States of America*, **110**, 15342–15347.
- Drzen J.C., Seibel B. (2007) Depth-related trends in metabolism of benthic and benthopelagic deep-sea fishes. *Limnology and Oceanography*, **52**, 2306–2316.
- Einbinder S., Mass T., Brokovich E., Dubinsky Z., Erez J., Tchernov D. (2009) Changes in morphology and diet of the coral *Stylophora pistillata* along a depth gradient. *Marine Ecology Progress Series*, **381**, 167–174.
- Form A.U., Riebesell U. (2012) Acclimation to ocean acidification during long-term CO<sub>2</sub> exposure in the cold-water coral *Lophelia pertusa*. *Global Change Biology*, **18**, 843–853.
- Fosså J.H., Skjoldal H.R. (2010) *Conservation of Cold-Water Coral Reefs in Norway*. Oxford University Press, New York, NY, USA: 215–230.
- Georgian S.E., Shedd W., Cordes E.E. (2014) High-resolution ecological niche modelling of the cold-water coral *Lophelia pertusa* in the Gulf of Mexico. *Marine Ecology Progress Series*, **506**, 145–161.
- Georgian S.E., DeLeo D., Durkin A., Gomez C.E., Kurman M., Lunden J.J., Cordes E.E. (2016) Oceanographic patterns and carbonate chemistry in the vicinity of cold-water coral reefs in the Gulf of Mexico: implications for resilience in a changing ocean. *Limnology and Oceanography*, **61**, 648–665.
- Guinotte J.M., Orr J., Cairns S., Freiwald A., Morgan L., George R. (2006) Will human-induced changes in seawater chemistry alter the distribution of deep-sea scleractinian corals? *Frontiers in Ecology and the Environment*, **4**, 141–146.
- Guppy M., Withers P. (1999) Metabolic depression in animals: physiological perspectives and biochemical generalizations. *Biological Reviews of the Cambridge Philosophical Society*, **74**, 1–40.
- Hennige S.J., Wicks L.C., Kamenos N.A., Bakker D.C.E., Findlay H.S., Dumousseaud C., Roberts J.M. (2014) Short-term metabolic and growth responses of the cold-water coral *Lophelia pertusa* to ocean acidification. *Deep Sea Research II*, **99**, 27–35.

- Hennige S.J., Wicks L.C., Kamenos N.A., Perna G., Findlay H.S., Roberts J.M. (2015) Hidden impacts of ocean acidification to live and dead coral framework. *Proceedings of the Royal Society B*, **282**, 20150990.
- Hoegh-Guldberg O. (2014) Coral reef sustainability through adaptation: glimmer of hope or persistent mirage? *Current Opinion in Environmental Sustainability*, **7**, 127–133.
- Hofmann G.E., Barry J.P., Edmunds P.J., Gates R.D., Hutchins D.A., Klinger T., Sewell M.A. (2010) The effect of ocean acidification on calcifying organisms in marine ecosystems: an organism-to-ecosystem perspective. *Annual Review of Ecology, Evolution, and Systematics*, **41**, 127–147.
- Holcomb M., McCorkle D.C., Cohen A.L. (2010) Long-term effects of nutrient and CO<sub>2</sub> enrichment on the temperate coral *Astrangia poculata* (Ellis and Solander, 1786). *Journal of Experimental Marine Biology and Ecology*, **386**, 27–33.
- IPCC (2013) Summary for policymakers. In: Stocker T.F., Qin D., Plattner G.K., et al. (Eds), *Climate Change 2013: The Physical Science Basis. Contribution of Working Group I to the Fifth Assessment Report of the Intergovernmental Panel on Climate Change*. Cambridge University Press, Cambridge: 1–1535.
- Jokiel P.L., Maragos J.W., Franzisket L. (1978) Coral growth buoyant weight technique. In: Stoddart D.R., Johannes R.E. (Eds), *Monographs on Oceanographic Methodology*. UNESCO, Paris: 529–542.
- Kaniewska P., Campbell P.R., Kline D.I., Rodriguez-Lanetty M., Miller D.J., Dove S., Hoegh-Guldberg O. (2012) Major cellular and physiological impacts of ocean acidification on a reef building coral. *PLoS ONE*, **7**, 34659.
- Langer G., Nehrke G., Probert I., Ly J., Ziveri P. (2009) Strain-specific responses of *Emiliania huxleyi* to changing seawater carbonate chemistry. *Biogeosciences*, **6**, 2637–2646.
- Larsson A.I., Lundälv T., van Oevelen D. (2013) Skeletal growth, respiration rate and fatty acid composition in the cold-water coral *Lophelia pertusa* under varying food conditions. *Marine Ecology Progress Series*, **483**, 169–184.
- Lavaley M.G., Duineveld T., Lundälv M., White M., Guihen D., Kiriakoulakis K., Wolff G.A. (2009) Cold-water corals on the Tisler Reef. *Oceanography*, **22**, 76–84.
- Le Goff-Vitry M.C., Pybus O.G., Rogers A.D. (2004) Genetic structure of the deep-sea coral *Lophelia pertusa* in the northeast Atlantic revealed by microsatellites and internal transcribed spacer sequences. *Molecular Ecology*, **13**, 537–549.
- Lessard-Pilon S., Podowski E.L., Cordes E.E., Fisher C.R. (2010) Megafauna community composition associated with *Lophelia pertusa* colonies in the Gulf of Mexico. *Deep Sea Research II*, **57**, 1882–1890.
- Lundälv T., Jonsson L. (2003) *Mapping of Deep-Water Corals and Fishery Impacts in the NE Skagerrak, using Acoustical and ROV Survey Techniques*. Proceedings of the 6th Underwater Science Symposium, Aberdeen, UK.
- Lunden J.J., Georgian S.E., Cordes E.E. (2013) Aragonite saturation states at cold-water coral reefs structured by *Lophelia pertusa* in the northern Gulf of Mexico. *Limnology and Oceanography*, **58**, 354–362.
- Lunden J.J., McNicholl C.G., Sears C.R., Morrison C.L., Cordes E.E. (2014a) Acute survivorship of the deep-sea coral *Lophelia pertusa* from the Gulf of Mexico under acidification, warming, and deoxygenation. *Frontiers in Marine Science*, **1**, 78.
- Lunden J.J., Turner J.M., McNicholl C.G., Glynn C.K., Cordes E.E. (2014b) Design, development, and implementation of recirculating aquaria for maintenance and experimentation of deep-sea corals and associated fauna. *Limnology and Oceanography: Methods*, **12**, 363–372.
- Maier C., Hegeman J., Weinbauer M.G., Gattuso J.P. (2009) Calcification of the cold-water coral *Lophelia pertusa* under ambient and reduced pH. *Biogeosciences*, **6**, 1671–1680.
- Maier C., Watremez P., Taviani M., Weinbauer M.G., Gattuso J.P. (2012) Calcification rates and the effect of ocean acidification on Mediterranean cold-water corals. *Proceedings of the Royal Society B: Biological Sciences*, **279**, 1716–1723.
- Maier C., Bils F., Weinbauer M.G., Watremez P., Peck M.A., Gattuso J.P. (2013a) Respiration of Mediterranean cold-water corals is not affected by ocean acidification as projected for the end of the century. *Biogeosciences*, **10**, 5671–5680.
- Maier C., Schubert A., Sánchez M.M.B., Weinbauer M.G., Watremez P., Gattuso J.P. (2013b) End of the century pCO<sub>2</sub> levels do not impact calcification in Mediterranean cold-water corals. *PLoS ONE*, **8**, e62655.
- Marchant H.K., Calosi P., Spicer J.I. (2010) Short-term exposure to hypercapnia does not compromise feeding, acid-base balance or respiration of *Patella vulgata* but surprisingly is accompanied by radula damage. *Journal of the Marine Biological Association of the United Kingdom*, **90**, 1379–1384.
- McCulloch M., Trotter J., Montagna P., Falter, J., Dunbar, R., Freiwald, A., Försterra, G., Correa, M. L., Maier, C., Rüggeberg, A., & Taviani, M. (2012) Resilience of cold-water scleractinian corals to ocean acidification: Boron isotopic systematics of pH and saturation state up-regulation. *Geochimica et Cosmochimica Acta*, **87**, 21–34.
- McFadden C.S. (1986) Colony fission increases particle capture rates of a soft coral: advantages of being a small colony. *Journal of Experimental Marine Biology and Ecology*, **103**, 1–20.
- Melzner F., Gutowska M.A., Langenbuch M., Dupont, S., Lucassen, M., Thorndyke, M. C., Bleich, M., & Portner, H. O. (2009) Physiological basis for high CO<sub>2</sub> tolerance in marine ectothermic animals: pre-adaptation through lifestyle and ontogeny? *Biogeosciences*, **6**, 2313–2331.
- Merks R.M., Hoekstra A.G., Kaandorp J.A., Sloop P.M. (2004) Polyp oriented modelling of coral growth. *Journal of Theoretical Biology*, **21**, 559–576.
- Meyer E., Davies S., Wang S., Willis B.L., Abrego D., Juenger T.E., Matz M.V. (2009) Genetic variation in responses to a

- settlement cue and elevated temperature in the reef-building coral *Acropora millepora*. *Marine Ecology Progress Series*, **392**, 81–92.
- Mienis F., Duineveld G.C.A., Davies A.J., Ross S.W., Seim H., Bane J., Van Weering T.C.E. (2012) The influence of near-bed hydrodynamic conditions on cold-water corals in the Viosca Knoll area, Gulf of Mexico. *Deep Sea Research I*, **60**, 32–45.
- Mora C., Wei C., Rollo A., Amaro, T., Baco, A. R., Billett, D., Bopp, L., Chen, Q., Collier, M., Danovaro, R., & Gooday, A. J. (2013) Biotic and human vulnerability to projected changes in ocean biogeochemistry over the 21st century. *PLoS Biology*, **11**, e1001682.
- Morrison C.L., Ross S.W., Nizinski M.S., Brooke, S., Järnegren, J., Waller, R. G., Johnson, R. L., & King, T. L. (2011) Genetic discontinuity among regional populations of *Lophelia pertusa* in the North Atlantic Ocean. *Conservation Genetics*, **12**, 713–729.
- Movilla J., Orejas C., Calvo E., Gori, A., López-Sanz, À., Grinyó, J., Domínguez-Carrió, C., & Pelejero, C. (2014) Differential response of two Mediterranean cold-water coral species to ocean acidification. *Coral Reefs*, **33**, 675–686.
- Mueller C.E., Larsson A.I., Veuger B., Middelburg J.J., van Oevelen D. (2014) Opportunistic feeding on various organic food sources by the cold-water coral *Lophelia pertusa*. *Biogeosciences*, **11**, 123–133.
- van Oevelen D., Duineveld G., Lavaley M., Mienis F., Soetaert K., Heip C.H.R. (2009) The cold-water coral community as a hot spot for carbon cycling on continental margins: a food-web analysis from Rockall Bank (northeast Atlantic). *Limnology and Oceanography*, **54**, 1829–1844.
- Ohde S., Hossain M.M.M. (2004) Effect of CaCO<sub>3</sub> (aragonite) saturation state of seawater on calcification of *Porites* coral. *Geochemical Journal*, **38**, 613–621.
- Orejas C., Ferrier-Pages C., Reynaud S., Gori, A., Beraud, E., Tsounis, G., Allemand, D., & Gili, J. M. (2011) Long-term growth rates of four Mediterranean cold-water coral species maintained in aquaria. *Marine Ecology Progress Series*, **429**, 57–65.
- Otoshi C.A., Arce S.M., Moss S.M. (2003) Growth and reproductive performance of broodstock shrimp reared in a biosecure recirculating aquaculture system versus a flow-through pond. *Aquacultural Engineering*, **29**, 93–107.
- Pancic M., Hansen P.H., Tammilehto A., Lundholm N. (2015) Resilience to temperature and pH changes in a future climate change scenario in six strains of the polar diatom *Fragilariopsis cylindrus*. *Biogeosciences Discussions*, **12**, 4627–4654.
- Pandolfi J.M., Connolly S.R., Marshall D.J., Cohen A.L. (2011) Projecting coral reef futures under global warming and ocean acidification. *Science*, **333**, 418–422.
- Parker L.M., Ross P.M., O'Connor W.A. (2011) Populations of the Sydney rock oyster, *Saccostrea glomerata*, vary in response to ocean acidification. *Marine Biology*, **158**, 689–697.
- Pierrot D., Lewis E., Wallace D.W.R. (2006) *MS Excel Program Developed for CO<sub>2</sub> System Calculations ORNL/CDIAC-105*. Carbon Dioxide Information Analysis Center, Oak Ridge National Laboratory, U.S. Department of Energy, Oak Ridge, TN.
- Pistevos J.C.A., Calosi P., Widdicombe S., Bishop J.D.D. (2011) Will variation among genetic individuals influence species responses to global climate change? *Oikos*, **120**, 675–689.
- Purser A., Larsson A.I., Thomsen L., van Oevelen D. (2010) The influence of flow velocity and food concentration on *Lophelia pertusa* (Scleractinia) zooplankton capture rates. *Journal of Experimental Marine Biology and Ecology*, **395**, 55–62.
- R Development Core Team. (2008). *R: A Language and environment for statistical computing*. Vienna: R Foundation for Statistical Computing. ISBN 3-900051-07-0. <http://www.R-project.org>.
- Rabouille C., Conley D.J., Dai M.H. (2008) Comparison of hypoxia among four river-dominated ocean margins: The Changjiang (Yangtze), Mississippi, Pearl, and Rhone rivers. *Continental Shelf Research*, **28**, 1527–1537.
- Riebesell U., Gattuso J.P. (2015) Lessons learned from ocean acidification research. *Nature Climate Change*, **5**, 12–14.
- Ries J.B., Cohen A.L., McCorkle D.C. (2010) A nonlinear calcification response to CO<sub>2</sub>-induced ocean acidification by the coral *Oculina arbuscula*. *Coral Reefs*, **29**, 661–674.
- Rodrigues L.J., Grotoli A.G. (2007) Energy reserves and metabolism as indicators of coral recovery from bleaching. *Limnology and Oceanography*, **52**, 1874–1882.
- Sabine C.L., Feely R.A. (2007) The oceanic sink for carbon dioxide. In: Reay D., Hewitt N., Grace J., Smith K. (Eds), *Greenhouse Gas Sinks*. CABI Publishing, Oxfordshire: 31–49.
- Schroeder W.W. (2002) Observations of *Lophelia pertusa* and the surficial geology at a deep-water site in the northeastern Gulf of Mexico. *Hydrobiologia*, **471**, 29–33.
- Seibel B.A., Drazen J.C. (2007) The rate of metabolism in marine animals: environmental constraints, ecological demands and energetic opportunities. *Philosophical Transactions of the Royal Society B: Biological Sciences*, **362**, 2061–2078.
- Seibel B.A., Walsh P.J. (2003) Biological impacts of deep-sea carbon dioxide injection inferred from indices of physiological performance. *Journal of Experimental Biology*, **206**, 641–650.
- Smith S.V., Key G.S. (1975) Carbon dioxide and metabolism in marine environments. *Limnology and Oceanography*, **20**, 493–495.
- Stramma L., Schmidtko S., Levin L.A., Johnson G.C. (2010) Ocean oxygen minima expansions and their biological impacts. *Deep Sea Research I*, **57**, 587–595.
- Stumpp M., Wren J., Melzner F., Thorndyke M.C., Dupont S.T. (2011) CO<sub>2</sub> induced seawater acidification impacts sea urchin larval development I: elevated metabolic rates decrease scope for growth and induce developmental delay. *Comparative Biochemistry and Physiology Part A: Molecular & Integrative Physiology*, **160**, 331–340.

- Sunday J.M., Crim R.N., Harley C.D.G., Hart M.W. (2011) Quantifying rates of evolutionary adaptation in response to ocean acidification. *PLoS ONE*, **6**, e22881.
- Thomsen J., Melzner F. (2010) Moderate seawater acidification does not elicit long-term metabolic depression in the blue mussel *Mytilus edulis*. *Marine Biology*, **157**, 2667–2676.
- Thresher R.E., Tilbrook B., Fallon S., Wilson N.C., Adkins J. (2011) Effects of chronic low carbonate saturation levels on the distribution, growth and skeletal chemistry of deep-sea corals and other seamount megabenthos. *Marine Ecology-Progress Series*, **442**, 87–99.
- Thurber A.R., Sweetman A.K., Narayanaswamy B.E., Jones D.O.B., Ingels J., Hansman R.L. (2014) Ecosystem function and services provided by the deep sea. *Biogeosciences*, **11**, 3941–3963.
- Tomoda T., Fushimi H., Kurokura H. (2005) Performance of a closed recirculation system for larviculture of red sea bream, *Pagrus major*. *Fisheries Science*, **71**, 1179–1181.
- Tsounis G., Orejas C., Reynaud S., Gili J.M., Allemand D., Ferrier-Pagès C. (2010) Prey-capture rates in four Mediterranean cold water corals. *Marine Ecology Progress Series*, **398**, 149–155.
- Wagner H., Purser A., Thomsen L., Jesus C.C., Lundälv T. (2011) Particulate organic matter fluxes and hydrodynamics at the Tisler cold-water coral reef. *Journal of Marine Systems*, **85**, 19–29.
- Wall M., Ragazzola F., Foster L.C., Form A., Schmidt D.N. (2015) Enhanced pH up-regulation enables the cold-water coral *Lophelia pertusa* to sustain growth in aragonite undersaturated conditions. *Biogeosciences Discussions*, **12**, 6757–6781.
- Wijgerde T., Diantari R., Lewaru M.W., Verreth J.A.J., Osinga R. (2011) Extracoelenteric zooplankton feeding is a key mechanism of nutrient acquisition for the scleractinian coral *Galaxea fascicularis*. *Journal of Experimental Biology*, **214**, 3351–3357.
- Wijgerde T., Spijkers P., Karruppannan E., Verreth J.A., Osinga R. (2012) Water flow affects zooplankton feeding by the scleractinian coral *Galaxea fascicularis* on a polyp and colony level. *Journal of Marine Biology*, **2012**, 854849.
- Wild C., Huettel M., Klüter A., Kremb S.G., Rasheed M.Y.M., Jørgensen B.B. (2004) Coral mucus functions as an energy carrier and particle trap in the reef ecosystem. *Nature*, **428**, 66–70.
- Wittmann A.C., Pörtner H. (2013) Sensitivities of extant animal taxa to ocean acidification. *Nature Climate Change*, **3**, 995–1001.



# Food selectivity and processing by the cold-water coral *Lophelia pertusa*

Dick van Oevelen<sup>1</sup>, Christina E. Mueller<sup>1</sup>, Tomas Lundälv<sup>2</sup>, and Jack J. Middelburg<sup>3</sup>

<sup>1</sup>Department of Estuarine and Delta Systems, Royal Netherlands Institute for Sea Research (NIOZ-Yerseke), and Utrecht University, PO Box 140, 4400 AC Yerseke, the Netherlands

<sup>2</sup>Sven Lovén Centre for Marine Sciences, Tjärnö, University of Gothenburg, 452 96 Strömstad, Sweden

<sup>3</sup>Department of Earth Sciences, Utrecht University, P.O. Box 80.021, 3508 TA Utrecht, the Netherlands

Correspondence to: Dick van Oevelen (dick.van.oevelen@nioz.nl)

Received: 15 July 2016 – Published in Biogeosciences Discuss.: 28 July 2016

Revised: 29 September 2016 – Accepted: 5 October 2016 – Published: 21 October 2016

**Abstract.** Cold-water corals form prominent reef ecosystems along ocean margins that depend on suspended resources produced in surface waters. In this study, we investigated food processing of <sup>13</sup>C and <sup>15</sup>N labelled bacteria and algae by the cold-water coral *Lophelia pertusa*. Coral respiration, tissue incorporation of C and N and metabolically derived C incorporation into the skeleton were traced following the additions of different food concentrations (100, 300, 1300 µg CL<sup>-1</sup>) and two ratios of suspended bacterial and algal biomass (1 : 1, 3 : 1). Respiration and tissue incorporation by *L. pertusa* increased markedly following exposure to higher food concentrations. The net growth efficiency of *L. pertusa* was low (0.08 ± 0.03), which is consistent with its slow growth rate. The contribution of algae and bacteria to total coral assimilation was proportional to the food mixture in the two lowest food concentrations, but algae were preferred over bacteria as a food source at the highest food concentration. Similarly, the stoichiometric uptake of C and N was coupled in the low and medium food treatment, but was uncoupled in the high food treatment and indicated a comparatively higher uptake or retention of bacterial carbon as compared to algal nitrogen. We argue that behavioural responses for these small-sized food particles, such as tentacle behaviour, mucus trapping and physiological processing, are more likely to explain the observed food selectivity as compared to physical–mechanical considerations. A comparison of the experimental food conditions to natural organic carbon concentrations above CWC reefs suggests that *L. pertusa* is well adapted to exploit temporal pulses of high or-

ganic matter concentrations in the bottom water caused by internal waves and downwelling events.

## 1 Introduction

Cold-water corals have a global distribution in the deep sea and are typically found at locations with high bottom-water velocities, such as continental margins, seamounts and mid-ocean ridges (Roberts et al., 2009; Davies and Guinotte, 2011; Yesson et al., 2012). Some cold-water corals are scleractinians and produce a three-dimensional carbonate structure, which provides settlement, refuge and feeding ground for many associated organisms (Henry and Roberts, 2007; Kutti et al., 2015). As a result, these reef communities are diverse, have high biomass and consume up to 20 times more organic carbon per square meter as compared to surrounding soft-sediment communities (Van Oevelen et al., 2009; White et al., 2012; Cathalot et al., 2015; Rovelli et al., 2015).

The main reef-building coral species in the North Atlantic Ocean is the branching coral *Lophelia pertusa*, which is a passive suspension feeder that uses tentacles to “catch” particles from the water column. Field observations on stable isotopes and fatty acids suggest that *L. pertusa* feeds on a broad range of food sources including particulate suspended matter, bacteria, phytoplankton and zooplankton (Kiriakoulakis et al., 2005; Duineveld et al., 2007; Sherwood et al., 2008; Dodds et al., 2009). Laboratory studies have confirmed the uptake of suspended particles, bacteria, phytoplankton and zooplankton by cold-water corals (Purser et al., 2010;

Mueller et al., 2014; Orejas et al., 2016). Recently, *L. pertusa* was also shown to take up dissolved organic matter in the form of free amino acids (Gori et al., 2014; Mueller et al., 2014) and to fix inorganic carbon into its biomass, supposedly through chemo-autotrophic activity of associated microbes (Middelburg et al., 2015). This flexibility in resource utilization clearly indicates an opportunistic feeding strategy (Mueller et al., 2014; Orejas et al., 2016).

In natural reefs the diversity of organic matter sources is high (Jensen et al., 2012) and it is presently unclear whether cold-water corals exhibit selective resource utilization or feed proportionally to resource availability. Moreover, organic matter supply to cold-water reefs is temporally variable due to seasonality in organic matter production in the surface ocean and the dynamic physical environment in which cold-water reefs occur (Duineveld et al., 2007; Davies et al., 2009; Findlay et al., 2013; Hebbeln et al., 2014; Mohn et al., 2014). Freshly hatched *Artemia salina* nauplii, which are often used as food in aquarium studies of scleractinians, were increasingly taken up by the cold-water coral *L. pertusa* with increasing concentration in the incubation vessel (Purser et al., 2010), indicating that *L. pertusa* responds to changes in food supply. In order to advance our understanding of cold-water coral physiology, we must better understand resource partitioning within the energy budget of the organism. For the cold-water coral *Desmophyllum dianthus* it was shown that zooplankton contributed to various components of the energy budget, including calcification, respiration and mucus release, following food withdrawal for 1 week (Naumann et al., 2011). The slow (i.e. months) response time of *L. pertusa* to changing food conditions renders this approach less effective in directly linking food uptake to physiological processing (Larsson et al., 2013).

The aims of this study are twofold. Firstly, we wanted to assess whether the cold-water coral *Lophelia pertusa* exhibits selective uptake when exposed to a mixed diet. Secondly, we aimed to quantitatively elucidate the energy budget of *L. pertusa* following feeding on different food quantities. To this end, we investigated food uptake, food selectivity and subsequent processing with a novel dual isotope labelling technique using mixed diets of  $^{13}\text{C}$ -labelled algae/ $^{15}\text{N}$ -labelled bacteria and  $^{15}\text{N}$ -labelled algae/ $^{13}\text{C}$ -labelled bacteria. This approach provided the high sensitivity needed to eliminate long-term incubations and allowed us to trace not only uptake, but also subsequent processing of algal and bacterial carbon and nitrogen. This experimental mixed diet study better represents the diversity of food available under natural coral reef conditions than traditional single food source studies and enables the quantitative tracing of individual food sources.

## 2 Materials and methods

### 2.1 Experimental design

Our dual isotope tracer design involved exposing separate coral fragments either to a food mixture of  $^{13}\text{C}$ -labelled algae ( $^{13}\text{C}$ -Algae) +  $^{15}\text{N}$ -labelled bacteria ( $^{15}\text{N}$ -Bacteria) or to a mixture of  $^{15}\text{N}$ -labelled algae ( $^{15}\text{N}$ -Algae) +  $^{13}\text{C}$ -labelled bacteria ( $^{13}\text{C}$ -Bacteria) (Fig. 1a). Uptake, respiration and calcification rates are subsequently summed to obtain total C or N uptake and processing (i.e. by dividing rates with the fractional  $^{13}\text{C}$  or  $^{15}\text{N}$  enrichment of each food source, see below). Three food concentrations were tested in this study: 8.3 ( $n = 2$  per food mixture), 25 ( $n = 3$  per food mixture) and 108 ( $n = 3$  per food mixture)  $\mu\text{mol CL}^{-1}$  (Fig. 1b). Replication in this study was limited due to collection restrictions for *Lophelia pertusa* from the Tisler Reef. The bacterial-C to algal-C ratio was 1:1 in the 8.3 and 25  $\mu\text{mol CL}^{-1}$  treatment, but due to technical issues, appeared to be 3:1 in the 108  $\mu\text{mol CL}^{-1}$  exposure.

### 2.2 Sampling location and maintenance

Corals were collected at the Tisler Reef, located 70 to 155 m deep in the Skagerrak, at the Norwegian-Swedish border. The Tisler Reef is located at a sill, which connects the Kosterfjord deep trough with the open Skagerrak. The current velocity at the reef varies from 0 to 50  $\text{cm s}^{-1}$ , with peaks in excess of 70  $\text{cm s}^{-1}$ , and the bottom-water temperature varies normally between 6 and 9 °C throughout the year (Lavaleye et al., 2009; Wagner et al., 2011), though peaks in excess of 12 °C have been observed in recent years (Guihen et al., 2012). The particulate organic carbon (POC) concentration at the reef varies between 3.6 and 8.9  $\mu\text{mol CL}^{-1}$  and the depositional POC fluxes average 38  $\text{mmol C m}^{-2} \text{d}^{-1}$  (Wagner et al., 2011).

Fragments of the cold-water coral *Lophelia pertusa* were collected from a depth of around 110 m using the remotely operated vehicle Sperre Subfighter 7500 DC. Fragments were placed in cooling boxes filled beforehand with cold seawater (7–8 °C) and transported within a few hours to the laboratory at the Sven Lovén Centre for Marine Sciences in Tjärnö, Sweden. After arrival, the coral fragments were clipped to approximately the same size ( $7.90 \pm 2.12$  g dry weight (DW) fragment $^{-1}$ ;  $14.1 \pm 2.4$  polyps fragment $^{-1}$  as mean  $\pm$  SD) and were subsequently acclimated for 6 weeks in aquaria ( $\sim 20$  L) placed in a dark thermo-constant room (7 °C). Sand-filtered (1–2 mm particle size) bottom water from 45 m depth out of the adjacent Koster fjord (salinity 31) was continuously flushed through the aquaria ( $\sim 1$  L min $^{-1}$ ). Experience at the station and our earlier experiments showed that the sand-filtered water still contains sufficient organic particles, so that no extra food was provided during the acclimation period (Mueller et al., 2014).

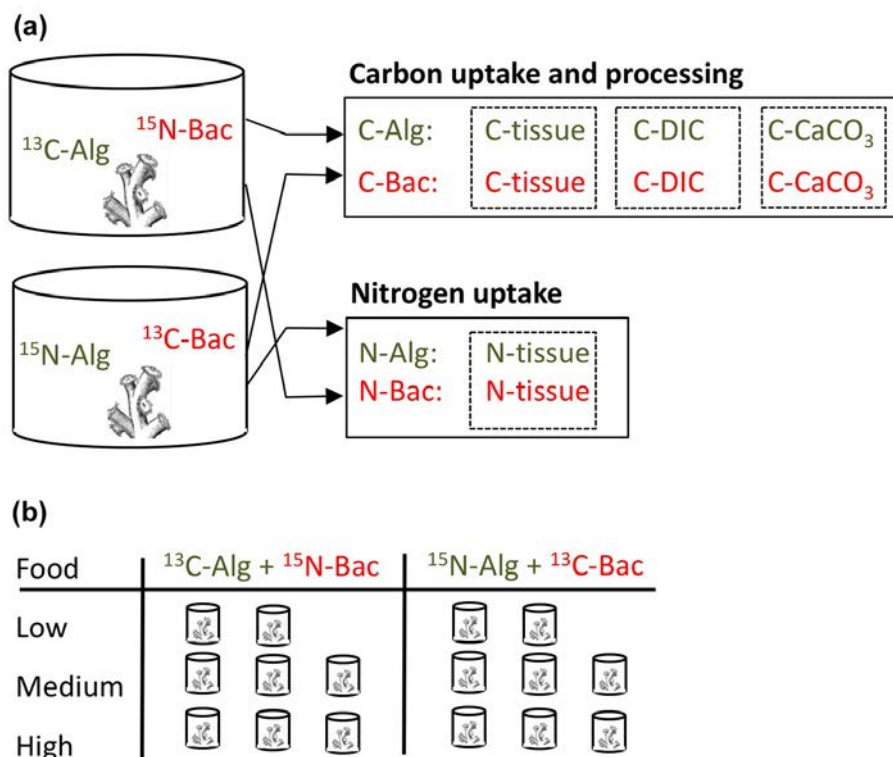


**Figure 1.** Experimental design of the dual-isotope labelling study. (a) Different coral fragments were exposed to a food mixture of  $^{13}\text{C}$ -labelled algae ( $^{13}\text{C}\text{-Alg}$ ) +  $^{15}\text{N}$ -labelled bacteria ( $^{15}\text{N}\text{-Bac}$ ) or to a mixture of  $^{15}\text{N}$ -labelled algae ( $^{15}\text{N}\text{-Alg}$ ) +  $^{13}\text{C}$ -labelled bacteria ( $^{13}\text{C}\text{-Bac}$ ). The N uptake in tissue (N-tissue), C uptake in tissue (C-tissue), respiration to dissolved inorganic carbon (C-DIC) and C incorporation into the skeleton (C- $\text{CaCO}_3$ ) was calculated for each incubation from the  $^{13}\text{C}$  and  $^{15}\text{N}$  transfer (see Methods). (b) Full experimental design with eight incubations for the  $^{13}\text{C}\text{-Alg} + ^{15}\text{N}\text{-Bac}$  treatment and eight incubations for the  $^{15}\text{N}\text{-Alg} + ^{13}\text{C}\text{-Bac}$  treatment, partitioned over a low, medium and high food concentration exposure.

### 2.3 Preparation of isotopically labelled algae and bacteria

$^{15}\text{N}$ -labelled algae were cultured axenically in F/2 culture medium adjusted after Guillard (1975). The culture medium was prepared by replacing 80 % of the  $\text{NaHCO}_3$  ( $^{13}\text{C}\text{-Algae}$ ) or 70 % of the  $\text{NaNO}_3$  ( $^{15}\text{N}\text{-Algae}$ ) with its heavy isotope equivalent (Cambridge Isotopes, 99 %  $^{13}\text{C}\text{-NaHCO}_3$ , 99 %  $^{15}\text{N}\text{-NaNO}_3$ ). Subsequently, a sterile inoculum of the diatom *Thalassiosira pseudonana* ( $\sim 5\ \mu\text{m}$ ) was added. After a 3 week culture period with a 12 h light–dark cycle, the culture had reached a cell density of  $3\text{--}4 \times 10^6$  cells  $\text{mL}^{-1}$ . The diatoms were concentrated by centrifugation at 450 g and the concentrate was rinsed three times with  $0.2\ \mu\text{m}$  filtered seawater to remove residual label and the algal suspension was kept frozen until further use.

Bacteria ( $\pm 1\ \mu\text{m}$  diameter) were cultured by adding a few mL of natural seawater from the Eastern Scheldt estuary (Netherlands) to M63 culture medium adjusted after Miller (1972). To obtain  $^{13}\text{C}$  or  $^{15}\text{N}$  isotopically labelled bacteria, 50 % of glucose ( $3\ \text{g L}^{-1}$ ) or 50 % of  $\text{NH}_4\text{Cl}$  ( $1.125\ \text{g L}^{-1}$ ) was replaced by its heavy isotope equivalent

(Cambridge Isotopes, 99 %  $^{13}\text{C}\text{-glucose}$ , 99 %  $^{15}\text{N}\text{-NH}_4\text{Cl}$ ) in the culture medium. After 3 days of culturing in the dark, bacteria were concentrated by centrifugation ( $14\ 500\ \text{g}$ ), rinsed three times with  $0.2\ \mu\text{m}$  filtered seawater to remove residual label and the bacterial suspension was stored frozen until the start of the experiment.

Subsamples of the algae ( $n = 3$ ) and bacteria ( $n = 3$ ) were measured for  $^{13}\text{C}$ ,  $^{15}\text{N}$ , C and N (see below). The algae used in the experiment had a molar C : N ratio of  $7.8 \pm 0.5$ , 44 at %  $^{13}\text{C}$  and 65 at %  $^{15}\text{N}$ , while bacteria had a C : N ratio of  $4.8 \pm 0.2$ , 58 at %  $^{13}\text{C}$  and 47 at % of  $^{15}\text{N}$ .

### 2.4 Experimental procedure

Prior to the start of the experiment, 10 L incubation chambers were filled with  $5\ \mu\text{m}$  of filtered bottom water from the nearby Koster fjord and placed in a temperature-controlled room that was maintained at  $7\ ^\circ\text{C}$ . Each coral fragment was inserted into an elastic silicone tube, which was mounted on an acrylic plate to allow easy fixing onto the chamber base and to ensure that the fragments retained an upright position. During the experiment, a continuous level of turbulence and water circulation was maintained by a motor-

driven paddle wheel in the upper part of the incubation chamber (speed = 2 rpm).

The corals were exposed to the isotopically labelled food for 12 h per day during 10 consecutive days (i.e. the “feeding period”). A food suspension dosage of a few millilitres was given at the beginning of each day during the feeding period with the respective concentration and ratio of  $^{13}\text{C}$  bacteria /  $^{15}\text{N}$  algae and  $^{13}\text{C}$  algae /  $^{15}\text{N}$  bacteria (see above and Fig. 1). After 12 h of exposure to the food dosage, the chambers were flushed with 5  $\mu\text{m}$  filtered Koster fjord water (140 mL  $\text{min}^{-1}$ ) for 12 h to remove food particles, avoid accumulation of waste products and renew the  $\text{O}_2$  supply. Corals for background isotope measurements (controls) were incubated in parallel under ‘acclimatization’ conditions, i.e. only exposed to sand-filtered seawater.

After the last flushing period on day 10, the incubation chambers were closed for 48 h to measure the production of  $^{13}\text{C}$  dissolved inorganic carbon ( $^{13}\text{C}$ -DIC) as a proxy for respiration (Moodley et al., 2000). Filtered (GF/F) water samples were taken for DIC analysis before (control) and after the incubation period and stored in a 10 mL headspace vial. Biological activity was stopped by adding 10  $\mu\text{L}$   $\text{HgCl}_2$  to the vials. The vials were closed with an aluminium cap fitted with a rubber septum and stored upside down for further analysis. Calculations based on literature respiration rates (Dodds et al., 2007) and pilot experiments indicated that the expected changes in pH and oxygen and ammonium concentration during the incubations are limited, so that no negative affect on coral or sponge physiology was expected. Coral fragments were stored frozen ( $-20^\circ\text{C}$ ) at the end of the incubation for further analysis.

## 2.5 Sample analysis

Coral fragments were freeze-dried, weighed and subsequent ground with a ball mill for 20 s (MM 2000, Retsch; Haan, Germany). This ground coral material, comprised of skeleton and organic tissue, was measured for the incorporation of isotopic tracers in the skeleton and tissue (following Tanaka et al., 2007; Mueller et al., 2013). Around 30 mg of a coral sample was transferred to silver measuring boats and measured for C content and  $^{13}\text{C}$  at % using a Thermo Electron Flash EA 1112 analyzer (EA) coupled to a Delta V isotope ratio mass spectrometer (IRMS). Another 30 mg of ground coral was transferred to pre-combusted silver boats and gently decalcified by acidification by placing them in an acidic fume for 3 to 4 days to remove most of the inorganic C. The ground coral was then further acidified by stepwise addition of HCl with increasing concentration (maximum concentration 12  $\text{mol L}^{-1}$ ) until the inorganic skeleton was removed (as evidenced by the absence of bubbling after further acid addition) (Mueller et al., 2013). After acidification, the samples were analysed on the EA-IRMS for C and N content and  $^{13}\text{C}$  and  $^{15}\text{N}$  at % in the organic fraction. Incorporation of  $^{13}\text{C}$  into the inorganic skeleton, as proxy for calcification

(sensu Tanaka et al., 2007), was obtained by subtracting the  $^{13}\text{C}$  in the organic fraction from the total  $^{13}\text{C}$  in the ground coral material. Note that this calcification proxy only tracks the incorporation of “metabolically derived” carbon, as the  $^{13}\text{C}$  needs to be liberated by metabolism from the organic resource (algae or bacteria) before it can be incorporated. Calcification based on metabolically derived C may only be a small fraction of total calcification, but it can still be used as a tracer to detect changes in calcification (Mueller et al., 2013).

In the headspace vials taken for DIC analysis, a headspace of  $\sim 3$  mL was created by injecting  $\text{N}_2$  gas through the vial septum (Mueller et al., 2013). Samples were acidified with 20  $\mu\text{L}$  of concentrated  $\text{H}_3\text{PO}_4$  to transform DIC into gaseous  $\text{CO}_2$ . A 10  $\mu\text{L}$  sample of the headspace was injected into the EA-IRMS for analysis of  $\text{CO}_2$  concentration and at % of  $^{13}\text{C}$ - $\text{CO}_2$ .

The incorporation of  $^{13}\text{C}$  and  $^{15}\text{N}$  in coral tissue and  $^{13}\text{C}$  in  $\text{CaCO}_3$  is the excess ( $E$ )  $^{13}\text{C}$  or  $^{15}\text{N}$  in a sample and is calculated as  $E = F_{\text{experiment}} - F_{\text{background}}$ , in which  $F$  represents the at % of  $^{13}\text{C}$  or  $^{15}\text{N}$  (i.e.  $^{13}\text{C} / [^{12}\text{C} + ^{13}\text{C}]$  and  $^{15}\text{N} / [^{14}\text{N} + ^{15}\text{N}]$ , respectively) in an experimental or background sample. Hence,  $E$  is the above-background at % of  $^{13}\text{C}$  or  $^{15}\text{N}$  and positive values indicate transfer of isotope from the original algal or bacterial source to the coral. The excess values are multiplied with the C or N content in the ground coral material (i.e.  $\mu\text{mol C g}^{-1}$  DW and  $\mu\text{mol N g}^{-1}$  DW, respectively) and divided with the at % enrichment of the specific food source to obtain total incorporation rate during the “feeding period” in  $\mu\text{mol C g}^{-1}$  DW and  $\mu\text{mol N g}^{-1}$  DW. Incorporation rates throughout the paper are expressed as the daily rates by dividing total incorporation with the length of the feeding period (i.e. 10 days). Total respiration is calculated similarly, in which excess values of DIC are multiplied with the DIC concentration ( $\mu\text{mol C L}^{-1}$ ) and chamber volume (10 L). Daily respiration rates are calculated over the length of the incubation period (2 days) and normalized to the coral weight (g DW) in an incubation chamber.

## 2.6 Data analysis

Selective uptake of algae or bacteria was assessed with the Chesson index (Chesson, 1983):

$$\alpha_i = \frac{r_i/n_i}{\sum_j r_j/n_j}, \quad (1)$$

in which  $\alpha_i$  is the selectivity index for resource  $i$ ,  $r_i$  is the uptake of resource  $i$  expressed as C or N uptake  $\text{g}^{-1}$  DW  $\text{d}^{-1}$ ,  $n_i$  is the initial concentration of resource  $i$  in the incubation chamber and  $j$  is the total number of resources ( $j = 2$  in this study). The Chesson index was calculated per food concentration tested and allows indicating selective uptake as the uptake is normalized to the respective food concentration, i.e. the algae vs. bacterial uptake is normalized for the dif-

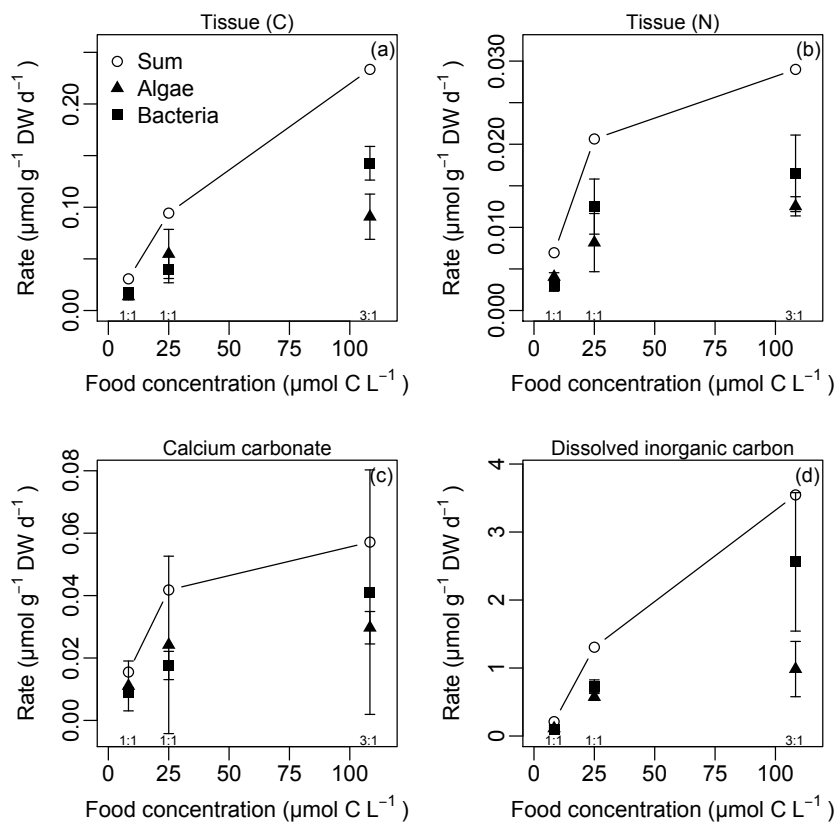


**Figure 2.** Food processing by the cold-water coral *L. pertusa* at different food concentrations and compositions. **(a)** Carbon assimilation in tissue, **(b)** nitrogen assimilation in tissue, **(c)** carbon incorporation into coral skeleton, **(d)** carbon respiration. The mean  $\pm$  range is shown for the low food concentration treatment ( $n = 2$ ). The ratios 1 : 1 and 3 : 1 in the sub-panels indicate the ratio of bacteria : algae in the respective food concentration treatment.

ferences in their availability. The selectivity indices sum to 1 and in the present experiment a selectivity index of 0.5 implies no selectivity,  $>0.5$  indicates “positive” selectivity (i.e. higher uptake than proportional availability) and  $<0.5$  indicates “negative” selectivity.

A net growth efficiency (NGE) was calculated from the C incorporation into tissue rate and the respiration rate as:  $\text{NGE} = \text{tissue incorporation} / (\text{tissue incorporation} + \text{respiration})$ . We also explored resource stoichiometric utilization by comparing the C : N ratio of food uptake from the algal and bacterial resources with the C : N ratio of the food in the incubation chamber (algal–bacterial mixture has a C : N of 5.9 in the low and medium food treatment and 5.3 in the high food treatment). Data are presented as mean  $\pm$  SD, except where stated otherwise, and figures were made in R (R Development Core Team, 2015). The bacteria : algae ratio was not constant over the food concentrations tested (see “Experimental design” above); therefore, we refrained from statistical comparisons and instead discuss the trends in the data.

### 3 Results

#### 3.1 Tissue incorporation and processing of food sources

Both bacterial and algal C and N were incorporated into the coral tissue and their incorporation rates increased with increasing food concentrations (Fig. 2a, b). Incorporation of algal C increased from 0.013 to 0.09  $\mu\text{g C g}^{-1} \text{DW d}^{-1}$  and bacterial C increased from 0.017 to 0.14  $\mu\text{g C g}^{-1} \text{DW d}^{-1}$  over the food concentration range (Fig. 2a). The incorporation rate into the carbonate skeleton tended to increase with food concentrations, but the estimated rates were associated with a high variability (Fig. 2c). Respiration of algal C increased substantially from 0.11 to 0.98  $\mu\text{g C g}^{-1} \text{DW d}^{-1}$  and bacterial C increased from 0.10 to 2.6  $\mu\text{g C g}^{-1} \text{DW d}^{-1}$  with increasing food concentration (Fig. 2d). The higher bacterial uptake and processing in the highest food treatment could be the result of the (unintended) higher bacteria : algae ratio in this treatment as compared to the other two treatments (3 : 1 vs. 1 : 1, respectively). A total of  $2.6 \pm 0.6$ ,  $4.8 \pm 0.8$  and  $3.6 \pm 1.4$  % of the total added organic carbon was recovered in the investigated pools with increasing food concentrations (low, medium, high) respectively.

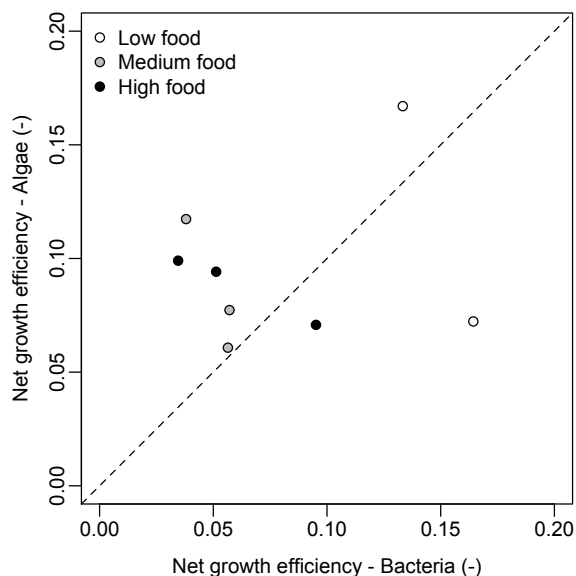


**Figure 3.** The net growth efficiency of *L. pertusa* when feeding on algae vs. bacteria. The colours represent the low, medium and high food concentrations, as in Fig. 2.

The incorporation rates into tissue were low compared to respiration losses (Fig. 3), resulting in low net growth efficiencies (NGEs) of  $0.08 \pm 0.03$ , independent of food concentration or type (Fig. 3).

The stoichiometric comparison shows that at low food concentrations the C:N incorporation into the coral tissue was equal to or lower than the bulk tissue C:N ratio of the coral ( $6.3 \pm 1.5$ , mean  $\pm$  SD) and the offered suspended food (i.e.  $^{13}\text{C}$ -algae +  $^{15}\text{N}$ -bacteria and  $^{15}\text{N}$ -algae +  $^{13}\text{C}$ -bacteria, Fig. 4). In the high food concentration treatment, however, the C:N incorporation into the coral tissue was evidently different between the two treatments (Fig. 4). The C:N values ranged from 4.9 to 6.8 in the  $^{13}\text{C}$ -algae +  $^{15}\text{N}$ -bacteria treatment and from 9.6 to 14.2 in the  $^{15}\text{N}$ -algae +  $^{13}\text{C}$ -bacteria treatment, indicating uncoupled processing of the available C and N.

### 3.2 Food selectivity

We found the mean C-based Chesson index for bacteria ranging from 0.56 to 0.35 over the food treatments and for algae ranging from 0.44 to 0.65 (Fig. 5a). When food concentration and food uptake are expressed in N-equivalents, the mean Chesson index ranged from 0.30 to 0.61 for bacteria and from 0.39 to 0.70 for algae (Fig. 5b). There was a clear tendency for selective uptake of algae at the higher food concentration treatment.

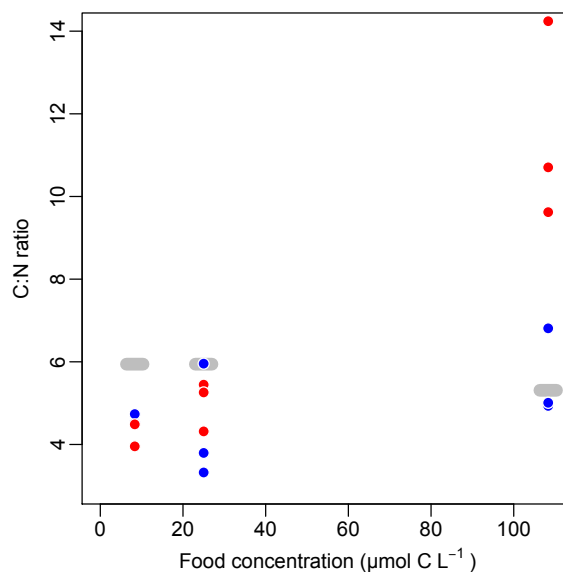


**Figure 4.** Resource stoichiometry in the experiment, presented as the C:N ratio of the resource vs. the C:N ratio in the coral tissue after the incubation. The grey bar is the C:N ratio of the suspended food (i.e. algae + bacteria), the blue dots are the C:N ratios of the coral tissue in the treatment  $^{13}\text{C}$ -algae +  $^{15}\text{N}$ -bacteria and the red dots are the C:N ratios of the coral tissue in the treatment  $^{15}\text{N}$ -algae +  $^{13}\text{C}$ -bacteria.

## 4 Discussion

### 4.1 Concentration-dependent food uptake and processing by *Lophelia pertusa*

Higher suspended food concentrations resulted in increased assimilation and respiration rates by *L. pertusa*, indicating that food uptake and metabolism is tightly coupled to food availability. This is consistent with observations by Purser et al. (2010) and Larsson et al. (2013) showing higher respiration and removal rates of zooplankton with increased particle concentration. Interestingly, food capture rates in Purser et al. (2010) and metabolic activity in this study start to saturate at a food concentration above  $100 \mu\text{mol C L}^{-1}$ . POC concentrations above cold-water coral (CWC) reefs vary between 1 and  $11 \mu\text{g C L}^{-1}$  (Kiriakoulakis et al., 2007; Wagner et al., 2011), which implies that *L. pertusa* is well adapted to exploit temporal pulses of high organic matter concentrations in the bottom water caused by internal waves and downwelling events such as observed in the Mingulay Reef complex (Davies et al., 2009), Tisler Reef (Wagner et al., 2011) and the Logachev Mounds at Rockall Bank (Duineveld et al., 2007; Soetaert et al., In press).

In contrast to assimilation and respiration rates, calcification rates increased less pronouncedly with increasing food concentration and were associated with a high variability. Hennige et al. (2014) found a short-term response in respiration rates by *L. pertusa* to higher  $p\text{CO}_2$  conditions, but calci-

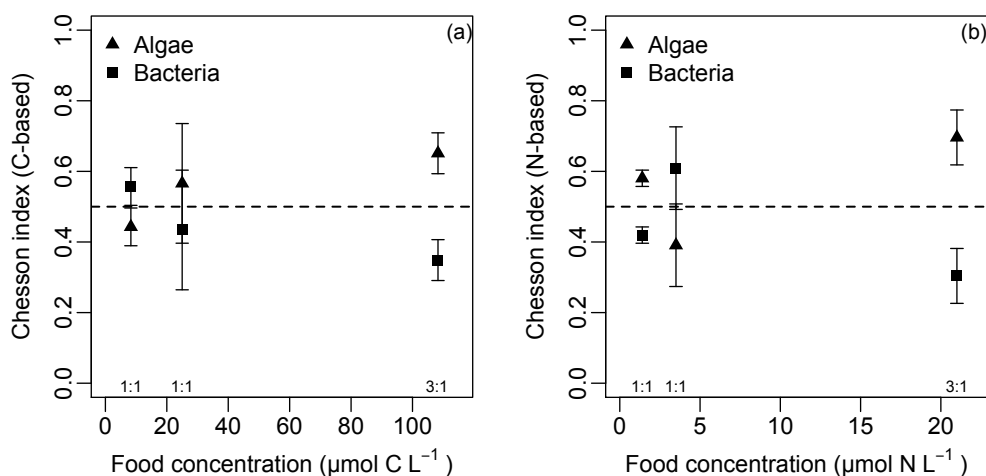


**Figure 5.** The Chesson index of *L. pertusa* for feeding on bacteria and algae expressed in (a) carbon and (b) nitrogen. The mean  $\pm$  range is shown for the low food concentration treatment ( $n = 2$ ). The ratios 1 : 1 and 3 : 1 in both sub-panels indicate the ratio of bacteria : algae in the respective food concentration treatment.

fication rates were not significantly affected. Similarly, Larsson et al. (2013) did not find a response in skeletal growth of *L. pertusa* after long-term exposure (months) to different food concentrations. Hence, it seems that the response time of calcification acts on a longer timescale than does food availability. Also, for tropical coral it is known that calcification processes can be less responsive to environmental conditions than tissue growth (Anthony and Fabricius, 2000; Tanaka et al., 2007; Tolosa et al., 2011). One explanation why a longer time period is needed before a response in calcification to altered food conditions can be measured may be the relatively low metabolic costs related to calcification in *L. pertusa* (McCulloch et al., 2012; Larsson et al., 2013). However, Naumann et al. (2011) did measure significantly higher calcification in fed compared to unfed specimens of the CWC *Desmophyllum dianthus*, but *D. dianthus* is a faster growing species and may therefore respond more rapidly to food availability.

The net growth efficiency (NGE) is the percentage of assimilated organic carbon that is transferred into biomass. Hence, a high NGE means that a food source is efficiently shunted into biomass. We are not aware of NGE estimates for cold-water corals in the literature. The NGEs of *L. pertusa* in our study ranged from 4 to 17%, and these values are low compared to values of > 50% for zooplankton (Anderson et al., 2005), a taxonomic group for which NGE is well studied. The shallow-water anemone *Anthopleura elegantissima*, taxonomically closely related to corals, also has substantially higher NGEs ranging from 30 to 60% (Zamer, 1986). The NGE is positively correlated with growth rate for the sponge *Halichondria panicea* (Thomassen and Riisgard, 1995) and the bivalve *Mytilus edulis* (Kiørboe et al., 1981), and we therefore speculate that the low NGE of the cold-water coral *L. pertusa* is related to its slow growth rate (Roberts et al.,

2009). The NGE tends to be higher when *L. pertusa* was feeding on algae compared to bacteria (Fig. 3), but these estimates are associated with a high variability. Hence, although it is known that the NGE can depend on food quality and quantity (Anderson et al., 2005), additional research is necessary to determine that relation for cold-water corals.

#### 4.2 Food-composition dependent uptake by *L. pertusa*

Food assimilation at the lower two food concentrations responded proportionally to resource stoichiometry (Fig. 4) and food composition (Fig. 5), which indicates that *L. pertusa* is an opportunistic and seemingly unselective feeder. This opportunistic feeding strategy is consistent with uptake of various organic resources in aquarium experiments (Gori et al., 2014; Mueller et al., 2014; Orejas et al., 2016) and inferences from natural abundance stable isotope and fatty acid compositions from field-collected CWC (Duineveld et al., 2007; Dodds et al., 2009). Interestingly however, at higher food concentrations it appears that *L. pertusa* feeds selectively on algae (Fig. 5) and the C : N uptake or retention becomes unbalanced, with a comparatively higher uptake or retention of bacterial carbon as compared to algal nitrogen in the <sup>15</sup>N-algae + <sup>13</sup>C-bacteria treatment (Fig. 4). This conclusion is tentative because the high food concentration treatment contained proportionally more bacteria than algae (see Sect. 2.1), but these results do suggest that *L. pertusa* assimilates food in proportion to availability at comparatively lower food concentrations. Whereas, when food is in ample supply, *L. pertusa* starts to feed preferentially on algal organic matter and differentially process the carbon and nitrogen derived from its resources.

Our data do not allow identification of which mechanisms drive the observed food selectivity. The algal cells (5 µm)

are a factor of 5 larger in diameter than bacteria, meaning food size may be a trigger that induces selective behaviour. Consistently, Tsounis et al. (2010) found that several CWCs, amongst other *L. pertusa*, fed at higher rates on adult *Artemia salina* compared to the smaller-sized *A. salina* nauplii. Shimeta and Koehl (1997) conducted a theoretical analysis of selective feeding by passive suspension feeders and found particle selection to be a function of encounter, retention and handling. For the particles considered in this study, i.e. bacteria and algae that are substantially smaller than the feeding tentacles, Shimeta and Koehl predict that encounter rates increase with particle size, while particle retention is likely to be independent of particle size. Sole mechanical predictions for the food handling stage provide only part of the story because behavioural choices may play an important role as well (Shimeta and Koehl, 1997). In this study, a role for behavioural and/or physiological responses is suggested by the uncoupling of C and N processing at a higher food concentration. Behavioural triggers that may increase encounter and retention, include enhanced polyp extension in the presence of the preferred food source or environmental conditions (Orejas et al., 2016) and trapping of food particles with the aid of mucus secretion (Mortensen, 2001). Zetsche et al. (2016) recently showed that mucus from *L. pertusa* is produced in small amounts and occurs localized in response to different stimuli. When exposed to *A. salina* nauplii, mucus strings and so-called “string balls” were observed to enhance food trapping. Given the comparatively small particle size used in this study and the uncoupling of C and N processing at higher food concentrations, we suggest that behavioural responses and subsequent physiological processing are more likely to explain the observed food selectivity as compared to the physical–mechanical considerations.

## 5 Data availability

The data underlying this manuscript are published in PANGAEA under <https://doi.pangaea.de/10.1594/PANGAEA.865313>.

**Acknowledgements.** Lisbeth Jonsson and Ann Larsson are thanked for their assistance with sampling and coral maintenance. Pieter van Rijswijk is thanked for his help whenever it was needed the most. The analytical lab of NIOZ-Yerseke is thanked for sample analysis. This research was supported by the CALMARO project (FP7/2007-2013) within the European Community’s Seventh Framework Program (FP7/2007-2013), by the Netherlands Earth System Science Center (NESSC) and by the Netherlands Organisation for Scientific Research (NWO-VIDI grant no. 864.13.007).

Edited by: C. Woulds

Reviewed by: E. Gontikaki and W. R. Hunter

## References

- Anderson, T. R., Hessen, D. O., Elser, J. J., and Urabe, J.: Metabolic stoichiometry and the fate of excess carbon and nutrients in consumers, *Am. Nat.*, 165, 1–15, 2005.
- Anthony, K. R. N. and Fabricius, K. E.: Shifting roles of heterotrophy and autotrophy in coral energetics under varying turbidity, *J. Exp. Mar. Biol. Ecol.*, 252, 221–253, 2000.
- Cathalot, C., Van Oevelen, D., Cox, T., Kutti, T., Lavaleye, M., Duineveld, G., and Meysman, F. J. R.: Cold-water coral reefs and adjacent sponge grounds: Hotspots of benthic respiration and organic carbon cycling in the deep sea, *Front. Mar. Sci.*, 2, 1–12, doi:10.3389/fmars.2015.00037, 2015.
- Chesson, J.: The estimation and analysis of preference and its relationship to foraging models, *Ecology*, 64, 1297–1304, 1983.
- Davies, A. J. and Guinotte, J. M.: Global habitat suitability for framework-forming cold-water corals, *PLoS One*, 6, e18483, doi:10.1371/journal.pone.0018483, 2011.
- Davies, A. J., Duineveld, G. C. A., Lavaleye, M. S. S., Bergman, M. J. N., Van Haren, H., and Roberts, J. M.: Downwelling and deep-water bottom currents as food supply mechanisms to the cold-water coral *Lophelia pertusa* (Scleractinia) at the Mingulay Reef complex, *Limnol. Oceanogr.*, 54, 620–629, 2009.
- Dodds, L. A., Roberts, J. M., Taylor, A. C., and Marubini, F.: Metabolic tolerance of the cold-water coral *Lophelia pertusa* (Scleractinia) to temperature and dissolved oxygen change, *J. Exp. Mar. Biol. Ecol.*, 349, 205–214, 2007.
- Dodds, L. A., Black, K. D., Orr, H., and Roberts, J. M.: Lipid biomarkers reveal geographical differences in food supply to the cold-water coral *Lophelia pertusa* (Scleractinia), *Mar. Ecol. Prog. Ser.*, 397, 113–124, 2009.
- Duineveld, G. C. A., Lavaleye, M. S. S., Bergman, M. I. N., De Stigter, H., and Mienis, F.: Trophic structure of a cold-water coral mound community (Rockall Bank, NE Atlantic) in relation to the near-bottom particle supply and current regime, *Bull. Mar. Sci.*, 81, 449–467, 2007.
- Findlay, H. S., Artioli, Y., Navas, J. M., Hennige, S. J., Wicks, L. C., Huvenne, V. A. I., Woodward, E. M. S., and Roberts, J. M.: Tidal downwelling and implications for the carbon biogeochemistry of cold-water corals in relation to future ocean acidification and warming, *Glob. Change Biol.*, 19, 2708–2719, 2013.
- Gori, A., Grover, R., Orejas, C., Sikorski, S., and Ferrier-Pages, C.: Uptake of dissolved free amino acids by four cold-water coral species from the Mediterranean Sea, *Deep-Sea Res. Pt. II*, 99, 42–50, 2014.
- Guihen, D., White, M., and Lundälv, T.: Temperature shocks and ecological implications at a cold-water coral reef, *Marine Biodiversity Records*, 5, 1–10, 2012.
- Guillard, R. R. L.: Culture of Phytoplankton for Feeding Marine Invertebrates, in: *Culture of Marine Invertebrate Animals*, edited by: Smith, W. L. and Chanley, M. H., Springer US, 1975.
- Hebbeln, D., Wienberg, C., Wintersteller, P., Freiwald, A., Becker, M., Beuck, L., Dullo, C., Eberli, G. P., Glogowski, S., Matos, L., Forster, N., Reyes-Bonilla, H., and Taviani, M.: Environmental forcing of the Campeche cold-water coral province, southern Gulf of Mexico, *Biogeosciences*, 11, 1799–1815, doi:10.5194/bg-11-1799-2014, 2014.
- Hennige, S. J., Wicks, L. C., Kamenos, N. A., Bakker, D. C. E., Findlay, H. S., Dumousseaud, C., and Roberts, J. M.: Short-term metabolic and growth responses of the cold-water coral *Lophelia*

- pertusa* to ocean acidification, *Deep-Sea Res. Pt. II*, 99, 27–35, 2014.
- Henry, L. A. and Roberts, J. M.: Biodiversity and ecological composition of macrobenthos on cold-water coral mounds and adjacent off-mound habitat in the bathyal Porcupine Seabight, NE Atlantic, *Deep-Sea Res. Pt. I*, 54, 654–672, 2007.
- Jensen, S., Bourne, D. G., Hovland, M., and Murrell, J. C.: High diversity of microplankton surrounds deep-water coral reef in the Norwegian Sea, *Fems Microbiol. Ecol.*, 82, 75–89, 2012.
- Kjørboe, T., Møhlenberg, F., and Nøhr, O.: Effect of suspended bottom material on growth and energetics in *Mytilus edulis*, *Mar. Biol.*, 61, 283–288, 1981.
- Kiriakoulakis, K., Fisher, E., Wolff, G. A., Freiwald, A., Grehan, A., and Roberts, J. M.: Lipids and nitrogen isotopes of two deep-water corals from the North-East Atlantic: initial results and implication for their nutrition, in: *Cold-water corals and ecosystems*, edited by: Freiwald, A. and Roberts, J. M., Springer-Verlag, Berlin Heidelberg, 2005.
- Kiriakoulakis, K., Freiwald, A., Fisher, E., and Wolff, G. A.: Organic matter quality and supply to deep-water coral/mound systems of the NW European Continental Margin, *Int. J. Earth Sci.*, 96, 159–170, 2007.
- Kutti, T., Fossa, J. H., and Bergstad, O. A.: Influence of structurally complex benthic habitats on fish distribution, *Mar. Ecol. Prog. Ser.*, 520, 175–190, 2015.
- Larsson, A. I., Lundälv, T., and van Oevelen, D.: Skeletal growth, respiration rate and fatty acid composition in the cold-water coral *Lophelia pertusa* under varying food conditions, *Mar. Ecol. Prog. Ser.*, 483, 169–184, 2013.
- Lavaleye, M., Duineveld, G., Lundälv, T., White, M., Guihen, D., Kiriakoulakis, K., and Wolff, G. A.: Cold-water corals on the Tisler reef: Preliminary observations on the dynamic reef environment, *Oceanography*, 22, 76–84, 2009.
- McCulloch, M., Falter, J., Trotter, J., and Montagna, P.: Coral resilience to ocean acidification and global warming through pH up-regulation, *Nature Climate Change*, 2, 623–633, 2012.
- Middelburg, J. J., Mueller, C. E., Veuger, B., Larsson, A. I., Form, A., and van Oevelen, D.: Discovery of symbiotic nitrogen fixation and chemoautotrophy in cold-water corals, *Sci. Rep.*, 5, 17962, doi:10.1038/srep17962, 2015.
- Miller, J. H.: Experiments in molecular genetics, Cold Spring Harbor Laboratory, 1972.
- Mohn, C., Rengstorf, A., White, M., Duineveld, G., Mienis, F., Soetaert, K., and Grehan, A.: Linking benthic hydrodynamics and cold-water coral occurrences: A high-resolution model study at three cold-water coral provinces in the NE Atlantic, *Prog. Oceanogr.*, 122, 92–104, 2014.
- Moodley, L., Boschker, H. T. S., Middelburg, J. J., Herman, P. M. J., De Deckere, E., and Heip, C. H. R.: The ecological significance of benthic Foraminifera:  $^{13}\text{C}$  labelling experiments, *Mar. Ecol. Prog. Ser.*, 202, 289–295, 2000.
- Mortensen, P. B.: Aquarium observations on the deep-water coral *Lophelia pertusa* (L., 1758) (Scleractinia) and selected associated invertebrates, *Ophelia*, 54, 83–104, 2001.
- Mueller, C. E., Lundälv, T., Middelburg, J. J., and van Oevelen, D.: The symbiosis between *Lophelia pertusa* and *Eunice norvegica* stimulates coral calcification and worm assimilation, *PLoS One*, 8, e58660, doi:10.1371/journal.pone.0058660, 2013.
- Mueller, C. E., Larsson, A. I., Veuger, B., Middelburg, J. J., and van Oevelen, D.: Opportunistic feeding on various organic food sources by the cold-water coral *Lophelia pertusa*, *Biogeosciences*, 11, 123–133, doi:10.5194/bg-11-123-2014, 2014.
- Naumann, M. S., Orejas, C., Wild, C., and Ferrier-Pages, C.: First evidence for zooplankton feeding sustaining key physiological processes in a scleractinian cold-water coral, *J. Exp. Biol.*, 214, 3570–3576, 2011.
- Orejas, C., Gori, A., Rad-Menéndez, C., Last, K. S., Davies, A. J., Beveridge, C. M., Sadd, D., Kiriakoulakis, K., Witte, U., and Roberts, J. M.: The effect of flow speed and food size on the capture efficiency and feeding behaviour of the cold-water coral *Lophelia pertusa*, *J. Exp. Mar. Biol. Ecol.*, 481, 34–40, 2016.
- Purser, A., Larsson, A. I., Thomsen, L., and van Oevelen, D.: The influence of flow velocity and food concentration on *Lophelia pertusa* (Scleractinia) zooplankton capture rates, *J. Exp. Mar. Biol. Ecol.*, 395, 55–62, 2010.
- R Development Core Team: R: A language and environment for statistical computing. R Foundation for Statistical Computing, Vienna, Austria, 2015.
- Roberts, J. M., Wheeler, A., Freiwald, A., and Cairns, S.: *Cold-water corals, The biology and geology of deep-sea coral habitats*, Cambridge University Press, Cambridge, 2009.
- Rovelli, L., Attard, K., Bryant, L., Flogel, S., Stahl, H., Roberts, J., Linke, P., and Glud, R.: Benthic  $\text{O}_2$  uptake of two cold-water coral communities estimated with the non-invasive eddy correlation technique, *Mar. Ecol. Prog. Ser.*, 525, 97–104, 2015.
- Sherwood, O. A., Jamieson, R. E., Edinger, E. N., and Wareham, V. E.: Stable C and N isotopic composition of cold-water corals from the Newfoundland and Labrador continental slope: Examination of trophic, depth and spatial effects, *Deep-Sea Res. Pt. I*, 55, 1392–1402, 2008.
- Shimeta, J. and Koehl, M. A. R.: Mechanisms of particle selection by tentaculate suspension feeders during encounter, retention, and handling, *J. Exp. Mar. Biol. Ecol.*, 209, 47–73, 1997.
- Soetaert, K., Mohn, C., Rengstorf, A., Grehan, A., and van Oevelen, D.: Ecosystem engineering creates a direct nutritional link between 600-m deep cold-water coral mounds and surface productivity, *Sci. Rep.*, 6, 35057, doi:10.1038/srep35057, 2016.
- Tanaka, Y., Miyajima, T., Koike, I., Hayashibara, T., and Ogawa, H.: Imbalanced coral growth between organic tissue and carbonate skeleton caused by nutrient enrichment, *Limnol. Oceanogr.*, 52, 1139–1146, 2007.
- Thomassen, S. and Riisgard, H. U.: Growth and energetics of the sponge *Halichondria panicea*, *Mar. Ecol. Prog. Ser.*, 128, 239–246, 1995.
- Tolosa, I., Treignier, C., Grover, R., and Ferrier-Pages, C.: Impact of feeding and short-term temperature stress on the content and isotopic signature of fatty acids, sterols, and alcohols in the scleractinian coral *Turbinaria reniformis*, *Coral Reefs*, 30, 763–774, 2011.
- Tsounis, G., Orejas, C., Reynaud, S., Gili, J. M., Allemand, D., and Ferrier-Pages, C.: Prey-capture rates in four Mediterranean cold water corals, *Mar. Ecol. Prog. Ser.*, 398, 149–155, 2010.
- Van Oevelen, D., Duineveld, G. C. A., Lavaleye, M. S. S., Mienis, F., Soetaert, K., and Heip, C. H. R.: The cold-water coral community as hotspot of carbon cycling on continental margins: a food web analysis from Rockall Bank (northeast Atlantic), *Limnol. Oceanogr.*, 54, 1829–1844, 2009.

- van Oevelen, D., Mueller, C. E., Lundälv, T., and Middelburg, J. J.: Food selectivity and processing by the cold-water coral *Lophelia pertusa*, Royal Netherlands Institute for Sea Research, Dataset #865313, 2016.
- Wagner, H., Purser, A., Thomsen, L., Jesus, C. C., and Lundälv, T.: Particulate organic matter fluxes and hydrodynamics at the Tisler cold-water coral reef, *J. Mar. Syst.*, 85, 19–29, 2011.
- White, M., Wolff, G. A., Lundälv, T., Guihen, D., Kiriakoulakis, K., Lavaleye, M., and Duineveld, G.: Cold-water coral ecosystem (Tisler Reef, Norwegian Shelf) may be a hotspot for carbon cycling, *Mar. Ecol. Prog. Ser.*, 465, 11–23, 2012.
- Yesson, C., Taylor, M. L., Tittensor, D. P., Davies, A. J., Guinotte, J., Baco, A., Black, J., Hall-Spencer, J. M., and Rogers, A. D.: Global habitat suitability of cold-water octocorals, *J. Biogeogr.*, 39, 1278–1292, 2012.
- Zamer, W. E.: Physiological energetics of the intertidal sea anemone *Anthopleura elegantissima*, *Mar. Biol.*, 92, 299–314, 1986.
- Zetsche, E.-M., Baussant, T., Meysman, F. J. R., and van Oevelen, D.: Direct Visualization of Mucus Production by the Cold-Water Coral *Lophelia pertusa* with Digital Holographic Microscopy, *PLoS One*, 11, e0146766, doi:10.1371/journal.pone.0146766, 2016.

# The cnidome and internal morphology of *Lophelia pertusa* (Linnaeus, 1758) (Cnidaria, Anthozoa)

Susanna M. Strömberg<sup>1</sup> and Carina Östman<sup>2</sup>

<sup>1</sup>Dept. of Marine Sciences, University of Gothenburg, SE-452 96 Strömstad, Sweden; <sup>2</sup>Evolutionary Biology Centre, Uppsala University, Norbyvägen 18 A, SE-752 36 Uppsala, Sweden

## Keywords:

*Lophohelia prolifera*, morphology, histology, cnidocyst, cnidoblast

Accepted for publication:

1 March 2016

## Abstract

Strömberg, S.M., Östman, C. 2017. The cnidome and internal morphology of *Lophelia pertusa* (Linnaeus, 1758) (Cnidaria, Anthozoa). – *Acta Zoologica* (Stockholm) 98: 191–213.

The cnidome of the scleractinian cold-water coral *Lophelia pertusa* (Linnaeus, 1758, syn. *Lophohelia prolifera*) was described by Carlgren in 1940. Due to a renewed interest in the cnidae of *L. pertusa*, specifically comparisons of adult and larval cnidae and their functions, we now redescribe the cnidome from material collected at the Tisler reef in Norway, close to Carlgren's collection site at Saekken (Sweden). Cnidae from column, tentacles, actinopharynx, mesenterial filaments and acontia were investigated. Fresh tissue preparations were compared to histological preparations of decalcified polyps to verify the presence of cnidocysts and secretory cells, and their composition and organization within tissues. The cnidome included microbasic b-mastigophores, microbasic and mesobasic p-mastigophores, holotrichous isorhizas and spirocysts. The nematocyst type cnidae (b-, p-mastigophores, isorhizas) appeared in different size classes with different distributions within the tissue. Spirocysts were highly variable in shape and size, without distinct size classes. In addition, developing stages of cnidae were documented, with new observations on the succession of p-mastigophore shaft development. The present observations were in general congruent with the cnidocyst descriptions from *L. prolifera* made by Carlgren; however, a tiny cnida, possibly of isorhiza type, has been added. Finally, the use of the term acontia is discussed.

Susanna M Strömberg, Dept. of Marine Sciences, University of Gothenburg, SE-452 96 Strömstad, Sweden. E-mail: susanna.stromberg@marine.gu.se

## Introduction

*Lophelia pertusa* (Linnaeus, 1758) is the most common reef-building cold-water coral with a nearly global distribution, ranging from Barents Sea to New Zealand. The depth range spans from 39 m in the Trondheim Fjord in Norway to 3383 m at the New England Seamount chain in the North Atlantic Ocean (Freiwald *et al.* 2004). The colonies have a branching growth pattern (Fig. 1A), with individual corallites of c. 10 mm diameter, and c. 20 mm in length (Gass and Roberts 2010). The vegetal growth consists of the budding of new individual polyps from the rim of the corallite of older polyps (Fig. 1B). Approximately the outermost 1 m layer of corallites contain live polyps, while older polyps beneath die due to reduced water exchange and food supply (Wilson 1979). The dead coral branches soon become colonized with

a wide range of associated fauna, while the live parts of the colonies tend to be devoid of epifauna.

Deep-sea corals such as *L. pertusa* are azooxanthellate, that is lacking symbiotic photosynthesizing dinoflagellates. Studies have shown *L. pertusa* to be opportunistic feeders, utilizing both dissolved and particulate organic matter, picoplankton (e.g. bacteria) and zooplankton (Dodds *et al.* 2009; Mueller *et al.* 2013). In the North Sea, the relatively large (2–4 mm) copepod *Calanus finmarchicus* is common and shown to be included in the diet of *L. pertusa* (Dodds *et al.* 2009). With such large prey, one could suspect that *L. pertusa* would invest in heavy cnidocyst armament.

Cnidocysts function in food capture, defence, aggression and locomotion and can be divided into three functional types: (i) penetrating (toxin delivering), (ii) ensnaring (or volvent) and (iii) glutinant cnidae (Mariscal 1984; Colin and

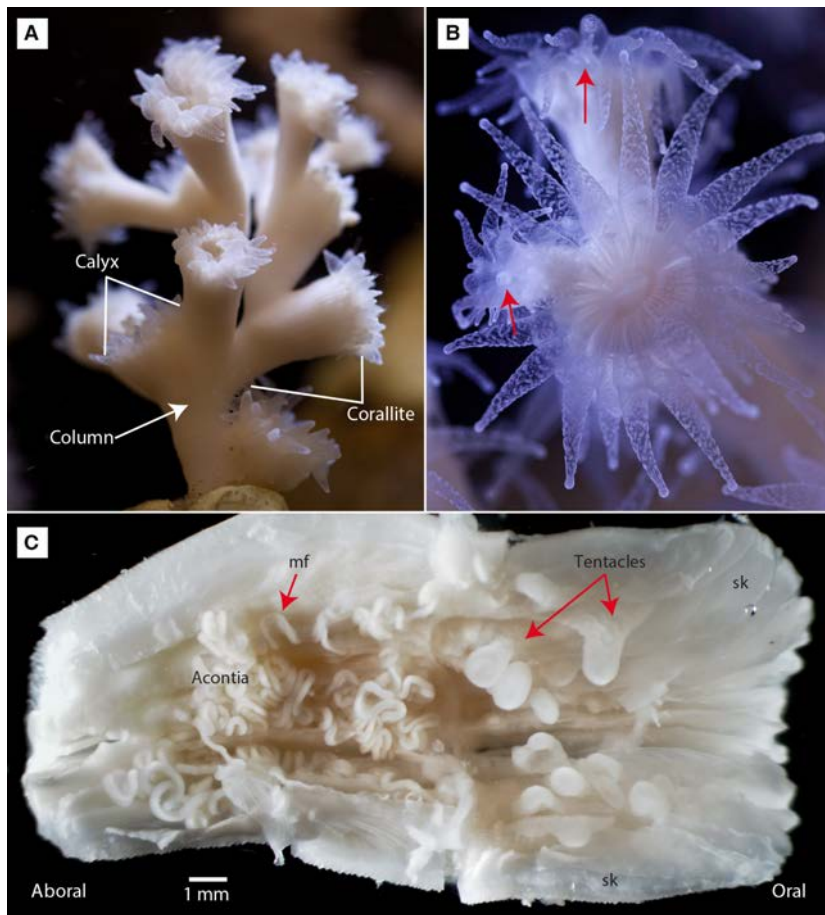


**Fig. 1**—General anatomy of *Lophelia pertusa*. – A. Colony morphology (tentacles semi-retracted). – B. Fully extended tentacles showing white blotches of cnidocyst batteries and the oral disk with mouth/actinopharynx in the centre. Red arrows point out young buds; on the lower, the actinopharynx is visible as a cylinder. – C. A corallite cut longitudinally: retracted tentacles at oral end, acontia at aboral end, mesenterial filaments (mf) attached via the mesenteries to the walls and part of the oral disk ripped apart in the middle. Skeletal lamellae/septa (sk). Corallites c. 10 mm in diameter.

Costello 2007). Glutinant cnidae are the most versatile and can function both in prey capture, tube building and in locomotion (Kass-Simon and Scappaticci 2002). Cnidocysts are classified into three categories based on morphological characters: nematocysts, spirocysts and ptychocysts. Nematocysts include penetrating and ensnaring cnidae. The other two categories are glutinant (Mariscal *et al.* 1977a,b). The highest diversity is found among nematocysts within Hydrozoa. In Anthozoa, a mere 10 of the total 30 types are present; instead, the anthozoans have added spirocysts and ptychocysts (Fautin and Mariscal 1991; Östman 2000; Kass-Simon and Scappaticci 2002; Fautin 2009).

Once a cnida is fired, it is wasted, and there is a constant replenishing of armament. Cnidogenesis has been described by Slautterback and Fawcett (1959), Skaer and Picken (1966), Westfall (1966), Skaer (1973), Holstein (1981), Tardent and Holstein (1982), among others, reviewed by Kass-Simon and Scappaticci (2002). Documentation of the morphology of developing cnidae (cnidoblasts) in different stages of maturation has been carried out for the anthozoans *Metridium senile* and *Sagartiogeton viduatus* by Östman *et al.* (2010a, b, 2013). Möbius (1866) suggested that cnidoblasts differentiate beneath the mature cnidocytes (commented in Robson

2004). Slautterback and Fawcett (1959) traced the origin of cnidoblasts from interstitial cells at the base of the epithelium. The maturing cnidae are subsequently migrating from the basal to the distal epithelium where the final maturation takes place (Skaer 1973; Tardent 1995).

The cnidome of *Lophohelia prolifera* was described by Carlgren in 1940 from material collected at Saekken in the Koster Trough (Bohuslän, Sweden, approx. 59°00.82'N, 11°06.96'E). He also included samples from the Drontheim Fjord (i.e. Trondheim Fjord, Norway). Carlgren separated the soft tissues from column, tentacles, actinopharynx and filaments (i.e. mesenterial filaments and acontia), and recorded cnidae type composition and size classes in the different tissues (Table 1).

The name *Lophohelia prolifera* is a homonym including *Lophelia pertusa*, *Madrepora oculata* and *Solenosmilia variabilis* (Fautin 2013). Later studies have confirmed the only species present at the sampling site of Carlgren to be *L. pertusa* (e.g. Dahl *et al.* 2012), and further studies on reproduction, embryology and larval development of *L. pertusa* from the area led to a renewed interest in the cnidome.

Larsson *et al.* (2014) observed cnidocyst discharge in planulae from 30 days of age and onwards, coinciding with

**Table 1** Cnidome of *Lophohelia prolifera* (syn. *Lophelia pertusa*), from Carlgren (1940, pp 44–46). Length-to-width ranges of capsules (in  $\mu\text{m}$ )

Tissue and cnidae type	Length $\times$ width ( $\mu\text{m}$ )	Carlgren's remarks
Column		
p-mastigophores	17–20 $\times$ 5.5	'very numerous'
Tentacles		
b-mastigophores	32.5–42.5 $\times$ 4–5	'fairly sparse, shaft very short, 3 spine rows'
p-mastigophores	18 $\times$ 5.5	
p-mastigophores	36–46 $\times$ 5	'common, hoplotelic <sup>2</sup> , everted shaft of capsule length, 10 spine rows'
holotrichs <sup>1</sup>	49–55 $\times$ 14–17	'sparse'
spirocysts	–	'very numerous'
Actinopharynx		
b-mastigophores	22–34 $\times$ 4–4.5	'sparse, like those of the tentacles'
p-mastigophores	14–17 $\times$ 5	'sparse, more or less oviform'
holotrichs <sup>1</sup>	60 $\times$ 12–14	'rare'
Filaments		
b-mastigophores	14–22.5 $\times$ 3	'sparse'
p-mastigophores	23–46 $\times$ 6–8	'possibly not hoplotelic <sup>2</sup> , numerous'
p-mastigophores	73–101 $\times$ 11–13	'hoplotelic <sup>2</sup> , only in the lower, strongly coiled parts of the filaments [i.e. acontia], sparse, 15 spine rows'
holotrichs <sup>1</sup>	79–94 $\times$ 13–16	'very closely situated, only in the lower, strongly coiled parts of the filaments' [i.e. acontia]
spirocysts	–	'very rare, seem to occur also in the mesenteries'

<sup>1</sup>holotrich = tubule spined throughout, corresponds to isorhizas.

<sup>2</sup>hoplotelic = shaft and distal tubule spined.

the onset of bottom-probing behaviour. The actinula larva of the hydrozoan *Tubularia mesembryanthemum*, Allman 1871 (accepted as *Ectopleura crocea* [Agassiz, 1862], WoRMS Editorial Board 2014) has been shown to use atrichous isorhizas for primary anchoring during settling (Yamashita *et al.* 2003). It was therefore hypothesized that the presence of cnidocysts in *L. pertusa* planulae is an indication of competence to settle and thus an interesting aspect of larval development. To be able to pinpoint the onset of settling competency is a valuable piece of information when constructing larval dispersal models, and the main incentive for conducting these studies.

The aim of this study was to redescribe the cnidome of adult polyps of *L. pertusa* to be able to compare cnidae of adults and planulae, with the purpose of investigating differences in adult and larval cnidae form and function.

## Materials and Methods

*Lophelia pertusa* were collected by an ROV (Remotely Operated Vehicle) from the Tisler reef in northeast Skagerrak, Norway, on 21 December 2012 (87–105 m depth at positions between 58°59'41.4"N, 10°58'07.4"E and 58°59'39.5"N, 10°58'06.4"E). The collected specimens were brought to the field station of the University of Gothenburg at Tjärnö (58°52'33.92"N, 11°8'46.60"E), situated on the west coast of Sweden and c. 10 nmi south of Tisler and Saekken. The cor-

als were kept in flow-through aquaria with filtered seawater (5  $\mu\text{m}$  Ametek polypropylene cartridges). Water temperature and salinity were kept close to *in situ* values (7–8 °C, 34–35 psu) in a constant temperature room. The corals were fed with homogenized *Calanus* copepods twice a week. The sampled corals were also used in reproductive and larval studies, and rearing methods are further described in Larsson *et al.* (2014).

Cnidocyst sizes and cnidae type composition in different tissues from newly collected *L. pertusa* were compared to the cnidocyst descriptions made by Carlgren (1940) from *Lophohelia prolifera*. In addition, preparations of live tissues of *L. pertusa* were compared to haematoxylin and eosin-stained sections of histological preparations of decalcified polyps to verify the presence of cnidocysts and secretory cells (unicellular glands), and their composition and organization within tissues.

### Fresh tissue preparation

Dissections were carried out by first cutting the corallite (skeletal cup) longitudinally with a microtome knife (Fig. 1C), and then soft tissue was pinched out with a fine forceps, trying to get clean isolated tissue samples from the five discernible tissue types, that is tentacles, actinopharynx, mesenterial filaments and acontia. Live tissue from the column (outer wall of corallites) was scraped off with a scalpel and smeared on a glass slide. Care was taken to avoid

cross-contamination of cnidocysts between tissue types; however, some cnidae were probably displaced.

The tissues were observed under an Olympus BX51 light microscope equipped with an Olympus DP70 camera, both as wet preparations of tissues with intact integrity immediately after dissection and as squash preparations, semi-dry to dry after a few hours. Usually, the cover slip was allowed to gently squash the tissues as the sample dried, rather than squashing by force. Some tissue slides were stained with a nigrosin and eosin mix (Hancock Stain). Nigrosin gives a background coloration to visualize transparent cells, as the cell membranes repel the negatively charged carbon particles and remain clear against the purplish black background. It was especially suitable for visualizing the everted shaft and tubule of nematocysts. Eosin stained some components of the spirocyst tubule well, even when still within the capsule. The developing stages of spirocysts stained with both nigrosin and eosin and were very well visualized with this method. Other cnidae types did not stain with eosin in fresh preparations.

#### Histological preparation

Coral samples were fixed in a modified Helly's solution (containing zinc chloride and potassium dichromate,  $K_2Cr_2O_7$ ), and postfixed with a 3% aqueous solution of potassium dichromate, washed in several water baths, decalcified with formic acid and stored in 50% or 70% ethanol, before and/or after decalcification. The polyps were embedded in paraffin with a melting point of 55–58 °C and cut into 4 or 6  $\mu\text{m}$  sections. Staining of sections was carried out with Harris's haematoxylin and eosin, sometimes with glacial acetic acid added to the eosin. The acid reduced the intensity of haematoxylin and gave more nuance and detail to some aspects of the morphology. Xylene was used for deparaffinization and clearing. The slides were finally mounted with Pertex and observed and photo documented under light microscopy (as described above).

#### Measurements

Cnidocyst measurements were made from photomicrographs with the image analysis software Image J (version 1.45s, Abramoff *et al.* 2004). A test of the accuracy was made by measuring cnidae of different size classes with 6 replicate measurements each. Measurements had a standard deviation with a range of  $\pm 0.1$ – $0.3$ . Cnidocysts with sufficient detail were measured, and the number of measured cnidae somewhat

reflects the abundance of each type, in each tissue. Smaller cnidae were, however, probably underestimated due to difficulties of observation. Likewise, very abundant cnidae types were left unmeasured when sufficient numbers were achieved. A total of 1376 cnidocysts were measured, from 7 different polyps, although not all tissues were covered in each polyp. The individual variation between polyps can therefore not be deduced from the present data. Whether cnidae types were divided into distinct size classes was investigated in a series of histograms on size frequency distributions presented in Fig. 2A–F and supplemental material (S1, Supplemental tables and graphs).

#### Nomenclature

Cnidae were identified by size, shape and morphology of their undischarged and discharged capsule, shaft and tubule, including spine armature. The classification system and nomenclature of cnidocysts, including nematocysts and spirocysts, established by Weill (1934) with modifications made by Carlgren (1940), Cutress (1955), Mariscal (1974), Östman (2000) and Östman *et al.* (2010a) were used.

Throughout this study, we will use *cnidocysts* as the common denotation for all cnidae types, while *nematocysts* will refer to isorhizas, p-mastigophores and b-mastigophores, thus excluding spirocysts. The *cnidocysts* are the organelles (capsule and content). The *cnidoblasts* are the cells housing the developing *cnidocysts*, while the cells containing the mature *cnidocysts* are called *cnidocytes*. The suffixes *-blast*, *-cytes* and *-cysts* will sometimes be added to the roots *nemato-* or *spiro-* when specific types are discussed.

The proper recognition of different types of secretory cells is beyond the scope of this paper. A distinction can be made between basophilic mucocytes and acidophilic granular gland cells; however, beyond this, the cellular detail in this study does not allow further distinction.

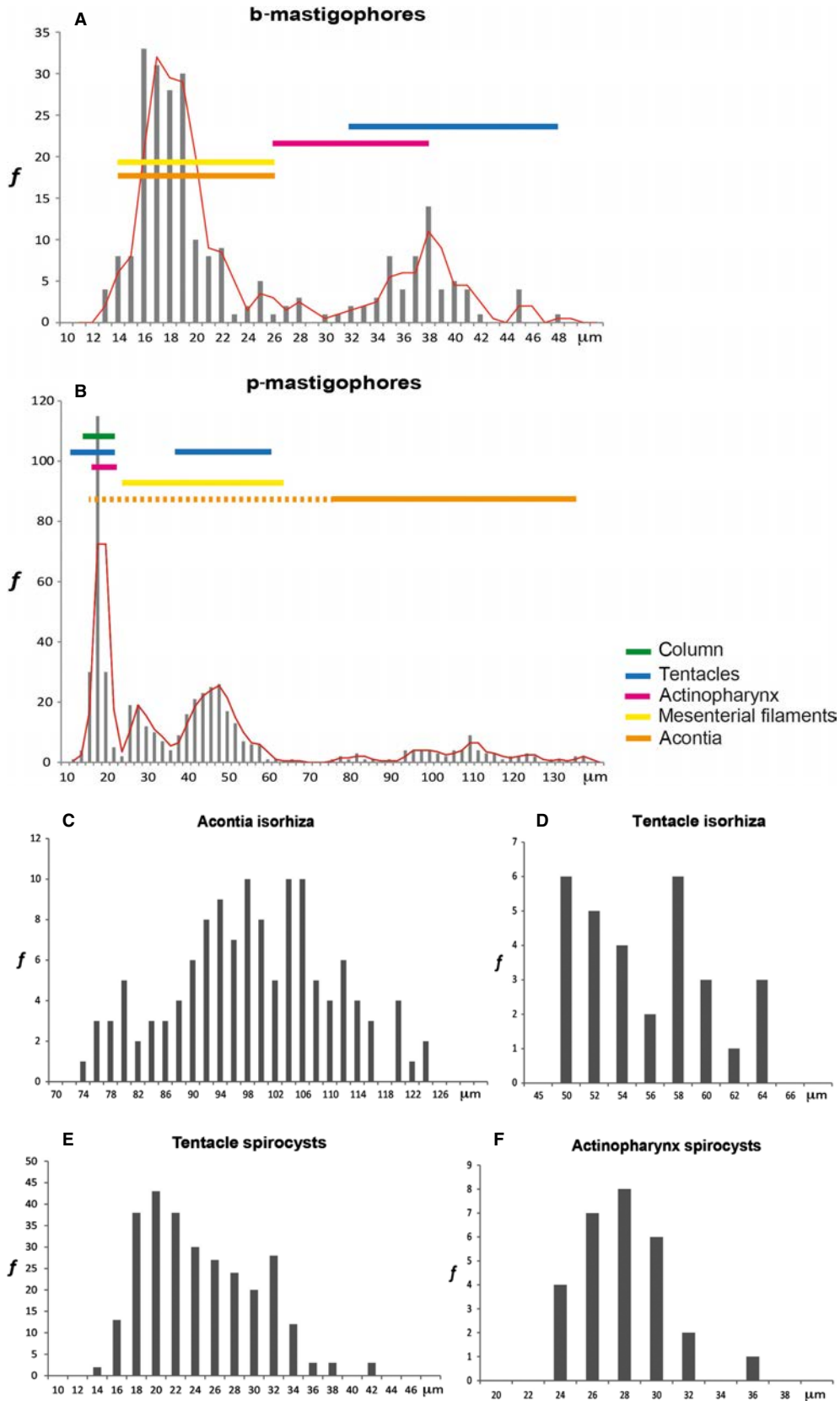
Finally, we have chosen to use the term *acontia* for the free coils of the mesenterial filaments. This term has previously not been used in scleractinian morphology; we therefore provide a justification for this in the discussion.

## Results

#### Tissue morphology and organization

*Column.* The thin tissue layer of the thecal wall (referred to as the column by Carlgren 1940) contained surprisingly

**Fig. 2**—Frequency distributions of cnidae sizes and their distribution over tissues. – A–B. Size distributions of b- and p-mastigophores in all tissues with size spans marked out for the separate tissues with color-coded lines. – A. The b-mastigophores are divided into two main size classes: small (12–22  $\mu\text{m}$ ) and large (30–48  $\mu\text{m}$ ), with a few intermediate (23–29  $\mu\text{m}$ ). – B. The p-mastigophores could be divided into four size classes: small (13–22  $\mu\text{m}$ ), medium (23–34  $\mu\text{m}$ ), large (35–69  $\mu\text{m}$ ) and very large (70–138  $\mu\text{m}$ ). Dotted part of the line for acontia p-mastigophores denotes low abundances. Trend lines in A–B are based on two point moving averages. C–D. Size distributions of isorhizas in acontia (C) and tentacles (D). Sizes were non-overlapping in the different tissues, with isorhizas in tentacles approx. half the length compared to acontia isorhizas. – E–F. Size distributions of spirocysts in tentacles (E) and actinopharynx (F) with overlapping size range.



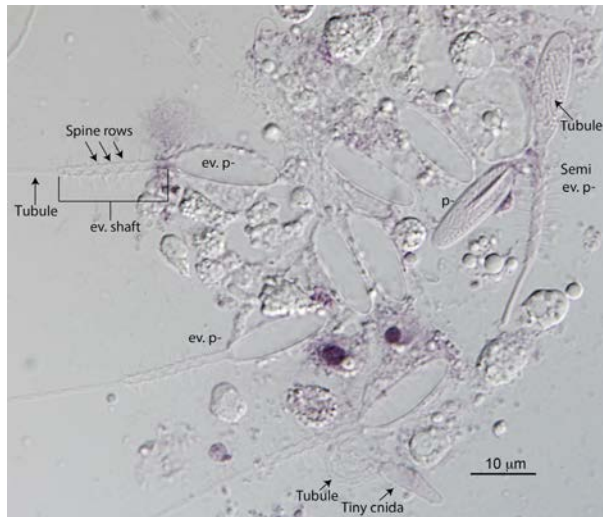


**Fig. 3**—Live tissue smear from corallite/theca wall (column). Small p-mastigophores: intact (p-); semi-everted (semi ev. p-) with everted shaft but tubule still in capsule; and fully everted (ev. p-). A tiny cnida (isorhiza) with its everted coiled tubule [Colour figure can be viewed at [wileyonlinelibrary.com](http://wileyonlinelibrary.com)].

abundant numbers of nematocysts, dominated by a homogeneous population of small microbasic p-mastigophores with rounded oval capsules (Fig. 3, Tables 2 and 3, S2 p.3). A few tiny (range: 7–9 µm) cnidae, probably of isorhiza type, were observed interspersed among the small p-mastigophores.

**Tentacles.** On live polyps with extended tentacles, the tentacle surface was spattered with irregular whitish blotches of reflective cnidocyst batteries, with translucent tissue in between (Fig. 1B). The terminal knobs (acrospheres) at the tentacle tips were uniformly whitish, capped with cnidocysts and with a slight constriction at the base of the knob. At the very apex of the tentacle tip a hydro pore (or terminal pore) was observed, visible with light microscopy in intact, fresh preparations of tentacles (Fig. 4A). The cnidocysts were oriented with their apical ends towards the pore. Dense aggregates of mucocytes were observed in the epidermis between cnidocyst batteries on the surfaces of the contracted tentacles (Fig. 4B–C).

All cnidae types were present in the tentacles (Tables 2, 3). Spirocysts dominated overall, while microbasic b- and p-mastigophores were numerous at the tip, and patchily dis-

**Table 2** Cnidome of *Lophelia pertusa* (present study). Length-to-width ranges of capsules (in µm)

Tissue and cnidae type	Length × width (µm)	n	Remarks
Column – dominated by homogenous small p-mastigophores			
p-mastigophores, small	13.9–20.8 × 3.8–6.2	111	Numerous
tiny cnidae	7.0–9.4 × 1.9–2.7	13	Sparse
Tentacles – dominated by spirocysts, all types present, rich in mucocytes			
b-mastigophores, large	31.4–47.6 × 4.0–6.0	50	Common, patchy, shaft with 4–5 spine rows
p-mastigophores, small-(medium) <sup>1</sup>	13.6–27.0 × 2.9–7.6	49	Common, patchy, shaft with 7–9 spine rows
p-mastigophores, large	35.2–58.3 × 5.0–9.6	102	Numerous, patchy, 15 and 18 spine rows
isorhizas, broad oval	45.6–63.0 × 13.9–23.1	30	Sparse
tiny cnidae	8.2–11.3 × 1.8–3.1	18	Sparse
spirocysts	12.3–41.7 × 1.7–7.2	284	Very numerous
Actinopharynx – oral disc epidermis dominated by mucocytes, actinopharynx epidermis ciliated and rich in secretory cells			
b-mastigophores, medium-large	24.4–37.9 × 2.8–5.1	19	Sparse
p-mastigophores, (small) <sup>1</sup> -medium	15.9–37.5 × 5.0–8.0	23	Sparse
spirocysts	23.7–34.7 × 1.0–7.0	28	Sparse
Mesenterial filament – secretory cells and medium p-mastigophores dominated			
b-mastigophores, small-(medium) <sup>1</sup>	12.3–24.1 × 2.3–5.1	108	Numerous, shaft with 3 spine rows
p-mastigophores, (small) <sup>1</sup> -medium	16.0–34.4 × 3.1–11.0	118	Numerous, shaft with 12 and 15 spine rows
p-mastigophores, large	35.2–63.4 × 4.9–13.3	105	Numerous, shaft with 18 and 20 spine rows
isorhizas, broad oval + large narrow	45.0–87.2 × 5.1–18.3	9	Contamination from acontia and tentacles? Not confirmed from histology
tiny cnidae	6.4–9.2 × 2.2–2.7	4	Rare
spirocysts	21.9–48.0 × 3.4–6.4	13	Contamination from tentacles? Not confirmed from histology
Acontia – dominated by large narrow isorhizas and very large p-mastigophores			
b-mastigophores, small-(medium) <sup>1</sup>	12.9–25.1 × 2.3–5.2	67	Shaft with 3 spine rows
p-mastigophores, small-large	13.9–64.8 × 4.2–13.6	22	Sparse
p-mastigophores, very large	74.7–137.7 × 9.8–16.9	75	Numerous, shaft with 28 or 38 spine rows
isorhizas, large narrow	73.4–123.9 × 14.0–21.8	126	Numerous
tiny cnidae	6.4–8.3 × 1.4–2.7	Rare	
		1376	N

<sup>1</sup>Minor contribution of size class in brackets, see Table 3.

**Table 3** *Lophelia pertusa*: cnidae type and size class distribution over tissues with ranked abundances (<sup>1</sup>)

Cnidae type	Size class	Range (µm)	Column <i>n</i>	Tentacles <i>n</i>	Actinoph <i>n</i>	Mesfil <i>n</i>	Acontia <i>n</i>
b-mast	Small	12–22				111 <sup>4</sup>	67 <sup>3</sup>
	Medium	23–29			8 <sup>1</sup>	2 <sup>1</sup>	2 <sup>1</sup>
	Large	30–48		50 <sup>3</sup>	11 <sup>2</sup>		
p-mast	Small	13–22	111 <sup>4</sup>	47 <sup>3</sup>	5 <sup>1</sup>	5 <sup>1</sup>	3 <sup>1</sup>
	Medium	23–34		3 <sup>1</sup>	18 <sup>2</sup>	113 <sup>4</sup>	7 <sup>1</sup>
	Large	35–69		102 <sup>4</sup>		105 <sup>4</sup>	12 <sup>2</sup>
	Very large	70–138					75 <sup>4</sup>
isorhiza	Large	46–63		30 <sup>2</sup>		8 <sup>1</sup>	
	Very large	73–124			1 <sup>1</sup>		128 <sup>5</sup>
tiny		6–11	13 <sup>2</sup>	17 <sup>2</sup>	4 <sup>1</sup>		2 <sup>1</sup>
spirocysts		z12–42	284 <sup>5</sup>	28 <sup>2</sup>	13 <sup>2</sup>		

<sup>1</sup>Rare.<sup>2</sup>Sparse.<sup>3</sup>Common.<sup>4</sup>Numerous.<sup>5</sup>Very numerous.

tributed along the tentacles. The microbasic b-mastigophores found in the tentacles were larger than those found in other tissues (Fig. 2A, 4E). The p-mastigophores were found in two discrete size classes, small and large (Figs 2B, 4D–E), with a few medium sized ( $n = 3$ ) included in the small category. Tiny cnidae of isorhiza type were also observed in the tentacle tissue, similar to those found in the column, with a spiraled or bent everted tubule. A few broad oval isorhizas were observed scattered among the other cnidocysts (Figs 2D, 4F). The spirocysts were highly variable in size (Figs 2E, 4D–F).

In histological preparations, the distal and basal epidermis, the mesoglea bordered by muscle fibres, the gastrodermis and tentacle lumen (i.e. endo-/exocoel) were clearly distinguishable (Fig. 5A–C). Cross sections at the base of the tentacles were oval, while sections through more apical parts were circular (Fig. 5B). The distal part of the epidermis was stained intensely pink and blue by abundant cnidocysts and mucocytes. The basal part of the epidermis was unusually wide in some tentacle cross sections. It was rich in nuclei and contained a frilly matrix of fibres, that is extensions of the myonemes from epitheliomuscular cells lining the mesoglea, and possibly components of the subepidermal nerve net. Cnidoblasts were found in the basal epidermis, close to the mesoglea (Fig. 5A, C).

Spirocysts were the most conspicuous cnidae type, while other types were less well visualized with the methods used. The spirocysts were found in bundles embedded between mucocytes, oriented with their broad apical tubule coil and capsule end towards the surface and their narrow end rooted in the epidermis (Fig. 5A–C). Their stark pink-stained coils of tubule easily identified them in the tissue. In cross-sectioned acontia, the spirocyst tubules were visible as red circles (Fig. 5A, right end). Possible p- or b-mastigophores were

sometimes seen as pale pink fusiform structures, surrounded by a pink haze, that is the shaft and tubule, respectively (Fig. 5C). The few holotrichous isorhizas observed in histological preparations of tentacles were occasionally embedded deeper in the epidermis than the other cnidae (S2 p.4) and could be identified by their larger size and more diffuse and oblique undulating coils.

*Actinopharynx.* In live corals, the actinopharynx is seen as a compressed cylinder in the middle of the oral disc, connecting the gastrovascular cavity to the outside (Figs 1B, 6A). The opening is surrounded by a protruding rim (similar to lips), that is the peristome. When the polyp opens the mouth the partition walls of the endo- and exocoelic compartments under the oral disc can be seen as white stripes in the opening (Fig. 6A). During dissections, this was also the character used for detecting the actinopharynx. When the stripes were observed, the tissue around them was pinched out with fine forceps.

The oral disc epidermis was dominated by mucocytes, sparingly interspersed with spirocysts (seen in histological sections). In fresh preparations, medium to large b-mastigophores (Figs 2A, 6C) and small oval p-mastigophores (Figs 2B, 6B) were present, but could not be confirmed on histological slides. In sections cut through the oral disc, lateral and parallel to the oral aperture, the endo- and exocoelic compartments under the oral disc were visible (Fig. 6D–D'). Large bundles of muscle fibres were observed lateral to the actinopharynx (Fig. 6E–E'). The epidermis of the actinopharynx was densely ciliated (Fig. 6F–F') and stained heavily from haematoxylin, rich in gland cells and possibly other basophilic components. Overall, the epidermis of the oral disc and the actinopharynx seems the least cnidocyst laden of all tissues (Tables 2, 3).

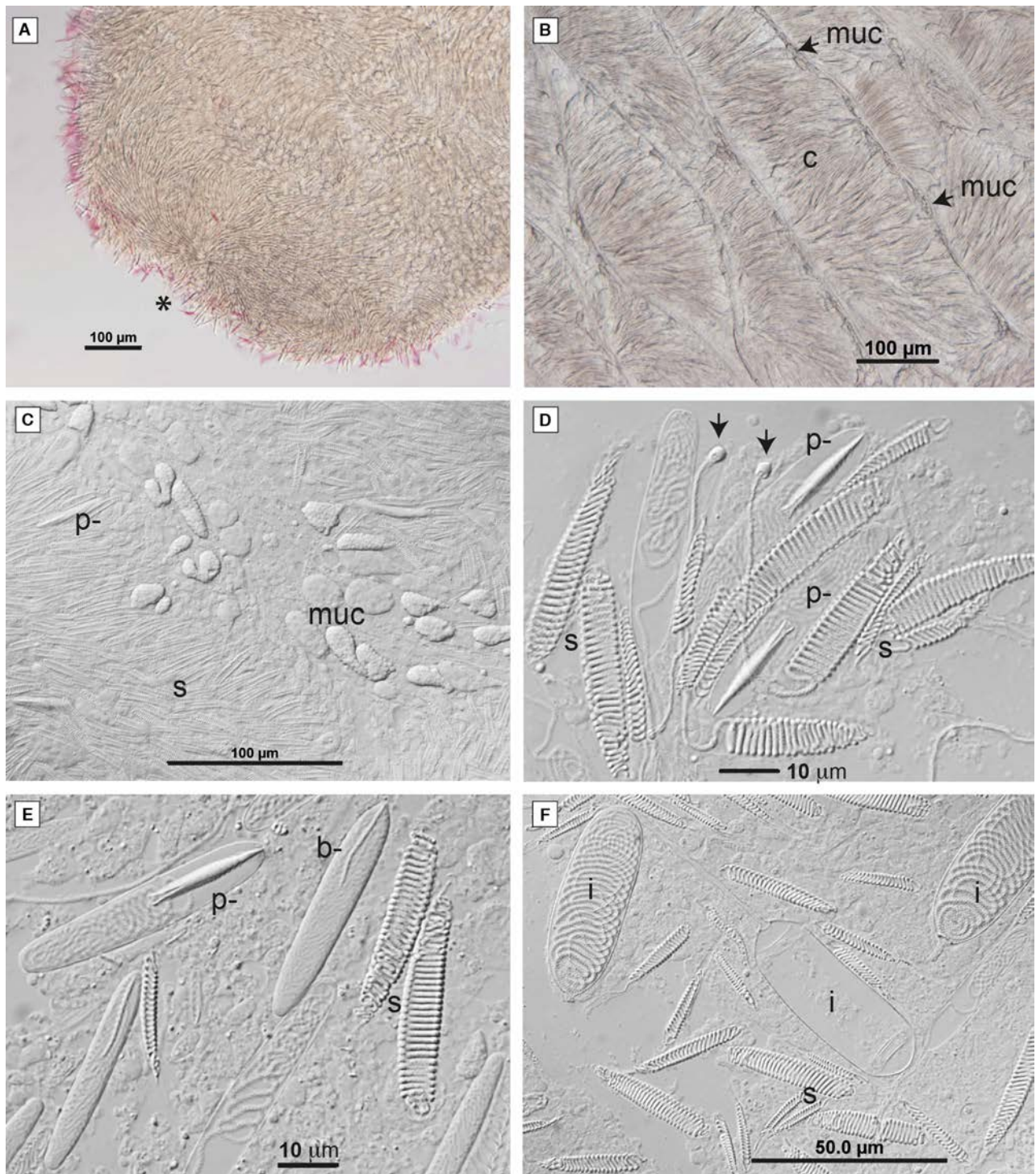


**Fig. 4**—Fresh preparations of tentacles. – A. Tentacle tip (acrosphere) with visible terminal pore (\*). Cnidae are oriented with their apical ends towards the pore. Some spirocysts are stained pink from eosin. – B. Close-up of contracted tentacle: cnidocyst batteries (c) with mucocytes (muc) in between. – C. Tentacle surface at higher magnification with spirocysts (s), p-mastigophore (p-) and mucocytes (muc). – D–F. Close-ups of tentacle cnidocytes. – D. Spirocysts (s) and p-mastigophores (p-). Distal ends of semi-everted tubules of spirocysts capped with agglutinant liquid (arrows). – E. Spirocysts (s), p-mastigophore (p-) and b-mastigophores (b-). – F. Spirocysts (s) and broad oval isorhizas (i), the latter both everted and intact [Colour figure can be viewed at [wileyonlinelibrary.com](http://wileyonlinelibrary.com)].

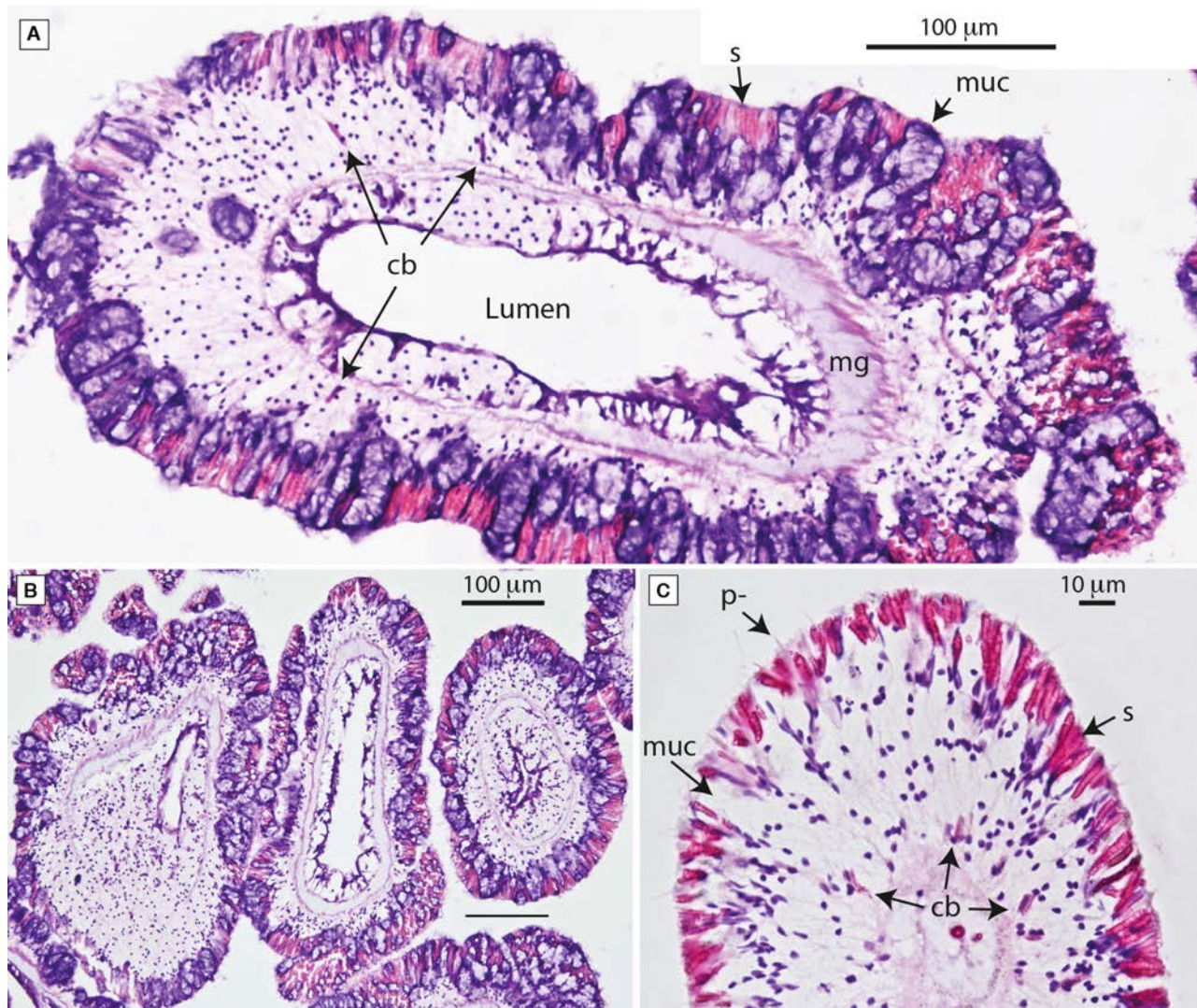


**Fig. 5**—Histological preparations of tentacles. — A. Cross section of tentacle, cut slightly oblique at the base. Epidermis facing outwards: distal part contains spirocysts (s) and mucocytes (muc); basal epidermis contains nuclei (dark dots) and a frilly matrix (pink fibres), possibly myonemes, that is extensions of the epitheliomuscular cells lining the mesoglea (mg). Arrows point out cnidoblasts (cb). The gastrodermis faces the lumen (left side intact, gastrodermal cells damaged on the right side). The tentacle lumen is continuous with the endo-/exocoels. — B. Cross sections of three tentacles. — C. Part of a cross-sectioned tentacle close to the tip (lumen not present). Acid was added to the eosin, and hematoxylin stain was partially lost; mucocytes (muc) are therefore seen as empty voids. Spirocysts (s) with dark pink-stained coils, possible pmastigophores (p-) seen as lighter pink fusiform shapes. Arrows point out cnidoblasts (cb).

*Mesenterial filaments.* In fresh squash preparations, the mesenteries were seen as muscular membranes with an undulating swollen edge, that is the cnidoglandular band (CGB, Fig. 7A–C). Adjacent to the CGB, the mesentery was thickened, and from their appearance in histological cross sections, this region has been named the *lateral lobes* (LL, Fig. 7E–F). Together, the CGB and lateral lobes constitute the mesenterial filament. The CGB were packed with cnidocysts, mucocytes and ciliated supporting cells (Fig. 7C–D). The lobes contained abundant secretory cells, and, if the animal had

been fed recently, assimilated nutrients in the phagocytic or absorptive cells, such as lipid droplets and inclusions of carotenoids from the food (Fig. 7C). In both histological and fresh preparations, there was a distinct translucent band of tissue between the CGB and lobes, lacking any refractive components (Fig. 7A–C, E).

The CGB was dominated by microbasic p-mastigophores with a large variation in size and shape, some rounded oval (prolate spheroids) and some more diamond shaped (Fig. 7D). The size distribution was bimodal (Fig. 2B, S1

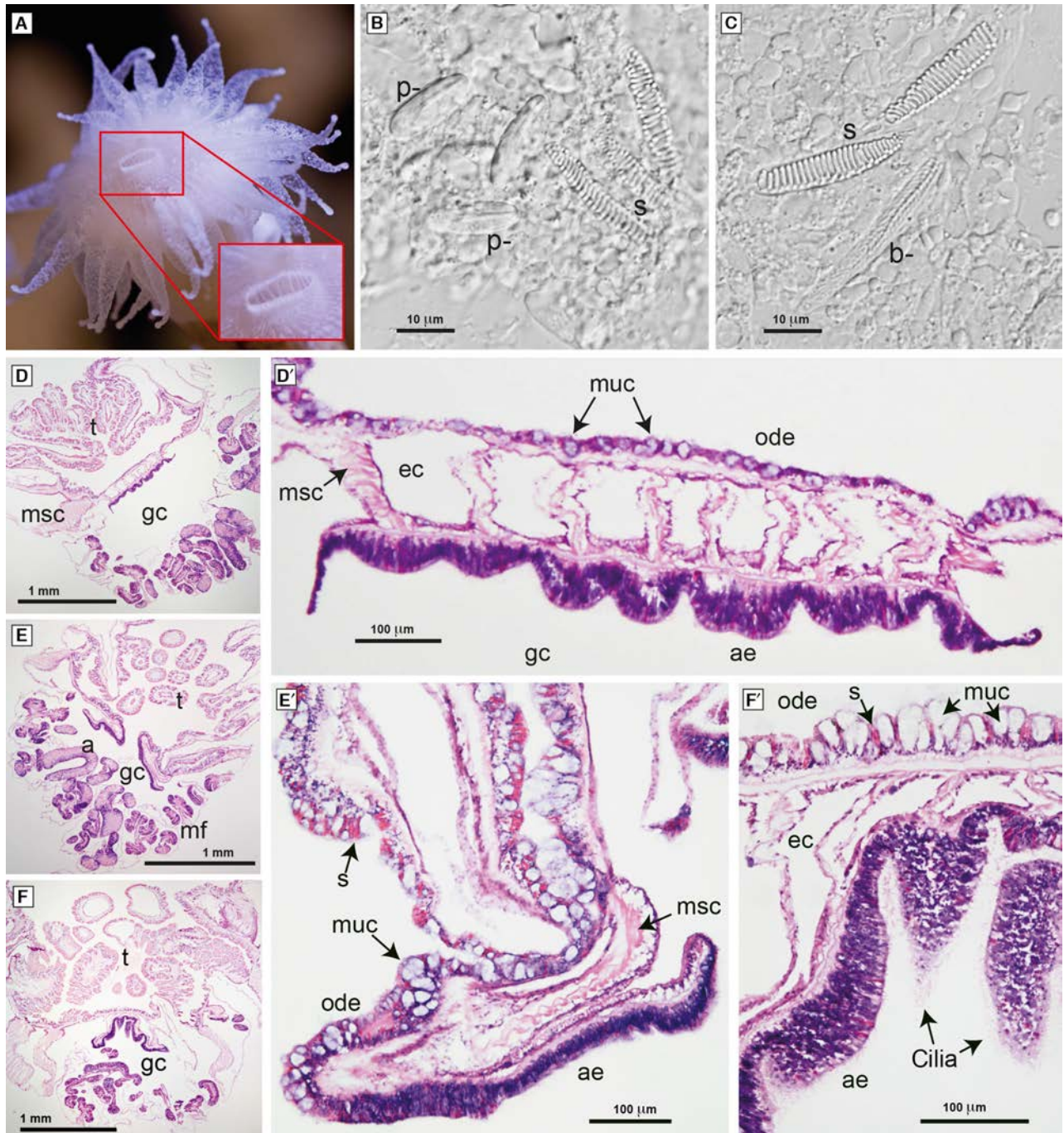


**Fig. 6**—Actinopharynx. – A. Polyp with open mouth: the white stripes are the partition walls of the body compartments (endo-/exocoels) under the oral disk, seen through the inner wall of the actinopharynx (inserted close-up). – B–C. Fresh tissue preparations from actinopharynx with small oval p-mastigophores (p-), spirocysts (s) and b-mastigophores (b-). – D, E, F. Whole-mounts of polyps with the actinopharynx centered and with corresponding close-ups in D', E' and F'. Gastrovascular cavity (gc) and tentacles (t) marked out for orientation. – D–D'. A parasagittal section of the actinopharynx, cut longitudinally adjacent to but not through, the opening. The body compartments, that is endo-/exocoels (ec), are visible between oral disk epidermis (ode) and actinopharynx epidermis (ae). Oral disk epidermis contains cnidocysts and mucocytes (muc), while the actinopharynx epidermis contains more basophilic components and is heavily ciliated. Muscle fibres (msc) in the mesenteries seen lateral to the actinopharynx. – E–E'. Actinopharynx cut through the oral pore. Acontia (a) and mesenterial filaments (mf). – F–F'. Actinopharynx cross-sectioned adjacent to the oral pore, with spirocysts (s), mucocytes (muc), endo-/exocoels (ec) and cilia visible in F'.

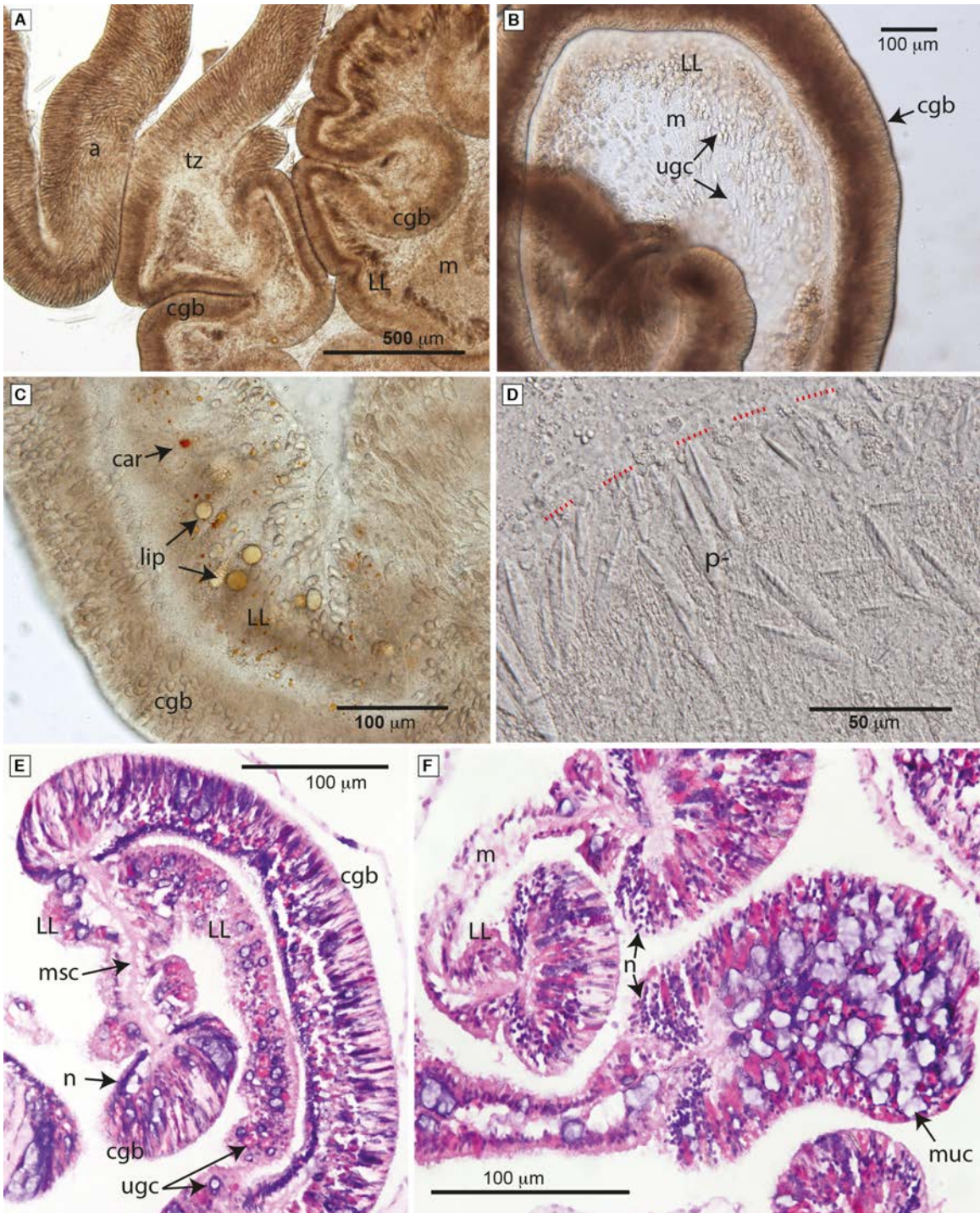


**Fig. 7**—Mesenterial filaments. – A. Transition zone (tz) between mesenterial filaments and acontia (a). The cnidoglandular band (cgb) and lateral lobes (LL) constitute the mesenterial filaments at the edge of the mesentery (m). – B. Part of mesentery (m) with cnidoglandular band (cgb) and lateral lobes (LL). Unicellular gland cells (ugc) are present throughout the mesentery, but appear denser in the lateral lobes (LL). – C. Stored nutrients in the lateral lobes (LL): lipid droplets (lip) and carotenoids (car). – D. Close-up of cnidoglandular band with diamond shaped p-mastigophores (p-); their apical ends with shafts towards the rim (red dotted lines). – E–F. Histological preparations of mesenterial filaments. – E. Longitudinal cut. Dense rows of nuclei (n) at the base of the cnidoglandular band (cgb) lateral to the attachments of muscle fibres (msc) from the mesentery. Lateral lobes (LL). Arrows also pointing out unicellular gland cells (ugc): mucocytes (blue) and acidophilic gland cells (pink). – F. Cross sections of cnidoglandular bands with large mucocytes (muc), nuclei (n), lateral lobes (LL) and part of mesentery (m) between.

p.12), including medium and large p-mastigophores (Tables 2, 3). Small b-mastigophores were abundant but inconspicuous. A few isorhizas and spirocysts were observed, although these were probably contaminations from other tissues, that is their presence could not be confirmed in histological sections.

In histological preparations, the mesenteries were heavily stained. Secretory cells were abundant, especially in the CGB and lobes (Fig. 7B, E–F). Unidentified dark purplish broad or elongate structures other than mucocytes were observed in the distal part of the gastrodermis in the CGB. Eosinophilic elongate structures were also observed, recognizable as p-mastigophores, while no spirocysts were observed (Fig. 7E–F). Also, in the lobes, pink blotches were observed, possibly acidophilic granular gland cells. Two dense lines of nuclei ran along the base of the CGB on each side of the muscle fibres from the mesentery anchored in between, with cnidocysts oriented in a fan-like manner from the base, with their apex towards the margin (Fig. 7E–F). Between the line of nuclei and the cnidocysts, pink and purple blotches were observed in the basal cell layer, probably cnidoblasts and gland cells. Even in lighter stained sections, the mesenterial filaments were too intensely stained to allow for reliable identification of all components, and thinner sections might have given better details.

*Acontia.* In fresh preparations, the acontia appeared as uniform long filaments densely packed with a distinct cnidae complement of very large nematocysts, different from the cnidae of the cnidoglandular band (CGB). Muscle fibres along the base mid-line allow them to contract in a spiral manner (Fig. 8A). Acontia emanated from the CGBs (along their lower parts), producing long free coils extending into the bottom of the gastrovascular cavity, and were of approximately twice the width compared to the CGB. Our examinations did not extend to investigating whether there were one or several acontia attached to each CGB. The transition zone between CGB and acontia was short and distinct (Fig. 7A).

Large and narrow holotrichous isorhizas dominated in the acontia, while very large p-mastigophores were patchily distributed, although sometimes abundant (Tables 2, 3, Fig. 8C). In between the very large nematocysts, small b-mastigophores and small p-mastigophores were observed. In squash preparations, medium and large p-mastigophores were also encountered, although not visible in intact acontia, and possibly associated with the transition zones, close to the CGB. A few cnidoblasts were observed among the densely packed nematocyst capsules (S2 p.5).

In histological sections of acontia, the densely packed isorhizas and p-mastigophores were found cushioned by abundant large mucocytes at the base and in between cnidae (Fig. 8E–F). Two dense rows of nuclei were observed lateral to the base mid-line on the concave side of the filament. In longitudinally cut sections, the cnidocysts were oriented with their apex pointing at the margin of the convex side (Fig. 8E). Isorhizas could be identified by their light pink-stained tubule

coils, making slightly oblique, transverse loops. The p-mastigophores were patchily distributed in between the isorhizas and stained a darker pink than the isorhiza tubules. Sometimes with the shaft recognizable as a fusiform shape surrounded by a pink haze of tubule, but mostly seen as a more diffuse strand (Fig. 8E). The capsule walls of cnidae were not visible in histological sections.

In cross-sectioned acontia, the isorhiza tubules were visible as bright pink circles, while the p-mastigophore tubules appeared as darker pink circles with a central dot (i.e. the shaft), or star-shaped, depending on where along the capsule and shaft they were sectioned (Fig. 8F). Mucocytes seemed to be confined to the margins and base, not in the central part of the acontia. The basal gastrodermis layer barely existed and was largely filled with mucocytes and a few pink blotches, possibly cnidoblasts.

### Cnidome

1. *Microbasic b-mastigophores.* These could roughly be split into two normally distributed major size classes: small (12–23  $\mu\text{m}$ ) and large (30–48  $\mu\text{m}$ ), with a few intermediate (24–29  $\mu\text{m}$ ) in between. The distribution over tissues differed between size classes (Table 3, Fig. 2A). Small b-mastigophores were restricted to the gastrodermis, that is mesenterial filaments and acontia. In intact acontia, they were observed in the tissues in among the large cnidocysts. Large b-mastigophores were restricted to the epidermis, common throughout the tentacles, and found sparingly in the actinopharynx. The intermediate sized b-mastigophores were mainly in the actinopharynx, although a few were found in the mesenterial filaments and acontia. The capsule of the b-mastigophores was narrow and elongated, with parallel sides or slightly tapering towards the basal end, that is broadest in the apical region along the shaft (Figs 6C, 9E–G). The inverted shaft was thread-like, sometimes undulating, and varied in length, reaching 0.3–0.6 of the capsule length. The tubule usually filled the capsule and made dense regular coils around the shaft, creating a characteristic pattern, and more irregularly coiled basal to the shaft. The discharged shaft was microbasic, that is shorter than the capsule (Fig. 9R–S). The homotrichous shaft armature showed 3 or 5 coils of 1–2  $\mu\text{m}$  long spines in triple helices for the respective size class. The transition between everted shaft and distal tubule was indistinct. The everted tubule was armed throughout with triple helices of tiny spines. The full length of a tubule of one small (capsule 15  $\mu\text{m}$ ) b-mastigophore was measured to c. 300  $\mu\text{m}$ , while the tubule of a large capsule (41  $\mu\text{m}$ ) had a total length of c. 1000  $\mu\text{m}$ .
2. *Microbasic and mesobasic p-mastigophores.* In all, the p-mastigophores could be divided into four size classes: small 13–22  $\mu\text{m}$ , medium 23–34  $\mu\text{m}$ , large 35–69  $\mu\text{m}$  and very large 70–138  $\mu\text{m}$  (Tables 2, 3, Figs 2B, 9B–C, H–I). The

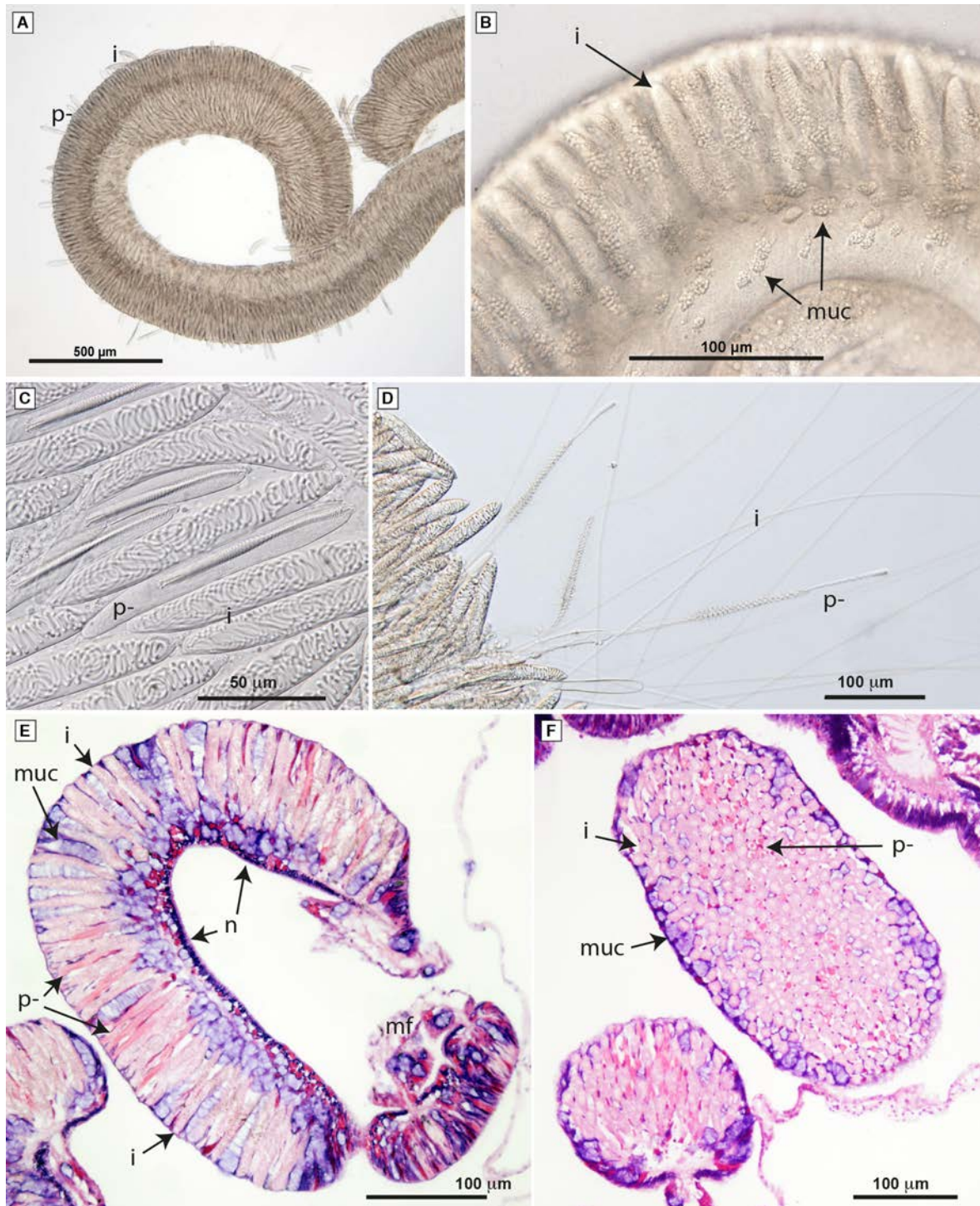


**Fig. 8**—Acontia. – A. Free coil of acontium packed with isorhizas (i) and p-mastigophores (p-). – B. Close-up of acontium with mucocytes (muc) interspersed among cnidae. – C. Densely packed cnidae: isorhizas (i) with capsules completely filled with irregular coils of tubule; p-mastigophores (p-) with shaft, and tubule coiled up in basal capsule. – D. Fired cnidae at the rim of an acontium: everted p-mastigophores (p-) with spined shafts, and holotrichous tubules of isorhizas (i). – E–F. Histological acontia preparations. – E. Longitudinally cut with pale pink isorhizas (i) with visible tubule coils and p-mastigophores (p-) as darker pink strands. Cnidae are cushioned by blue-stained mucocytes (muc). Dense rows of nuclei (n) seen at concave side (referred to as base midline in text) of acontium. – F. In cross-sectioned acontia the isorhiza (i) tubules are seen as bright pink circles, while p-mastigophore (p-) tubules are visible as circles with a central dot (shaft).

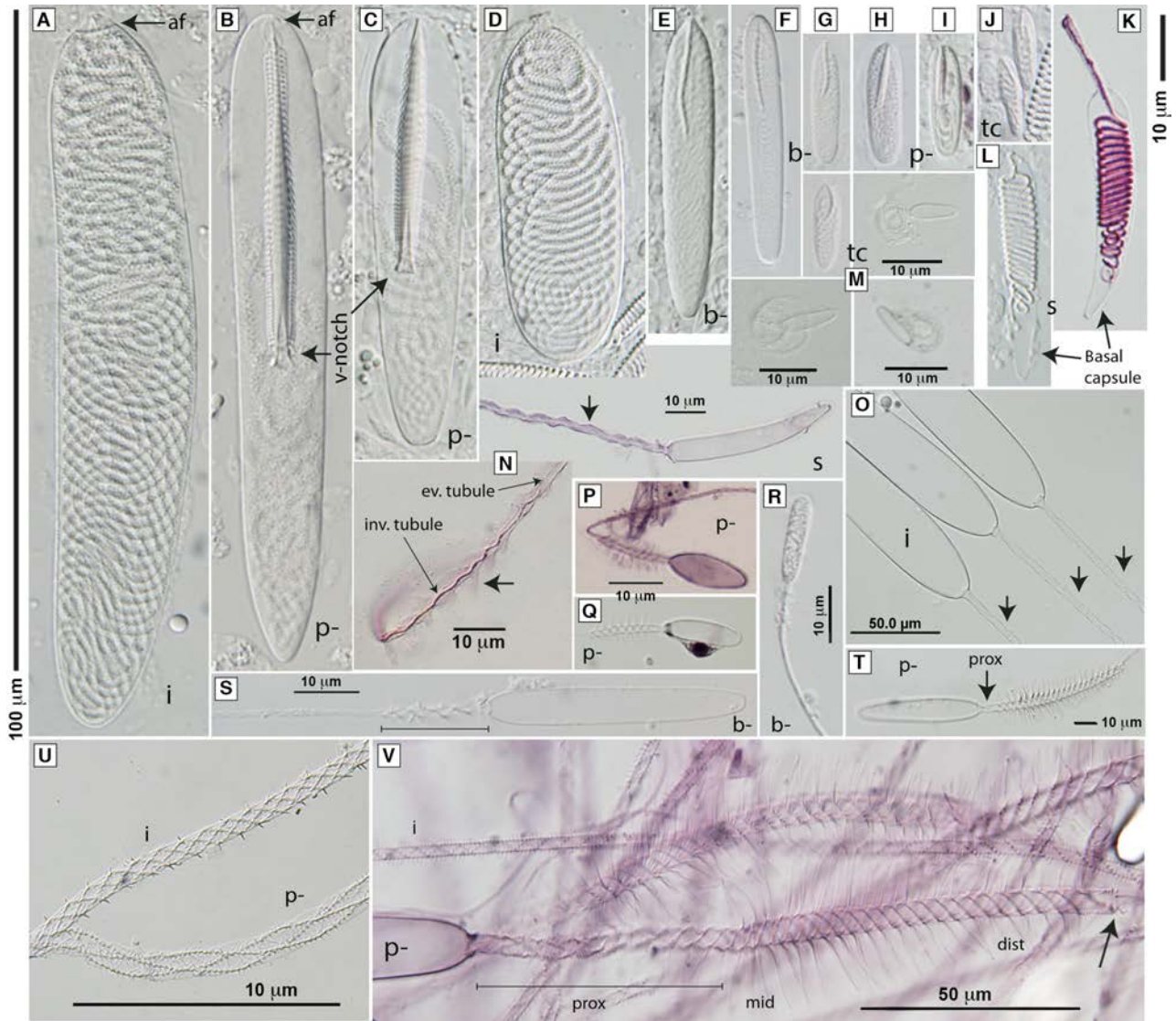


**Fig. 9**—Cnidome of *Lophelia pertusa*. – A–L and upper left M: intact capsules, all oriented with their apical ends up and basal ends down and in scale with the lateral scale bars. – M–V: Fired cnidae. – A. Very large acontia isorhiza (i) with visible apical flaps (af). Note pattern on tubule. – B. Very large acontia p-mastigophore (p-) with its sharp point (rod) of the shaft towards the apical flaps. – C. Large p-mastigophore (p-) from tentacles and mesenterial filaments. – D. Short, broad isorhiza (i) from tentacles. – E–G. b-mastigophores (b-) with typical thread-like shafts. – H–I. Small p-mastigophores (p-); present in all tissues, most abundant in column (v-notch vaguely visible). – J and upper left M: tiny cnidae (tc) of isorhiza-type. – K–L. Spirocysts (s), most abundant in tentacles; in K stained with eosin. – M. Everted tiny cnidae (tc) with coiled tubules. – N. Upper image: empty capsule of spirocyst (s) and everted tubule with single helix of eosinophilic microfibrillae still attached to tubule. Lower image: distal end of everted (ev.) tubule with microfibrillae adhering to glass slide. Note that the tubule is not fully everted; inverted (inv.) part is still inside. – O. Isorhiza (i) capsules with everted tubules showing variation in length of proximal spineless part (arrows point out first spine rows). – P–Q. Everted small p-mastigophore (p-) stained with nigrosin and eosin (note nucleus in Q). – R. Small b-mastigophore (b-) from mesenterial filaments and acontia. – S. Large b-mastigophore (b-) from tentacles and oral disk. – T. Medium p-mastigophore (p-) from mesenterial filaments; note short proximal (prox) part. – U. Everted tubules of isorhiza (i) and p-mastigophore (p-). – V. Stained everted very large p-mastigophore (p-). Shaft with long proximal part (prox), mid-part (mid) with long spines, distal part (dist) with successively shorter spines, and transition between shaft and tubule (arrow). Isorhiza (i) tubule also visible [Colour figure can be viewed at [wileyonlinelibrary.com](http://wileyonlinelibrary.com)].

small were present in all tissues, albeit most abundant in tentacles and column. In actinopharynx and column, they were the only size class represented. The medium and

large size classes were present in tentacles, mesenterial filaments and acontia, approximately equally common in the mesenterial filaments, while the large size class dominated

in the tentacles. The very large p-mastigophores were specific for the acontia and were there the second most abundant cnidocyst type after the large narrow isorhizas (Tables 2, 3). The p-mastigophores of the acontia were approximately twice the size compared to the large p-mastigophores in the tentacles and mesenterial filaments.

The capsule shape was highly variable in p-mastigophores of the mesenterial filaments, from rounded oval (prolate spheroids) to diamond shaped (Fig. 7D). The latter capsules were broadest alongside the v-notch of the shaft, and narrower at the apical and basal ends. The capsules of the small p-mastigophores were usually broad and symmetrically rounded oval, while capsules of the large ones were broader at the apical ends and slightly tapering towards the basal ends. The very large acontia p-mastigophores were narrow with almost parallel sides, sometimes slightly bent, and often tapering towards the basal ends that were either blunt or pointed.

The inverted shaft of the large and very large p-mastigophores was highly elaborate with its sharp point (rod) directed to the sometimes visible flaps at the apical end of the capsule (capsule aperture), and a conspicuous v-notch at the distal end of the shaft (Fig. 9B–C). The shaft reached half, or more than half (0.5–0.7), of the capsule length in the very large p-mastigophores (S1 p.5), and 0.4–0.6 of the capsule length in the small (S1 p.4). The shaft could be divided into three regions: the narrow proximal region towards the apical flaps, the broad mid-region and the distal part with the v-notch. In very large p-mastigophores (Fig. 9B), the narrow proximal end was longer than in the large p-mastigophores. The helical pattern on the twisted shaft was broader in the mid-region (Fig. 9B–C, S2 p.9), corresponding with the length of spines on the everted shaft, which were shorter at the proximal and distal ends and longest in the mid-region (Fig. 9V). The distal shaft region had a large, prominent v-shaped notch at its end (Fig. 9B–C). The v-notch depth varied between 1.5  $\mu\text{m}$  in the small p-mastigophores and 11.5  $\mu\text{m}$  in the largest. The cusps of the v-notch were sometimes bent and gave the notch the appearance of the forceps (i.e. cerci) of a male earwig (insect of the order Dermaptera).

The everted shaft was heterotrichous. The shaft of the very large p-mastigophores ( $158.4 \pm 18.8 \mu\text{m}$ ) was mesobasic ( $>1.5\times$  the capsule length) and had 28 or 38 spine rows along the shaft (Fig. 9V). The proximal shaft was long and loose, and had approximately 1 spine row  $10 \mu\text{m}^{-1}$ , armed with tiny (1–5  $\mu\text{m}$ ) spines. The mid-region was more regular, with 3 spine rows  $10 \mu\text{m}^{-1}$  and armed with 10–13  $\mu\text{m}$  long spines, which gradually grew shorter towards the distal end (Fig. 9V).

Small to large p-mastigophores were microbasic, with the everted shafts approximately as long, or shorter than, the capsule (Fig. 9P–Q, T). In large p-mastigophores (capsule c. 50  $\mu\text{m}$ ), the shaft had a short proximal part, and a mid-part with up to 6  $\mu\text{m}$  long spines, and 18 or 20 spine rows

on the entire shaft. The everted shafts of medium and small p-mastigophores had 12 or 15, and 5 or 7 spine rows, respectively. Roughly, the shaft doubled its length during eversion (S2 p.12).

The inverted tubule made a few irregular coils around the inverted shaft. Loose, irregular coils basal to the shaft nearly filled the remaining capsule of medium, large and very large p-mastigophores (Fig. 9B–C). In small p-mastigophores, the tubule seemed to fill the entire capsule (Fig. 9H).

The everted tubules were armed throughout with 1–2  $\mu\text{m}$  long spines forming three helically arranged spine rows. Small p-mastigophores had 300–400  $\mu\text{m}$  long tubules. The tubules of very large p-mastigophores were c. 4000  $\mu\text{m}$  long and c. 4.1  $\mu\text{m}$  broad, with 0.4–0.6 rows  $10 \mu\text{m}^{-1}$ . The spine rows were widely spaced compared to the more regular rows of the isorhizas, and their everted tubules were thereby easily distinguished (Fig. 9U). The tubule of medium p-mastigophores was c. 1.5  $\mu\text{m}$  broad. The full length of medium and large p-mastigophore tubules is unknown.

3. *Isorhizas* were present in tentacles and acontia with distinct populations in each tissue type. Broad oval isorhizas were sparsely scattered throughout the tentacles ( $54.4 \pm 4.9 \mu\text{m}$  long,  $18.3 \pm 2.0 \mu\text{m}$  wide, length-to-width ratio 3 : 1, Fig. 9D). The large narrow isorhizas of the acontia were approximately twice as long ( $97.2 \pm 12.6 \mu\text{m}$  long,  $17.0 \pm 1.6 \mu\text{m}$  wide, length-to-width ratio 6 : 1, Fig. 9A).

The capsules of tentacle isorhizas were stout, symmetrically rounded oval (prolate spheroids), while acontia isorhizas were long and narrow, tapering to the basal end and often bent (Fig. 9A). The apical flaps were generally visible, sometimes with a protruding tip (Fig. 4F).

The inverted tubule of the isorhizas made regular to irregular, slightly oblique coils, which mostly filled the entire capsule; however, a few isorhizas were observed in which the tubule did not fill the capsule.

The everted tubule was holotrichous and reached up to 5000  $\mu\text{m}$  in its full length. Proximally, the tubule was 2.6–3.8  $\mu\text{m}$  broad, tapering slightly towards its end. It was armed throughout with uniform thorn-like spines (Fig. 9U) in very regular spine rows (1.8–2.2 spine rows  $10 \mu\text{m}^{-1}$ ), except for on the short proximal region close to the capsule that was more loose and free of spines. This proximal region varied in length (Fig. 9O).

4. *Tiny cnidae* (6–11  $\mu\text{m}$ ) were found sparingly in column and tentacles, and rarely in mesenterial filaments and acontia (Fig. 9J, M). Non-everted capsules appeared to have a shaft, although it could simply be a loop of the proximal tubule. When everted ones were found, they had a bent or spiraled and spined tubule, but no visible shaft. These tiny cnidae were most likely of isorhiza type.
5. *Spirocysts* were overwhelmingly numerous in the tentacles, extending down to the oral disc (Tables 2, 3, Figs 4, 5,

9K–L). A few spirocysts were found in other tissues but could not be confirmed in histological sections, therefore assumed to be cross-tissue contamination. The size distribution of the spirocysts was left-skewed and unimodal, with no discernible size classes ( $23.5 \pm 5.7 \mu\text{m}$ , mean  $\pm$  SD; mode  $20.4 \mu\text{m}$ ; range  $12\text{--}42 \mu\text{m}$ , Fig. 2E–F).

The capsule shape varied from narrow, almost needle shaped, to broad. The length-to-width ratio varied between 3 : 1 and 10 : 1 with no indication of discrete types, that is capsule length-to-width ratios were normally distributed (S1 p.9). The capsules were broadest apically and tapered towards the narrow basal end (Fig. 9K–L).

The inverted tubule formed 20–30 distinct regular coils, transverse or slightly oblique, to the capsule axis and filled the capsule except for the narrow basal part. The first tubule coil in the apical part of the capsule was often seen as a loop perpendicular to the rest of the coils. The empty basal capsule part varied in length.

The everted tubule was broad, with a single helix of eosinophilic substance, probably microfibrillae or some component of these, winding along the entire tubule (Fig. 9N, upper). The microfibrillae sometimes spread out, giving a feathery appearance, and adhering to the glass slide surface (Fig. 9N, lower). The tips of semi-discharged tubules were sometimes capped, presumably by a droplet of agglutinant liquid (Fig. 4D).

#### Developing stages – cnidoblasts

Early stages of developing cnidocysts were either found in spherical cnidoblasts (Fig. 10A–B), or if the cnidoblasts were lysed, with the capsule and external tubule spread out (Fig. 10C). In fresh squash preparations, abundant developmental stages were present often in discrete regions sparse in mature cnidocysts (proliferation zones), although sometimes also interspersed among mature ones (Fig. 11A–B). As seen in histological sections, the cnidoblasts could be found mainly in the basal epidermis. In the tentacles, where the basal zones were wide the cnidoblasts were observed close to the mesoglea, completely separated from mature cnidae (Fig. 5A, C). In acontia and mesenterial filaments where the basal epidermis zones were narrower or almost absent, the cnidoblasts were found more interspersed among the bases of mature cni-

dae. The developing stages of isorhizas, p- and b-mastigophores (i.e. nematoblasts) seemed to develop in a very similar pattern (Fig. 10A–O), while spirocysts had a unique morphology during development (Fig. 11A–R).

**Nematoblasts.** Early nematoblasts had capsules with smooth external tubules (Fig. 10A–C). The developing p-mastigophores had heterogeneous tubule diameter; that is, the shaft region of the external tubule was wider than the tubule (Fig. 10A–B). Isorhizas could be identified by their larger capsule and homogeneous diameter of the external tubule (Fig. 10C).

In later stage nematoblasts with internalized tubules, isorhizas could be identified by their broad capsule, a tubule filling the entire capsule, and sometimes with a small protruding tip at the apical capsule end. The proximal part of the inverted tubule seemed to condense first, making the pattern of the tubule visible, while the remaining tubule was still obscure (Fig. 10D). The shafts of the b- and p-mastigophores were conspicuous, with the undulating thread-like shafts of b-mastigophores (Fig. 10M–N), and shafts with a v-notch of the p-mastigophores (Fig. 10E–L).

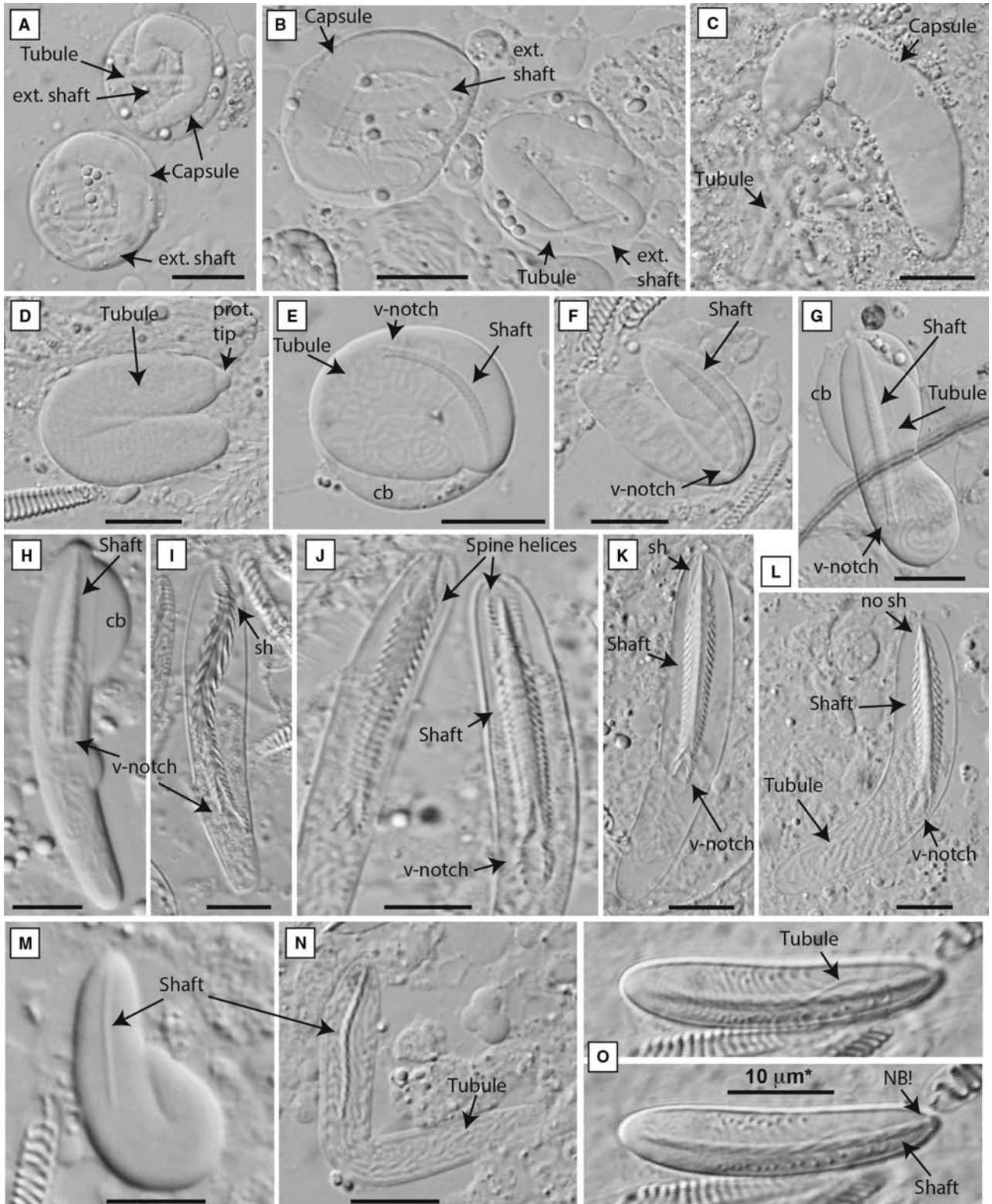
The shafts of p-mastigophores, however, seemed to invaginate primarily into an immature, slender and flexible shaft (Fig. 10E–F). A v-notch was present, but small. In addition, the immature capsules were more opaque than later stages, shafts and tubules diffused by capsule contents (Fig. 10D–H, M, S2 p.6). The shaft later untwined, that is relaxed its spiral twist around its axis, to allow for spines to develop (Fig. 10I–J). Spine helices were conspicuous in the loosened shafts, and the shaft could then reach the basal end of the capsule (Fig. 10I–J, S2 p.7). At this stage, the capsules became clear, with details of shaft and tubule distinct. When spines had been assembled, the spine helices were twisted and tightly tucked in along the shaft, sometimes displaying a double v-notch in the process (Fig. 10K).

Some shafts in immature capsules appeared fully developed, with a broader mid-region and a deep v-notch (Fig. 10G–H), although the opacity of the capsule did not allow any details to be discerned. Further, it seemed as if most of the still bent p-mastigophores were in an immature stage (Fig. 10E–G), although a few capsules were still bent at later stages (Fig. 10L). In a mature shaft, the spines are seen as

**Fig. 10**—Developing stages of nematocysts. – A–B. Intact cnidoblasts (p-mastigophores) with capsules and heterogeneous diameter of external (ext.) shaft and tubule. – C. Isorhiza with broad large capsule, and homogenous tubule diameter (cnidoblast has lysed). – D. Isorhiza at later stage of development; tubule internalized and with its proximal part condensed, spines developing. A protruding (prot.) tip at the apical end. – E–L. Different stages of p-mastigophore development; internalized tubule and recognizable shaft with v-notch. – E–F. Shafts slender and immature, before spines are formed. Cnidoblast (cb) intact in E. – F. Capsule is starting to unfold. – G–H. Still present cnidoblast, capsule unfolding. – I–J. Final maturation: the shaft is untwined to make room for spine development, spine helices (sh) projecting, the v-notch sometimes reaching basal end of capsule. – K–L. The shaft is re-packed, getting shorter as it is twisted tighter, and spine helices (sh) are less projecting. – M–O. Developing b-mastigophores with typical thread-like, sometimes undulating shafts. – M. Shaft visible, tubule is diffuse. – N. The tubule has condensed and is seen filling up the entire capsule. – O. Shaft untwined, almost reaching the basal end. Note the even diameter of the proximal shaft at its point of attachment to the apical capsule end, unlike the pointed shaft of p-mastigophores. \*All scale bars  $10 \mu\text{m}$  [Colour figure can be viewed at [wileyonlinelibrary.com](http://wileyonlinelibrary.com)].

indentations along the sides of the shaft, although, when focus is placed on top of the shaft, the tightly packed spine helices can be seen as transverse bands (Fig. 9B–C, S2 p.9).

Developing b-mastigophores displayed a similar stage with an untwined shaft reaching the basal end of the capsule (Fig. 10O). Very few b-mastigophore cnidoblasts were



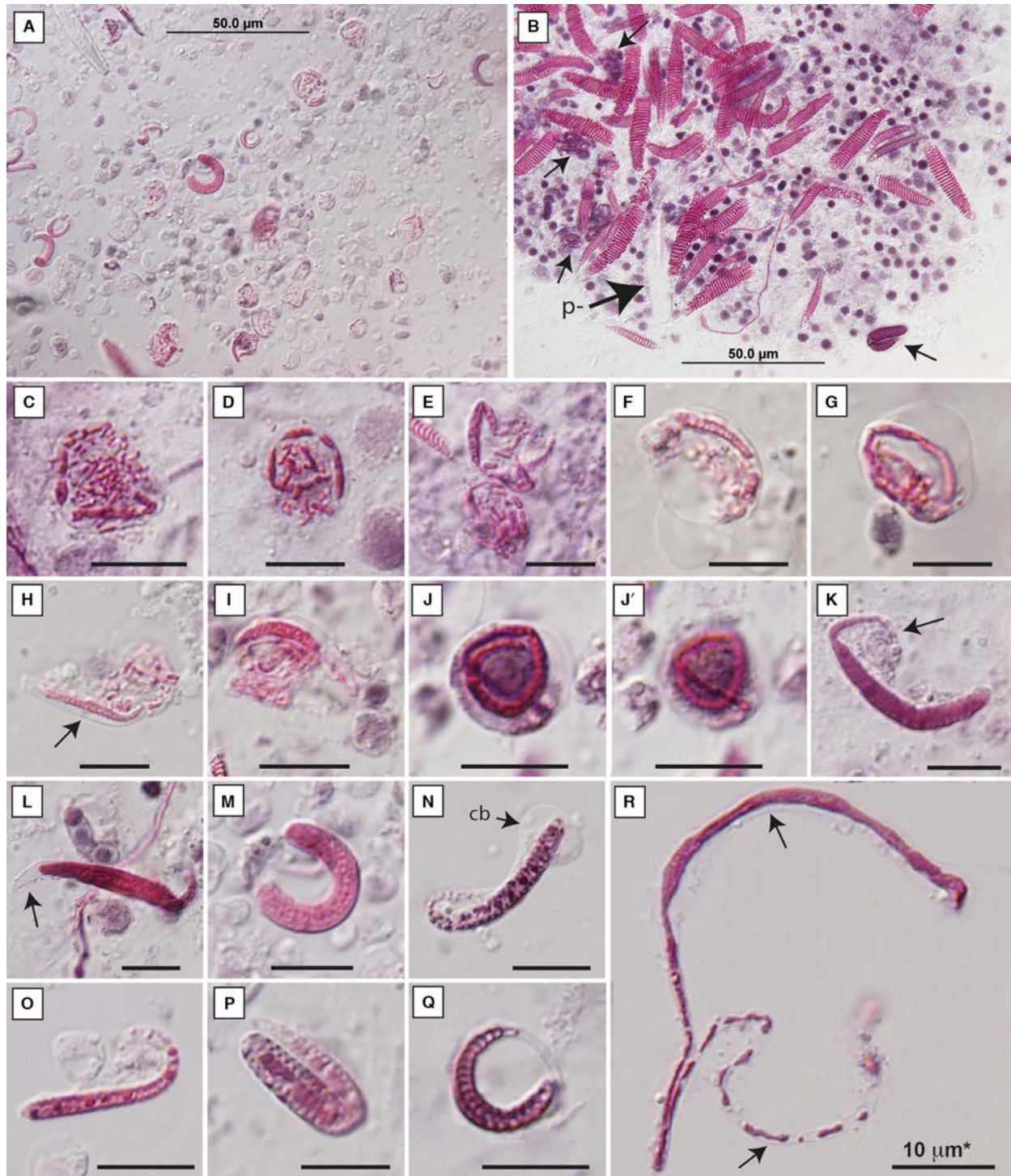


**Fig. 11**—Developing stages of spirocysts. – A. Area dominated by developing stages. – B. Cnidoblasts (small arrows) among mature spirocysts. The p-mastigophores (p-) not stained. – C–E. Early stages of developing spirocysts. The eosinophilic substance inside the external tubule is excreted in fragments. – F–I. Tubule with eosinophilic substance is packed into the capsule. Arrow in H point out capsule. – J–J'. Intact spiroblast (the same taken in two different focus planes). – K–L. Lysed cnidoblasts: the external tubule is almost completely internalized into the capsules (arrow in K point out external tubule). – L. Empty basal capsule end (arrow). – M. The entire tubule internalized. – N–P. Late stage spiroblasts where the eosinophilic substance seems to rearrange. – Q. Maturing spirocyst: the coils are discernable. – R. A lysed spiroblast has released an external tubule with its eosinophilic content, making the tubule walls visible (arrows). \*Scale bars in C–R 10 µm.

observed, and the details of the stages of development cannot be resolved here. The untwined shaft had a homogeneous diameter, with no visible pointed rod towards the apical end as in p-mastigophores.

*Spiroblasts.* Developing spirocysts was easily identified in stained preparations. The tubule was filled with eosinophilic substance, initially built up by short fragments (Fig. 11C–F). In a lysed spiroblast, with its external tubule spread out on the glass slide, the eosinophilic substance clearly was contained within a thin-walled tubule (Fig. 10R). In non-stained preparations, using Normarski light microscopy, the spiroblast tubule seemed to be completely fragmented because the tubule itself was not visible (S2 p.8). The fragments were subsequently merging and packed into the capsule (Fig. 11F–I). In some spiroblasts, it seemed as if an outer tubule were left outside the capsule, that is not inverted along with the eosinophilic matrix and inner tubule (Fig. 11K). The eosinophilic substance was initially packed into the capsule as a seemingly undifferentiated mass (Fig. 11J–L), that later rearranged and condensed until the tubule coils were visible (Fig. 11M–Q). In everted tubules of fired spirocysts, the eosinophilic substance was found in a single helix along the tubule, or feathering out attaching to the glass slide (Fig. 9N), and is assumed to be the microfibrillae described by Mariscal *et al.* (1977b) or a component thereof.

## Discussion

### *Comparison with the description of Carlgren*

The cnidome of polyps of *Lophelia pertusa* (Linnaeus, 1758) from newly collected material was in close agreement with the cnidae descriptions of *Lophohelia prolifera* (Pallas, 1766) made by Carlgren (1940). Carlgren reported microbasal b-mastigophores, microbasal p-mastigophores, holotrichs (=holotrichous isorhizas) and spirocysts (Table 1). The size ranges of cnidae examined by Carlgren were within the size ranges in this study (Table 2). Carlgren did not provide data on the number of measurements taken, but one can assume that he measured fewer than in the present study, and the discrepancy is probably mostly due to chance, or possibly that he examined preserved material.

The smallest cnidae observed by Carlgren were 14 µm (b- and p-mastigophores from filaments and actinopharynx, Table 1). In our examinations, we have identified b-mastigophores down to 12 µm, p-mastigophores down to 13 µm and, in addition, a new tiny cnida of isorhiza type of 6–11 µm (Table 2).

The *microbasal b-mastigophores* reported by Carlgren (1940, pp. 44–45) were found sparsely in tentacles, actinopharynx and filaments. The inverted shaft of the tentacle b-mastigophores he described as very short, with 3 spine rows in the everted shaft armature (Carlgren 1940; p. 46, Fig. XV13–14). The size ranges of medium microbasal

b-mastigophores in our material corresponded well to the size ranges of the microbasal b-mastigophores in Carlgren's material (see Tables 1, 2). The number of spine rows on everted shafts was usually 3, but 5 spine rows were found in the larger b-mastigophores. He found large b-mastigophores in the tentacles and small in the filaments, and the same pattern of distribution was found in our study. Although Carlgren defined b-mastigophores as sparse in all tissues, they were found to be common (tentacles, acontia), or numerous (mesenterial filaments) in the present material.

*Microbasal p-mastigophores.* Carlgren (1940, pp. 44–46) divided into three size classes. Small p-mastigophores he reported from column, tentacles and actinopharynx, congruent with the present study. The largest p-mastigophores Carlgren reported 'only in the lower, strongly coiled parts of the filaments': interpreted as the acontia and correlating with the very large p-mastigophores in our study. The intermediate size class Carlgren reported from tentacles and filaments are corresponding to our medium and large size classes (from tentacles and mesenterial filaments). While Carlgren observed 10 spine rows in the everted shafts of the tentacle p-mastigophores, and 15 spine rows in the largest p-mastigophores (Carlgren 1940; pp. 45, 46, Fig. XV17), the corresponding p-mastigophores in our study showed 15 or 18, and 28 or 38 spine rows, respectively (Tables 1, 2). Most probably, Carlgren did not observe the small spines on the proximal and distal shaft regions and had thus only counted the spine rows from the mid-shaft region with the most conspicuous spines. Carlgren reported the larger p-mastigophore shafts as being 'somewhat longer than the capsule'. In our material, it was clear that they were more than 1.5 times longer than the capsule, and therefore, we here re-classify them as mesobasal according to the nomenclature of Östman (2000). Carlgren made a note on the smaller p-mastigophores in the filaments that they were 'possibly not hoplotelic' (i.e. spined on both shaft and tubule), but in the present material spines were present along the full length of the everted tubules.

*Holotrichs* were sparingly distributed in tentacles and actinopharynx, and dense in acontia (i.e. 'the strongly coiled part of filaments'), according to Carlgren. The large holotrichs observed by Carlgren correspond to our large and narrow holotrichous isorhizas from the acontia, and the sizes of holotrichs in tentacles and actinopharynx correspond to the broad oval isorhizas. The holotrichs he found in the actinopharynx could be contamination from the tentacles, but it is also possible that they extend to the oral disc although we did not find any. The difficulties of reliably dissecting out tissue from the actinopharynx left us with very few samples of that specific tissue type.

*Spirocysts.* Carlgren found to be very numerous in the tentacles, rare in the filaments, and not present in the actinopharynx. As spirocysts were so conspicuous in eosin-stained preparations, we are confident that they are not present in mesenterial filaments or acontia because they were absent in stained histological preparations of those tissues. Contrary to

the mesenterial filaments, spirocysts are confirmed on the oral disc close to the actinopharynx.

#### *Comparison between fresh and histological preparations*

Comparing preparations of live tissues with haematoxylin and eosin-stained histological sections of the same tissues was useful to verify the presence or non-presence of cnidocysts and secretory cells, and their organization within tissues. In some cases, the comparisons could be of help in identifying cross-tissue contaminations of cnidae, as mentioned above. This was especially useful considering spirocysts that were highly eosinophilic and easily identified. If they were present, they could not be missed in stained tissues. The nematocysts, however, were less well visualized. The poor fixation and staining of nematocysts in the histological preparations is probably due to improper methods. The capsules are soluble in alkaline reducing agents, especially disulphide reducing agents (Blanquet and Lenhoff 1966; David *et al.* 2008). The collapsing of capsules made it more difficult to recognize nematocysts in the tissues. The shaft and tubules of the nematocysts were also eosinophilic, although much less so than the tubule content of spirocysts. It was therefore less useful to use histological slides to confirm presence of nematocysts in tissues, especially in the mesenterial filaments and oral gastrodermis that were intensely stained by basophilic components.

#### *Developing cnidae*

The different *developing stages* observed in this study are to a large extent congruent with previous descriptions of cnidogenesis (Slautterback and Fawcett 1959; Westfall 1966; Skaer 1973; Holstein 1981; Tardent and Holstein 1982; Östman *et al.* 2010a,b, 2013). The location of cnidoblasts mainly in the basal epidermis below mature cnidae is in agreement with Möbius (1866) and Slautterback and Fawcett (1959), although cnidoblasts were also found among mature cnidae. Dense populations of cnidoblasts in discrete proliferation zones, with few or no mature cnidae were also observed (Fig. 11A), as previously noted in the sea anemones *Metridium senile* and *Sagartiogeton viduatus* (Östman *et al.* 2010a,b, 2013).

The novelty of cnidogenesis observed in this study concerns the p-mastigophore shaft and its v-notch. It has been stated that spines differentiate immediately after invagination of the external tubule (Holstein 1981). In this study, we have observed a time lag, with untwining of the shaft (relaxation of the spiral twist around its axis) between invagination and spine assembly; before the final packaging of the mature shaft in which the shaft again is tightly twisted around its axis. The p-mastigophore shafts thus undergo invagination, in which they are twisted and pleated into a recognizable, but immature, shaft with a v-notch. Immature shafts have a less pronounced increase of the diameter of the mid-region,

appearing more slender, and a small v-notch. Later, the shaft untwines to allow for spine development. When this is completed, the shaft undergoes a second packaging, twisted and pleated into the mature, spined shaft, now with a larger v-notch. The small v-notch in the immature shaft is due to the difference in diameter between shaft region and tubule, and when spines are added, this difference increases.

In *Hydra*, spine development has been thoroughly mapped, and a glycine- and histidine-rich protein named spinalin identified as the major component (Koch *et al.* 1998). Spines develop in the lumen of the inverted tubule and shaft, with the electron-dense precursors first present in the matrix of the capsule before invagination of the external tubule (Holstein 1981; Koch *et al.* 1998; Hellstern *et al.* 2006). This protein has not yet been identified in anthozoans; however, it is likely the same (or a similar) protein responsible for spine assembly within Anthozoa. The opacity of the immature capsules seen in Fig. 10E–H could thus be due to the precursors of spines, that is electron-dense subunits. Once the spines have assembled, the subunits are used-up and the capsule is clear (Figs 9B–C, 10I–L). The shafts in Fig. 10G–H that appear to be mature, with broader mid-diameter and larger v-notch, could possibly be due to the shaft beginning to loosen up and untwine before spine development. The opacity of the capsule suggests that spine assembly has not yet taken place.

Early stages of developing cnidae of different types are difficult to discern from one another at the very earliest stages of development, although there are some early indicators of the complexity of the end product. It appears that the extension of the endoplasmic reticulum (Slautterback and Fawcett 1959) and the number of microtubuli formed by the centrioles (forming the cage around the growing tip of the external tubule) is related to the size and complexity of the capsule and shaft region under construction (Holstein 1981). This is however only visible in TEM sections. In light microscopy, it is sometimes possible to see that the external tubule has a heterogeneous diameter, that is the shaft region is wider than the tubule. This could be observed in some of the nematoblasts (Fig. 10A–B), and was described also by Holstein (1981). As p-mastigophores have a more elaborate shaft than b-mastigophores, with larger difference in diameter between shaft and tubule, it should be possible to discern the two types, although during this study we did not find any distinct examples. The nematoblasts of isorhizas were more readily discerned from the other nematocyst types, due to their lack of shaft and therefore homogenous diameter of the external tubule, and the large size of the capsule. The spiroblasts were the easiest ones to discern from the others, especially in stained preparations, due to their highly eosinophilic substance.

Most efforts in describing cnidocyst development have been devoted to nematocysts, while spirocyst development has been addressed only by Kupson and Greenwood (1989), published as an abstract in *American Zoologist*. The

fundamentals of spirocyst development seem to be the same as for nematocysts; however, the morphological differences, such as the thin tubule wall and the eosinophilic substance, can produce artefacts using light microscopy. The apparent fragmentation of the tubule as seen in unstained Normarski micrographs (S2 p.8) is due to the thin tubule wall and fragmented eosinophilic substance. When the material was stained with eosin and documented in fresh preparations, the tubule wall was visible, and it was obvious that only the eosinophilic substance was fragmented. The single helix of microfibrillae, in contrast to the triple helices of spines on nematocysts, is another unique characteristic of spirocysts. This is congruent with previous descriptions of spirocyst tubules (Schmidt 1969; Mariscal *et al.* 1977b).

The lack of attention given to spiroblasts in previous literature prompted us to devote more effort into their development. The abundance of developing stages varies over time, and between polyps, depending on a recent event of large-scale discharge. One dissected polyp was especially rich in spiroblasts in the tentacles, and almost all images of spiroblasts are from that one polyp. It is estimated that replenishing takes almost a week (Schmidt 1982), and thus, cnidoblasts could be experimentally induced by poking or air exposure of tentacles to stimulate large-scale discharge. Cnidoblasts should be present within the next few days. This probably occurred in the dissected polyp rich in spiroblasts, although not planned.

#### *A remark on the function of cnidae*

The distribution of different cnidae types and size classes in different tissues probably reflect their function. Coral polyps are delicate, and feeding involves high risk when handling prey such as copepods with exoskeletons and sharp appendages. The agglutinant spirocysts and entangling isorhizas in the tentacles are perfect adaptations, efficiently immobilizing the prey until the toxins delivered by the penetrating large b- and p-mastigophores take effect.

The largest cnidae in the acontia has been attributed to a function mainly in aggression (Kramer and Francis 2004; Nevalainen *et al.* 2004). As a predator or aggressor approaches the polyp, the acontia are extruded through the mouth as the polyp quickly retracts, and the very large cnidae can fire. These very large cnidae are also found in the mucus strands released by *L. pertusa* when they have been handled, after quick polyp retraction when touched (personal observation). The dominance of penetrating cnidae in the mesenterial filaments could be due to the nature of the toxins, which contain enzymes and thus aid in digestion of the captured prey (Nevalainen *et al.* 2004). A study by Schlesinger *et al.* (2009) showed that the acontial microbasic p-mastigophores of the sea anemone *Aiptasia diaphena* penetrates prey inside the gastrovascular cavity when the animal is feeding. A function in feeding and digestion is thus also probable for the large acontia cnidae.

The tiny cnidae and abundant small p-mastigophores in the external tissue layer (column) on the theca could provide an explanation for the absence of epifauna on the surfaces of the skeleton covered with live tissue. Only, a few species are seen in direct contact with living branches of *Lophelia pertusa*, for example the crustacean *Munidopsis serricornis* and the polychaete *Eunice norvegica* (usually protected within its tube), while dead coral branches house a myriad of fouling invertebrates. The cnidae of the column could thus be an efficient antifouling agent.

#### *A final remark on the use of the term acontia*

The authors are aware that the term *acontia* has not previously been used to distinguish the free coils of the mesenterial filaments in scleractinians. However, the descriptions of acontia from sea anemones fit well with the structures observed in *Lophelia pertusa*.

Carlgren (1949) describes acontia as: ‘thin threads attached at one end to mesenteries, as a rule below the filaments, while the other end is free. They are laden with extraordinarily numerous nematocysts of variable categories’. Gosse (1860, p. XXV of the Introduction) provided more detail in the morphology by describing the point of insertion to be anywhere along the cnidoglandular band (named ‘craspeda’ by Gosse) of the mesenteries, rather than ‘below the filaments’ as Carlgren (1949) stated. Stephenson (1920, pp. 443–445) provided the most detailed description of acontia. He made a comparison between acontia and mesenterial filaments, and distinguished one from the other, simultaneously stating: ‘an acontium can only be regarded as a specialized form of mesenterial filament’. In addition, Stephenson (1920) suggested that acontia ‘help to paralyse prey and to defend the animal’. He further warned that acontia of some species can be ‘partially reduced or even quite rudimentary’. An example of rudimentary acontia is the nematosomes of *Nematostella vectensis*, that is small globular bodies containing cnidocysts, rotating freely in the gastrovascular cavity. These were suggested by Williams (1979) to be homologous to acontia and acontoids (thicker filaments with less cnidae, Carlgren 1949), because they bud off from the cnidoglandular bands.

The descriptions fit well with the morphology of the structures we have chosen to call acontia in *L. pertusa*: that is, firstly, they emanate from the cnidoglandular band; secondly, they are structurally distinct from the mesenterial filaments, both in morphology and function, and in this aspect congruent with acontia. Generally, the cnidae of the acontia are larger than in the mesenterial filaments, although marginally so in some species (Stephenson 1920; Carlgren 1945). In *L. pertusa*, they are much larger than the cnidae in the mesenterial filament, similar to what is found in the sea anemone family Sagartiidae, described by Carlgren (1945).

Following that mesenteries and their filaments are a common character of the basic bauplan within Anthozoa (Daly

et al. 2003), and the acontia are specialized parts of the mesenterial filaments, then acontia might well be an ancestral condition within Anthozoa that has been lost multiple times. Rodríguez et al. (2012), for example, have found acontia to be lost, or reduced, several times within Actiniaria (sea anemones).

We suggest that a more thorough examination of acontia within scleractinians should be carried out to re-evaluate the status of acontia within Anthozoa as a whole. Other species of azooxanthellate, temperate or deep-sea scleractinians, which feed on larger prey such as copepods, might also have retained their acontia; for instance, we have observed similar structures in the temperate cup-coral *Caryophyllia smithii*.

### Acknowledgements

The study was carried out at the Sven Lovén Center for Marine Sciences, Tjärnö, a marine field station belonging to the University of Gothenburg. Financial support was obtained from FORMAS (contract No. 2010-1604), and the faculty of Science of Uppsala University. We would like to express deep gratitude to the anonymous reviewer who provided us with many knowledgeable and useful comments that helped us improve this manuscript.

### Supporting Information

Additional supporting information may be found in the online version of this article:

**Data S1.** Supplemental tables and graphs.

**Data S2.** Supplemental images.

### References

Abramoff, M. D., Magalhaes, P. J. and Ram, S. J. 2004. Image processing with Image J. – *Biophotonics International* 11: 36–42.

Blanquet, R. and Lenhoff, H. M. 1966. A disulfide-linked collagenous protein of nematocyst capsules. – *Science* 154: 152–8.

Carlgrén, O. 1940. A contribution to the knowledge of the structure and distribution of cnidae in the Anthozoa. – *Acta Universitatis Lundensis (ser 2)* 36: 1–62.

Carlgrén, O. 1945. Further contributions to the knowledge of the cnidome in the Anthozoa especially in the Actiniaria. – *Lunds Universitets Årsskrift* 41: 1–24.

Carlgrén, O. 1949. A survey of the Ptychodactiaria, Corallimorpharia and Actiniaria. – *Kungliga Svenska Vetenskapsakademiens Handlingar* 1: 1–121.

Colin, S. P. and Costello, J. H. 2007. Functional characteristics of nematocysts found on the scyphomedusa *Cyanea capillata*. – *Journal of Experimental Marine Biology and Ecology* 351: 114–120.

Cutress, C. E. 1955. An interpretation of the structure and distribution of cnidae in Anthozoa. – *Systematic Zoology* 4: 120–137.

Dahl, M. P., Pereyra, R. T., Lundälv, T. and André, C. 2012. Fine-scale spatial genetic structure and clonal distribution of the cold-water coral *Lophelia pertusa*. – *Coral Reefs* 31: 1135–1148.

Daly, M., Fautin, D. G. and Cappola, V. A. 2003. Systematics of the Hexacorallia (Cnidaria: Anthozoa). – *Zoological Journal of the Linnean Society* 139: 419–437.

David, C. N., Ozbek, S., Adamczyk, P., Meier, S., Pauly, B., Chapman, J., Hwang, J. S., Bojoberi, T. and Holstein, T. W. 2008. Evolution of complex structures: Minicollagens shape the cnidarian nematocyst. – *Trends Genet* 24: 431–438.

Dodds, L. A., Black, K. D., Orr, H. and Roberts, J. M. 2009. Lipid biomarkers reveal geographical differences in food supply to the cold-water coral *Lophelia pertusa* (Scleractinia). – *Marine Ecology-Progress Series* 397: 113–124.

Fautin, D. G. 2009. Structural diversity, systematics, and evolution of cnidae. – *Toxicon* 54: 1054–1064.

Fautin, D. G. 2013. Hexacorallians of the world. Sea anemones, Corals, and their allies. <http://geoportal.kgs.ku.edu.edu/hexacorall/anemone2/index.cfm>. Recent update of functionality: 2nd January 2013.

Fautin, D. G. and Mariscal, R. N. 1991. Cnidaria: Anthozoa. In: Harrison, F. W. and Westfall, J. A., (Eds): *Microscopic anatomy of Invertebrates*, vol. 2, pp. 267–358. – Wiley-Liss, N.Y.

Freiwald, A., Fosså, J. H., Grehan, A., Koslow, T. and Roberts, M. J. 2004. Cold-water coral reefs: Out of sight – no longer out of mind. 83 pp. UNEP-WCMC, Cambridge, UK.

Gass, S. E. and Roberts, J. M. 2010. Growth and branching patterns of *Lophelia pertusa* (Scleractinia) from the North Sea. – *Journal of the Marine Biological Association of the United Kingdom* 91: 831–835.

Gosse, P. H. 1860. *Actinologia Britannica: A history of the British sea-anemones and corals*, 362 pp. Van Voorst, Paternoster Row, London.

Hellstern, S., Stetefeld, J., Fauser, C., Lustig, A., Engel, J., Holstein, T. W. and Özbek, S. 2006. Structure/function analysis of spinalin, a spine protein of *Hydra* nematocysts. – *Federation of European Biochemical Societies Journal* 273: 3230–3237.

Holstein, T. 1981. The morphogenesis of nematocytes in *Hydra* and *Forskalia*: An ultrastructural study. – *Journal of Ultrastructure Research* 75: 276–290.

Kass-Simon, G. and Scappaticci, A. A. 2002. The behavioral and developmental physiology of nematocysts. – *Canadian Journal of Zoology-Revue Canadienne De Zoologie* 80: 1772–1794.

Koch, A. W., Holstein, T. W., Mala, C., Kurz, E., Engel, J. and David, C. N. 1998. Spinalin, a new glycine- and histidine-rich protein in spines of *Hydra* nematocysts. – *Journal of Cell Science* 111: 1545–1554.

Kramer, A. and Francis, L. 2004. Predation resistance and nematocyst scaling for *Metridium senile* and *M. farcimen*. – *The Biological Bulletin* 207: 130–140.

Kupson, J. E. and Greenwood, P. G. 1989. Spirocyst development in the sea-anemone *Haliplanella luciae*. – *American Zoologist* 29: A110–A110.

Larsson, A. I., Järnegren, J., Strömberg, S. M., Dahl, M. P., Lundälv, T. and Brooke, S. 2014. Embryogenesis and larval biology of the cold-water coral *Lophelia pertusa*. – *Plos One* 9: e102222.

Mariscal, R. N. 1974. Scanning electron microscopy of the sensory surface of the tentacles of sea anemones and corals. – *Cell and Tissue Research* 147: 149–156.

Mariscal, R. 1984. Cnidaria: Cnidae. In: Bereiter-Hahn, J., Matoltsy, A. G. and Richards, K. S., (Eds): *Biology of the Integument*, pp. 57–68. – Springer, Berlin Heidelberg.

Mariscal, R. N., Conklin, E. J. and Bigger, C. H. 1977a. The ptychocyst, a major new category of cnidae used in tube construction by a cerianthid anemone. – *The Biological Bulletin* 152: 392–405.

Mariscal, R. N., McLean, R. B. and Hand, C. 1977b. The form and function of cnidarian spirocysts. 3. Ultrastructure of the thread and the function of spirocysts. – *Cell and Tissue Research* 178: 427–433.

Möbius, K. A. 1866. Ueber den Bau, den mechanismus und die entwicklung der nesselkapseln einiger polypen und quallen.

- *Abhandlungen aus dem Gebiete der Naturwissenschaften Hamburg V*: 1–22, pls. 1–2.
- Mueller, C. E., Larsson, A. I., Veuger, B., Middelburg, J. J. and van Oevelen, D. 2013. Opportunistic feeding on various organic food sources by the cold-water coral *Lophelia pertusa*. – *Biogeosciences Discussions* 10: 11375–11403.
- Nevalainen, T. J., Peuravuori, H. J., Quinn, R. J., Llewellyn, L. E., Benzie, J. A. H., Fenner, P. J. and Winkel, K. D. 2004. Phospholipase A2 in Cnidaria. – *Comparative Biochemistry and Physiology B-Biochemistry & Molecular Biology* 139: 731–735.
- Östman, C. 2000. A guideline to nematocyst nomenclature and classification, and some notes on the systematic value of nematocysts. – *Scientia Marina* 64: 31–46.
- Östman, C., Kultima, J. R. and Roat, C. 2010a. Tentacle cnidae of the sea anemone *Metridium senile* (Linnaeus, 1761) (Cnidaria: Anthozoa). – *Scientia Marina* 74: 511–521.
- Östman, C., Kultima, J. R., Roat, C. and Rundblom, K. 2010b. Acontia and mesentery nematocysts of the sea anemone *Metridium senile* (Linnaeus, 1761) (Cnidaria: Anthozoa). – *Scientia Marina* 74: 483–497.
- Östman, C., Borg, F., Roat, C., Roat Kultima, J. and Wong, S.Y.G. 2013. Cnidae in the sea anemone *Sagartiogeton viduatus* (Müller, 1776) (Cnidaria, Anthozoa); A comparison to cnidae in the sea anemone *Metridium senile* (Linnaeus, 1761) (Cnidaria, Anthozoa). – *Acta Zoologica* 94: 392–409.
- Robson, E. A. 2004. Cnidogenesis in the jewel anemone *Corynactis californica* (Carlgren, 1936) and *C. viridis* (Allman, 1846) (Anthozoa: Corallimorpharia). – *Zoologische Mededelingen (Leiden)* 78: 461–476.
- Rodríguez, E., Barbeitos, M., Daly, M., Gusmão, L. C. and Häussermann, V. 2012. Toward a natural classification: Phylogeny of acontiate sea anemones (Cnidaria, Anthozoa, Actiniaria). – *Cladistics* 28: 375–392.
- Schlesinger, A., Zlotkin, E., Kramarsky-Winter, E. and Loya, Y. 2009. Cnidarian internal stinging mechanism. – *Proceedings of the Royal Society of London B: Biological Sciences* 276: 1063–1067.
- Schmidt, H. 1969. Die Nesselkapseln der Aktinien und ihre differentialdiagnostische Bedeutung. – *Helgolander Wissenschaftliche Meeresuntersuchungen* 19: 284–317.
- Schmidt, G. H. 1982. Replacement of discharged cnidae in the tentacles of *Anemonia sulcata*. – *Journal of the Marine Biological Association of the United Kingdom* 62: 685–691.
- Skaer, R. J. 1973. The secretion and development of nematocysts in a siphonophore. – *Journal of Cell Science* 13: 371–393.
- Skaer, R. J. and Picken, L. E. R. 1966. The pleated surface of the undischarged thread of a nematocyst and its simulation by models. – *Journal of Experimental Biology* 45: 173–177.
- Slautterback, D. B. and Fawcett, D. W. 1959. The development of the cnidoblasts of *Hydra*: An electron microscope study of cell differentiation. – *Journal of Biophysical and Biochemical Cytology* 5: 441–467.
- Stephenson, T. A. 1920. Memoirs: On the Classification of Actiniaria. – Part I. – Forms with acontia and forms with a mesogloal sphincter. – *Journal of Cell Science* s2-64: 425–572.
- Tardent, P. 1995. The cnidarian cnidocyte, a high-tech cellular weaponry. – *Bioessays* 17: 351–362.
- Tardent, P. and Holstein, T. 1982. Morphology and morphodynamics of the stenotele nematocyst of *Hydra attenuata* Pall. (Hydrozoa, Cnidaria). – *Cell and Tissue Research* 224: 269–290.
- Weill, R. 1934. Contribution à l'étude des cnidaires et de leurs nématocystes. I, II. – *Travaux de la Station Zoologique de Wimereux* 10,11: 1–701.
- Westfall, J. A. 1966. Differentiation of nematocysts and associated structures in Cnidaria. – *Zeitschrift Fur Zellforschung Und Mikroskopische Anatomie* 75: 381–403.
- Williams, R. B. 1979. Studies on the nematosomes of *Nematostella vectensis* Stephenson (Coelenterata: Actiniaria). – *Journal of Natural History* 13: 69–80.
- Wilson, J. B. 1979. Patch development of the deep-water coral *Lophelia pertusa* (Linnaeus, 1758) on Rockall Bank. – *Journal of the Marine Biological Association of the United Kingdom* 59: 165–177.
- WoRMS Editorial Board. 2014. World Register of Marine Species. Available from <http://www.marinespecies.org> at VLIZ.
- Yamashita, K., Kawai, S., Nakai, M. and Fusetani, N. 2003. Larval behavioral, morphological changes, and nematocyte dynamics during settlement of actinulae of *Tubularia mesembryanthemum*, Allman 1871 (Hydrozoa: Tubulariidae). – *Biological Bulletin* 204: 256–269.

Thesis for the Degree of Doctor of Philosophy

**EARLY LIFE HISTORY OF                      -WATER CORAL**

***Lophelia pertusa***

– WITH

**Susanna M Strömberg**

2016



**UNIVERSITY OF GOTHENBURG**

ACULTY OF SCIENCE  
EPARTMENT OF MARINE SCIENCES

Akademisk avhandling för filosofie doktorexamen i Naturvetenskap med inriktning

Fakultetsopponent: Associate Professor Rhian G. Waller,

Early Life History of the cold





**BSTRACT**

**OPULÄRVETENSKAPLIG S**

vi nu är på väg mot samma kemiska sammansättning i haven som tidigare har lett till

massutdöenden.

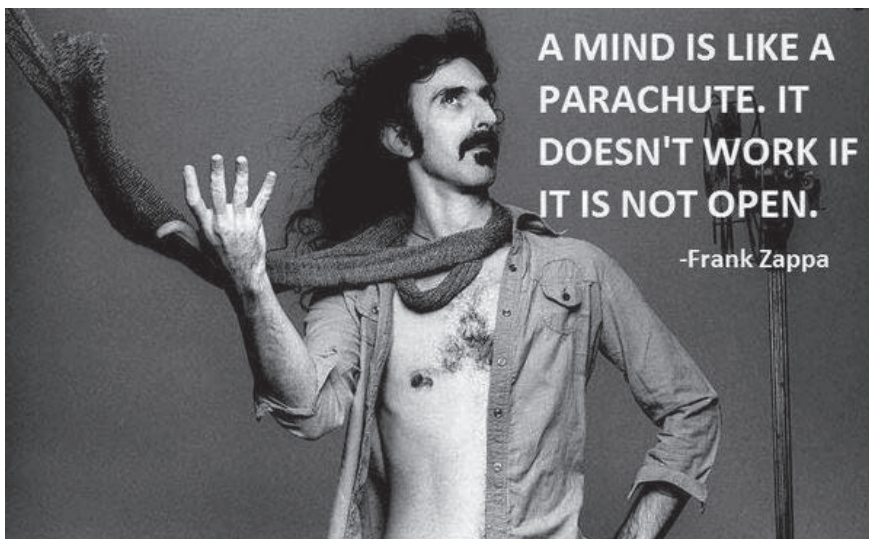
## **ELATED WORK**

## LIST OF PAPERS

This thesis is a summary of the following papers:

- PAPER I.** Larsson, A. I., Järnegren, J., Strömberg, S. M., Dahl, M. P., Lundälv, T. and Brooke, S. 2014. Embryogenesis and larval biology of the cold-water coral *Lophelia pertusa*. – *PLoS One* **9**: e102222.
- PAPER II.** Strömberg, S. M., Östman, C. 2016. The cnidome and internal morphology of *Lophelia pertusa* (Linnaeus, 1758) (Cnidaria, Anthozoa). – *Acta Zoologica*  
In press
- PAPER III.** Strömberg, S. M., Östman, C., Larsson, A. I. The cnidome and external morphology of late planulae in *Lophelia pertusa* (Linnaeus, 1758) – with implications for settling competency. Manuscript
- PAPER IV.** Strömberg, S. M., Larsson, A. I. Larval behavior and longevity in the cold-water coral *Lophelia pertusa* indicate potential for long distance dispersal. Manuscript

Paper I and II are included in this thesis with permission from PLoS One and Acta Zoologica.



A MIND IS LIKE A  
PARACHUTE. IT  
DOESN'T WORK IF  
IT IS NOT OPEN.

-Frank Zappa

**ABLE OF CONTENTS**

**INTRODUCTION**

**A** *BRIEF HISTORY OF THE MEDITERRANEAN REEF* .....

*ECOLOGICAL IMPORTANCE* - *WATER CORAL REEFS* .....

*THREATS* .....

*Natural resource extractions*

*Ocean acidification*

*A historic perspective of ocean acidification*

*DISTRIBUTION AND PHYSIOLOGY* .....

*DISPERSAL AND POPULATION DYNAMICS* .....

*MORPHOLOGY AND BIOLOGY* .....

*Cnidaria*

*TAXONOMIC CLASSIFICATION* .....

*Etymology*

*Remarks on phylogeny and history*

**AIM OF THE THESIS**

*RESULTS IN SUMMARY* .....

*Timeline*

*Timing of spawning*

*Embryogenesis and early planulae*

*Comparison of adult and larval cnidome*

*Larval feeding behavior*

*CONCLUSIONS* .....

*FUTURE PERSPECTIVES* .....

**ACKNOWLEDGMENTS**

**THE COLD**

*THE COLD- WATER CORAL BREEDER'S NIGHTMARE* .....

**ECOLOGICAL RESTORATION**

**REFERENCES**

**APER I**

**APER II**

**APER III**

**APER IV**

## INTRODUCTION

Thinking of corals brings to mind colorful tropical corals in luscious reefs, conveniently situated at diving depth. But surprisingly, over half of the approximately 5100 known coral species lives in the deep (Roberts *et al.* 2009). Deep-sea, or cold-water corals, span from the Barents Sea in the Arctic to the Antarctic shelf, from 40 m depth in areas where deep oceanic water is forced up to shallower depths by bottom topography and currents, while the deepest known coral species is found below 6000 m. There are solitary species and species capable of building continuous reefs covering areas up to 100 km<sup>2</sup>. Most deep-sea corals thrive at temperatures of 4–13°C, while some corals in the Polar Regions tolerate near-zero, or even periods of sub-zero temperatures (Bett 2000; Freiwald *et al.* 2004; Waller and Feehan 2013).

The main difference between tropical and deep-sea corals is that the tropical corals rely to a large extent on photosynthesizing symbionts (zooxanthellae) for nutrients, while deep-sea corals are predators and opportunistic heterotrophs, i.e. feeding foremost on zooplankton, but also on particulate organic matter, pico- and nanoplankton (Houlbrèque *et al.* 2004; Dodds *et al.* 2009; Mueller *et al.* 2014; Naumann *et al.* 2015). And while the corals themselves contribute to a large amount of the biodiversity in tropical reefs, by the assemblage of many different coral species, deep-sea coral reefs usually is made up by only one, or a few species. Nonetheless, deep-sea coral reefs are diversity hot spots, fully comparable to, or even exceeding, tropical reefs in species richness (Jensen and Frederiksen 1992; Freiwald *et al.* 2004).

### **A brief history on deep-sea scleractinian research**

The very first to take interest in cold-water corals were the Danish author, bishop, and historian Erik Pontoppidan (1698–1764) during his years as Bishop of Bergen in 1747–1754. Chapter 6 of his book *The natural History of Norway* (1755) was dedicated to “Sea-vegetables”, and he described a specimen of what three years later would be described by Carl von Linné as *Madrepora pertusa* (syn. *Lophelia pertusa*) with the words: “entirely white, the flowers much larger than the former, some of them even exceeding a shilling; and likewise expanded like a flower in full bloom, for which singular beauty I caused a draught of it to be taken” (Roberts *et al.* 2009). The confusion on what kingdom corals belong to was understandable, whether plants or animals. Aristotle (384–322 BC), the great Greek philosopher and father of natural philosophy, classified corals as zoophyta (animal-plants) recognizing their dual characteristics in his *Scala Naturae*. Not until the eighteenth century, with the help of the microscope, William Herschel, a British astronomer and constructor of telescopes, established that coral cells had the characteristics of animal cells (Wikipedia). About this time, the “father of biology”, Abraham Trembley (1710–1784) had made the entire Europe perplexed with his and the Bentinck boy’s descriptions of another cnidarian, the tiny pond creature, *Hydra*, a freshwater cnidarian polyp that intrigued by its confusing attributes of both plant and animal, and capacity for regeneration. The enigmatic *Hydra* was first recognized as a plant, due to its green color derived from their photosynthesizing symbionts, but then it was observed “walking”. Trembley’s nephew Bennet wrote in an excited letter: “One can say that you have discovered the point of passage from the Vegetable to the Animal” (Stott 2012).

Deep-sea scleractinian coral taxonomy has mostly been based on skeletal characteristics. Much of the sampled materials came from dredging expeditions and

soft tissues were probably not in a condition for description. The first to take interest in the biology, rather than skeleton morphology, were the British naturalist Philip Henry Gosse (1810–1888). Gosse was also the one bringing the deep sea to the public, by equipping London Zoo with the first aquarium in 1853, and at this point coined the term “aquarium”. Gosse provided detailed descriptions of the soft tissues, for instance in his generously illustrated work *The British sea anemones and corals* (1860). Cairns (2001) has provided a historic overview of the taxonomic research. Some of the earliest scleractinian taxonomists worth mentioning are Henri Milne Edwards, Jules Haime, Louis François de Pourtalès, and later Helmut Zibrowius. Stephen Cairns himself has made great contributions to scleractinian taxonomy.

Beginning in 1868, a series of deep-sea dredging expeditions went out to explore the deep sea to challenge the British naturalist Edward Forbes’ “azoic theory”. Forbes’ had broad interests covering geology, paleontology, and marine biology, and he believed that below 600 m depth (300 fathoms) the environmental conditions were not suitable for animal life, and the deep seafloor was expected to be a barren landscape. However, the Scotsman Charles Wyville Thomson, natural historian and marine zoologist, had seen what Michael Sars (theologian and biologist) had recovered in his dredge hauls in Norway from even greater depths. Thomson led the first expedition on the *HMS Lightning* covering the waters between the Faeroe Islands and Scotland, followed by expeditions with *HMS Porcupine* (1869), and the first great global expedition with the *HMS Challenger* during the years 1872–1876 (Roberts *et al.* 2009). The *HMS Challenger* journey covered 68000 nautical miles (c. 126 thousand km) and sounded the depth of a sampling station in the Mariana Trench to 8184 m (4475 fathoms), very close to the now deepest known place in Earth’s seabed of almost 11000 m. Thomson found life, covering all marine invertebrate groups, as deep as 1200 m (650 fathoms), and thereby proved Forbes wrong.

Since then great technical progress has been made, with sonar and multibeam echosounders for seabed mapping, manned submarines, and smaller unmanned submersibles—so called remotely operated vehicles (ROV) connected to the vessel with cables—and autonomous underwater vehicles (AUV) programmed onboard to follow a specific route and return to the vessel or surface after completed mission. These technological advances has made deep-sea habitat mapping and monitoring possible, and has revealed diverse habitat types and life forms in the oceans deepest abysses proving Forbes wrong many times over (Roberts *et al.* 2009).

In the Skagerrak area where the present work was conducted, Tomas Lundäl and Lisbeth Jonsson started mapping the cold-water coral reefs and other deep habitats, especially in the Koster-Hvaler area, beginning in the late 1990’s. First with rented ROVs, and later with ROV’s purchased for the Gothenburg University field station at Tjärnö, using the dedicated research vessel R/V *Lophelia* for their surveys. The Norwegian Trench and the bathymetry of the Koster-Hvaler area funnels deep oceanic water from the Atlantic to relatively shallow depths in the Koster-Hvaler archipelagos, creating suitable conditions for deep-sea fauna (Wisshak *et al.* 2005), resulting in a uniquely accessible area for deep-sea research. The presence of the University of Gothenburg’s field station on Tjärnö, adjacent to the Koster Fjord, and the ROV surveys has lead to that a 450-km<sup>2</sup> area was made the first marine National Park in Sweden in 2009. An equal sized area in Hvaler, on the Norwegian side, was simultaneously made a marine National Park in Norway.

### **Ecological importance of cold-water coral reefs**

Reef building deep-sea scleractinian corals are constructing three-dimensional frameworks, creating habitats for other organisms. They change the environment they inhabit by their own growth, modulating the availability of resources. Their three-dimensional skeleton matrix slows down near-bed currents and induces the precipitation of particles (“marine snow”, i.e. particulate organic material, POM) and pelagic larvae within the matrix, thus at the same time enhancing nutrient availability and concentrating life to the reef habitat. This kind of influence on the environment is defined as “autogenic engineering” (Lawton and Jones 1995). Most of the associated fauna found within cold-water coral reefs are the same fauna found in the geographic area in general, although highly concentrated. There are a few exceptions of specialized inhabitants that are found solely in reef habitats, sometimes in species-specific symbiotic associations (Jensen and Fredriksen 1992). Examples of organisms found almost uniquely in for example *Lophelia pertusa* reefs are the large polychaete *Eunice norvegica*, the squat lobster *Munidopsis serricornis*, and the hemichordate *Rhabdopleura normani*.

This habitat engineering quality of some of the deep-sea scleractinians is making them profoundly important for the associated fauna, and for the ecosystem functioning at a scale we do not fully comprehend yet. They have been suggested to be important nursing or feeding grounds for some commercially important fishes, such as rockfish (*Sebastes* sp.), cod (*Gadhus morhua*), and pollock (*Polachius virens*). Costello *et al.* (2005) found that 80% of individual fishes and 92% of species were associated to *Lophelia pertusa* reef habitat. The reef habitat commonly attract abundant zooplankton that hide amongst the coral branches, besides the many polychaetes and other invertebrate fauna accumulating within the coral matrix. Many of which are recovered in the stomach contents of associated fishes.

### **Threats**

#### *Natural resource extractions*

This important ecosystem service that deep-sea scleractinians are providing us is threatened in several ways. The most devastating and direct destruction is caused by deep-sea trawling; in heavily trawled areas large reefs can soon be completely leveled to the seafloor, leaving unconsolidated coral rubble with no three-dimensional structure left intact and no recovery observed even decades later (Althaus *et al.* 2009). Up to 95–98% reduction of coral cover has been observed in some trawled areas, leading to a subsequent depletion of the targeted fish stocks (Gianni 2004). Norse and Watling (1999) compared the impact of mobile fishing gear with forest clear-cutting, and alerted to the potential harm trawling could do to biodiversity. In Norway, long-line and gillnet fishermen contacted the Institute of Marine Research (IMR) in the 1990s, due to their concerns of the impacts that trawling fisheries seemed to cause to their fishing grounds (Fosså 2002). The long-line and gillnet fishermen commonly target coral reef areas due to the rich catches they usually get there. When these fishing grounds also had been targeted for trawling, catches went down. A series of ROV surveys conducted during 1998–1999 (Fosså 2002) in response to these

concerns revealed that the coral cover had been reduced by 30–50% of the estimated original total cover, with some of the reef sites inspected completely leveled.

The importance of three-dimensional structures were evident when a revisit at a reef site at Väderöarna, in the very southern part of the Koster Fjord, suddenly displayed dense mats of very young coral colonies, or single polyp juveniles, seemingly recently settled (Tomas Lundälv and Lisbeth Jonsson, personal comments). This reef site had been observed to no longer host any live corals during previous visits. The newly settled corals had used old lumps of dead coral skeleton as substrate. This is in contrast to other old reef sites in the area that consist of unconsolidated coral rubble with no three-dimensional structures left, and where no signs of new recruitment and recovery have been observed. Samples for DNA analysis to investigate the origin of these newly settled have been taken, but a full analysis is not yet done.

Even if not the entire reef is leveled, partial destruction of a reef could seriously hamper the reproductive success. Since *L. pertusa* and most other deep-sea scleractinians are gonochoric (separate sexes, see Waller 2005), one colony usually is the result of one settled planula and therefore is of one sex. The density and distribution of colonies of different sexes are crucial for reproductive success, and furthermore, not all parental crosses are compatible (Baums *et al.* 2013), thus the unfortunate destruction of specific coral colonies during a sweep with a trawl could easily leave the reef reproductively dead.

Other threats to these ecosystems are the extraction of oil and gas (Fosså 2002; Gianni 2004; Davies *et al.* 2007). The installations of offshore platforms for oil and gas extraction has ambiguous effects on cold-water corals, on one hand, platforms usually harbor healthy colonies of both *L. pertusa* and other fauna; however, colonies found close to the discharge chutes have been observed to have discoloration and 30% polyp mortality (Gass and Roberts 2006). Bakke *et al.* (2013) did a review on the present knowledge of potential effects of operational discharge from oil and gas platforms. There is evidence of fish being attracted to the structures, as well as negative physiological effects in fish sampled in areas with extensive production.

Besides the direct effects of increased sedimentation load by the released drill cuttings, and possible direct toxicity of petroleum products, there are also endocrine disruptive components in the discharge products. This has the potential of affecting reproduction and growth of exposed fauna. Fish are mobile and might be able to avoid the highest concentrations of discharge fluids, in contrast, the sessile invertebrate fauna has little chance of avoidance. The endocrine disruptive components of drill discharge have the potential to disturb coral reproduction since gametogenesis and reproduction is controlled by estradiol and testosterone, just as in vertebrates (Atkinson and Atkinson 1992; Twan *et al.* 2006). In a study by Negri and Heyward (2000) fertilization success was observed to decrease by exposure to petroleum products, especially crude oil in combination with dispersant chemicals. The most sensitive stage was metamorphosis—the transition from larva to juvenile—that was almost completely inhibited by the crude oil and dispersant combination. These effects were probably caused by other than endocrine disruptive properties of the dispersant chemicals, and no direct studies of reproductive effects on coral populations in the vicinity of platforms has been made.

Studies of the direct smothering or toxic effects of discharged sediments from oil extraction have been undertaken. For example, Larsson and Purser (2011) found partial tissue loss in *L. pertusa* exposed to realistic sedimentation loads of drill cuttings, but with an overall efficiency of sediment shedding and only slight decrease

of calcification rates. While normal operational running of platforms may have limited negative effects on surrounding fauna—with the reservation of disturbances in hormone regulation and reproduction that is not yet fully investigated—there is always the risk of a blowout. After the Deepwater Horizon disastrous oil spill in the Gulf of Mexico in 2010, affected coral communities was observed up to 11 km from the site, with tissue loss, and other stress responses in corals in the visual consensus made by White *et al.* (2012).

There is also an emerging threat of deep-sea mining that has caused researchers to lift a warning finger, and stress the importance of assessing the potential impacts on benthic fauna (Boschen *et al.* 2013). Deep-sea mining has been an issue since the 1970's, with a patent for an apparatus for harvesting mineral nodules filed already in 1977 (Diggs 1977). Many more patents have been registered since, but falling prizes of minerals has delayed harvesting (Glasby 2000), and deep-sea researchers such as Van Dover (2011) are calling out for tight regulations before any large-scale harvesting projects are launched.

### *Ocean acidification*

While the above anthropogenic impacts are fairly localized and easy to address through management and regulations—and an increasing amount of marine protected areas are established—the increasing carbon dioxide concentration in the atmosphere with decreasing ocean pH as a consequence, i.e. ocean acidification, is a far more challenging threat.

Several studies have been done examining the effects of ocean acidification on different marine organisms, including scleractinian corals. There have been variable results considering the sensitivity of coral calcification rates to ocean acidification. The study of Maier *et al.* (2009) found a positive net calcification in corals exposed to predicted future values of oceanic pH and aragonite saturation state ( $\Omega_a$ ), although there was a 40–59% reduction. The fastest growing apical polyps showed the largest reduction. Hennige *et al.* (2014) found decreasing respiration rates with maintained calcification rates in response to lowered pH correlating to a CO<sub>2</sub> partial pressure of 750 ppm, and this maintenance of calcification was attributed to the utilization of lipid reserves. The experiment was running for 21 days and was performed on freshly collected coral material, and thus the corals may not have depleted their energy reserves during the experimental period. A study by Tambutté *et al.* (2015) revealed that the skeleton of corals exposed to acidified conditions were more porous than the skeletons in control conditions. Linear growth apparently does not reveal the full story considering calcification rates in corals.

Calcification is a blunt instrument for measuring the effects of ocean acidification, and a study by Kaniewska *et al.* (2012) on the tropical coral *Acropora millepora* revealed that before effects on calcification were observed, there were changes in gene expression consistent with metabolic suppression, evidence of oxidative stress, and upregulation of genes involved in cytoskeletal remodeling. There was a down-regulation of genes involved in the mitochondrial electron transport chain, indicating a reduced capacity of generating ATP and NADPH. A similar study was done on the cold-water coral *Desmophyllum dianthus* by Carreiro-Silva *et al.* (2014), in which they found no significant differences in calcification or respiration. Contrary to this, they found significant effects in gene expression, with upregulation of genes involved in stress responses and immune defense. The corals also

upregulated genes involved in skeleton synthesis; apparently compensating for the less favorable conditions for calcification. It is obvious that calcification rates are kept up to a cost, and that this is depending on ample food availability.

While there is evidence for some ability of corals to compensate for acidified conditions (Form and Riebesell 2011; McCulloch *et al.* 2012; Carreiro-Silva *et al.* 2014), this is usually tested on pieces of coral with a full cover of live tissue on the skeleton. The calcifying compartments are isolated from the surrounding water and their environment is strictly regulated with alkalinity upregulated through ion pumping to create conditions favorable for calcification. The coral itself provides the nucleation sites for aragonite crystallization through an organic matrix laid down within the calcifying compartment, and through proton and calcium ion pumping the pH is elevated to allow for spontaneous precipitation of crystals (Allemann *et al.* 2004). This gives corals some leverage to counteract acidification. It is the naked skeleton of the dead parts at the base of, and in the center of the reefs, that are in more immediate danger, and there is a risk of reef collapse and loss of three-dimensional complexity. There have even been observations of ability of corals to survive complete decalcification as soft-bodied polyps that after return to normal conditions picked up on calcification and rebuilt colonies (Fine and Tchernov 2007). As soft-bodied polyps they are, however, vulnerable to predation and does not provide the large three-dimensional habitat for other organisms to utilize. The problems with acidification might therefore lie more in the ecosystem services coral reefs provide for other organisms, rather than a threat of extinction of the corals themselves. There is, however, emerging evidence that the early life history of corals is more sensitive. For example, a study of Albright *et al.* (2010) has shown that ocean acidification compromised fertilization success and thereby reduced larval availability in the studied species, *Acropora palmata*. Furthermore, ocean acidification reduced settling success and postsettlement growth.

In a study by Morabito *et al.* (2013) the effect of lower pH on cnida discharge capability in the jellyfish *Pelagia noctiluca* was tested, and low pH was observed to reduce the discharge response. The tested pH values were 6.5 and 4.5 (control pH 7.65), and thus lower than what is ecologically relevant in comparison to plausible scenarios of ocean acidification. Nonetheless, it is a very important aspect to investigate. If pH values within the plausible ranges for future ocean acidification could hamper cnidae discharge, it could hamper coral feeding, and thus the ability of the corals to compensate for the increased energy demand for maintaining calcification rates in a more acidic environment.

The second aspect of climate change due to rising carbon dioxide is the ongoing warming of the oceans. Embryo and larval development rates are temperature dependent, i.e. in cold waters development is slow, while a rise in temperature speeds up development. A rise in the temperature of the oceans will reduce pelagic larval durations (PLD), resulting in shorter dispersal distances (Hoegh-Guldberg and Pearse 1995; O'Connor *et al.* 2007). So, not only do the environmental conditions deteriorate due to ocean acidification, it will also be harder for most larvae to disperse long enough distances to escape into more favorable conditions.

The full consequences of ocean acidification are difficult to anticipate, and any recovery back to the pre-industrial baseline will take centuries or millennia, if at all possible. These are large-scale processes and once the wheels have turned there is no turning back, just the slow route of change, working at geological timescales.

*A historic perspective of ocean acidification*

The potential problem with ocean acidification is not a novel insight to the research community; already in 1951 William W. Rubey stated in his *Geologic history of seawater—An attempt to state the problem*, and I quote: “Carbon plays a significant part in the chemistry of sea water and in the realm of living matter. The amount now buried as carbonates and organic carbon in sedimentary rocks is about 600 times as great as that in today’s atmosphere, hydrosphere, and biosphere. If only 1/100 of this buried carbon were suddenly added to the present atmosphere and ocean, many species of marine organisms would probably be exterminated”.

Rubey referred back to a range of studies made on the physiological effects of different levels of pH that had been undertaken. Gattuso and Hansson (2011) have synthesized the history of ocean acidification in their book *Ocean acidification: background and history*, most certainly hair-raising reading for those who dare.

Another notable early alarm signal is from an educational documentary produced in 1958 by Frank Capra for Bells Labs called *Unchained Goddess* (available on YouTube at <https://youtu.be/0lgzz-L7GFg>), in which Richard Carlson discussed the potential effects of human induced increase of atmospheric carbon dioxide concentrations: global warming, melting polar ice caps, and sea level rise, were all mentioned in the video. Despite the early rise of awareness of the potential problem, the inertia of the human population to respond to these warnings has led to that we now, in the eleventh-hour, stand at the verge of the tipping-point when our last-minute attempts to mitigate our influence on the planet just might not make the difference we need. The only thing exceeding the inertia of the human population is the inertia of the planet itself, to our demise—a painful proof of Newton’s first law.

***Distribution and physical environment***

The distribution of deep-sea scleractinian corals (fig. 1) is largely explained by four environmental variables: temperature, aragonite saturation, depth, and salinity (Davies and Guinotte 2011). They are restricted to oceanic conditions (4–12°C, 34–36 psu) and topographic highs with enhanced current velocities on continental slopes or seamounts (Freiwald *et al.* 2004; Roberts *et al.* 2009). In addition, their global distribution follows the distribution of water masses supersaturated with respect to aragonite (Guinotte *et al.* 2006; Davies and Guinotte 2011). This is probably the reason why deep-sea scleractinian corals barely exist in the Pacific Ocean while they thrive in abundance in the North Atlantic and other ocean basins. The aragonite saturation horizon (ASH<sup>1</sup>) is at a mere 140 m in the Pacific, compared to 2000 m in the North Atlantic, due to large-scale oceanic processes. These ASH depths will change as the effects of the increasing atmospheric carbon dioxide concentrations progress, with increasing ocean acidification as a result. The ASH is largely determined by pH and pressure, the lower the pH, the less pressure needed to flip the

---

<sup>1</sup> The aragonite saturation horizon (ASH) is the depth at which there is a shift in the occurrence of dissolution or precipitation of the aragonite form of calcium carbonate. Above the ASH, aragonite will precipitate, i.e. the chemical equilibrium reactions will favor the solid phase, while below the ASH the equilibrium will favor dissolution into ions. Aragonite is more readily dissolved than calcite due to the orthorhombic crystal structure, in contrast to the more stable tetragonal structure of calcite. Calcite thus has a saturation horizon that lies deeper than the ASH. *Lophelia pertusa* produces a skeleton of aragonite, but other invertebrates can have shells or skeletons made of calcite.

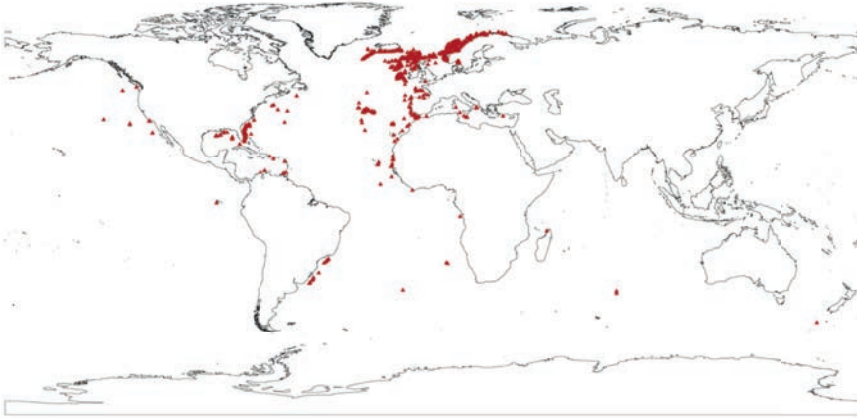


**Fig. 1** – The global distribution of *Lophelia pertusa* shown with red triangles. Other species of cold-water corals is distributed more in the southern hemisphere, e.g. in the Indian and Pacific Oceans, and around Australia and New Zealand. Map from Davies *et al.* 2008.

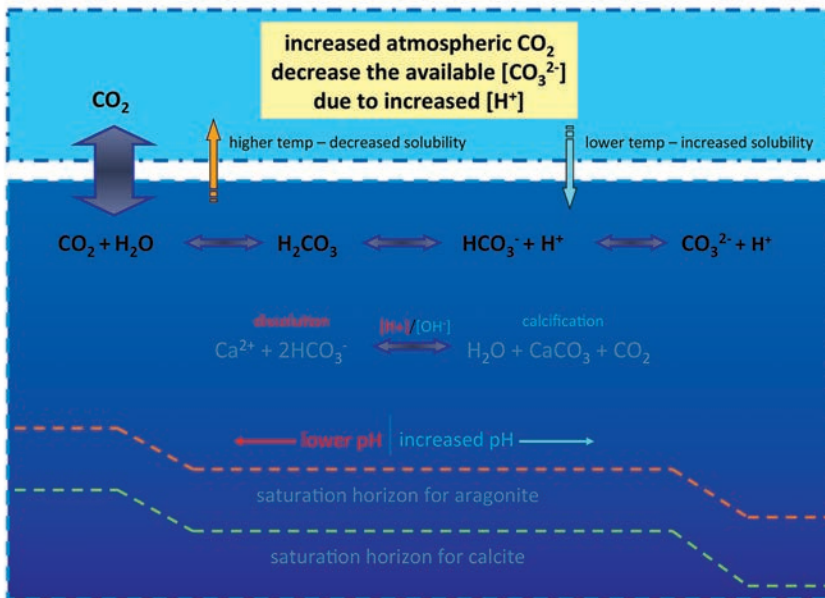


**Fig. 2** – Water chemistry under ocean acidification: the increase in atmospheric carbon dioxide leads to more free hydrogen, and thus a lowering of the pH of the ocean. The equilibrium reactions of dissolution and precipitation (calcification) of aragonite is depending on pH and pressure, and thus, with lower pH follows that less pressure is needed to flip the equilibrium towards dissolution, and the aragonite saturation horizon will shoal to lesser depth. Gasses are more readily dissolved in colder water, thus uptake of atmospheric carbon dioxide increase at higher latitudes.

chemistry over to dissolution (fig. 2). Orr *et al.* (2005) estimated that the ASH depth in the Pacific will shoal from the present day 140 m to 70 m by 2100. For the North Atlantic the rise will be from 2000 m to 610 m. These figures were based on their “conservative scenario”. In the study by Guinotte *et al.* (2006), more than 95% of deep-sea corals were found in locations that were saturated during pre-industrial times; locations of which 70% will be undersaturated by 2100 if the projections of Orr *et al.* (2005) will prove correct. The distribution of deep-sea corals will surely change dramatically the coming centuries.

Deep-sea hard substrate habitats are naturally patchy, separated by vast plains of siliceous soft sediments. Available surface for settling is scarce, and the competition is furious. The period after the last glaciation during the Pleistocene–Holocene transition (12 ka BP) was a splendid example of the contrary. As the ice retreated from Scandinavia it left clean hard surfaces in surplus, and as soon as oceanographic conditions allowed, cold-water corals established in the area (Correa *et al.* 2012). Over a period of 400 years *Lophelia pertusa* made a 7500 km range-expansion from deglacial refugia, according to the tracing of the genetic origin of the present *L. pertusa* populations in the North Sea done by Henry *et al.* (2014). In present days we see *L. pertusa* establishing on man-made structures such as offshore oil platforms. On North Sea oil rigs the depth distribution is observed to be 60–130 m, with peak density between 90–110 m, corresponding to depths around or below the summer stratification level and temperatures between 7° and 11°C (Roberts 2002; Gass and Roberts 2006). The potential for spread is enormous in this species, as long as the conditions are right.

### ***Dispersal and population connectivity***

For sessile marine benthos such as *Lophelia pertusa*, and other sessile invertebrates, the only chance of dispersal is during the pelagic larval stage. Once settled and metamorphosed into their sessile adult form, they are stuck. The pelagic larval stage is also the means of connecting different populations. Larvae are transported by ocean currents, and since the major oceanic currents usually are uni-directional and stable, this results in one-way transport of larvae from source to sink populations<sup>2</sup>. Henry *et al.* (2014; see also Dahl *et al.* 2013) traced the origins of the northeastern Atlantic populations of *L. pertusa* to Mediterranean populations, that through the Strait of Gibraltar connected northern populations via the Mediterranean outflow water (MOW), with populations at Galicia Banks, Aviles Canyon, and British Isles as stepping stones for further dispersal to the Norwegian shelf and Barents Sea. Most populations in the northeast Atlantic enjoy high gene flow, while populations in Skagerrak and the Norwegian Fjords show high clonality in the most hydrodynamically isolated locations (Le Goff-Vitry *et al.* 2004; Dahl *et al.* 2012; Flot *et al.* 2013).

At smaller scales, neighboring populations could potentially have multi-lateral connectivity through alternating current directions, such as tidal currents or regular

<sup>2</sup> A source population is defined as a population “in which birth rates are greater than death rates, and emigration rates are greater than immigration rates”, thus a net contributor to neighbouring meta-populations. A sink population is defined by the opposite: i.e. “birth rates are less than death rates and emigration is less than immigration”, and thus a net receiver of propagules (Crowder *et al.* 2000). A theory originally formalized by Pulliam (1988).

upwelling and downwelling events, depending on the main current regimes working during spawning season and larval drift periods. Although genetic studies like the above can trace genetic origins and establish the connectivity between metapopulations, they cannot resolve the question of how far larvae can be transported in one step. This is confounded by the contributions of larvae from populations acting as stepping-stones, in which the reproducing individuals have the same genetic origin as an upstream source population.

Previously, marine invertebrate larvae were conceived to be dispersed more or less like passive particles, with no means of affecting their dispersal routes. Recent studies have, however, shown that larvae can exert an influence on their vertical depth distribution and that this affects dispersal directions and distance. Only a slight capacity for vertical positioning potentially has profound effects on dispersal. By vertical migration the larvae have the potential of catching counter-directional currents at different depths and thereby change the direction of dispersal (Fiksen *et al.* 2007; Metaxas and Saunders 2009; Shanks 2009; Corell *et al.* 2012; Drake 2013). While larval behavior is increasingly recognized as influential during dispersal, and biophysical dispersal models are developed to include these biological drivers, very little is yet known about the swimming abilities and ontogenic shifts in the properties and behavior of deep-sea invertebrate embryos and larvae.

### **Morphology and biology**

*Lophelia pertusa* belongs to the stony corals, i.e. scleractinians, and build large arborescent colonies that can extend continuously over hundreds of square kilometers. Usually, the upper one-meter of the colonies contain live polyps, while older polyps below dies off due to age, reduced water circulation and food availability (Wilson 1979; Cairns and Kitahara 2012). One colony is the result of the asexual growth of one settling sexually produced larva, with budding occurring from the rim of the older polyp. It is possible that colonies can originate from several larvae that have anastomosed (fused) during growth, since gregarious settling is common in corals. However, while chimerism and fusing of closely related juveniles is a common phenomenon; as the colonies grows this self-recognition of siblings and acceptance of each others tissues can be reversed, and later one individual will take over (Rinkevich 2004). Pires *et al.* (2014) have found gametes of both sexes from different polyps in the same colony of *L. pertusa*, so there are some evidence that this species could have anastomosed colonies, although it seem rare. Each polyp resides in a skeletal cup, i.e. a *corallite*, up to 20 mm long and 10 mm wide (Gass and Roberts 2010).

Shick (1991) aptly described anthozoans as being at “*the origami level of construction*”, as their bauplan basically consist of epithelial sheets of either epidermis and gastrodermis, or two layers of gastrodermis (as in the mesenteries), with a layer of acellular mesoglea in between. This play on word is derived from the terminology *tissue* or *organ grade of construction*. Anthozoans do not possess organs, and thus are at the tissue grade of construction. Each epithelial layer consists of single cells, sometimes elongate with differentiation between distal and basal part of cells, thereby giving the epithelia a pseudostratified appearance. These sheets are folded into the few tissue types and appendages that make up the animal, such as the tentacles, mesenteries, and the actinopharynx, i.e. the passage from the mouth into the gastrovascular cavity (Fautin and Mariscal 1991; Fautin 2009). Rather than having cells organized into organs, there are specialized cells carrying out the necessary

functions, and these cells are clustered in the epidermis or gastrodermis according to their function. For instance, calicoblastic cells are the ones excreting the aragonitic skeleton of scleractinians. These constitute the epithelial layer of cells aligning the skeleton both on the outside and the inside of the corallite. The gastrodermis lining the mesenteries contain unicellular gland cells excreting enzymes and mucus for digestion. Simple gonads, without oviducts or sperm ducts, are produced as outpocketings of the mesenteries. All epidermal and gastrodermal layers contain ciliated supporting cells that govern cross surface transport: on the external surfaces they help shedding sediment off the living tissues, and in the actinopharynx they help in food transport into the gastrovascular cavity and general water circulation. There are also neurons, epitheliomuscular cells, and sensory cells with mechano- and chemoreceptors.

*Lophelia pertusa* are predators and opportunistic heterotrophs, as most deep-sea scleractinians. They feed foremost on zooplankton, but also on particulate and dissolved organic matter, pico- and nanoplankton (Houlbrèque *et al.* 2004; Dodds *et al.* 2009; Gori *et al.* 2014; Mueller *et al.* 2014; Naumann *et al.* 2015), and recently it has been discovered that they possibly also house chemoautotrophic sulfur oxidizing, and nitrogen fixing symbiotic bacteria (Middelburg *et al.* 2015).



**Fig. 3** – Egg release in *Lophelia pertusa*. Female polyps forcefully eject thousands of eggs in one big squirt, followed by a couple of smaller squirts with 15–20 minutes in between. Male polyps let their sperm slowly ooze out, like a trail of smoke.

Reproduction in *L. pertusa* is by broadcast spawning, i.e. release of gametes to the surrounding water, and subsequent external fertilization (fig. 3). Gonochoric broadcast spawning is the dominating sexual system and reproductive mode in deep-sea reef-building scleractinians, while hermaphroditic spawning dominates in tropical corals. Brooding of embryos and larvae are common in solitary species, and more prevalent in temperate and cold-water Atlantic species than in other ocean basins (Waller 2005; Kerr *et al.* 2010).

Gametogenesis and spawning is probably regulated by estradiol and testosterone, as in vertebrates. Peak levels of glucuronidated testosterone and 17 $\beta$ -estradiol have been measured during spawning over reefs, with a 100-fold increase in glucuronidated estrogen at spawning compared to one month prior to spawning (Atkinson and Atkinson 1992; Twan et al. 2006). In *L. pertusa*, gametogenesis takes a full year, or more, for the oocytes (eggs), while spermatocytes developed faster (Waller and Tyler 2005; Brooke and Järnegren 2012). Spawning occurs in January-February in Skagerrak, and February-March in the Trondheim Fjord populations (Larsson et al. 2014), while populations in the Gulf of Mexico and off Brazil is estimated to spawn during September-November and May-July, respectively (Waller and Tyler 2005; Pires et al. 2014). The annual spawning of *L. pertusa* is in contrast to other reef-forming deep-sea scleractinians that shows continuous or multiple spawning over the year (Pires et al. 2014).

The synchronization of spawning is most likely regulated by hormones; however, this has not yet been fully investigated. Most research on spawning periodicity has been connecting spawning with lunar cycles (Babcock et al. 1986; Harrison et al 1984; Hayashibara et al. 1993), with lunar periodicity in spawning synchrony of other invertebrates extending even into the deep-sea (Mercier et al. 2011). Solar insolation (Penland et al. 2004) and calm periods with a reduction in wind driven currents (van Woesik 2010) has also been linked to spawning periodicity in tropical corals. The calm periods could potentially induce spawning due to that concentrations of water soluble hormonal signals builds up in the more still water; however, this possibility was not investigated.

While annual cycles in environmental conditions can govern the onset of gametogenesis and the general annual cyclicity of reproduction, the final maturation and release of gametes should be governed by hormones. Atkinson and Atkinson (1992) suggested that, as gametes have matured, the release of conjugated hormones will give a negative feedback on gonadotropin to decrease hormone production, and thus affect the mesogleal lining of the oocyte and spermatocyte pockets so that they disintegrate, and gametes can be released into the gastrovascular cavity and subsequently expelled by the polyp. The hormone system of cnidarians is not fully understood yet (Tarrant 2005), but teleost fish use conjugated hormones as exogenous signals, i.e. pheromones, to synchronize gamete maturation and spawning in conspecific mates (Kobayashi et al. 2003; Stacey 2003), and it is thus likely that there are similar functions in corals.

## *Cnidae*

One cannot discuss the morphology and biology of cnidarians without the mentioning of the defining character of the entire phylum, i.e. *cnidae*<sup>3</sup>. The name Cnidaria is derived from the Greek word κνίδη (*knidē*), meaning nettle, based on the burning sensation received by the encounter with certain jellyfish (e.g. Lion's mane jellyfish, *Cyanea capillata*). It is apparent while looking through a microscope at a coral tentacle that *cnidae* is of profound importance, since *cnidocysts* are just about everything you see in the tentacle epidermis as well as in other tissues. The density of

---

<sup>3</sup> *Cnidae* is the umbrella term for a range of different types of *cnidae*, and different levels of *cnidae* terminology. *Cnidocyte* is the cell bearing a *cnidocyst*, i.e. a stinging organell with a capsule and a tubule, sometimes equipped with a shaft. A *cnidoblast* is a cell containing a developing *cnidocyst*.

these stinging organelles is impressive. Cnidae are used by corals to catch prey and to defend themselves from aggressors or predators.

Cnidocysts are considered the most complex organelles in the animal kingdom (Shick 1991; Beckmann and Özbek 2012), a complexity that is in stark contrast to the animal's structural simplicity at the tissue level and number of cell types present. Although as many as 25 to 30, or more, morphological types of cnidocysts have been described (reviewed in: Östman 2000; Kass-Simon and Scappaticci 2002; Fautin 2009), there are only a few functional types: i.e. penetrating, ensnaring, and glutinant.

*Penetrating* cnidae usually has a distinct shaft that pierce through the epithelia or cuticle of the prey (or aggressor), however, some cnidae types without shaft can also penetrate if the trajectory of the everting tubule is straight and the discharge kinetics is sufficient (Östman *et al.* 1997; Colin and Costello 2007).

The everting tubule of *ensnaring* cnidae has a sweeping discharge trajectory and small spines along the entire tubule, effectively entangling the prey (Colin and Costello 2007). A special case of the ensnaring type is desmonemes: their spring-like thread has so much spring tension that they can crush the cuticle of copepods (Östman *et al.* 1991).

*Glutinant* cnidae secrete a sticky substance, and/or, are equipped with adhesive microfibrillae along the everted tubule, as in spirocysts (Mariscal *et al.* 1977a) and ptychocysts (Mariscal *et al.* 1977b). While spirocysts is present in all anthozoans (concentrated to the tentacle epidermis), ptychocysts are highly specialized and only occurring in burrowing cerianthid anemones. They are used for building the framework of their dwelling-tube, in which particles adhere to add to the construction.

Certain types of cnidae (i.e. atrichous isorhiza, without spines on the tubule), is used both by adult polyps of *Hydra sp.* (Ewer 1947, in Kass-Simon and Scappaticci 2002), and the actinula larvae of the hydrozoan *Tubularia mesembryanthemum*, as a means of temporary attachment during locomotion or settling (Yamashita *et al.* 2003). These cnidae types have yet to be functionally described to be able to classify them as either of the above functional types, although it seems from manuscript III in this thesis that they should be grouped with the glutinant types, which explains their function in temporary attachment; a function that was in no sense obvious from the smooth appearance of the tubule.

Cnidocysts are also grouped into three categories based on morphological characters: nematocysts, spirocysts, and ptychocysts. The highest diversity is found amongst nematocysts, the other two being basically monomorphic. Within Anthozoa the diversity of nematocysts is lower than in Hydrozoa (aprox. 10 of 30 types); however, the spirocysts and ptychocysts are specific for Anthozoa (Fautin and Mariscal 1991).

Cnidogenesis has been described by Slautterback and Fawcett (1959), Skaer and Picken (1966), Westfall (1966), Skaer (1973), Holstein (1981), Tardent and Holstein (1982), amongst others, reviewed by Kass-Simon and Scappaticci (2002). These early works have described the ultrastructure of the developing cnidae, and identified the role of the Golgi apparatus in the excretion of capsule and tubule. The capsule is excreted first, and the tubule is added externally to the capsule in the form of a cylindrical tube. This process is orchestrated by centrioles and microtubuli, also responsible for the correct split of the chromosomes during cell division. The microtubuli forms a funnel around the progressing tubule, and the number of microtubuli involved decides the width of the tubule produced. If the cnidocyst in the making is equipped with a shaft, the proximal part of the tubule will be made wider,

i.e. more microtubuli involved, and then the number of microtubuli will be reduced when the remaining tubule is built. Building blocks of sub-units of the proteins and mini-collagens involved gets lined up inside the microtubuli and bonds are formed. The tubule is made up of two or three layers with different properties. If spines are in line for production, the capsule is filled up with sub-units for the specific proteins making up the spines, and as soon as the external tubule has been invaginated into the capsule, the spine proteins will neatly fit in where they belong along the inverted tubule. A spine protein is identified for *Hydra*, and aptly named spinalin by Hellstern *et al.* (2006). Detailed presentations of this intricate process of invagination, folding, and packaging of the external tubule, to produce the mature, and ready to fire, stinging organelle with internalized tubule has been given by the work of e.g. Skaer and Picken (1966), and Tardent and Holstein (1982). More recent work has described the process of cnidogenesis in more molecular detail, identifying different mini-collagens as the building blocks of capsule and tubule walls (e.g. Engel *et al.* 2002; Adamczyk *et al.* 2007; David *et al.* 2008).

Documentation of the morphology of cnidoblasts in different stages of maturation has been done for the anthozoans *Metridium senile* and *Sagartiogeton viduatus* by Östman *et al.* (2010a-b; 2013). Already Möbius (1866) suggested that cnidoblasts differentiate beneath the mature cnidocytes (commented in Robson 2004), and Slautterback and Fawcett (1959) traced the origin of cnidoblasts from interstitial cells at the base of the epithelium. The maturing cnidae then migrates from the basal to the distal epithelium where final maturation takes place (Skaer 1973; Tardent 1995).

### *Trigger mechanisms*

As if the cnidogenesis, and the resulting cnidocysts, was not exquisite enough, their mode of action brings it to a complete new level. The firing mechanisms for cnidocysts are exquisite in an insidious way, and some the most interesting studies on the subject have been done by Watson and Hessinger (1994), and Watson and Roberts (1994). Cnidae discharge is triggered by mechano- and chemoreceptors working in concert. These receptors are situated on supporting cells adjacent to the cnidocyte itself. The mechanoreceptors consist of stereocilia, or “hair bundles”, that are sensitive to vibrations of specific frequencies, tuned to trigger cnidae discharge when a suitable prey gets close to the cnidae laden tentacles. As the first round of fire has been executed, the prey finds itself pierced with penetrating nematocysts, and entangled in a sticky web of spirocysts. The more it fights to get free, the more it gets entangled with the sticky web. And soon the toxins and enzymes delivered by the nematocysts will subdue the prey that subsequently will be less active, i.e. its frequency of muscle activity will go down. This is when things get insidious. The pierced prey is now leaking body fluids, for instance the amino acid proline. The chemoreceptors are binding sites for proline, and what happens when proline binds in is that, the hair bundles will grow a little bit longer, and thereby become sensitive to lower frequencies. The next round of fire is executed. Game over. Now, the polyp can safely move the prey into the gut and enjoy the meal.

A coral polyp is an extremely delicate creature, with only two cell layers and the acellular mesoglea to protect them. Still, they take on prey with exoskeletons and sharp appendages, and they have evolved the perfect armory to do so.

**Taxonomic classification**

Phylum:	CNIDARIA
Class:	ANTHOZOA
Subclass:	Hexacorallia
Order:	Scleractinia
Family:	Caryophylliidae
Genus:	<i>Lophelia</i> H. Milne Edwards & Haime, 1849 Syn. <i>Lophohelia</i> Milne Edwards & Haime, 1857 (misspelling)
Species:	<i>Lophelia pertusa</i> (Linnaeus, 1758)

Type species: *Madrepora prolifera* Pallas, 1766

Original name: *Madrepora pertusa* Linnaeus, 1758

Synonyms: *Madrepora prolifera* Pallas, 1766; *Lophelia californica* Durham, 1947 (junior synonym representing the *gracilis* variation sensu Duncan, 1873); *Dendrosmlia nomlandi* Durham and Barnard, 1952 (junior synonym representing the more robust *brachycephala* variation sensu Moseley, 1881); *Lophohelia oculifera* Whiteaves, 1901 (*nomen nudum*)

Referred to as *Lophohelia prolifera* by Gosse (1860) and Carlgren (1940), and *Lophelia prolifera* by Cairns (1979); finally receiving its now accepted name *Lophelia pertusa* in a revision by Zibrowius (1980).

*Etymology*

Gosse (1860) provided an etymology of the name *Lophohelia* as derived from the Greek words *lophos* (a tuft), and *helios* (the sun). *Lophos* refer to the arborescent branching (like a bouquet, a tuft). *Helios* refer to the radiating skeletal lamellae (septa) as seen when viewing the calyx from above, a characteristic feature of *Lophelia pertusa* (Cairns and Kitahara 2012). Further, *pertusus* means perforated and could refer to fine perforations of the skeleton.

*Remarks on phylogeny and history*

Milne Edwards and Haime (1849) first put the genus *Lophelia* within the scleractinian family Oculinidae but later it has been assigned to the family Caryophylliidae Dana, 1846. Caryophylliidae presently comprise 89 valid genera of which 38 are extinct, known only from fossil records Kitahara *et al.* (2010a). The Caryophylliidae is, however, not a monophyletic group, and a revision is likely to reduce the number of genera assigned to the family (Romano and Cairns 2000; Kitahara *et al.* 2010b).

The oldest known fossil assigned to the Caryophylliidae is from the Jurassic era (180 Mya), while some of the earliest fossil records of “scleractiniamorph” corals with characteristics indistinguishable from those of modern corals dates all the way back to the Ordovician 450 Mya (Stolarski *et al.* 2011).

The 51 extant genera of Caryophylliidae are found in all oceans, at all depths, including both zooxanthellate (with photosynthesizing symbionts) and azooxanthellate species (without symbionts). Two genera within Caryophylliidae with exclusively zooxanthellate and reef-building taxa group together in phylogenetic trees and has been gathered in the subfamily Eusmiliinae (Romano *et al.* 2000), thus it is

possible that the diversity of caryophylliids regarding symbiosis and growth pattern will be altered after a revision.

It has been suggested that the solitary azooxanthellate corals, possibly with a deep-sea origin, are the ancestral forms (Kitahara *et al.* 2010a; Stolarski *et al.* 2011), while shallow-water tropical corals seems to have invaded shallow waters at several occasions (Lindner *et al.* 2008).

While the majority of deep-sea scleractinians are solitary there are six prominent reef framework-building representatives: *L. pertusa*, *Solenosmilia variabilis*, *Goniocorella dumosa* (Fam. Caryophylliidae), *Oculina varicosa*, *Madrepora oculata* (Fam. Oculinidae), and *Enallopsammia rostrata* (Fam. Dendrophylliidae) (Freiwald *et al.* 2004; Davies *et al.* 2011). All with a similarly wide cosmopolitan distribution as *L. pertusa*, except for *G. dumosa* and *O. varicosa* that has a more geographically restricted distribution. However, *L. pertusa* is standing out as the species producing by far the most extensive reefs (Cairns 2007; Kitahara *et al.* 2010b).

## AIM OF THE THESIS

For sessile marine organisms the pelagic larval phase is what connects populations, maintains genetic diversity, and provides a security against extinctions due to changing environmental conditions by letting the organisms spread to potentially more suitable habitats. Knowing the prerequisites for successful reproduction and the biological drivers for dispersal is of paramount importance in the work of finding sustainable management strategies so that we can mitigate the anthropogenic impacts imposed on these ecosystems, and hopefully help increase their resilience. Knowledge of the biological aspects that influence dispersal is very limited considering deep-sea benthos (Cowen *et al.* 2007; Cowen and Sponaugle 2009; Davies and Guinotte 2011; Hilario *et al.* 2015; Trembl *et al.* 2015), and the aim for this thesis was to provide biophysical modelers with the biological data needed to improve the accuracy of the predictions from dispersal models for one of the major deep-sea habitat engineers, the cold-water scleractinian *Lophelia pertusa*.

The dispersive phase of marine organisms can be divided into several stages. Trembl *et al.* (2015) provided a conceptual framework of these stages, and the intrinsic and extrinsic drivers affecting dispersal during each stage. The initiation—*stage 1*—of dispersal is affected by the abundance and density of the reproducing population, with reproductive mode (brooding or broadcast spawning), and fecundity (number of gametes per individual) as key intrinsic factors. The habitat quality and structure, as well as depth and timing will affect the outcome of the reproductive effort. *Stage 2*—the actual dispersal stage—is affected by mortality rates, intrinsic properties of the propagule such as morphology, buoyancy, and behavior, and extrinsic factors such as water quality, hydrodynamics at different scales, and predator-prey dynamics. The settlement stage of dispersal—*stage 3*—is determined by when and how metamorphic and settling competency is achieved by the larva, and for how long this competency window lasts; thus setting the limits for the pelagic larval duration (PLD). The availability of suitable substrate and habitat will influence the outcome. The final step—*step 4*—is the actual recruitment, which is depending on the condition of the larva at the time when it finds suitable substrate and its capacity to cope with the competition with other organisms, and the environmental qualities of the chosen habitat.

As noted by Hilário *et al.* (2015) the dispersal stage (stage 2) can be further broken down into sub-stages depending on ontogenic shifts, i.e. during embryo and larval development the propagules can alter between passive and active stages. The term PLD is often used independent of whether the embryogenesis is included in the pelagic phase or not—as is the case in broadcast spawning—leading to the suggestion by Hilário *et al.* (2015) of changing PLD to PPD—pelagic propagule duration—to get a terminology that encompasses the embryogenesis.

With the framework of Trembl *et al.* (2015) in mind, and with the additional aspects presented by Hilário *et al.* (2015), we aimed at mapping the early life history of *L. pertusa*, from spawning to settling.

## Results in Summary

### Timeline – from spawning to settling competency

In summary, we have established that after gamete release and fertilization, the zygotes and developing embryos are transported as passive particles until day five, when they become swimming blastulae (fig. 4). During this period they are positively buoyant, slowly ascending, and most probably transported by advection away from the reef (paper I). Day 6–9 they are alternating between modest swimming and being passive during the process of gastrulation. From day 10 to 20 they are in the pre-competency phase, actively swimming upwards in the water column with a swimming speed of  $0.44 \pm 0.16 \text{ mm s}^{-1}$  (mean  $\pm$ SD, measured day 14).

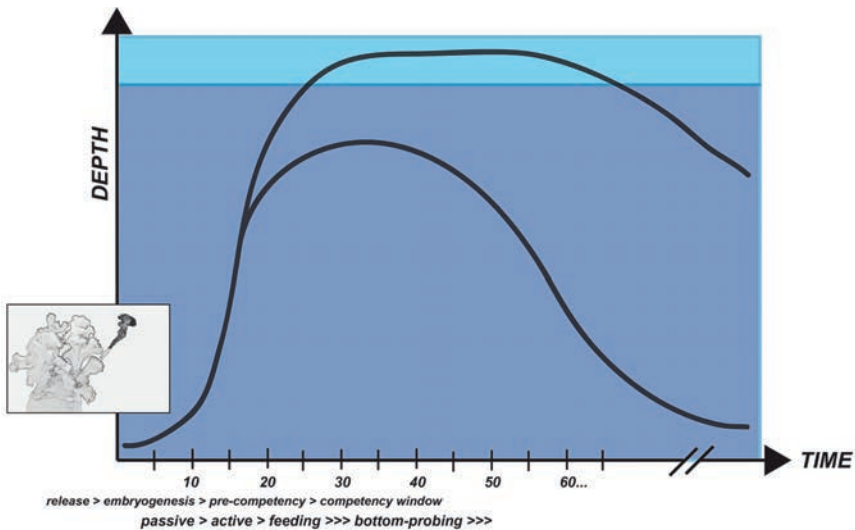


**Fig. 4** – Timeline for the pelagic phase of *Lophelia pertusa* embryos and larvae, indicating the ontogenic shifts and behavior of the planulae that affect dispersal. Until day 5 embryos are positively buoyant and transported by advection as passive particles. Between day 5 and 9 they are capable of moderate swimming, but remain still while they undergo gastrulation. From day 10 they are actively swimming upwards. They enter their settling competency period after day 20 and starts feeding. After approximately 30–40 days they start their search for suitable habitat for settling, and can probably spend several months searching. Potentially they can enter the photic zone.

After this pre-competency period they simultaneously develop a flexible mouth and starts foraging actively, as well as developing functional cnidocysts, and start actively swimming downward and displaying bottom-probing behavior (paper I and IV). They have now entered their competency window, in which they are capable of metamorphosis—possibly only after successful foraging to gain necessary nutrients—and ready to settle. Although the bottom-probing behavior started day 21, not all larvae started swimming downward immediately. The downward swimming became increasingly common over a period of two weeks (day 21–35), after which

almost all larvae displayed the same behavior. At the same time, vertical upward swimming was still observed in 36 days old planulae, measured to  $0.74 \pm 0.20 \text{ mm s}^{-1}$  (mean  $\pm$ SD), corresponding to a potential vertical migration of 64 m per 24 hours. It is plausible that planulae will alter between downward and upward swimming during a period expanding beyond 35 days. And foraging will influence their swimming.

The duration of the competency window is yet to be resolved, but a few of the larvae from the spawning season 2015 have survived in lab for a full year, although in very poor condition by the end. The interesting aspect is that they seem to spend almost all of their competency window period further down in the water column since they start downward swimming simultaneously with foraging and gaining functional cnidae. And although planulae in lab was showing interest in small size microalgae their main diet seemed to be of animal origin, or picoplankton, similar to the diet of the adults. Potentially they are capable of spending long periods near-bottom, after the initial 20–30 days of dispersal higher up, searching for suitable habitat and foraging.

The above described developmental rates was observed in planulae reared at a temperature of 7–8°C, and are likely to be affected by *in situ* temperatures during the dispersal period of naturally dispersing larvae. For example, in the Koster-Hvaler area the spawning season coincide with dropping temperatures, from c. 8°C in January to c. 6°C in March-April (fig. 5), measurements taken in 2015 with a Aanderaa RCM9 acoustic Doppler current profiler, ADCP, with turbidity meter). These are the temperatures at the reef site, at 120 m depth, and do not necessarily reflect the temperature at the depth occupied by the larvae. During the corresponding period, the water temperature of the deep-water from the Koster Fjord, taken from 45 m depth and continuously measured in lab (with a few gaps in the data due to technical failure), dropped from c. 9°C in December down to c. 5°C in February-March, but were then rising to 8°C by April (data from the Sven Lovén Centre water inlet loggers). We have yet to resolve the question of how high up in the water column the planulae ascend during the pelagic phase; however, since they did show interest in small size microalgae and passed through haloclines with no hesitation (paper IV), they can potentially ascend to the photic zone. The depth distribution of *L. pertusa* on oil rigs (60–130 m, Gass and Roberts 2006) gives at least an indication of the depth distribution at settling competency. It is important to consider the ambient temperatures and the effect it has on the development rates of larvae when modeling, and allow for variation. These data will, nevertheless, greatly enhance the accuracy of predictions of larval dispersal for *L. pertusa*.

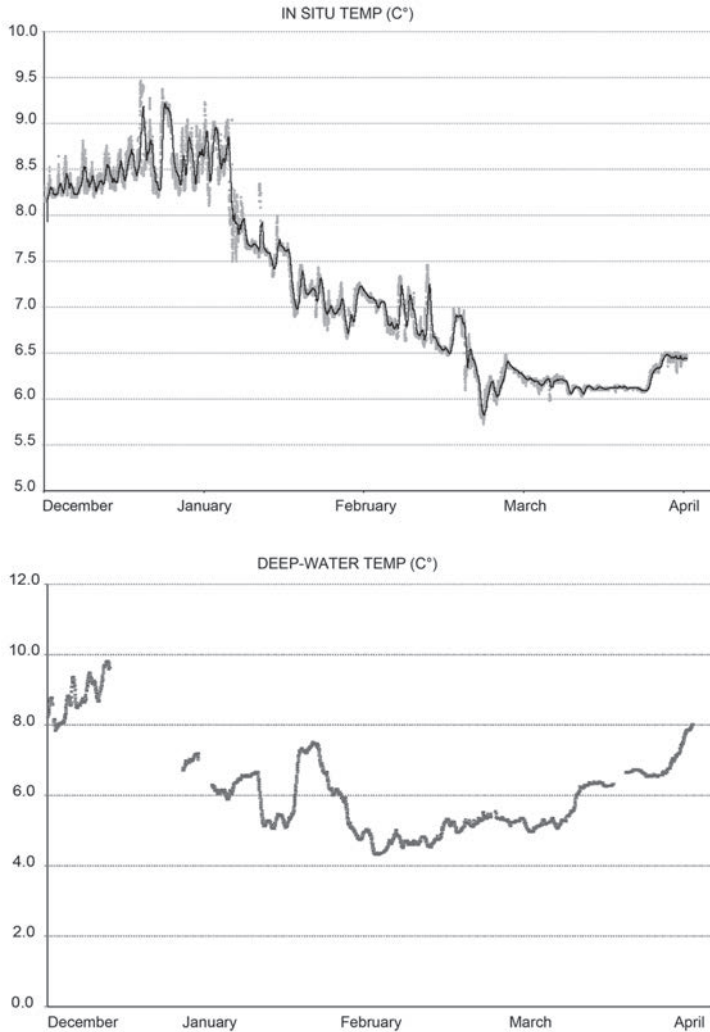


**Fig. 5** – *In situ* water temperature (°C) at 120 m depth at the Tisler reef during December 9, 2014 to April 27, 2015 in the top graph. The bottom graph shows the temperature of the deep-water of the flow-through system at the laboratory (water inlet at 45 m depth in the Koster Fjord) for the corresponding period. The *in situ* measurements were taken with an ADCP (Aanderaa RCM9), and the data from the deep-water system in the lab were extracted from the Sven Lovén Centre web page. The water temperature and salinity is continuously logged. Note the different scales of the y-axes.

### *Timing of spawning*

In the two most successful years of spawning, 2013 and 2015, the timing of spawning varied between years. In 2013 the first spawning event occurred in early January, starting the 9<sup>th</sup> and 10<sup>th</sup>, followed by a quiet period until January 20, when an intense spawning period started. This period lasted a full week, until January 27, which happened to also be the time for full moon. Two more occasions with minor gamete release was observed at February 14–15 and 28, which was the last observed spawning this year. The February full moon was the 25<sup>th</sup>.

In 2015 there was no intense week of spawning. The first event was observed in January 22, followed by release on January 25, 27\*, 29\*, and in February 2\*, 4, 13, 18\*, 19\*, 20, 23\*\*, and finally the 25<sup>th</sup>. Those marked with an asterisk (\*) were major releases, with February 23<sup>rd</sup> being the major event. Full moon occurred January 5 and February 4, and thus no apparent connection could be found to the moon cycle this year.

In an attempt of resolving the question if spawning in lab coincided with spawning in the field, we made a long-term deployment of an ADCP (Aanderaa RCM9) to measure *in situ* turbidity (NTU) and current directions and speed (cm s<sup>-1</sup>) at the Tisler reef, where the parental colonies had been collected. The equipment was deployed over a period between December 9 (2014) and April 27 (2015), to cover the spawning season with good margins. To our surprise the equipment came back with a single peak in turbidity registered at January 18, lasting for one hour at 06:10–07:10, and slightly elevated turbidity values following after that for almost the entire remaining period (fig. 6). This is too early to coincide with early spring phytoplankton blooms, and no dredging activity was reported during this time. The gametes of *L. pertusa* are highly reflective and should be easily detectable with an NTU-type (Nephelometric Turbidity Units) of turbidity meter that measures light backscatter. The single peak reached almost 6.0 NTU, while the background turbidity was relatively low at 0.2–1.2, with occasional smaller peaks <1.8 NTU. The ADCP was standing at the edge of a larger reef patch, unfortunately in a slope and in a depression between *L. pertusa* colonies. The position was not optimal, but promising. In hindsight it is apparent that to be able to accurately pick up peaks in turbidity caused by spawning we need to put out several measuring devices coupled to time-lapse cameras to verify that the peaks are indeed caused by spawning products. This single peak could be caused by a dense aggregation of zooplankton or what not, and further deployments needs to be done to resolve the question of the timing of spawning in the field.

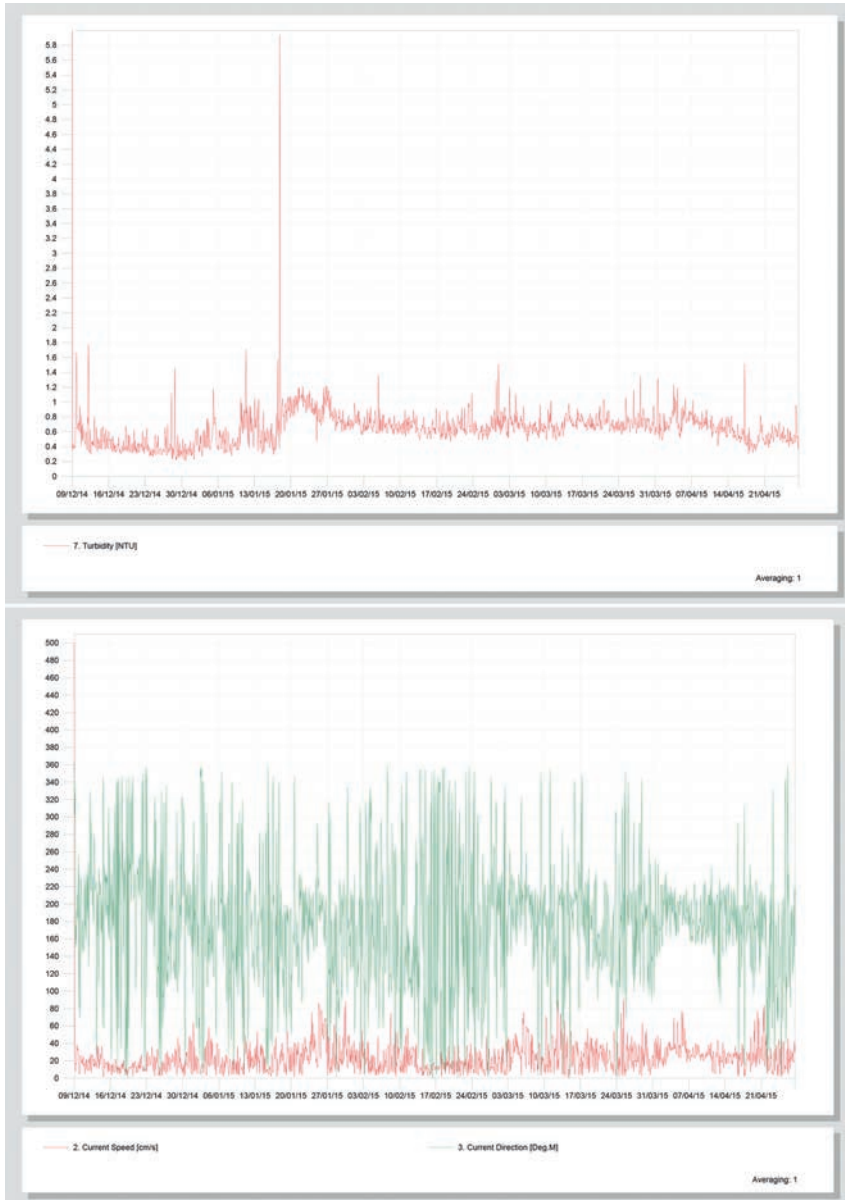


**Fig. 6** – *In situ* measurements of turbidity (NTU) in the top graph, and current speed ( $\text{cm s}^{-1}$ , red) and direction (green) in the bottom graph. Measurements were taken at 120 m depth at the Tisler reef during the period December 9, 2014, to April 27, 2015. The turbidity shows a single peak at January 18, for one hour between 06:10–07:10 hours. The single peak was an unexpected outcome, since the corals in lab were spawning on several occasions and we expected to see several peaks in January–February caused by spawning products. Further field measurements are needed, in combination with cameras, to verify that any peaks are indeed spawning events and not caused by something else. Measurements were taken with an Aanderaa RCM9 acoustic Doppler current profiler (ADCP) with turbidity meter.

*Embryogenesis and early planulae*

In paper I (Larsson *et al.* 2014) we established the timeline for embryogenesis and larval development, with focus mostly on the embryogenesis. The embryo development of *L. pertusa* is slow, compared to development times in temperate and tropical corals. At 7–8°C it took 48 hours to reach the 64-cell stage, and 5 days to become ciliated blastulae. They did not develop into planulae until after accomplished gastrulation day 9–10, and starting the onset of settling competency after three weeks. As seen in paper IV, the development rate doubled in embryos reared at 11–12°C, i.e. what normally took six days, was achieved in only three days at the higher temperature. A full developmental series of scanning electron micrographs (SEM) from non-hydrated egg to mature planula can be seen in fig. 7.

These development rates can be compared to those of the temperate cup coral *Caryophyllia smithii* that become fully developed feeding planulae after only 48 hours and ready to settle after 8–10 weeks, reared at 15°C (Tranter *et al.* 1982). In broadcasting tropical corals planulae are commonly formed 24–36 hours after spawning, with feeding starting day two or three, and settling from day five, or even as early as 2.5 days post-spawning (Krupp 1983; Hayashibara *et al.* 1997; Schwarz *et al.* 1999; Miller and Mundy 2003; Chui *et al.* 2014), with competency periods and longevity spanning over periods of 10 days to over 200 days (Wilson and Harrison 1998; Graham *et al.* 2008).

The only deep-sea corals followed from release to settling are brooding soft coral species (Octocorallia), and thus release is of fully developed planulae. These have been observed to be either demersal larvae, crawling over the substrate, or swimming close to the bottom, with settling and metamorphosis occurring from day 1–30 in two species (Sun *et al.* 2010a,b) and day 3–70 after release in two other species (Sun *et al.* 2011). Planula release is probably continuous over the year in these species, and furthermore, planulae can be produced via parthenogenesis, i.e. without fertilization. One interesting aspect with the studies on these octocorals was that larvae with an origin from deeper (1200 m) populations seemed less selective considering substrates than those from the same species collected at more shallow depths (500 m, Sun *et al.* 2010a).

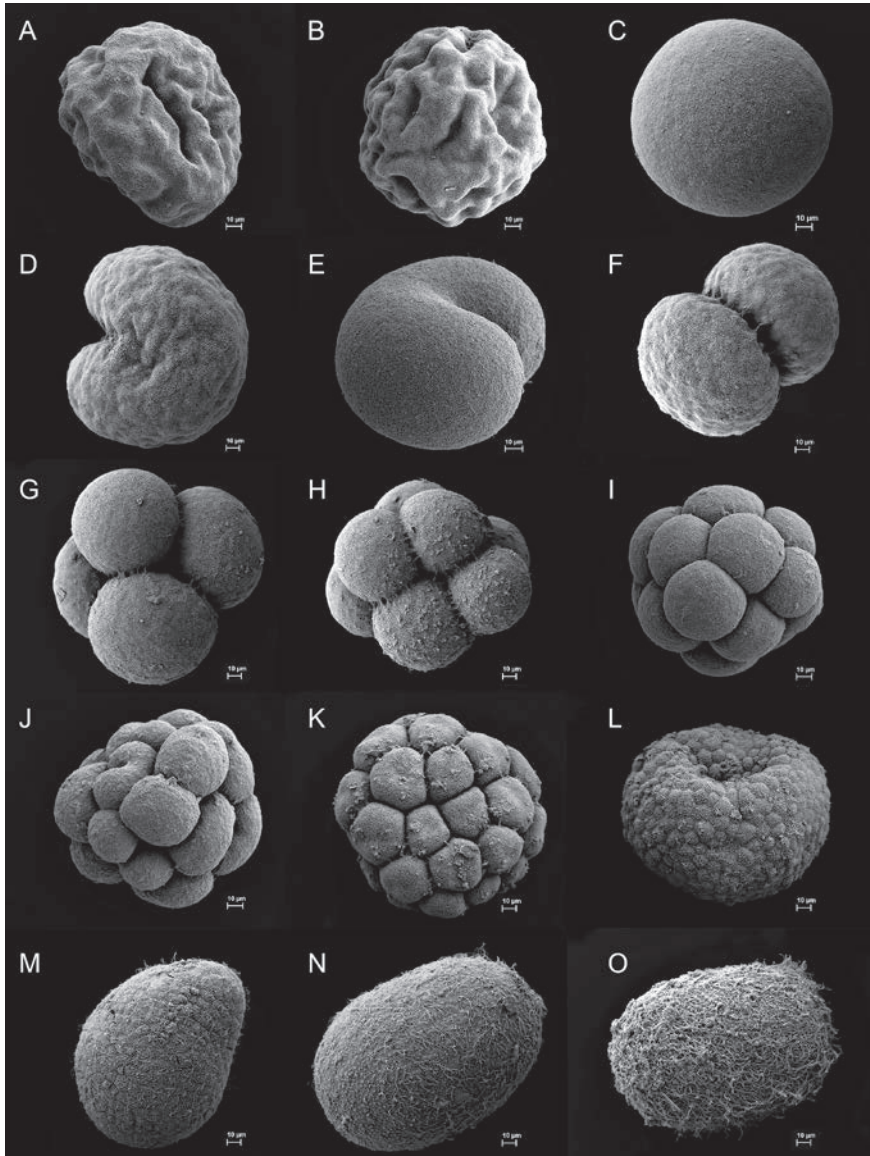


**Fig 7** – A development panel for *Lophelia pertusa*, from recently released egg (A-B), not yet fully hydrated, to a planula (O). The 64-cell stage (L) was reached after 48 hours and ciliation occurred day 3–5 (M) followed by gastrulation. N represent a 14 days old early planula with an oral pore, and O is a fully developed planula. Scanning electron micrographs.

*Comparison of adult and larval cnidome*

In paper II we present the internal morphology of *L. pertusa*, with focus on the cnidome (i.e. the cnidae complement) of the adult polyps. This study was done to be able to compare the adult and larval cnidome and from this derive differences in cnidae function between adults and larvae, in combination with observations of larval cnidae usage. The cnidome of *L. pertusa* had previously been described by Carlgren (1940); however, to make a proper analysis of the differences we needed more detail in the cnidocyst morphology. Very few studies have been done comparing adult and larval cnidae (e.g. Yamashita *et al.* 2003; Holst *et al.* 2007; Zenkert *et al.* 2011), but those done have shown that the planulae have a unique cnidae complement. We suspected that cnidae are used by planulae for preliminary anchoring before attaching more permanently, and therefore a sign of settling competency. In paper III we concluded that the larval cnidome indeed is very different from the adult's, and could confirm that planulae use them for temporary anchoring. The evidence is still not completely to satisfaction and more studies needs to be done to verify cnidae function in planulae. For instance, we wanted to fix settled planulae for scanning electron microscopy (SEM), so that both planulae and their attachments by cnidae tubules were visible. Unfortunately only one planula was observed to settle on one of the substrates adapted for fixation, and subsequently fixed for SEM, but the planula itself was lost in the process, leaving only cnidae tubules. The types of tubules present on the substrate where the planula had attached had adhesive microfibrillae or other adhesive strands; however, they were not verified on the surface of planulae in SEM preparations and there is therefore still an uncertainty about these results. Observations under dissection microscope and light microscope confirmed attachment by cnidae tubules, although not the exact type of cnidae or mode of attachment.

From the observations made during this study (paper III), it is also apparent that the planulae could use cnidae as a defense, to evade predators. The atrichous isorhizas (i.e. nematocysts without shafts, and with smooth tubules) had rigid tubules that could hold off potential predators, or rather, holding the planulae off the predators. Cnidae also fired in response to water turbulence which can be an effect of a predator closing in; however, potentially this could also be a mechanism for planulae to avoid being swept out of a reef matrix by eddies. If they have managed to find a suitable reef habitat for settling they will need to have a means of staying there, despite small-scale hydrodynamic forces that could sweep them away. These cnidae functions need further investigation, but are an interesting avenue for further research.

The investigation of the internal morphology in paper II also resulted in some controversy considering the free extensions of the mesenterial filaments, what we chose to call acontia, as in sea anemone anatomy. The focus on skeletal characters in scleractinian taxonomy has probably led to some confusion considering the naming of soft tissues in scleractinians. Since the early taxonomist had not provided names for soft tissue homologs to other anthozoans, such as sea anemones that has been generously described according to their soft tissue anatomy since they lack a skeleton, it seems as if later researchers has been shy to apply names of anthozoan soft tissue anatomy to scleractinians. The basic bauplan of scleractinians is homologous to that of sea anemones, both groups belonging to the subclass Hexacorallia. In the synthesis of anatomical and molecular taxonomic evidence made by Daly *et al.* (2003) this controversy is discussed, and their conclusion is that Actiniaria (sea anemones), Antipatharia (black corals), Ceriantharia (tube-dwelling anemones), Corallimorpharia, Zoanthidea, and Scleractinia are a monophyletic group. In addition, Actiniaria,

Corallimorpharia, and Scleractinia share the paired hexamerously arrangement of the mesenteries, i.e. the soft tissue compartments of the polyp. The soft tissue anatomy is complicated by the high variation within groups, and that different features are shared across different pairs of groups. Daly *et al.* (2003) also discuss the complications that arise from differences in terminology between groups of hexacorallians. The free extensions of the mesenterial filaments in *L. pertusa* are fitting the descriptions of acontia for sea anemones, as we discuss in paper II.

### *Larval feeding behavior*

In paper IV we have confirmed that *L. pertusa* planulae are planktotrophic, feeding mainly on animal derivatives, but also showing interest in picoplankton and small size microalgae. It was apparent from our feeding trials that 14 days old planulae were not yet capable of feeding, while fully mature planula after developing the flexible mouth (>20 days old) responded strongly to the presence of food. The food choice is of interest, since different food types are distributed differently in the ocean; microalgae being present in the photic zone with a predictable depth distribution, while other food sources is expected to be more patchy and spread out. Knowing the preferred food of *L. pertusa* planulae could therefore give an indication of their vertical distribution during their pelagic period.

We found no limitations to the upward distribution of the planulae; they pass through haloclines and are interested in microalgae. Although, since foraging coincide with settling competency and onset of downward swimming, it is more likely that planulae will forage in random patches of animal derived detritus and picoplankton below the photic zone. Marine invertebrate larvae are known to be able to utilize dissolved organic matter and free amino acids, as well as bacteria and detritus (Manahan 1990; Boidron-Métairon 1995), and in a study by Ben-David-Zaslow and Benayahu (2000) it was estimated that uptake of free amino acids by coral planulae could cover 11% of the metabolic demand for the investigated species. Our planulae were enthusiastically feeding on crustacean homogenate, as been observed in other scleractinian and sea anemone planulae (Tranter *et al.* 1982; Schwarz *et al.* 1999; Schwarz *et al.* 2002). However, such high-quality food should be rather rare in the field.

### **Conclusions**

From our results we can conclude that *Lophelia pertusa* embryos and planula ascend slowly the first ten days after release, and then show a more steep upward movement the following ten days. After this initial constant upward movement it is still unclear if they reside in the photic zone or stay at the depth indicated by settlement on the oilrigs at 60–130 m depth. The longest period of dispersal, beyond thirty-forty days, should be deeper down, actively searching for suitable habitat for settling. Planulae are potentially long-lived; a full year is not impossible, but perhaps unlikely. Setting a proper mortality rate for the modeling should give an end point sooner than one year.

### **Future perspectives**

These studies has answered some of the questions regarding the dispersal potential and plausible routes for *L. pertusa* planulae and raised many more. The *in situ* timing for spawning to verify that spawning is prolonged over two months, or if concentrated to a peak spawning period still needs to be resolved. The timing for release is important for dispersal, and could also be valuable information for management. For example, one could regulate trawling activities, drilling or dredging, within a certain radius around cold-water coral reefs during spawning season to alleviate negative effects on reproduction from sedimentation and toxic substances.

Whether cnidae discharge is affected by ocean acidification is an important issue to investigate, since successful feeding is necessary for corals to maintain calcification rates under acidified conditions. And we now understand that cnidae plays an important role in larval settling; how this is affected by ocean acidification is also a very important question.

Now that we know how to rear *L. pertusa* larvae successfully (with a reservation for the parasites that needs to be managed) this opens up for running experiments on embryos and larvae, for instance, how these early stages are affected by ocean acidification, or even rearing larvae to juveniles for restoration purposes to replant *L. pertusa* in areas depleted of corals. More needs to be known of the *in situ* cyclicity of environmental conditions to be able to maintain reproductive periodicity in lab. Some of our parental colonies did spawn a second year in lab, but to keep the same corals fit to spawn in lab over several years we need to know more about what in the environmental conditions that maintain the reproductive periodicity.

Since we have not yet managed to rear larvae all the way to settling, there is still a question whether planulae when competent for settling are sensitive to pressure. Some deep-sea organisms are known to demand a certain hydrostatic pressure for successful embryonic development; this has been shown by Young and Tyler (1993) for the deep-sea echinoid *Echinus affinis*. Although *L. pertusa* embryos develop well in lab, and early planulae does not seem bothered by low pressure since they reside just below the surface in culture flasks, barotactic sensitivities could develop toward settling competency to assure that larvae will seek out deeper habitats. On the other hand, *L. pertusa* has such a vertiginous depth range—from 39 m to over 3000 m—that pressure does not seem to be the limiting factor. The poor results in settling probably are due to the late realization of the demand for cryptic habitat, with substrates offering minute crevices. This will be investigated further, if opportunity arises.

## ACKNOWLEDGMENTS

First I would like to thank Tomas Lundälv and Lisbeth Jonsson for their work on mapping the *Lophelia pertusa* reefs starting in the late 1990's—without their work I would never have been able to do mine. When first contacting them I was wondering if I could do a Master project on the echinuran *Bonellia viridis*, I had seen that Tomas and Lisbeth had observed them with the ROV. No such projects were at hand, but they had some settling panels that needed attention. And so I began.

Secondly, I would like to thank Kerstin Johannesson for making it possible to get funding for this project. Without her name on the application I would still be sending in grant proposals.

I would also like to thank Roger Johansson and Thore Hilmersson for technical help with my rotating gadgets.

Talking about gadgets, I would also like to send a thanks to the company that helped me build them, the company with the fantastically swinglish name Plastic Produkter AB. Excellent work!



My cnidocyst friend and mentor, Carina Östman, deserves a big warm hug and many thanks for her generosity and enthusiasm letting all her knowledge spill over on me. After 40 years working with cnidocysts she is still childishly enthusiastic! I'm sorry you can't be with me the day of my defense. On the picture below Carina and a friend is standing on the Chinese wall. That's where she was while I was writing, and when it's time for the defense she'll be on her way to Åre to ski, as she does every year. She is the most energetic 77-year-old lady the world ever saw.

My friend and colleague and supervisor Ann Larsson is also worth a big thank you. We complement each other well, and I hope we will continue working together!

Further, I would like to thank Pink Floyd for making such excellent music. Whenever my mind strayed from the work on the thesis, I could turn on Pink Floyd and immediately I would feel just fine where I was. Sivert Høyem and Madrugada is not a bad company while writing either.

There are many more to thank at the lab at Tjärnö, thank you all!

## THE COLD-WATER CORAL BREEDER'S HANDBOOK

The present work was depending on the successful rearing of *Lophelia pertusa* larvae, and when it came to keeping the parental colonies happy we were very successful. The corals were maintained in two polycarbonate chamber-sets, with each set divided into four 18 L chambers, equipped with Mississippi-type paddles providing that extra water movement to keep the corals in good shape (fig. 8A-B). It is apparent (from long hours of watching the corals while rearing them) that vigorous water movement is crucial to keeping the polyps fit. When corals have spent a long period in low water turbulence their tentacles become long slender and floppy. The muscles in the tentacles wither. Kept in high turbulence water flow the tentacles get stout and strong, and they get more control of their tentacle movements, which possibly affect their feeding capacity positively. It is difficult to advice on an exact rpm for the paddle rotation; the paddles were turned up to what seemed to be the maximum turbulence the polyps could manage without loosing control of tentacle movements. The suitable rpm is depending on both the condition of the corals, the exact dimensions of the paddles and tanks, and surely also on the specific set of corals in the tank, i.e. their morphology, mode of mounting, etc. factors affecting the hydrodynamics. This extra water movement also seemed to add the environmental factor that stimulated the corals to display what appeared to be a natural spawning behavior, and provided us with a plentitude of gametes.

The design of the chambers was inspired from an experimental set-up previously done by our colleagues from Jacobs University in Bremen (Annika Moje, Hannes Wagner, Majk Dressel and Torsten Behnke). The set-up was then designed to provide sealable chambers, where the Mississippi-paddles were to govern the internal water circulation while flow-through of water was turned off over-night, to be able to measure oxygen consumption in corals exposed to drill-cuttings from offshore oil extraction (Larsson *et al.* 2013). During that experiment, the first successful rearing of larvae was achieved in 2009, accidentally, as my supervisor Ann Larsson in the sealed-up chambers found gametes one morning while preparing for oxygen measurements. This encouraged us to apply for funding for the present PhD project and try to rear *L. pertusa* planulae to be able to conduct experimental work such as settling experiments, and general mapping of embryo and larval development. The tank design was modified to suit the new purposes, the chambers were made larger, and the back walls were made black to make it easier to see the small whitish eggs.

### *Experimental set-up for settling*

The experimental set-up for the planned settling experiment consisted of 18 rotating 1 L beakers with submerged substrates on holders, originally designed by myself for this project. Small pieces (~10×10 mm) of four different substrates were glued onto glass slides and then conditioned in flow-through of seawater to get a cover of bacterial film (fig. 8C-E). There were double controls: control #1 with glass slides without substrates, and control #2 with substrates but no additional treatment. The treatments consisted of added food (fine fraction of centrifuged copepod homogenate) and/or adult signal (water from the tanks with adult corals). We wanted to know the prerequisites and cues for the planulae to achieve metamorphic and settling competency. This experimental set-up was not sufficiently tested to be able to evaluate the effectiveness of the set-up. And the rearing of *L. pertusa* larvae proved to be a bigger challenge than rearing the adult corals.

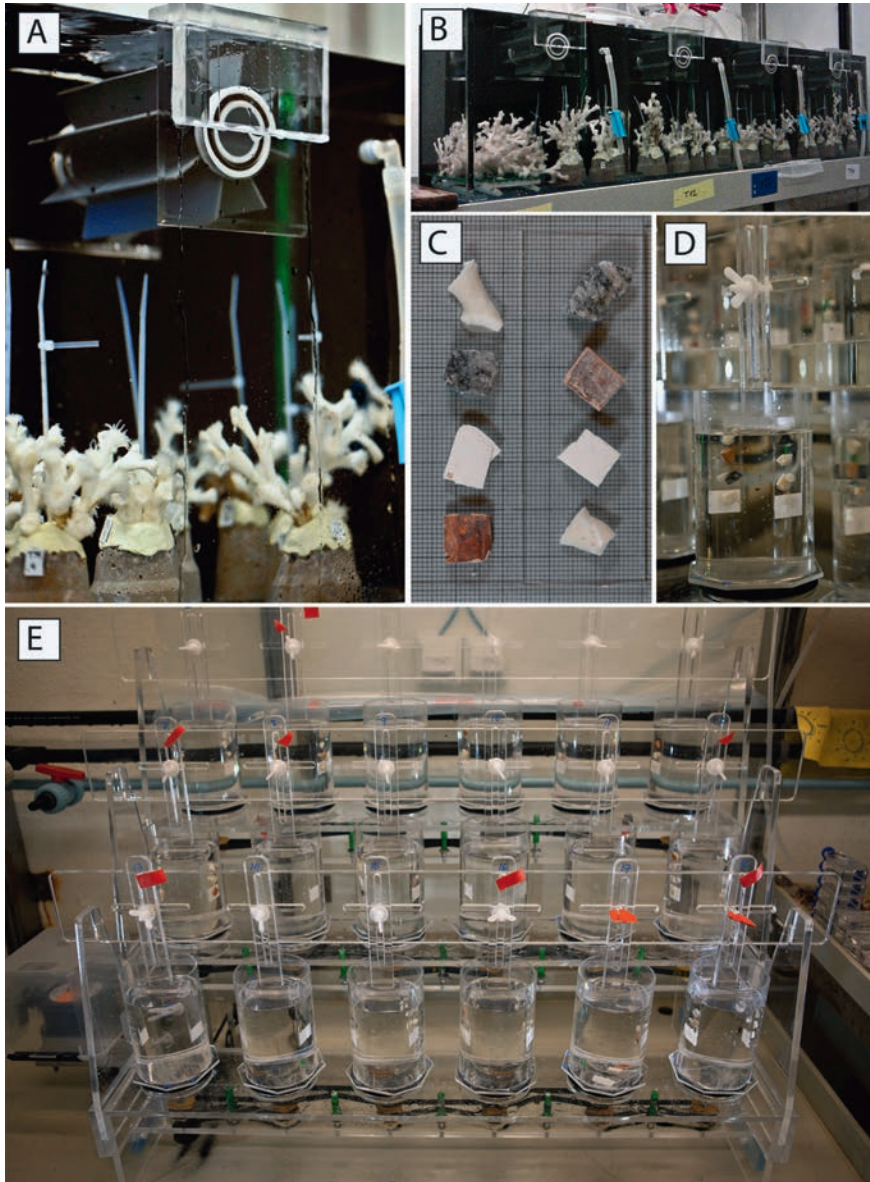


**Fig. 8** – **A.** The much-appreciated (by the corals) Mississippi-type paddles to increase water turbulence in the aquaria. – **B.** The parental colonies were maintained in a chamber-set with four separated chambers (18 L), each equipped with a Mississippi-paddle to govern water movement. – **C.** The settling experiment aimed at testing four different substrates: coral skeleton, bivalve shell (*Arctica islandica*), stone, and a piece of ceramic tile. The glass slides with either plain glass, polylysine-coated glass, frosted area, and the thin space between the glass slides mounted in pairs, and the walls of the polycarbonate beakers provided additional substrates. – **D.** Two pairs of glass slides were submerged in the beakers. – **E.** The full set-up of the settling experiment consisted of 18 rotating 1 L beakers. Six treatments, three replicates each, were divided over the beakers.

### ***The Cold-Water Coral Breeder's Nightmare***

The gametes, embryos, and planulae were kept in filtered seawater (50 + 5  $\mu\text{m}$  Ametek polypropylene cartridges) at 7–8°C, and a salinity of 33–35 psu. The water intake for the seawater flow-through system is situated at 45 m in the Koster Fjord, and thus sensitive to downwelling of less saline surface waters during hard weather. After a period of strong wind the salinity could drop to 28–29 psu. The water thus had to be spiked with additional salt occasionally to maintain suitable salinity. This water treatment was usually sufficient for keeping the planulae in good condition; however, over the years we had an increasing problem with parasites in our larval cultures. A shift to a 1- $\mu\text{m}$  filter cartridge was tested, but the planulae did not develop well in that water. In addition, running a settling experiment it is crucial to condition the substrates to get a bacterial film, as proven by several studies on settling in tropical coral planulae.

Usually, in cultures of marine invertebrate larvae, it is ciliates that cause problems. But the two different parasites observed in these cultures were other types of protozoans. A flagellate was seen probing the planulae, using its flagella as a mosquito's feeding tube (proboscis), inserting it into the planulae. This parasite was rare, and did not seem to cause much damage. There was a more insidious parasite that proved to be able to cause considerable damage, wiping out culture flask after culture flask of planulae. This parasite had no visible cilia or flagella; it was a spherical entity with granular interior and a dented surface (fig. 9A-B). It was observed to move over the planula ectoderm, nibbling off the cilia, leaving the planulae incapacitated, with short and dysfunctional cilia. As a second step, the parasites were sinking into the larval ectoderm. The parasites then proliferated inside the planulae, sometimes causing abnormal growth (fig. 9C-F). Swarms of small parasites were later seen leaving the infested planulae. The parasites were captured in a SEM preparation (fig 9E-F), but the high-resolution SEM images did not reveal any cilia or other distinct characters that could give a clue of what kind of protozoan it was. These parasites were present already in 2013, but did not cause major problems until the spawning season in 2015. They probably thrive in the bends of the water pipes supplying the seawater flow-through, where organic matter and sediments builds up.

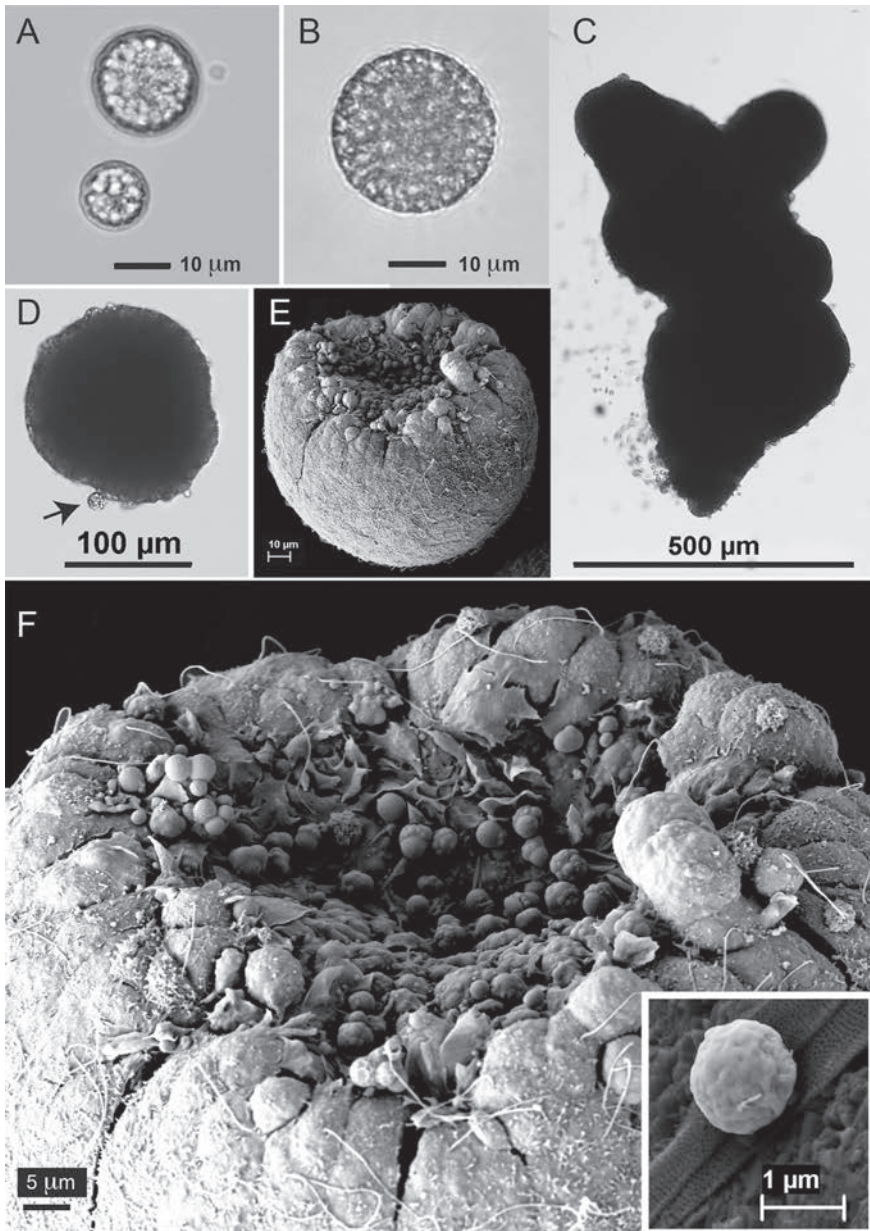


**Fig 9** – A-B. The unidentified protozoan parasite under light microscopy. – C. An infested planula showing abnormal growth. – D. A planula in an early stage of infestation; a parasite is seen on the ectoderm, close to the oral pore (arrow). – E-F. A SEM preparation of an infested planula, the oral pore looks like a crater filled with small parasites. Two large parasites are seen at the edge of the crater to the right. The inset in the bottom right corner shows a parasite with what seems to be a cilia being phagocytized.

“If you build it they will come”

## ECOLOGICAL RESTORATION

This doctoral project initially included a restoration experiment, and although initiated during the project period, it was not ready for evaluation within the project time frame. The aim for this part of the studies was to test if one can enhance settling rates of associated fauna by the design of the artificial reefs (AR), and/or the mode of deployment (i.e. solitary or clustered ARs). Three different designs of concrete AR units were built: 1) simple cubes; 2) irregular lumps; and 3) units with pinnacles (fig. 10). The simple cubes were controls, and the two following were to test the level of complexity necessary to enhance settling. Forty-five of these units were constructed, three of each type was deployed solitary, and three groups of four units deployed as clusters to see if nearness of units could enhance settling. The upstream unit were hypothesized to affect the downstream settling by creating eddies that would favor settling. The surfaces of the ARs were also enhanced by the inclusion of pebbles and shells to create many microhabitats.

On the ARs fragments of live corals were transplanted to test for coral growth on the different designs, and if growth were affected by transplanting corals in groups or as satellites (solitary fragments). Corals were stained with Alizarin that gets incorporated into the skeleton during incubations, and will be seen as pink bands on the fragments. New growth will be of normal coral color and can easily be measured from images.

The quote at the top of this page comes from the novel *Shoeless Joe* by the author W.P. Kinsella. The novel was adapted for the screen by Phil Alden Robinson in the 1989 drama *Field of Dreams*, starring Kevin Costner. The original quote was: “If you build it, he will come”, alluding to the ghost of a famous baseball player that would come and play on a baseball field—if built by the farmer on his cornfield. The quote has later been adopted and adapted by researchers working in the field of restoration ecology, e.g. Palmer *et al.* (1997), to exemplify the *Field of Dreams hypothesis*. In essence the hypothesis is that if you get the conditions right, propagules will come and settle in the restored area.

With the complex design of the ARs I wanted to mimic the complexity of a reef, so that any transplanted corals would be sufficiently elevated from the boundary layer and that the AR would function as the dead parts of a reef, offering habitats for reef associated fauna until the coral transplants grows up to a functioning reef.

At revisits to check how the settling progressed, and document coral transplant survival and growth; it was obvious that the experiment would take longer than the project time frame due to the dense population of feather stars at the chosen site at Saekken (fig. 11). The feather stars *Hathrometra tenella* (Crinoidea, syn. *H. sarsii*) are mobile animals that settle on any protruding object on the seafloor. When other fauna finally manage to settle and establish themselves on the surfaces, the feather stars usually withdraw to peripheral spots on the objects (personal observation). At the time of revisits, however, they were still covering the entire AR units.

*To be continued.*

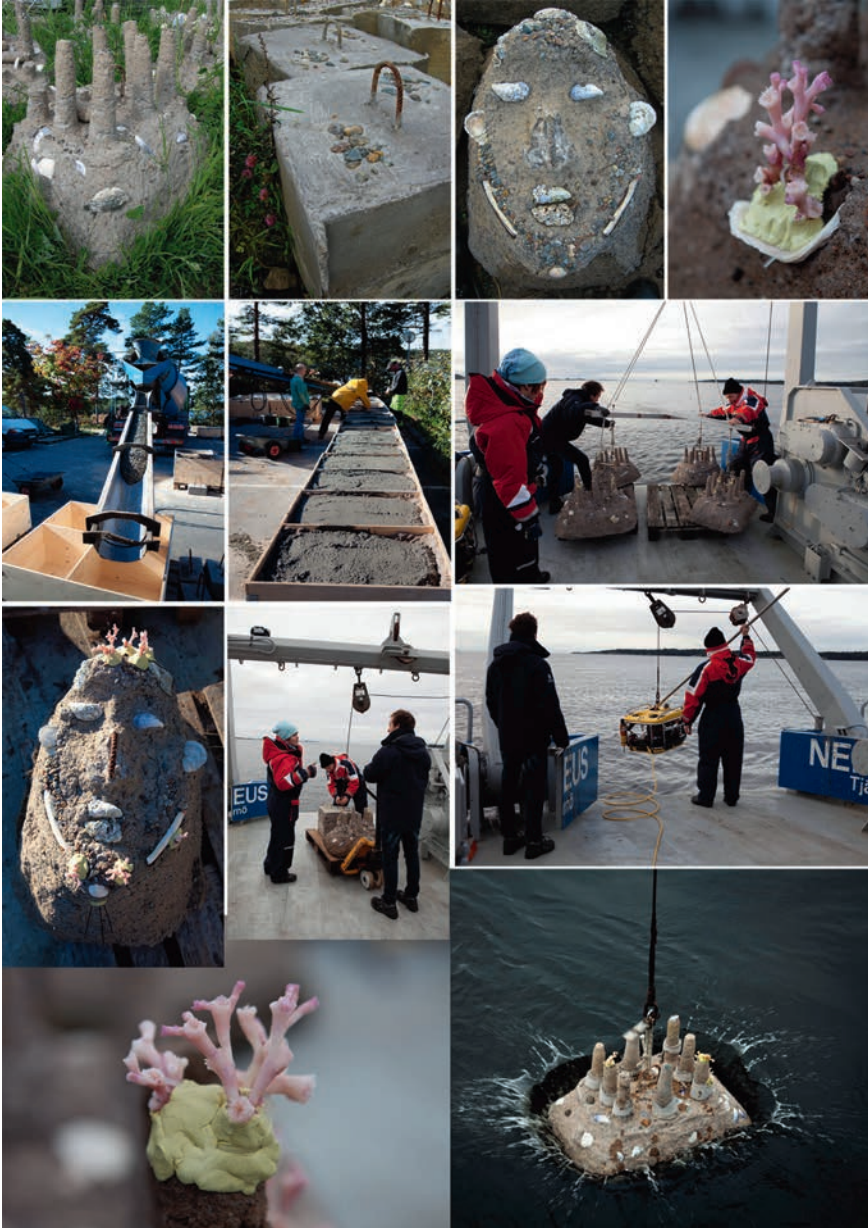


**Fig 10** – Images of the artificial reefs (ARs): AR with pinnacles, simple cubes, and medium complex irregular lumps (thanks to Mårten Duvetorp for the fantastic design of this particular one). The casting of these concrete lumps were a big job, and I was grateful to get help from Mårten, Daniel Johansson, and my internship student Laurence de Clippele. Deployments were done from the R/V Nereus with the help from the skippers and technical staff at Sven Lovén Center. The pink coral transplants are stained with Alizarin.

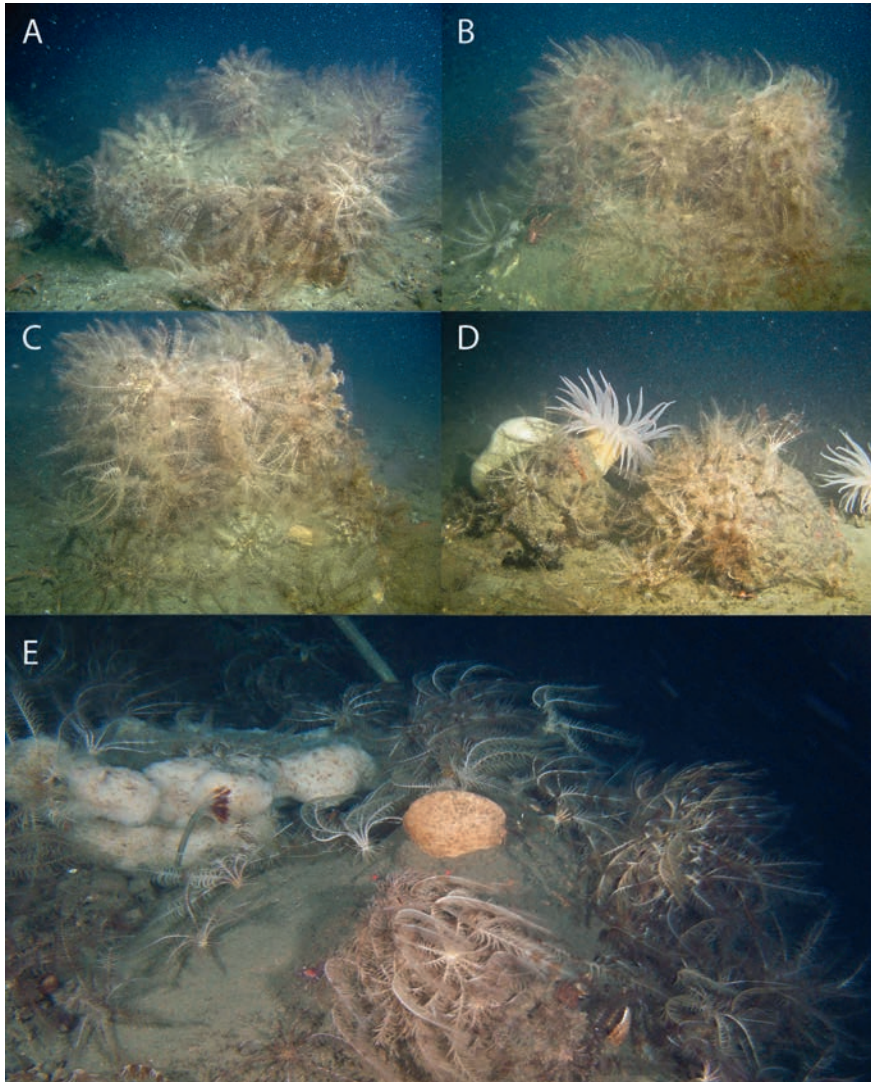


**Fig 11** – UW-images from the restoration site. – A. A simple cube. – B. An irregular AR. – C. An AR with pinnacles. – D. Natural rock habitat for comparison. – E. Close-up of an irregular AR with sponges, a *Sabella pavonina* (polychaete), plenty of crinoids (feather stars), and a small crustacean.

## REFERENCES

- Adamczyk, P., Meier, S., Gross, T., Hobmayer, B., Grzesiek, S., Bachinger, H. P., Holstein, T. W. and Ozbek, S. 2008. Minicollagen-15, a novel minicollagen isolated from *Hydra*, forms tubule structures in nematocysts. – *J Mol Biol* **376**: 1008–1020.
- Albright, R., Mason, B., Miller, M. and Langdon, C. 2010. Ocean acidification compromises recruitment success of the threatened Caribbean coral *Acropora palmata*. – *Proceedings of the National Academy of Sciences* **107** (47): 20400–20404.
- Allemand, D., Ferrier-Pagès, C., Furla, P., Houlbrèque, F., Puverel, S., Reynaud, S., Tambutté, É., Tambutté, S. and Zoccola, D. 2004. Biomineralisation in reef-building corals: from molecular mechanisms to environmental control. – *Comptes Rendus Palevol* **3** (6-7): 453–467.
- Althaus, F., Williams, A., Schlacher, T., Kloser, R., Green, M., Barker, B., Bax, N., Brodie, P. and Schlacher-Hoenlinger, M. 2009. Impacts of bottom trawling on deep-coral ecosystems of seamounts are long-lasting. – *Marine Ecology Progress Series* **397** (279–294): 40.
- Atkinson, S. and Atkinson, M. J. 1992. Detection of estradiol-17 $\beta$  during a mass coral spawn. – *Coral Reefs* **11**: 33–35.
- Babcock, R. C., Bullard, G. D., Harrison, P. L., Heyward, A. J., Oliver, J. K., Wallace, C. C. and Willis, B. L. 1986. Synchronous spawnings of 105 scleractinian coral species on the Great Barrier Reef. – *Marine Biology* **90**: 379–394.
- Bakke, T., Klungsoyr, J. and Sanni, S. 2013. Environmental impacts of produced water and drilling waste discharges from the Norwegian offshore petroleum industry. – *Marine Environmental Research* **92**: 154–169.
- Baums, I., Devlin-Durante, M., Polato, N., Xu, D., Giri, S., Altman, N., Ruiz, D., Parkinson, J. and Boulay, J. 2013. Genotypic variation influences reproductive success and thermal stress tolerance in the reef building coral, *Acropora palmata*. – *Coral Reefs* **32** (3): 703–717.
- Beckmann, A. and Özbek, S. 2012. The nematocyst: a molecular map of the cnidarian stinging organelle. – *International Journal for Development Biology* **56**: 577–582.
- Ben-David-Zaslow, R. and Benayahu, Y. 2000. Biochemical composition, metabolism, and amino acid transport in planula-larvae of the soft coral *Heteroxenia fuscescens*. – *Journal of Experimental Zoology* **287** (6): 401–412.
- Bett, B. 2000. Benthic ecology of Faeroe-Shetland Channel, Section 4.3. 1 in Environmental survey of the seafloor of the UK Atlantic Margin. Atlantic Frontier Environmental Network [CD-ROM]. – *Geotek Limited, Daventry, Northants NN11 5EA, UK*.
- Boidron-Métairon, I. 1995. Larval nutrition. – Ecology of marine invertebrate larvae. *CRC Press, Boca Raton, FL*: 223–248.
- Boschen, R., Rowden, A., Clark, M. and Gardner, J. 2013. Mining of deep-sea seafloor massive sulfides: a review of the deposits, their benthic communities, impacts from mining, regulatory frameworks and management strategies. – *Ocean & coastal management* **84**: 54–67.
- Brooke, S. and Järnegren, J. 2012. Reproductive periodicity of the scleractinian coral *Lophelia pertusa* from the Trondheim Fjord, Norway. – *Marine Biology* **160** (1): 139–153.
- Cairns, S. D. 2001. A brief history of taxonomic research on azooxanthellate Scleractinia (Cnidaria: Anthozoa). – *Bulletin of the Biological Society of Washington* **10**: 191–203.
- Cairns, S. D. and Kitahara, M. V. 2012. An illustrated key to the genera and subgenera of the recent azooxanthellate Scleractinia (Cnidaria, Anthozoa), with an attached glossary. – *ZooKeys* (227): 1–47.
- Cairns, S. D. 2007. Deep-water corals: An overview with special reference to diversity and distribution of deep-water scleractinian corals. – *Bulletin of Marine Science* **81** (3): 311–322.
- Carlgrén, O. 1940. A contribution to the knowledge of the structure and distribution of cnidae in the Anthozoa. – *Acta Universitatis Lundensis (ser 2)* **36** (3): 1–62.
- Carreiro-Silva, M., Cerqueira, T., Godinho, A., Caetano, M., Santos, R. and Bettencourt, R. 2014. Molecular mechanisms underlying the physiological responses of the cold-water coral *Desmophyllum dianthus* to ocean acidification. – *Coral Reefs* **33** (2): 465–476.
- Chui, A. P. Y., Wong, M. C., Liu, S. H., Lee, G. W., Chan, S. W., Lau, P. L., Leung, S. M. and Ang, P. 2014. Gametogenesis, embryogenesis, and fertilization ecology of *Platygyra acutain* marginal nonreefal coral communities in Hong Kong. – *Journal of Marine Biology* **2014**: 1–9.
- Colin, S. P. and Costello, J. H. 2007. Functional characteristics of nematocysts found on the scyphomedusa *Cyanea capillata*. – *Journal of Experimental Marine Biology and Ecology* **351**: 114–120.

- Corell, H., Moksnes, P.-O., Engqvist, A., Döös, K. and Jonsson, P. R. 2012. Depth distribution of larvae critically affects their dispersal and the efficiency of marine protected areas. – *Marine Ecology Progress Series* **467**: 29.
- Correa, M. L., Montagna, P., Joseph, N., Rüggeberg, A., Fietzke, J., Flögel, S., Dorschel, B., Goldstein, S., Wheeler, A. and Freiwald, A. 2012. Preboreal onset of cold-water coral growth beyond the Arctic Circle revealed by coupled radiocarbon and U-series dating and neodymium isotopes. – *Quaternary Science Reviews* **34**: 24–43.
- Costello, M. J., McCrea, M., Freiwald, A., Lundälv, T., Jonsson, L., Bett, B. J., van Weering, T. C. E., de Haas, H., Roberts, M. J. and Allen, D. 2005. Role of cold-water *Lophelia pertusa* coral reefs as fish habitat in the NE Atlantic. In: Roberts, F., (Ed.) *Cold-water corals and ecosystems* pp. 771–805. Springer-Verlag Berlin Heidelberg.
- Cowen, R. K. and Sponaugle, S. 2009. Larval dispersal and marine population connectivity. – *Ann Rev Mar Sci* **1**: 443–466.
- Cowen, R. K., Gawarkiewicz, G. G., Pineda, J., Thorrold, S. R. and Werner, F. E. 2007. Population connectivity in marine systems: an overview. – *Oceanography* **20**: No. 3, 14–21.
- Crowder, L. B., Lyman, S., Figueira, W. and Priddy, J. 2000. Source-sink population dynamics and the problem of siting marine reserves. – *Bulletin of Marine Science* **66** (3): 799–820.
- Dahl, M. P., Pereyra, R. T., Lundälv, T. and André, C. 2012. Fine-scale spatial genetic structure and clonal distribution of the cold-water coral *Lophelia pertusa*. – *Coral Reefs* **31** (4): 1135–1148.
- Dahl, M. P., Pereyra, R. T., Lundälv, T., Järnægren, J., Arnaud-Haond, S., and André, C. 2013. Genetic structure and the postglacial colonization process in the East Atlantic Ocean of the cold-water coral *Lophelia pertusa*. Paper II in the thesis *Conservation genetics of Lophelia pertusa*, Faculty of Science at University of Gothenburg, 2013.
- Daly, M., Fautin, D. G. and Cappola, V. A. 2003. Systematics of the Hexacorallia (Cnidaria: Anthozoa). – *Zoological Journal of the Linnean Society* **139** (3): 419–437.
- David, C. N., Ozbek, S., Adamczyk, P., Meier, S., Pauly, B., Chapman, J., Hwang, J. S., Gojobori, T. and Holstein, T. W. 2008. Evolution of complex structures: minicollagens shape the cnidarian nematocyst. – *Trends Genet* **24**: 431–438.
- Davies, A. J., Roberts, M. J. and Hall-Spencer, J. 2007. Preserving deep-sea natural heritage: emerging issues in offshore conservation and management. – *Biological Conservation* **138**: 299–312.
- Davies, A. J., Wisshak, M., Orr, J. C. and Murray Roberts, J. 2008. Predicting suitable habitat for the cold-water coral *Lophelia pertusa* (Scleractinia). – *Deep Sea Research Part I: Oceanographic Research Papers* **55** (8): 1048–1062.
- Davies, A. J. and Guinotte, J. M. 2011. Global habitat suitability for framework-forming cold-water corals. – *PLoS One* **6** (4).
- Diggs, R. E. 1977. Deep sea mining apparatus and method. Patent US 05/577,343,1977.
- Dodds, L. A., Black, K. D., Orr, H. and Roberts, J. M. 2009. Lipid biomarkers reveal geographical differences in food supply to the cold-water coral *Lophelia pertusa* (Scleractinia). – *Marine Ecology-Progress Series* **397**: 113–124.
- Drake, P. T., Edwards, C. A., Morgan, S. G. and Dever, E. P. 2013. Influence of larval behavior on transport and population connectivity in a realistic simulation of the California Current System. – *Journal of Marine Research* **71** (4): 317–350.
- Engel, U. 2002. Nowa, a novel protein with minicollagen Cys-rich domains, is involved in nematocyst formation in *Hydra*. – *Journal of Cell Science* **115** (20): 3923–3934.
- Ewer, R. F. 1947. On the functions and mode of action of the nematocysts of *Hydra*. – *Proceedings of the Zoological Society of London* **117** (2-3): 365–376.
- Fautin, D. G. and Mariscal, R. N. 1991. Cnidaria: Anthozoa. In: Harrison, F. W. and Westfall, J. A., (Eds.) *Microscopic anatomy of Invertebrates*, vol. **2**, pp. 267–358. – *Wiley-Liss, N.Y.*
- Fautin, D. G. 2009. Structural diversity, systematics, and evolution of cnidae. – *Toxicon* **54**: 1054–1064.
- Fiksen, Ø., Jørgensen, C., Kristiansen, T., Vikebø, F. and Huse, G. 2007. Linking behavioural ecology and oceanography: larval behaviour determines growth, mortality and dispersal. – *Marine Ecology Progress Series* **347**: 195–205.
- Fine, M. and Tchernov, D. 2007. Scleractinian coral species survive and recover from decalcification. – *Science* **315** (5820): 1811.
- Flot, J.-F., Dahl, M. and André, C. 2013. *Lophelia pertusa* corals from the Ionian and Barents seas share identical nuclear ITS2 and near-identical mitochondrial genome sequences. – *BMC research notes* **6** (1): 144.
- Form, A. U. and Riebesell, U. 2011. Acclimation to ocean acidification during long-term exposure in the cold-water coral *Lophelia pertusa*. – *Global Change Biology*: 1–11.

- Fosså, J. H., Mortensen, P. B. and Furevik, D. M. 2002. The deep-water coral *Lophelia pertusa* in Norwegian waters: distribution and fishery impacts. – *Hydrobiologia* **471**: 12.
- Freiwald, A., Fosså, J. H., Grehan, A., Koslow, T. and Roberts, M. J. 2004. Cold-water coral reefs: out of sight - no longer out of mind. 83 pp. UNEP-WCMC, Cambridge, UK.
- Gass, S. E. and Roberts, J. M. 2006. The occurrence of the cold-water coral *Lophelia pertusa* (Scleractinia) on oil and gas platforms in the North Sea: colony growth, recruitment and environmental controls on distribution. – *Mar Pollut Bull* **52** (5): 549–559.
- Gattuso, J.-P. and Hansson, L. 2011. Ocean acidification: background and history. – *Ocean acidification*: 1–20.
- Gianni, M. 2004. *High seas bottom trawl fisheries and their impacts on the biodiversity of vulnerable deep-sea ecosystems: options for international action*. IUCN.
- Glasby, G. P. 2000. Lessons Learned from Deep-Sea Mining. – *Science* **289** (5479): 551–553.
- Gori, A., Grover, R., Orejas, C., Sikorski, S. and Ferrier-Pagès, C. 2014. Uptake of dissolved free amino acids by four cold-water coral species from the Mediterranean Sea. – *Deep Sea Research Part II: Topical Studies in Oceanography* **99**: 42–50.
- Gosse, P. H. 1860. *Actinologia Britannica: A history of the British sea-anemones and corals*. – *Van Voorst, Paternoster Row, London*. 362 pp.
- Graham, E. M., Baird, A. H. and Connolly, S. R. 2008. Survival dynamics of scleractinian coral larvae and implications for dispersal. – *Coral Reefs* **27**: 529–539.
- Guinotte, J. M., Orr, J., Cairns, S., Freiwald, A., Morgan, L. and George, R. 2006. Will human-induced changes in seawater chemistry alter the distribution of deep-sea scleractinian corals? – *Front Ecol Environ* **4**(3): 141–146.
- Harrison, P. L., Babcock, R. C., Bull, G. D., Oliver, J. K., Wallace, C. C. and Willis, B. L. 1984. Mass spawning in tropical reef corals. – *Science* **223** (4641): 1186–1189.
- Hayashibara, T., Ohike, S. and Kakinuma, Y. 1997. Embryonic and larval development and planula metamorphosis of four gamete-spawning *Acropora* (Anthozoa, Scleractinia). *Proceedings of the 8th International Coral Reef Symposium, Panama*. 1231–1236 pp. 1997.
- Hellstern, S., Stetefeld, J., Fauser, C., Lustig, A., Engel, J., Holstein, T. W. and Özbek, S. 2006. Structure/function analysis of spinalin, a spine protein of *Hydra* nematocysts. – *Federation of European Biochemical Societies Journal* **273**: 3230–3237.
- Hennige, S. J., Wicks, L. C., Kamenos, N. A., Bakker, D. C. E., Findlay, H. S., Dumousseaud, C. and Roberts, J. M. 2014. Short-term metabolic and growth responses of the cold-water coral *Lophelia pertusa* to ocean acidification. – *Deep Sea Research Part II: Topical Studies in Oceanography* **99**: 27–35.
- Henry, L.-A., Frank, N., Hebbeln, D., Wienberg, C., Robinson, L., de Flierd, T. v., Dahl, M., Douarin, M., Morrison, C. L., Correa, M. L., Rogers, A. D., Ruckelshausen, M. and Roberts, J. M. 2014. Global ocean conveyor lowers extinction risk in the deep sea. – *Deep Sea Research Part I: Oceanographic Research Papers* **88**: 8–16.
- Hilário, A., Metaxas, A., Gaudron, S., Howell, K., Mercier, A., Mestre, N., Ross, R. E., Thurnherr, A. and Young, C. 2015. Estimating dispersal distance in the deep sea: challenges and applications to marine reserves. – *Frontiers in Marine Science* **2**.
- Hoegh-Guldberg, O. and Pearse, J. S. 1995. Temperature, food availability, and the development of marine invertebrate larvae. – *American Zoologist* **35** (4): 415–425.
- Holst, S., Sötje, I., Tiemann, H. and Jarms, G. 2007. Life cycle of the rhizostome jellyfish *Rhizostoma octopus* (L.) (Scyphozoa, Rhizostomeae), with studies on cnidocysts and statoliths. – *Marine Biology* **151**: 1695–1710.
- Holstein, T. 1981. The morphogenesis of nematocytes in *Hydra* and *Forskålia*: An ultrastructural study. – *Journal of Ultrastructure Research* **75**: 276–290.
- Houlbreque, F., Tambutte, E., Richard, C. and Ferrier-Pages, C. 2004. Importance of a micro-diet for scleractinian corals. – *Marine Ecology-Progress Series* **282**: 151–160.
- Jensen, A. and Frederiksen, R. 1992. The fauna associated with the bank-forming deepwater coral *Lophelia pertusa* (Scleractinia) on the Faroe Shelf. – *Sarsia* **77**: 53–69.
- Kaniewska, P., Campbell, P. R., Kline, D. I., Rodriguez-Lanetty, M., Miller, D. J., Dove, S. and Hoegh-Guldberg, O. 2012. Major cellular and physiological impacts of ocean acidification on a reef building coral. – *PLoS One* **7** (4): e34659.
- Kass-Simon, G. and Scappaticci, A. A. 2002. The behavioral and developmental physiology of nematocysts. – *Canadian Journal of Zoology-Revue Canadienne De Zoologie* **80**: 1772–1794.
- Kerr, A. M., Baird, A. H. and Hughes, T. P. 2010. Correlated evolution of sex and reproductive mode in corals (Anthozoa: Scleractinia). – *Proceedings of the Royal Society B-Biological Sciences* **278** (1702): 75–81.

- Kitahara, M. V., Cairns, S. D., Stolarski, J., Blair, D. and Miller, D. J. 2010a. A comprehensive phylogenetic analysis of the Scleractinia (Cnidaria, Anthozoa) based on mitochondrial COI sequence data. – *PLoS One* **5**: e11490.
- Kitahara, M. V., Cairns, S. D. and Miller, D. J. 2010b. Monophyletic origin of Caryophyllia (Scleractinia, Caryophylliidae), with descriptions of six new species. – *Systematics and Biodiversity* **8**: 91–118.
- Kobayashi, M., Sorensen, P. W. and Stacey, N. E. 2002. Hormonal and pheromonal control of spawning behavior in the goldfish. – *Fish Physiology and Biochemistry* **26** (1): 71–84.
- Krupp, D. A. 1983. Sexual reproduction and early development of the solitary coral *Fungia scutaria*; (Anthozoa: Scleractinia). – *Coral Reefs* **2** (3): 159–164.
- Larsson, A. I., Järnegren, J., Strömberg, S. M., Dahl, M. P., Lundälv, T. and Brooke, S. 2014. Embryogenesis and larval biology of the cold-water coral *Lophelia pertusa*. – *Plos One* **9**: e102222.
- Larsson, A. I. and Purser, A. 2011. Sedimentation on the cold-water coral *Lophelia pertusa*: cleaning efficiency from natural sediments and drill cuttings. – *Mar Pollut Bull* **62** (6): 1159–1168.
- Larsson, A. I., van Oevelen, D., Purser, A. and Thomsen, L. 2013. Tolerance to long-term exposure of suspended benthic sediments and drill cuttings in the cold-water coral *Lophelia pertusa*. – *Marine Pollution Bulletin* **70** (1): 176–188.
- Lawton, J. H. and Jones, C. G. 1995. Linking Species and Ecosystems: Organisms as Ecosystem Engineers. In: Jones, C. G. and Lawton, J. H., (Eds.) *Linking Species & Ecosystems*, pp. 141–150. Springer US, Boston, MA.
- Le Goff-Vitry, M. C., Pybus, O. G. and Rogers, A. D. 2004. Genetic structure of the deep-sea coral *Lophelia pertusa* in the northeast Atlantic revealed by microsatellites and internal transcribed spacer sequences. – *Molecular Ecology* **13**: 537–549.
- Lindner, A., Cairns, S. D. and Cunningham, C. W. 2008. From offshore to onshore: multiple origins of shallow-water corals from deep-sea ancestors. – *PLoS One* **3**: e2429.
- Maier, C., Hegeman, J., Weinbauer, M. G. and Gattuso, J.-P. 2009. Calcification of the cold-water coral *Lophelia pertusa* under ambient and reduced pH. – *Biogeosciences* **6**: 1875–1901.
- Manahan, D. T. 1990. Adaptations by invertebrate larvae for nutrient acquisition from seawater – *American Zoologist* **30** (1): 147–160.
- Mariscal, R. N., Conklin, E. J. and Bigger, C. H. 1977a. The ptychocyst, a major new category of cnidae used in tube construction by a cerianthid anemone. – *The Biological Bulletin* **152**: 392–405.
- Mariscal, R. N., McLean, R. B. and Hand, C. 1977b. The form and function of cnidarian spirocysts. 3. Ultrastructure of the thread and the function of spirocysts. – *Cell and Tissue Research* **178**: 427–433.
- McCulloch, M., Falter, J., Trotter, J. and Montagna, P. 2012. Coral resilience to ocean acidification and global warming through pH up-regulation. – *Nature Climate Change* **2** (8): 623–627.
- Mercier, A., Sun, Z., Baillon, S. and Hamel, J.-F. 2011. Lunar Rhythms in the Deep Sea: Evidence from the Reproductive Periodicity of Several Marine Invertebrates. – *Journal of Biological Rhythms* **26** (1): 82–86.
- Metaxas, A. and Saunders, M. 2009. Quantifying the “bio-” components in biophysical models of larval transport in marine benthic invertebrates: advances and pitfalls. – *The Biological Bulletin* **216** (3): 257–272.
- Middelburg, J. J., Mueller, C. E., Veuger, B., Larsson, A. I., Form, A. and van Oevelen, D. 2015. Discovery of symbiotic nitrogen fixation and chemoautotrophy in cold-water corals. – *Scientific reports* **5**.
- Miller, K. and Mundy, C. 2003. Rapid settlement in broadcast spawning corals: implications for larval dispersal. – *Coral Reefs* **22** (2): 99–106.
- Morabito, R., Marino, A., Lauf, P. K., Adragna, N. C. and La Spada, G. 2013. Sea water acidification affects osmotic swelling, regulatory volume decrease and discharge in nematocytes of the jellyfish *Pelagia noctiluca*. – *Cell Physiol Biochem* **32** (7): 77–85.
- Mueller, C. E., Larsson, A. I., Veuger, B., Middelburg, J. J. and van Oevelen, D. 2014. Opportunistic feeding on various organic food sources by the cold-water coral *Lophelia pertusa*. – *Biogeosciences Discussions* **10**: 11375–11403.
- Möbius, K. A. 1866. Ueber den Bau, den mechanismus und die entwicklung der nesselkapseln einiger polypen und quallen. – *Abhandlungen aus dem Gebiete der Naturwissenschaften Hamburg* V(1): 1–22, pls. 1–2.

- Naumann, M. S., Orejas, C., Wild, C. and Ferrier-Pages, C. 2011. First evidence for zooplankton feeding sustaining key physiological processes in a scleractinian cold-water coral. – *J Exp Biol* **214** (Pt 21): 3570–3576.
- Naumann, M. S., Tolosa, I., Taviani, M., Grover, R. and Ferrier-Pagès, C. 2015. Trophic ecology of two cold-water coral species from the Mediterranean Sea revealed by lipid biomarkers and compound-specific isotope analyses. – *Coral Reefs* **34** (4): 1165–1175.
- Norse, E. A. and Watling, L. 1999. Impacts of mobile fishing gear: the biodiversity perspective. *American Fisheries Society Symposium*. 31–40 pp. 1999.
- Negri, A. P. and Heyward, A. J. 2000. Inhibition of fertilization and larval metamorphosis of the coral *Acropora millepora* (Ehrenberg, 1834) by petroleum products. – *Marine Pollution Bulletin* **41** (7-12): 420–427.
- O'Connor, M. I., Bruno, J. F., Gaines, S. D., Halpern, B. S., Lester, S. E., Kinlan, B. P. and Weiss, J. M. 2007. Temperature control of larval dispersal and the implications for marine ecology, evolution, and conservation. – *Proc Natl Acad Sci U S A* **104** (4): 1266–1271.
- Orr, J. C., Fabry, V. J., Aumont, O., Bopp, L., Doney, S. C., Feely, R. A., Gnanadesikan, A., Gruber, N., Ishida, A., Joos, F., Key, R. M., Lindsay, K., Maier-Reimer, E., Matear, R., Monfray, P., Mouchet, A., Najjar, R. G., Plattner, G.-K., Rogers, K. B., Sabine, C. L., Sarmiento, J. L., Schlitzer, R., Slater, R. D., Totterdell, I. J., Weirig, M.-F., Yamanaka, Y. and Yool, A. 2005. Anthropogenic ocean acidification over the twenty-first century and its impact on calcifying organisms. – *Nature* **Vol. 437**: 681–686.
- Palmer, M. A., Ambrose, R. F. and Poff, N. L. 1997. Ecological theory and community restoration ecology. – *Restoration Ecology* **5** (No. 4): 291–300.
- Penland, L., Klouechad, J., Idip, D. and Van Woesik, R. 2004. Coral spawning in the western Pacific Ocean is related to solar insolation: evidence of multiple spawning events in Palau. – *Coral Reefs* **23** (1): 133–140.
- Pires, D., Silva, J. and Bastos, N. 2014. Reproduction of deep-sea reef-building corals from the southwestern Atlantic. – *Deep Sea Research Part II: Topical Studies in Oceanography* **99**: 51–63.
- Pulliam, H. R. 1988. Sources, sinks, and population regulation. – *American Naturalist*: 652–661.
- Rinkevich, B. 2004. Allorecognition and xenorecognition in reef corals: a decade of interactions. *Coelenterate Biology 2003*, pp. 443–450. Springer.
- Roberts, J. 2002. The occurrence of the coral *Lophelia pertusa* and other conspicuous epifauna around an oil platform in the North Sea. – *Underwater Technology* **25** (2): 83–92.
- Roberts, J. M., Wheeler, A., Freiwald, A. and Cairns, S. D. 2009. *Cold-water corals: the biology and geology of deep-sea coral habitats*. Cambridge University Press.
- Robson, E. A. 2004. Cnidogenesis in the jewel anemone *Corynactis californica* (Carlgren, 1936) and *C. viridis* (Allman, 1846) (Anthozoa: Corallimorpharia). – *Zoologische Mededelingen (Leiden)* **78** (18–28): 461–476.
- Romano, S. L. and Cairns, S. D. 2000. Molecular phylogenetic hypotheses for the evolution of scleractinian corals. – *Bulletin of Marine Science* **67**: 1043–1068.
- Rubey, W. W. 1951. Geologic history of sea water an attempt to state the problem. – *Geological Society of America Bulletin* **62** (9): 1111–1148.
- Schwarz, J. A., Krupp, D. A. and Weis, V. M. 1999. Late larval development and onset of symbiosis in the scleractinian coral *Fungia scutaria*. – *The Biological Bulletin* **196**: 70–79.
- Schwarz, J. A., Weis, V. M. and Potts, D. C. 2002. Feeding behavior and acquisition of zooxanthellae by planula larvae of the sea anemone *Anthopleura elegantissima*. – *Marine Biology* **140**: 471–478.
- Shanks, A. L. 2009. Pelagic larval duration and dispersal distance revisited. – *The Biological Bulletin* **216** (3): 373–385.
- Shick, J. M. 1991. *A functional biology of sea anemones*. Chapman & Hall, London, New York etc.
- Skaer, R. J. and Picken, L. E. R. 1966. The pleated surface of the undischarged thread of a nematocyst and its simulation by models. – *Journal of Experimental Biology* **45**: 173–177.
- Skaer, R. J. 1973. The secretion and development of nematocysts in a siphonophore. – *Journal of Cell Science* **13**: 371–393.
- Slautterback, D. B. and Fawcett, D. W. 1959. The development of the cnidoblasts of *Hydra*: An electron microscope study of cell differentiation. – *Journal of Biophysical and Biochemical Cytology* **5**: 441–467.
- Stacey, N. 2003. Hormones, pheromones and reproductive behavior. – *Fish Physiology and Biochemistry* **28** (1-4): 229–235.

- Stolarski, J., Kitahara, M., Miller, D., Cairns, S., Mazur, M. and Meibom, A. 2011. The ancient evolutionary origins of scleractinia revealed by azooxanthellate corals. – *BMC Evol Biol* **11**: 316.
- Stott, R. 2012. Darwin's ghosts – the secret history of evolution. Book. *Spiegel & Grau, The Random House Publishing Group*. ISBN: 978-1-4000-6937-8
- Sun, Z., Hamel, J.-F., Edinger, E. and Mercier, A. 2010a. Reproductive biology of the deep-sea octocoral *Drifa glomerata* in the Northwest Atlantic. – *Marine Biology* **157** (4): 863–873.
- Sun, Z., Hamel, J.-F. and Mercier, A. 2010b. Planulation periodicity, settlement preferences and growth of two deep-sea octocorals from the northwest Atlantic. – *Marine Ecology-Progress Series* **410**: 71–87.
- Sun, Z., Hamel, J.-F. and Mercier, A. 2011. Planulation, larval biology, and early growth of the deep-sea soft corals *Gersemia fruticosa* and *Duva florida* (Octocorallia: Alcyonacea). – *Invertebrate Biology* **130** (2): 91–99.
- Tambutte, E., Venn, A. A., Holcomb, M., Segonds, N., Techer, N., Zoccola, D., Allemand, D. and Tambutte, S. 2015. Morphological plasticity of the coral skeleton under CO<sub>2</sub>-driven seawater acidification. – *Nat Commun* **6**: 7368.
- Tardent, P. and Holstein, T. 1982. Morphology and morphodynamics of the stenotele nematocyst of *Hydra attenuata* Pall. (Hydrozoa, Cnidaria). – *Cell and Tissue Research* **224**: 269–290.
- Tarrant, A. M. 2005. Endocrine-like signaling in Cnidarians: Current understanding and implications for ecophysiology. – *Integrative and Comparative Biology* **45**: 201–214.
- Tranter, P. R. G., Nicholson, D. N. and Kinchington, D. 1982. A description of spawning and post-gastrula development of the cool temperate coral, *Caryophyllia smithii*. . – *Journal of the Marine Biological Association of the United Kingdom* **62** (4): 845–854.
- Treml, E. A., Ford, J. R., Black, K. P. and Swearer, S. E. 2015. Identifying the key biophysical drivers, connectivity outcomes, and metapopulation consequences of larval dispersal in the sea. – *Mov Ecol* **3** (1): 17.
- Twan, W.-H., Hwang, J.-S., Lee, Y.-H., Jeng, S.-R., Yueh, W.-S., Tung, Y.-H., Wu, H.-F., Dufour, S. and Chang, C.-F. 2006. The presence and ancestral role of Gonadotropin-releasing hormone in the reproduction of Scleractinian coral, *Euphyllia ancora*. – *Endocrinology* **147**: 397–406.
- Van Dover, C. L. 2011. Tighten regulations on deep-sea mining. – *Nature* **470** (7332): 31–33.
- van Woesik, R. 2010. Calm before the spawn: global coral spawning patterns are explained by regional wind fields. – *Proc Biol Sci* **277** (1682): 715–722.
- Waller, R. G. 2005. Deep-water Scleractinia (Cnidaria: Anthozoa): current knowledge of reproductive processes. In: Freiwald, A. and Roberts, J. M., (Eds.) *Cold-water corals and ecosystems*, pp. 691-700. Springer-Verlag.
- Waller, R. G. and Feehan, K. A. 2013. Reproductive ecology of a polar deep-sea scleractinian, *Fungiacyathus marezelleri* (Vaughan, 1906). – *Deep Sea Research Part II: Topical Studies in Oceanography* **92**: 201–206.
- Waller, R. G. and Tyler, P. A. 2005. The reproductive biology of two deep-water, reef-building scleractinians from the NE Atlantic Ocean. – *Coral Reefs* **24** (3): 514–522.
- Watson, G. and Hessinger, D. 1994. Antagonistic frequency tuning of hair bundles by different chemoreceptors regulates nematocyst discharge. – *Journal of Experimental Biology* **187** (1): 57–73.
- Watson, G. M. and Roberts, J. 1994. Localization of proline receptors involved in regulating nematocyst discharge. – *Journal of Experimental Zoology* **270** (6): 527–537.
- Westfall, J. A. 1966. Differentiation of nematocysts and associated structures in Cnidaria. – *Zeitschrift Fur Zellforschung Und Mikroskopische Anatomie* **75**: 381–403.
- White, H. K., Hsing, P.-Y., Cho, W., Shank, T. M., Cordes, E. E., Quattrini, A. M., Nelson, R. K., Camilli, R., Demopoulos, A. W. and German, C. R. 2012. Impact of the Deepwater Horizon oil spill on a deep-water coral community in the Gulf of Mexico. – *Proceedings of the National Academy of Sciences* **109** (50): 20303–20308.
- Wilson, J. B. 1979. Patch development of the deep-water coral *Lophelia pertusa* (Linnaeus, 1758) on Rockall Bank – *Journal of the Marine Biological Association of the United Kingdom* **59**: 165–177.
- Wilson, J. and Harrison, P. 1998. Settlement-competency periods of larvae of three species of scleractinian corals. – *Marine Biology* **131** (2): 339–345.
- Wisshak, M., Freiwald, A., Lundälv, T. and Gektidis, M. 2005. The physical niche of the bathyal *Lophelia pertusa* in a non-bathyal setting: environmental controls and palaeoecological implications. In: JM, F. A. R., (Ed.) *Cold-water corals and ecosystems*, pp. 979–1001. Springer-Verlag Berlin Heidelberg.

- Young, C. M. and Tyler, P. A. 1993. Embryos of the deep-sea echinoid *Echinus affinis* require high pressure for development. – *Limnology and Oceanography* **38** (1): 178–181.
- Zenkert, C., Takahashi, T., Diesner, M.-O. and Özbek, S. 2011. Morphological and molecular analysis of the *Nematostella vectensis* cnidom. – *PLoS One* **6** (7): e22725.
- Yamashita, K., Kawaii, S., Nakai, M. and Fusetani, N. 2003. Larval behavioral, morphological changes, and nematocyte dynamics during settlement of actinulae of *Tubularia mesembryanthemum*, Allman 1871 (Hydrozoa : Tubulariidae). – *Biological Bulletin* **204**: 256–269.
- Östman, C., Piraino, S. and Kem, W. 1991. Nematocysts of the Mediterranean hydroid *Halorcordyle disticha* – *Hydrobiologia* **216**: 607–613.
- Östman, C. and Hydman, J. 1997. Nematocyst analysis of *Cyanea capillata* and *Cyanea lamarckii* (Scyphozoa, Cnidaria). – *Scientia Marina* **61** (3): 313–344.
- Östman, C. 2000. A guideline to nematocyst nomenclature and classification, and some notes on the systematic value of nematocysts. – *Scientia Marina* **64**: 31–46.
- Östman, C., Kultima, J. R. and Roat, C. 2010a. Tentacle cnidae of the sea anemone *Metridium senile* (Linnaeus, 1761) (Cnidaria: Anthozoa). – *Scientia Marina* **74**: 511–521.
- Östman, C., Kultima, J. R., Roat, C. and Rundblom, K. 2010b. Acontia and mesentery nematocysts of the sea anemone *Metridium senile* (Linnaeus, 1761) (Cnidaria: Anthozoa). – *Scientia Marina* **74**: 483–497.
- Östman, C., Borg, F., Roat, C., Kultima, J. R. and Wong, S. Y. G. 2013. Cnidae in the sea anemone *Sagartiogeton viduatus* (Muller, 1776) (Cnidaria, Anthozoa); A comparison to cnidae in the sea anemone *Metridium senile* (Linnaeus, 1761) (Cnidaria, Anthozoa). – *Acta Zoologica* **94** (4): 392–409.